

General Disclaimer

One or more of the Following Statements may affect this Document

- This document has been reproduced from the best copy furnished by the organizational source. It is being released in the interest of making available as much information as possible.
- This document may contain data, which exceeds the sheet parameters. It was furnished in this condition by the organizational source and is the best copy available.
- This document may contain tone-on-tone or color graphs, charts and/or pictures, which have been reproduced in black and white.
- This document is paginated as submitted by the original source.
- Portions of this document are not fully legible due to the historical nature of some of the material. However, it is the best reproduction available from the original submission.

OPTIMIZATION OF MLS RECEIVERS
FOR MULTIPATH ENVIRONMENTS

Interim Report
Grant No. NSG-1128

Submitted to:

NASA Scientific and Technical Information Facility
P. O. Box 8757
Baltimore/Washington International Airport
Maryland 21240

Submitted by:

G. A. McAlpine
Associate Professor

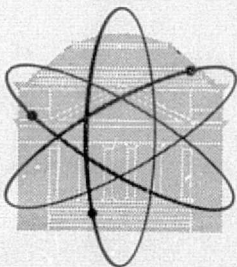
J. H. Highfill, III
Senior Engineer

S. H. Irwin, Jr.
Graduate Research Assistant

J. E. Padgett
Student Assistant

SCHOOL OF ENGINEERING AND
APPLIED SCIENCE

RESEARCH LABORATORIES FOR THE ENGINEERING SCIENCES



UNIVERSITY OF VIRGINIA

CHARLOTTESVILLE, VIRGINIA 22901

Report No. EE-4033-101-75

December 1975

(NASA-CR-145906) OPTIMIZATION OF MLS
RECEIVERS FOR MULTIPATH ENVIRONMENTS
Interim Report (Virginia Univ.) 165 p HC
\$6.75

N76-14056

CSCL 01E

Unclas
05615

G3/03

TABLE OF CONTENTS

Chapter	Page
I. Introduction	1
II. Signal Modeling	2
III. Optimal MLS Receiver Design	16
Locally Optimum Estimation	16
Recursive State Estimation	31
Conclusions	34
IV. Suboptimal Design and Simulation Evaluation	36
Receiver Algorithm Design	36
Simulation Modeling	41
Performance Evaluation	47
Conclusion	59
V. Conclusions and Recommendations	61
References	63
Appendix A Computer Programs	
Appendix B Computer Plots	

LIST OF FIGURES

- Figure II-1 Coordinate System
- Figure II-2 Reflection Geometry
- Figure III-1 Structure of a Locally Optimum Estimator Receiver for the Direct-Path Signal + Noise Case
- Figure IV-1 Envelope and Gating Functions
- Figure IV-2 Flowchart for Simulation Program MLSRCVR
- Figure IV-2a Initialization
- Figure IV-2b A/C and Reflector Initial Conditions
- Figure IV-2c Updating Signal to kth Scan
- Figure IV-2d Computing Envelope Samples
- Figure IV-2e Estimate Calculation
- Figure IV-2f Short-Term Plotting Decisions
- Figure IV-2g Advancing Geometry to Next Scan
- Figure IV-3 Square-Gate Receiver Flowchart
- Figure IV-4 Flowchart for Plotting Program MLSPLOT
- Figure IV-5 Simulation Results
- Figure B-1 SNR = 20 db, no multipath
- a. Long-Term Plot
 - b. Selected Envelopes Plot
 - c. Short-Term Plot
- Figure B-2 SNR = 8 db, no multipath
- a. Long-Term Plot
 - b. Selected Envelopes Plot
 - c. Short-Term Plot
- Figure B-3 SNR = 8 db, 1 reflector, $\alpha_1 = 0.8$, phase difference = 180° at pulse coincidence
- a. Long-Term Plot
 - b. Selected Envelopes Plot
 - c. Short-Term Plot
- Figure B-4 SNR = 20 db, 1 reflector, phase difference = 180° at pulse coincidence
- a. Long-Term Plot
 - b. Selected Envelopes Plot
 - c. Short-Term Plot

Figure B-5 SNR = 20 db, 1 reflector, phase difference = 0° at pulse coincidence

- a. Long-Term Plot
- b. Selected Envelopes Plot
- c. Short-Term Plot

Figure B-6 SNR = 20 db, 1 reflector, phase difference = 90° at pulse coincidence

- a. Long-Term Plot
- b. Selected Envelopes Plot
- c. Short-Term Plot

Figure B-7 SNR = 20 db, 1 reflector, phase difference = 270° at pulse coincidence

- a. Long-Term Plot
- b. Selected Envelope Plot
- c. Short-Term Plot

CHAPTER 1

INTRODUCTION

This is a report of the initial phase of research under Grant NSG 1128, awarded to the University in December 1974. The project is part of a program to design a receiver for aircraft (A/C), which, as a component of the proposed Microwave Landing System (MLS), is capable of optimal performance in the multipath environments found in air terminal areas [1]. This project focuses on the angle-tracking problem of the MLS receiver and deals with signal modeling, preliminary approaches to optimal design, suboptimal design and simulation study. This effort was integrated in part with the work under contract NAS1-12754-1, which was summarized in a final report dated May 1975 [2].

CHAPTER II
SIGNAL MODELING

The angular coordinate determination capability of the MLS has been tentatively established by a provision potentially for six (6) angle channels [1]. The signals in all channels have similar forms, however, and without loss of generality, this study has employed the azimuth channel as a focus to provide concrete interpretations of the models and results developed. Parallel results for other channels would obtain from suitable adjustments of parameter values.

The coordinate system in use is the right-handed system shown in Figure 1-1 with the origin located at the center of the azimuth transmitting antenna. The relevant variables r , θ , ϕ are range (n.mi.), azimuth (degrees, positive clockwise looking down) and elevation (degrees, positive up). Let $p(\cdot)$ and $\theta_A(\cdot)$, respectively the antenna selectivity and scanning functions, be defined as follows:

$p(\theta_e) \triangleq$ the far-field strength of the transmitted signal (field) relative to the boresight signal strength at the same range, where θ_e is the azimuth angle of the observer relative to the antenna boresight axis, and thus $p(0) = 1$. (2-1)

$\theta_A(t) \triangleq$ the angular orientation in azimuth of the antenna boresight axis as observed at time t at the transmitting antenna site. (2-2)

The definition of $p(\cdot)$ above does not recognize explicitly a dependency on observer elevation, which is present due to phased array radiation pattern properties. The effect is recognized implicitly however, with notation suppressed until cross-coupling of the various angular coordinate estimators (and the DME) is considered.

Further, letting

$t_k \triangleq$ the time (as observed at the antenna site) that the k th TO-FRO antenna scan begins; (2-3)

$T \triangleq$ the duration of the TO-FRO scan as observed by a stationary observer, (2-4)

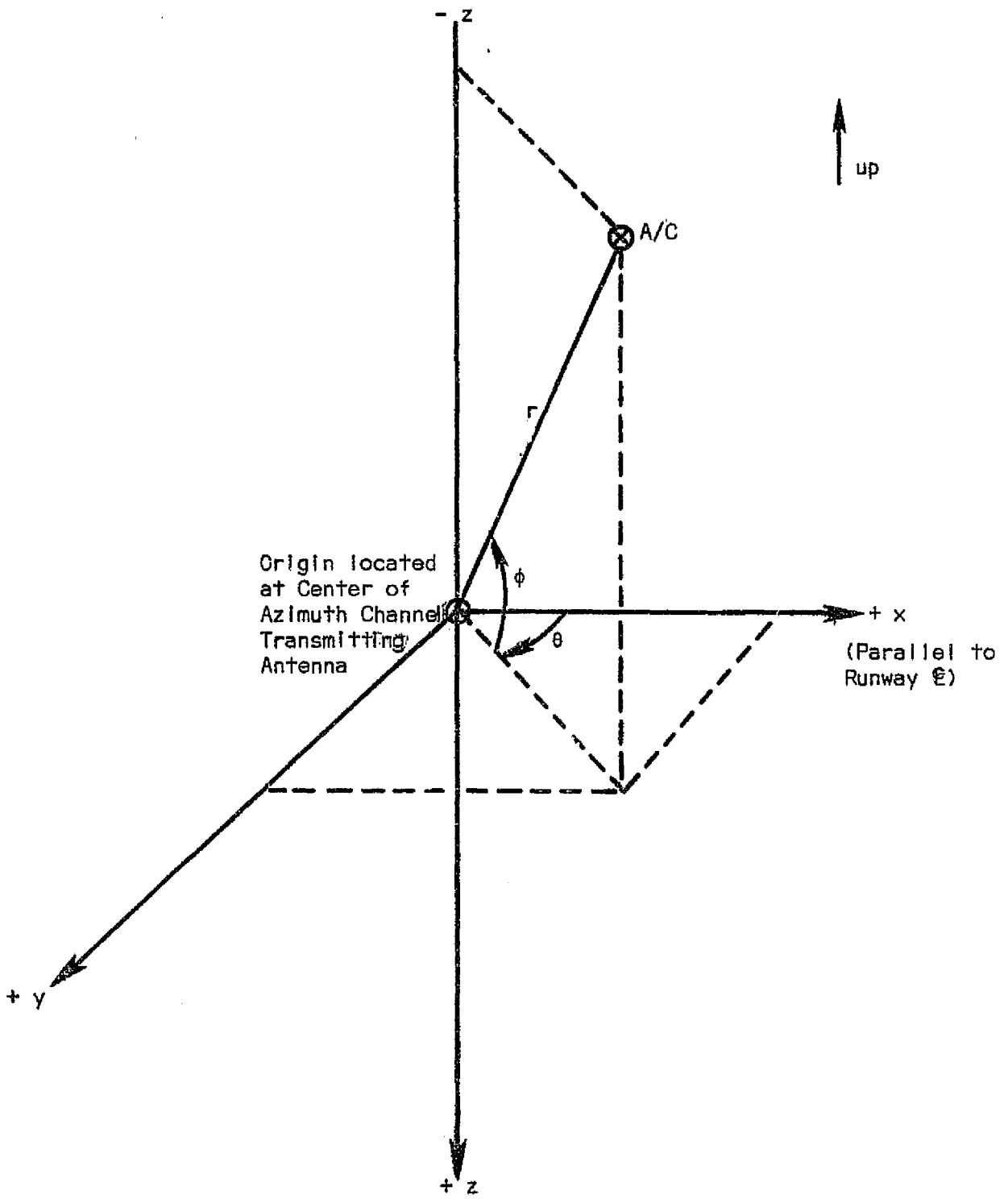


Figure 11-1 Coordinate System

then $\theta_A(\cdot)$ is specifically defined by the antenna scanning motion as a function of its argument on the interval $[t_k, t_k + T]$.

The coordinates of the receiver (the A/C) at time t are $r(t)$, $\theta(t)$, $\phi(t)$. A direct-path-signal event arriving at the A/C at time t is one that necessarily left the transmitting antenna at time $t - \frac{r(t)}{c}$, where c is the propagation velocity of light. Hence, the component of the received signal observed at time t and due to transmitter emissions derives from transmission occurring when $t_k \leq t - \frac{r(t)}{c} \leq t_k + T$. This component itself comprises two contributions $y_D(t)$, $y_R(t)$, as follows, due respectively to direct-path and reflection-path propagation:

$$y_D(t) = \alpha(t) p [\theta_A(t - \frac{r(t)}{c}) - \theta(t)] \cos[\omega_c(t - \frac{r(t)}{c}) + \beta_D] \quad (2-5)$$

$$y_R(t) = \sum_i y_{R_i}(t) \quad (2-6)$$

where

$$y_{R_i}(t) = \alpha_i(t) p [\theta_A(t - \frac{r_{T_i}(t)}{c}) - \theta_{R_i}(t)] \cos[\omega_c(t - \frac{r_{T_i}(t)}{c}) + \beta_{R_i}] \quad (2-7)$$

and

$$\alpha(t), \beta_D = \text{amplitude and phase of the direct path component} \quad (2-8)$$

$$\omega_c = \text{radian frequency of propagating r-f energy} \quad (2-9)$$

$$r_{T_i}(t), \theta_{R_i}(t) = \text{range thru and azimuth of the } i\text{th reflection point} \quad (2-10)$$

$$\alpha_i(t), \beta_{R_i} = \text{amplitude and phase of the component reflected by the } i\text{th reflection point (where, for each } i, \alpha_i(t) = 0, \text{ if } t - \frac{r_{T_i}(t)}{c} < t_k). \quad (2-11)$$

Under the assumption of isotropic reflection at the i th reflection point, located at $r_{T_i}(t)$, $\theta_{R_i}(t)$, $\phi_{R_i}(t)$, the range through reflection, $r_{T_i}(t)$, is easily shown (see Figure 11-2) to be

$$r_{T_i}(t) = r_{R_i}(t) + r_{AR_i}(t) \quad (2-12)$$

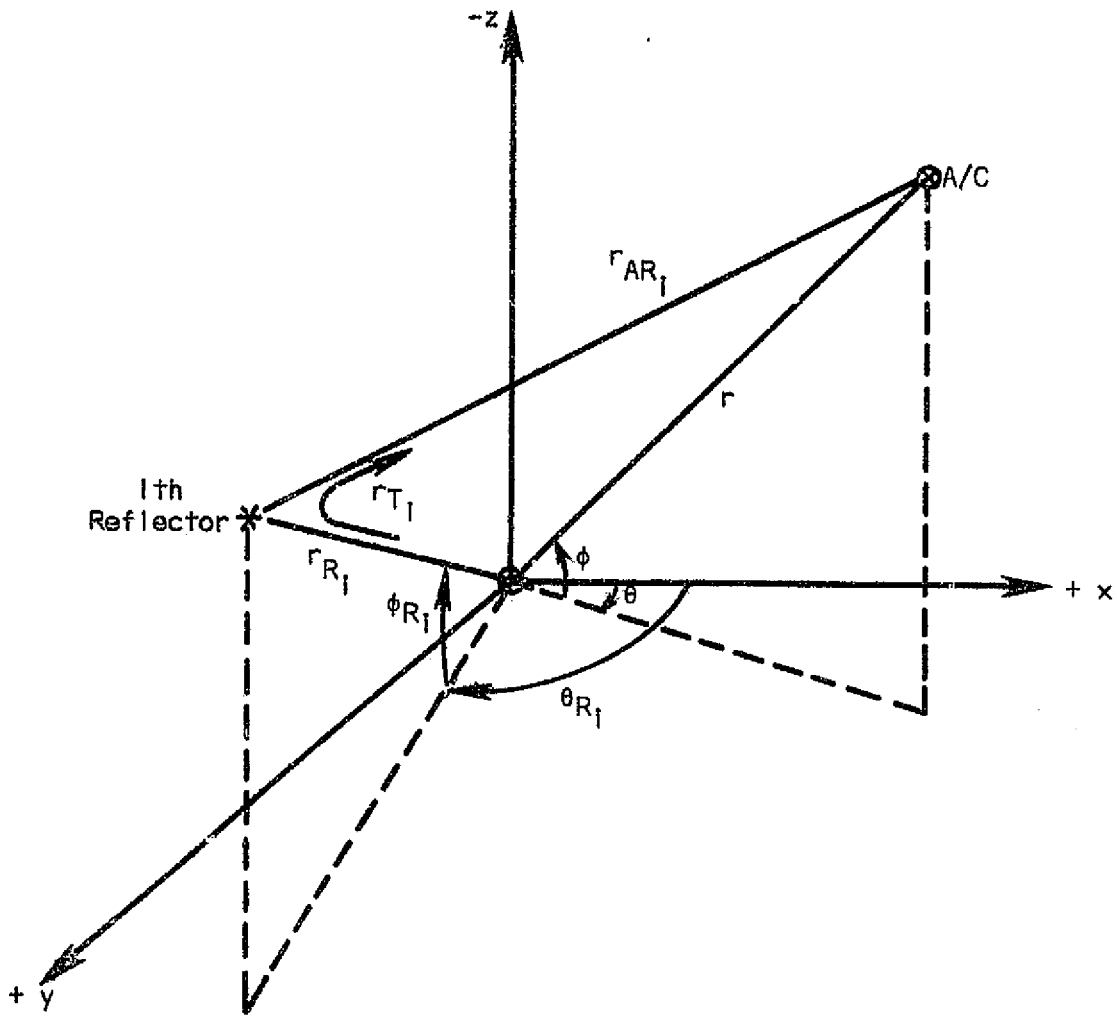


Figure 11-2 Reflection Geometry

where

$$r_{AR_i}(t) = [r^2(t) - 2r(t)r_{R_i}(t)\zeta(t) + r_{R_i}^2(t)]^{1/2} \quad (2-13)$$

and

$$\zeta(t) = \cos\phi(t) \cos\phi_{R_i}(t) \cos[\theta(t) - \theta_{R_i}(t)] + \sin\phi(t) \sin\phi_{R_i}(t) \quad (2-14)$$

In view of the generally independent motions of the A/C and a reflector, the equations (2-7) and (2-12) through (2-14) are clearly approximations. A more exact expression for, say t_x , the time of transmission, given receipt at time t (i.e., t_x would be the argument of $\theta_A(\)$ in $y_{R_i}(t)$ generally) would have the form

$$t_x = t - \frac{r_{AR_i}(t)}{c} - \frac{r_{R_i}}{c} \left(t - \frac{r_{AR_i}(t)}{c} \right), \quad (2-14a)$$

based on an argument similar to that preceding (2-5) above. On the basis of the linear approximation

$$r_{R_i} \left(t - \frac{r_{AR_i}(t)}{c} \right) = r_{R_i}(t) - \dot{r}_{R_i}(t) \frac{r_{AR_i}(t)}{c}$$

the expression for t_x becomes

$$\begin{aligned} t_x &= t - \frac{r_{AR_i}(t)}{c} - \frac{r_{R_i}(t)}{c} + \frac{\dot{r}_{R_i}(t)r_{AR_i}(t)}{c^2} \\ &= t - \frac{r_{T_i}(t)}{c} + \frac{\dot{r}_{R_i}(t)r_{AR_i}(t)}{c^2} \end{aligned}$$

The original approximation for t_x (in (2-7)) results when the term $\dot{r}_{R_i} r_{AR_i} / c^2$ is dropped, which seems reasonable under the circumstances.

In the strict sense the expression in (2-14a) does not give the exact value for t_x , but is adequate to show the approximate magnitude of error in the original approximation (in (2-7)).

The basic model has now been presented in terms of a number of parameters potentially time-varying within a scan interval in an unspecified manner. The update rate of the MLS (13.3 Hz in Azimuth) is sufficiently high relative to the dynamics of the environment to allow simple approximations for these parametric functions within a scan interval. For $t_k \leq t \leq t_{k+1}$ (which contains the kth scan interval, $t_k \leq t - \frac{r(t)}{c} \leq t_k + T$, at the A/C), the approximations used are the following, which seem reasonable:

$$\alpha(t) \approx \alpha(t_k) \quad (2-15)$$

$$\theta(t) \approx \theta(t_k) \quad (2-16)$$

$$r(t) \approx r(t_k) + \dot{r}(t_k)[t - t_k] \quad (2-17)$$

$$\alpha_i(t) \approx \alpha_i(t_k) \quad (2-18)$$

$$\theta_{R_i}(t) \approx \theta_{R_i}(t_k) \quad (2-19)$$

$$r_{T_i}(t) \approx r_{T_i}(t_k) + \dot{r}_{T_i}(t_k)[t - t_k] \quad (2-20)$$

It is emphasized these approximations are limited to a given scan. Clearly, the result in (2-12) through (2-14) generally invalidates (2-20) in any but a local sense, with $r_{T_i}(t_k)$ determined even then by (2-12) through (2-14), (and $\dot{r}_{T_i}(t_k)$ by the derivative of the expression in (2-12), as was done in the simulation study; see Section IV).

Under the assumptions (2-15) through (2-20) the received signal can be expressed in terms of a time variable local to the scan being received at the A/C. First, note that $t - \frac{r(t)}{c}$, the argument of $\theta_A(\cdot)$ in the received direct path component, $y_D(t)$, (2-5), as a direct result of (2-17), can be written as

$$t - \frac{r(t)}{c} = t \left(1 - \frac{\dot{r}(t_k)}{c}\right) - \frac{r(t_k)}{c} + t_k \frac{\dot{r}(t_k)}{c} \quad (2-21)$$

Consequently, the "received scan interval," defined heretofore by $t_k \leq t - \frac{r(t)}{c} \leq t_k + T$, can be described as follows:

$$\left(t_k + \frac{r(t_k)/c}{1 - \dot{r}(t_k)/c} \right) \leq t \leq \left(t_k + \frac{r(t_k)/c}{1 - \dot{r}(t_k)/c} \right) + \frac{T}{1 - \dot{r}(t_k)/c} \quad (2-22)$$

and thus on the k th scan interval we may write in general

$$t = \left(t_k + \frac{r(t_k)/c}{1 - \dot{r}(t_k)/c} \right) + \tau = t_{Rk} + \tau \quad (2-23)$$

where τ is a local time variable on the k th received scan interval, varying as follows:

$$0 \leq \tau \leq \frac{T}{1 - \dot{r}(t_k)/c} \quad (2-24)$$

with the same scaling as t , i.e., $dt/d\tau = 1$. (note a change in the duration of the received scan period in (2-22) and (2-24) due to A/C motion). The quantity

$$t_{Rk} \triangleq t_k + \frac{r(t_k)/c}{1 - \dot{r}(t_k)/c} \quad (2-25)$$

is the time of reception at the A/C of a signal event transmitted at time t_k , in particular the start of the k th scan. Errors in determining the arrival of this event at the A/C translate into errors in starting the local τ -clock. It is the function of the Barker code, however, to keep these errors small.

As a consequence of the above development

$$t - \frac{r(t)}{c} = t_k + \left(1 - \frac{\dot{r}(t_k)}{c} \right) \tau, \quad (2-26)$$

and, using approximations (2-15) and (2-16), the direct path component y_D can be redefined as a function of a global discrete-time variable t_k and a local continuous-time variable τ , as follows:

$$y_D(t_k, \tau) = \alpha(t_k) p[\theta_A(t_k + \tau) - \theta(t_k)] \cos[\omega_0(t_k)\tau + \beta(t_k)] \quad (2-27)$$

In which the $-\dot{r}(t_k)\tau/c$ term of (2-26) has been dropped from the argument of $\theta_A(\cdot)$ because of its relative insignificance, and $\omega_0(t_k)$, $\beta(t_k)$ are defined as follows:

$$\omega_0(t_k) \triangleq \begin{cases} \omega_c(1 - \dot{r}(t_k)/c), & \text{as the apparent r-f carrier frequency} & (2-28a) \\ \omega_{IF} - \omega_c \dot{r}(t_k)/c, & \text{as the apparent i-f carrier frequency} & (2-28b) \end{cases}$$

$$\beta(t_k) = \beta_D + \omega_c t_k, \text{ initial phase on the } k\text{th scan period} \quad (2-29)$$

The expected doppler shift (neglecting relativity) is present in (2-28).

The phase parameter β_D in (2-5) and (2-8) was modeled originally as an independent random variable uniformly distributed on $[-\pi, \pi]$. Equation (2-29) above for $\beta(t_k)$ suggests that $\beta(t_k)$ then is also a random variable but one possibly highly correlated with β_D . As a practical matter, however, the increment $\omega_c(t_k - t_{k-1})$ is a large multiple of 2π radians and can never be determined accurately enough to make valid use of the correlation implied by (2-29) above, for two reasons:

1. The t_k are determined from the Barker decoder output via (2-25), and with a noisy input the uncertainty may become a significant part of a bit pulse width (approximately 67 μ s, also many periods of the 5000 MHz r-f carrier).
2. The quantity $t_k - t_{k-1}$ is not constant from scan-to-scan, and may even be jittered to suppress propeller modulation effects.

On this basis the $\beta(t_k)$ also were modeled as independent random variables uniformly distributed on $[-\pi, \pi]$, which seems reasonable.

The i th reflection component, $y_{R_i}(t)$, (2-7), can also be expressed in terms of the local receiver time variable τ , associated above with the direct path signal. Under the approximation of $r_{T_i}(t)$, (2-20), we may write

$$t - \frac{r_{T_i}(t)}{c} = t \left(1 - \frac{\dot{r}_{T_i}(t_k)}{c} \right) - \frac{r_{T_i}(t_k)}{c} + t_k \frac{\dot{r}(t_k)}{c} \quad (2-30)$$

Substituting from (2-33) for t and (2-25) for t_{R_k} gives

$$t - \frac{r_{T_i}(t)}{c} = t_{R_k} - \frac{r_{T_i}(t_{R_k})}{c} + \tau(1 - \dot{r}_{T_i}(t_k)/c) \quad (2-31)$$

$$= t_k - \frac{\Delta r_i(t_k)}{c} - \frac{\Delta \dot{r}_i(t_k)}{c} \cdot \frac{r(t_k)/c}{1 - \dot{r}(t_k)/c} + \tau(1 - \dot{r}_{T_i}(t_k)/c) \quad (2-32)$$

where, in general

$$\Delta r_i(t) \triangleq r_{T_i}(t) - r(t) \quad (2-33)$$

$$\Delta \dot{r}_i(t) \triangleq \dot{r}_{T_i}(t) - \dot{r}(t) \quad (2-34)$$

Scan data is received through the reflection path, clearly, when

$$\tau \geq \frac{1}{1 - \dot{r}(t_k)/c} \left[\frac{\Delta r_i(t_k)}{c} + \left(\frac{\Delta \dot{r}_i(t_k)}{c} \right) \left(\frac{r(t_k)/c}{1 - \dot{r}(t_k)/c} \right) \right] = \frac{\Delta r_i(t_k)}{c} \quad (2-34a)$$

Neither of the terms involving the time derivatives $\Delta \dot{r}_i(t_k)$ and $\dot{r}_{T_i}(t_k)$ in (2-32) is important in the argument of $\theta_A(\cdot)$, hence, using the approximations (2-18, 2-19) for $\alpha_i(t)$, $\theta_{R_i}(t)$ respectively, the i th reflection component y_{R_i} can be redefined with bivariate argument (t_k, τ) as follows, for $0 \leq \tau \leq \frac{T}{1 - \dot{r}(t_k)/c}$:

$$y_{R_i}(t_k, \tau) = \begin{cases} \alpha_i(t_k) p \left[\theta_A \left(t_k + \tau - \frac{\Delta r_i(t_k)}{c} \right) - \theta_{R_i}(t_k) \right] \\ \cos[\omega_{0_i}(t_k)\tau + \beta_i(t_k)], & \frac{\Delta r_i(t_k)}{c} \leq \tau \leq \frac{T}{1 - \dot{r}(t_k)/c} \\ 0, & 0 \leq \tau < \Delta r_i(t_k)/c \end{cases} \quad (2-35a)$$

$$(2-35b)$$

where

$$\omega_{0_i}(t_k) = \begin{cases} \omega_c (1 - \dot{r}_{T_i}(t_k)/c), & \text{as r-f carrier frequency} \\ \omega_{IF} - \omega_c \dot{r}_{T_i}(t_k)/c, & \text{as i-f carrier frequency} \end{cases} \quad (2-36a)$$

$$(2-36b)$$

$$\beta_i(t_k) = \beta_{R_i} + \omega_c [t_{R_k} - r_{T_i}(t_{R_k})/c] \quad (2-37)$$

$$= \beta_{R_i} + \omega_c \left[t_k - \frac{\Delta r_i(t_{R_k})}{c} \right] \quad (2-37a)$$

$$= \beta_{R_i} + \omega_c \left[t_k - \frac{\Delta r_i(t_k)}{c} + \frac{\Delta \dot{r}_i(t_k)}{c} \cdot \frac{r(t_k)/c}{1 - \dot{r}(t_k)/c} \right] \quad (2-37b)$$

A more compact form of (2-35), which will be useful, employs a bivariate argument in α_i , as follows:

$$Y_{R_i}(t_k, \tau) = \alpha_i(t_k, \tau) p \left[\theta_A \left(t_k + \tau - \frac{\Delta r_i(t_k)}{c} \right) - \theta_{R_i}(t_k) \right] \cos[\omega_{0_i}(t_k)\tau + \beta_i(t_k)] \quad (2-38)$$

where

$$\alpha_i(t_k, \tau) = \begin{cases} \alpha_i(t_k), & \Delta r_i(t_k)/c \leq \tau \leq \frac{T}{1 - \dot{r}(t_k)/c} \\ 0, & 0 \leq \tau < \Delta r_i(t_k)/c \end{cases} \quad (2-39a)$$

$$(2-39b)$$

It was established, following equation (2-29) for the $\beta(t_k)$ in the direct path component, that the $\beta(t_k)$ were independent random variables. The $\beta(t_k)$, however, are functions of properties of the transmitted signal which the $\beta_i(t_k)$ in the reflection components share. For each i , the initial value of $\beta_i(t_k)$, say $\beta_i(t_1)$, was modeled as an independent random variable uniformly distributed on $[-\pi, \pi]$, but as a consequence of the above, it was felt that the scan-to-scan change in β_i , e.g., $\beta_i(t_{k+1}) - \beta_i(t_k)$, should be related to the corresponding change in β , i.e. $\beta(t_{k+1}) - \beta(t_k)$. Use of (2-29) and (2-37) gave the relations

$$[\beta_i(t_{k+1}) - \beta_i(t_k)] = [\beta(t_{k+1}) - \beta(t_k)] - \frac{\omega_c}{c} [\Delta r_i(t_{R_{k+1}}) - \Delta r_i(t_{R_k})] \quad (2-40)$$

$$= [\beta(t_{k+1}) - \beta(t_k)] - \frac{\omega_c}{c} (t_{k+1} - t_k) \Delta \dot{r}_i(t_k) \quad (2-40a)$$

in the latter of which relatively insignificant terms corresponding to

the last in (2-37b) were dropped. In the simulation this relation assured the smooth evolution of the simulated multipath interference phenomena.

Specializing more concretely now to the signal in the (linear) i-f channel of the receiver, where the total signal, y , comprises direct path, reflection path and receiver noise components, we assume the i-f bandpass characteristic is appropriately symmetrical about the nominal bandcenter frequency, ω_{IF} . The noise then, a process generated at the receiver and hence modeled with sample function $n(\tau)$, is assumed to be a stationary, bandpass, zero-mean Gaussian process with variance σ_n^2 . A quadrature expansion of the noise $n(\tau)$ is possible, therefore, and the following formulation of the composite signal y with bivariate argument (t_k, τ) results:

$$y(t_k, \tau) = y_D(t_k, \tau) + y_R(t_k, \tau) + n(\tau) \quad (2-41)$$

where

$$y_D(t_k, \tau) = \alpha(t_k) p [\theta_A(t_k + \tau) - \theta(t_k)] \cos[\omega_{IF}\tau + (\beta(t_k) - \omega_c \tau \dot{r}(t_k)/c)] \quad (2-42)$$

$$= y_{D_C}(t_k, \tau) \cos \omega_{IF}\tau - y_{D_S}(t_k, \tau) \sin \omega_{IF}\tau \quad (2-43)$$

$$y_R(t_k, \tau) = \sum_i \alpha_i(t_k, \tau) p [\theta_A(t_k + \tau - \frac{\Delta r_i(t_k)}{c}) - \theta_{R_i}(t_k)] \cos[\omega_{IF}\tau + (\beta_i(t_k) - \omega_c \tau \dot{r}_{T_i}(t_k)/c)] \quad (2-44)$$

$$= y_{R_C}(t_k, \tau) \cos \omega_{IF}\tau - y_{R_S}(t_k, \tau) \sin \omega_{IF}\tau \quad (2-45)$$

$$n(\tau) = n_C(\tau) \cos \omega_{IF}\tau - n_S(\tau) \sin \omega_{IF}\tau \quad (2-46)$$

in which

$$y_{D_C}(t_k, \tau) = \alpha(t_k) p [\theta_A(t_k + \tau) - \theta(t_k)] \cos[\beta(t_k) - \omega_c \tau \dot{r}(t_k)/c] \quad (2-47)$$

$$y_{D_S}^i(t_k, \tau) = \alpha(t_k) p[\theta_A(t_k + \tau) - \theta(t_k)] \sin[\beta(t_n) - \omega_c \tau \dot{r}(t_k)/c] \quad (2-48)$$

$$y_{R_C}^i(t_k, \tau) = \sum_i \alpha_i(t_k, \tau) p[\theta_A(t_k + \tau - \frac{\Delta r_i(t_k)}{c}) - \theta_{R_i}(t_k)] \cos[\beta_i(t_k) - \omega_c \tau \dot{r}_{T_i}(t_k)/c] \quad (2-49)$$

$$y_{R_S}^i(t_k, \tau) = \sum_i \alpha_i(t_k, \tau) p[\theta_A(t_k + \tau - \frac{\Delta r_i(t_k)}{c}) - \theta_{R_i}(t_k)] \sin[\beta_i(t_k) - \omega_c \tau \dot{r}_{T_i}(t_k)/c] \quad (2-50)$$

and

$n_c(\tau)$, $n_s(\tau)$, the quadrature components of the noise, are independent, stationary low-pass Gaussian processes, each with mean zero, variance σ_n^2 , and two-sided bandwidth equal to the i-f bandwidth. (2-51)

Hence

$$y(t_k, \tau) = m_C(t_k, \tau) \cos \omega_{IF} \tau - m_S(t_k, \tau) \sin \omega_{IF} \tau \quad (2-52)$$

$$= M(t_k, \tau) \cos[\omega_{IF} \tau - \Gamma(t_k, \tau)] \quad (2-53)$$

where

$$m_C(t_k, \tau) = y_{D_C}^i(t_k, \tau) + y_{R_C}^i(t_k, \tau) + n_C(\tau) \quad (2-54)$$

$$m_S(t_k, \tau) = y_{D_S}^i(t_k, \tau) + y_{R_S}^i(t_k, \tau) + n_S(\tau) \quad (2-55)$$

$$M(t_k, \tau) = \sqrt{m_C^2(t_k, \tau) + m_S^2(t_k, \tau)} \quad (2-56)$$

$$\Gamma(t_k, \tau) = \arctan[m_S(t_k, \tau)/m_C(t_k, \tau)] \quad (2-57)$$

The principal signal modeling results to date have been presented. These results have been used in the digital simulation studies described in Chapter IV and in the optimal receiver design analysis of Chapter III. In the simulation the local time variable τ was discretized, of course, a sampling rate equal to the i-f bandwidth (160 kHz) being chosen.

Other small refinements, such as dropping certain i/c terms, etc., were made also where permissible; reference is made to Chapter IV for a more detailed description of the simulation study.

The optimal design studies undertaken to date and reported in Chapter III were specialized to a signal model involving only the direct-path and receiver noise components. This initial focus on the multipath-free case was justified on several counts:

1. The study establishes for reference purposes the optimum level of performance obtainable in a multipath-free environment.
2. It provides insight into the structural properties of MLS receivers resulting from the requirement for optimal performance in a very basic and generally applicable disruptive environment.
3. The algorithms that result under this specialization represent lower bounds in computational complexity in relation to those optimal processors associated with the more complex environment of interest.

The first point cannot be overemphasized; the MLS receiver will operate most of the time without significant multipath interference, and its performance during such periods is not outside our concern in this study.

In re-extending our concern to the multipath-corrupted signal, the results obtained above will probably not be used directly because of the very high dimension of the parameter space associated with the total reflected signal

$$Y_R(t_k, \tau) = \sum_i Y_{R_i}(t_k, \tau) \quad (2-58)$$

where Y_{R_i} is given in equation (2-38). Instead a stochastic process model (really a random field model) with associated sample function $Y_R(t_k, \tau)$ is being considered. This is done in conjunction with considerations of the estimation algorithm to be used, since the statistics of interest

depend to some extent on the latter. Second-order statistics on the scan interval and local to the arrival time of the direct-path pulse are expected to be important; variations of these statistics with t_k are the basis for an adaptive approach to the suppression of multipath interference. If first- and second-order statistics turn out to be sufficient, a unique Gaussian random field model is implied and the possibility of an adaptive algorithm of manageable dimensions.

Lastly, a state-variable model is needed as a prerequisite to the application of modern recursive estimation techniques to this problem. Such a model generally would describe the (short-term) evolution of the A/C angular coordinate and other parameters of interest and relate these to the observed receiver signal. In the desired model the "state" should include the A/C angular coordinate, of course, but also all unknown parameters whose estimates are needed for use in the angular coordinate estimate calculation. In the locally optimum estimation scheme to be described in Chapter III, for example, the latter parameter set included the signal strength parameter $\alpha(t)$ and the apparent i-f carrier frequency $\omega_0(t)$ (Note: the latter estimate may not be needed if the nominal i-f carrier frequency is sufficiently great with respect to the doppler shift (which is about 800 Hz/100 kts speed, for a 5000 MHz r-f carrier frequency)). In addition, in an adaptive design an "augmented state" may appear and include some parameters associated with evolution of the "state-proper," thus allowing some estimation of the model as well as the variables of prime interest. The forms of models needed in the recursive estimation study will be determined later when recursive estimation algorithms are considered in greater detail.

CHAPTER III

OPTIMAL MLS RECEIVER DESIGN

Under the optimal tracking criterion two approaches to receiver design were considered:

1. Locally optimum estimation [3] in which it is assumed the tracking error is always small and constant on the interval of observation (the scan interval), and thus can be estimated as a parameter without requiring a knowledge of the a priori statistics of the A/C angular coordinate of interest.
2. Recursive state estimation [4, Chapters 7,8,and 9] in which a state space model is assumed and used to provide smoothing of the evolving estimates and also extrapolation into and possible through periods of signal fade.

Quadrature detection of the I-F signal arises in these algorithms, and to preserve the option for analog implementation of these stages continuous-time formulations were used mostly. The principal signal model used in the initial studies was the direct-path-component-plus-noise specialization.

Locally Optimum Estimation [3]

In this formulation the received signal on the present scan interval is modeled as an observations process $\{y(t), t \in [0, T]\}$ with sample function of the general form

$$y(t) = s(t, mte, a) + n(t), \quad t \in [0, T] \quad (3-1)$$

where

$$t = \text{local receiver time on the present scan interval} \quad (3-2)$$

$$[0, T] = \text{the present scan interval wrt local receiver time} \quad (3-3)$$

$s(t, \cdot, \cdot) =$ a sample function of a process or a sure function with which the modulation or parameter of interest is associated. (3-4)

$n(t) =$ a sample function of a white Gaussian noise process $\{n(t), t \in [0, T]\}$ with known power density N_0 . (3-5)

$mte =$ true present value of the unknown parameter (or parameter vector)

to be estimated, assumed constant for $t \in [0, T]$ (3-6)

m = estimate of the unknown parameter, based on observations through the last, but not the present, scan interval (possible extrapolated to the present, however) (3-7)

e = error in the last estimate, m (3-8)

a = a random parameter (or parameter vector) in which we have no estimation interest (3-9)

To avoid technical difficulty with mathematical processing of white noise the integrated observations process $\{Y(t), t \in [0, T]\}$ is considered instead of $\{y(t), t \in [0, T]\}$, where

$$Y(t) = \int_0^t s(\tau, m+e, a) d\tau + N(t) \quad (3-10)$$

and $N(t)$ is a Wiener process for which

$$\langle N(t)N(\tau) \rangle = N_0 \min(t, \tau) \quad (3-11)$$

(and where $\langle \rangle$ denotes mathematical expectation).

The objective is to estimate the (unobservable) error e and to refine the parameter estimate m using the error estimate. Following Murphy [3], probability measures relevant to this objective in a locally optimum estimation context are the following:

$$Q = \text{measure corresponding to } \{N(t), t \in [0, T]\} \quad (3-12)$$

$$S = \text{measure corresponding to } \{s(t, m+e, a), t \in [0, T]\} \quad (3-13)$$

$$Y_S = \text{measure corresponding to } \{Y(t), t \in [0, T] | s\} \quad (3-14)$$

$$P_e = \text{measure corresponding to } \{Y(t), t \in [0, T]\} \quad (3-15)$$

An estimate \hat{e} of e is said to be locally optimum [3] at $e = e_0$ if two conditions, stated below, are satisfied; all integrations are taken over the underlying elementary event space (universe), denoted Ω :

1.) The estimate \hat{e} is locally unbiased at e_0 , i.e.,

$$a) \int_{\Omega} (\hat{e} - e_0) dP_{e_0} = 0 \text{ (a vector), and} \quad (3-16)$$

$$b) \frac{\partial}{\partial e} \int_{\Omega} (e - e_0)^T dP_{e_0} = I (\text{the unity matrix}), \quad (3-17)$$

where $()^T$ denotes the transpose of $()$.

- 2.) The estimate \hat{e} has minimum mean square error among all locally unbiased estimates of e at e_0 , i.e. if $\hat{\sigma}$ is any estimate of e locally unbiased at e_0 , then

$$\int (\hat{e} - e_0)(\hat{e} - e_0)^T dP_{e_0} \leq \int (\hat{\sigma} - e_0)(\hat{\sigma} - e_0)^T dP_{e_0} \quad (3-18)$$

in the sense of the usual "weak" order relation on a set of non-negative definite square matrices of the same dimension.

Murphy [3] has shown that the locally optimum estimate \hat{e} of e at $e = 0$ is given by

$$\hat{e} = \Phi_0^{-1} \Lambda_0(Y) \quad (3-19)$$

where Λ_0 is the vector whose i th component, Λ_{0_i} , is given by

$$\Lambda_{0_i}(Y) = \begin{cases} \frac{\partial}{\partial e_i} \ln \left(\frac{dP_e}{dQ} \right) \Big|_{e=0}, & \text{if } \frac{dP_e}{dQ} \neq 0 \\ 0, & \text{otherwise} \end{cases} \quad (3-20)$$

and

$$\Phi_0 = \int_{\Omega} \Lambda_0(Y_0) \Lambda_0^T(Y_0) dP_0 \quad (3-21)$$

in which Y_0 is given by (3-10) with $e = 0$. If $e = 0$, the residual mean square error (i.e., the error covariance matrix) associated with this estimate is Φ_0^{-1} , that is

$$\int_{\Omega} \hat{e} \hat{e}^T dP_0 = \Phi_0^{-1} \quad (3-22)$$

Radon-Nikodym derivatives associated with this estimate are the following:

$$\frac{dY_s}{dQ} = \exp \left(\frac{1}{N_0} \int_0^T s(t, m+e, a) dY(t) - \frac{1}{2N_0} \int_0^T s^2(t, m+e, a) dt \right) \quad (3-23)$$

(the first integral above being a Wiener integral) and

$$\frac{dP_e}{dQ} = \int \frac{dY_s}{dQ} S(ds), \quad (3-24)$$

this latter integral being taken over the space of realizations of $\{s(t, m+e, a), t \in [0, T]\}$. When $s(t, m+e, a) = s(t, m+e)$, i.e. is deterministic, then S is degenerate, i.e., there exists a realization of the process $\{s(t, m+e), t \in [0, T]\}$ such that $S(\{s\}) = 1$, in which case $\frac{dP_e}{dQ} = \frac{dY_s}{dQ}$. Another special case of interest is when $s(t, m+e, a)$ is a deterministic function of random parameter a , which ranges on the reals, R_1 , with induced probability measure P . Then the collection of realizations of the process $\{s(t, m+e, a), t \in [0, T]\}$ is indexed by $a \in R_1$, and we may write

$$\frac{dP_e}{dQ} = \int_{R_1} \frac{dY_s(t, m+e, a)}{dQ} P(da) \quad (3-25)$$

where $dY_s(t, m+e, a)/dQ$ denotes the form in (3-23) with the functional form of $s(t, m+e, a)$ substituted as required. If μ is Lebesgue measure on R_1 and P is absolutely continuous with respect to μ , then we may also write

$$\frac{dP_e}{dQ} = \int_{R_1} \frac{dY_s(t, m+e, a)}{dQ} \frac{dP}{d\mu}(a) d\mu(a) \quad (3-26)$$

where $\frac{dP}{d\mu}(a)$ is the probability density of the random variable a .

Application of locally optimum estimation to the MLS receiver design problem, specialized to the direct-path-signal-plus-noise case, is made by letting $s = y_D$, i.e., referring to (2-27),

$$s(t, m+e, a) = \alpha p[\theta_A(t) - \theta] \cos[\omega_0 t + \beta], \quad t \in [0, T] \quad (3-27)$$

and making the associations

$$m+e = \begin{pmatrix} \theta \\ \alpha \\ \omega_0 \end{pmatrix} \quad (3-28)$$

$$a = \beta \quad (3-29)$$

It is illuminating to regard β as a known parameter temporarily and regard $s(\cdot)$ as a "sure" function of t and the parameters θ , α , ω_0 . In this case, as explained following (3-24), the measure S is degenerate and

$$\frac{dP_e}{dQ} = \frac{dY_s(\cdot)}{dQ} = \exp\left[\frac{\alpha}{N_0} \int_0^T p[\theta_A(t) - \theta] \cos[\omega_0 t + \beta] dY(t) - \frac{\alpha^2}{4N_0} q_1(\theta)\right] \quad (3-30)$$

where

$$q_1(\theta) \triangleq 2 \int_0^T p^2[\theta_A(t) - \theta] \cos^2[\omega_0 t + \beta] dt \quad (3-31)$$

$$= \int_0^T p^2[\theta_A(t) - \theta] dt \quad (3-32)$$

Then, from (3-20)

$$\Lambda_0(Y) = \frac{1}{N_0} \begin{pmatrix} -\hat{\alpha} \int_0^T p[\theta_A(t) - \hat{\theta}] \cos[\hat{\omega}_0 t + \beta] dY(t) - \frac{\hat{\alpha}^2}{4} \hat{q}_1(\hat{\theta}) \\ \int_0^T p[\theta_A(t) - \hat{\theta}] \cos[\hat{\omega}_0 t + \beta] dY(t) - \frac{\hat{\alpha}}{2} q_1(\hat{\theta}) \\ -\hat{\alpha} \int_0^T p[\theta_A(t) - \hat{\theta}] t \sin[\hat{\omega}_0 t + \beta] dY(t) \end{pmatrix} \quad (3-33)$$

where

$$\hat{\theta}, \hat{\alpha}, \hat{\omega}_0 \text{ are last estimates, corresponding to } m \quad (3-34)$$

$$\hat{p}(\theta_A(t) - \hat{\theta}) \triangleq \left. \frac{dp(\theta_e)}{d\theta_e} \right|_{\theta_e = (\theta_A(t) - \hat{\theta})} \quad (3-35)$$

$$\hat{q}_1(\hat{\theta}) \triangleq \frac{dq_1(\hat{\theta})}{d\hat{\theta}} = -2 \int_0^T p[\theta_A(t) - \hat{\theta}] \hat{p}[\theta_A(t) - \hat{\theta}] dt. \quad (3-36)$$

The last quantity, $\hat{q}_1(\hat{\theta})$, is very nearly zero (hence $q_1(\hat{\theta})$ is very nearly a constant), except when $\hat{\theta}$ is near the ends of the interval of coverage, e.g. $(-60^\circ, +60^\circ)$ for azimuth. To an extent the bivariate nature of $p(\cdot)$, i.e. the channel-cross-coupling effect discussed following (2-2),

also affects the functions $q_1(\cdot)$ and $\dot{q}_1(\cdot)$. Under the assumption these combined effects are negligible, the approximations

$$q_1(\hat{\theta}) = \text{constant} (= \int_0^T p^2[\theta_A(t)] dt) \quad (3-37)$$

$$\dot{q}_1(\hat{\theta}) = 0 \quad (3-38)$$

are made with the result that

$$\Lambda_0(Y_0) = \frac{1}{N_0} \int_0^T M dN(t) \quad (3-39)$$

where

$$M = \begin{pmatrix} -\hat{\alpha} \dot{p}[\theta_A(t) - \hat{\theta}] \cos[\hat{\omega}_0 t + \beta] \\ p[\theta_A(t) - \hat{\theta}] \cos[\hat{\omega}_0 t + \beta] \\ -\hat{\alpha} t p[\theta_A(t) - \hat{\theta}] \sin[\hat{\omega}_0 t + \beta] \end{pmatrix} \quad (3-40)$$

The result (3-39) follows from setting $e = 0$ in $Y(t)$ in (3-10) and then substituting the resulting Y_0 into (3-33) and simplifying.

The above implies, then, by (3-21) that

$$\Phi_0 = \frac{1}{N_0^2} \int_{\Omega} \left[\int_0^T M dN(t) \right] \left[\int_0^T M^T dN(t) \right] dP_0 \quad (3-41)$$

$$= \frac{1}{N_0^2} \left\langle \left[\int_0^T M dN(t) \right] \left[\int_0^T M^T dN(t) \right] \right\rangle \quad (3-42)$$

which, since $\{N(t), t \in [0, T]\}$ is a Wiener process with $\langle N(t), N(\tau) \rangle$ as given in (3-11), can be written

$$\Phi_0 = \frac{1}{N_0} \int_0^T M M^T dt \quad (3-43)$$

Substitution from (3-40) and use of some trigonometric identities (and some nearly obvious notational shorthand) gives

$$\Phi_0 = \frac{1}{N_0} \int_0^T \begin{pmatrix} \hat{\alpha}^2 \dot{p}^2 \left(\frac{1 + \cos 2[\]}{2} \right) & -\hat{\alpha} \dot{p} \left(\frac{1 + \cos 2[\]}{2} \right) & \hat{\alpha}^2 t \dot{p} \left(\frac{\sin 2[\]}{2} \right) \\ -\hat{\alpha} \dot{p} \left(\frac{1 + \cos 2[\]}{2} \right) & p^2 \left(\frac{1 + \cos 2[\]}{2} \right) & -\hat{\alpha} t p^2 \left(\frac{\sin 2[\]}{2} \right) \\ \hat{\alpha}^2 t \dot{p} \left(\frac{\sin 2[\]}{2} \right) & -\hat{\alpha} t p^2 \left(\frac{\sin 2[\]}{2} \right) & \hat{\alpha}^2 t^2 p^2 \left(\frac{1 - \cos 2[\]}{2} \right) \end{pmatrix} dt \quad (3-44)$$

And asymptotically as $\hat{\omega}_0 \rightarrow \infty$ (or gets very large),

$$\Phi_0 \approx \frac{1}{N_0} \begin{pmatrix} \frac{\hat{\alpha}^2 q_2}{2} & 0 & 0 \\ 0 & \frac{q_1}{2} & 0 \\ 0 & 0 & \frac{\hat{\alpha}^2 q_3(\hat{\theta})}{2} \end{pmatrix} \quad (3-45)$$

where, under the approximating assumptions made,

$$q_1(\hat{\theta}) = \int_0^T p^2[\theta_A(t) - \hat{\theta}] dt \Big|_{\dot{q}_1 \approx 0} = \int_0^T p^2[\theta_A(t)] dt = q_1, \text{ a constant} \quad (3-46)$$

$$q_2(\hat{\theta}) = \int_0^T \dot{p}^2[\theta_A(t) - \hat{\theta}] dt \Big|_{\dot{q}_1 \approx 0} = \int_0^T \dot{p}^2[\theta_A(t)] dt = q_2, \text{ a constant} \quad (3-47)$$

$$q_3(\hat{\theta}) = \int p^2[\theta_A(t) - \hat{\theta}] t^2 dt \Big|_{\dot{q}_1 \approx 0} = q_1 t_{RMS}^2(\hat{\theta}). \quad (3-48)$$

Consequently, the covariance matrix, Φ_0^{-1} , for the estimation error, $\hat{e} - e_0$, is approximately

$$\Phi_0^{-1} \approx N_0 \begin{pmatrix} 2/(\hat{\alpha}^2 q_2) & 0 & 0 \\ 0 & 2/q_1 & 0 \\ 0 & 0 & 2/(\hat{\alpha}^2 q_3(\hat{\theta})) \end{pmatrix} \quad (3-49)$$

and the locally optimum estimate \hat{e} is obtained by combining (3-46) through (3-49) and (3-33) with (3-19):

$$\hat{e} = \begin{pmatrix} -\frac{2}{\hat{\alpha}q_2} \int_0^T p^*[\theta_A(t) - \hat{\theta}] \cos[\hat{\omega}_0 t + \beta] dY(t) \\ \frac{2}{q_1} \int_0^T p^*[\theta_A(t) - \hat{\theta}] \cos[\hat{\omega}_0 t + \beta] dY(t) - \hat{\alpha} \\ -\frac{2}{\hat{\alpha}q_3(\hat{\theta})} \int_0^T p^*[\theta_A(t) - \hat{\theta}] t \sin[\hat{\omega}_0 t + \beta] dY(t) \end{pmatrix} = \begin{pmatrix} \hat{e}_\theta \\ \hat{e}_\alpha \\ \hat{e}_{\omega_0} \end{pmatrix} \quad (3-50)$$

or, alternatively (recall β was assumed known)

$$\hat{e} = \begin{pmatrix} -\frac{2}{\hat{\alpha}q_2} [\cos\beta(\int_0^T p^*[\theta_A(t) - \hat{\theta}] \cos\hat{\omega}_0 t dY(t)) \\ - \sin\beta(\int_0^T p^*[\theta_A(t) - \hat{\theta}] \sin\hat{\omega}_0 t dY(t))] \\ -\hat{\alpha} + \frac{2}{q_1} [\cos\beta(\int_0^T p^*[\theta_A(t) - \hat{\theta}] \cos\hat{\omega}_0 t dY(t)) \\ - \sin\beta(\int_0^T p^*[\theta_A(t) - \hat{\theta}] \sin\hat{\omega}_0 t dY(t))] \\ -\frac{2}{\hat{\alpha}q_3(\hat{\theta})} [\cos\beta(\int_0^T p^*[\theta_A(t) - \hat{\theta}] t \sin\hat{\omega}_0 t dY(t)) \\ + \sin\beta(\int_0^T p^*[\theta_A(t) - \hat{\theta}] t \cos\hat{\omega}_0 t dY(t))] \end{pmatrix} \quad (3-51)$$

For instrumentation purposes, $dY(t)$ would be replaced with $y(t)dt$ and physical dumping integrators employed to integrate the six outputs of three weighted or gated quadrature detectors, corresponding to the above. Other significant observations that can be made include:

1. The estimator is dependent upon the prior estimate values but not the noise variance parameter, N_0 .
2. The error covariance is proportional to noise parameter N_0 , and of particular interest is the variance associated with \hat{e}_θ , the estimated A/C angular parameter:

$$\langle \hat{e}_\theta^2 \rangle = \left(\frac{2N_0}{\hat{\alpha}^2} \right) \left(\frac{1}{q_2} \right) \quad (3-52)$$

where the first factor is a measure of the ratio of noise-to-

estimated signal power, and the second factor is the reciprocal of the integral of \dot{p}^2 , given in (3-47).

3. The estimate $\hat{\alpha}$ in (3-50) involves an integral less the prior estimate of α , $\hat{\alpha}$. Hence the integral is a global estimate of α , given $y(t)$ and prior estimates of θ and ω_0 . The error covariance of the estimate is proportional to N_0 , but independent of other parameters (under the stated assumption $\dot{q}_1(\theta) \approx 0$ for all θ of interest).

Returning now to the more realistic situation in which β is regarded as a random variable uniformly distributed on the interval $[-\pi, \pi]$, as described following (2-29), we have from (3-30)

$$\begin{aligned} \frac{dY_s(t, m+e, a)}{dQ} &= \exp\left(-\frac{\alpha^2 q_1(\theta)}{4N_0}\right) \exp\left(\frac{\alpha}{N_0} \int_0^T p[\theta_A(t) - \theta] \cos[\omega_0 t + \beta] dY(t)\right) \\ &= C_e \exp\left[\frac{\alpha}{N_0} (I_{c_e}(Y) \cos \beta - I_{s_e}(Y) \sin \beta)\right] \\ &= C_e \exp\left[\frac{\alpha}{N_0} \sqrt{I_{c_e}^2(Y) + I_{s_e}^2(Y)} \cos(\beta - \arctan\left(\frac{I_{s_e}(Y)}{I_{c_e}(Y)}\right))\right] \end{aligned}$$

where

$$C_e \triangleq \exp\left(-\frac{\alpha^2 q_1(\theta)}{4N_0}\right) \quad (3-56)$$

$$I_{c_e}(Y) \triangleq \int_0^T p[\theta_A(t) - \theta] \cos \omega_0 t dY(t) \quad (3-57)$$

$$I_{s_e}(Y) \triangleq \int_0^T p[\theta_A(t) - \theta] \sin \omega_0 t dY(t) \quad (3-58)$$

and $q_1(\theta)$ is as given in (3-32). Hence from (3-26)

$$\frac{dP_e}{dQ} = \frac{C_e}{2\pi} \int_{-\pi}^{\pi} \exp\left[\frac{\alpha}{N_0} \sqrt{I_{c_e}^2 + I_{s_e}^2} \cos(\beta - \arctan\left(\frac{I_{s_e}}{I_{c_e}}\right))\right] d\beta \quad (3-59)$$

$$= C_e I_0\left(\frac{\alpha}{N_0} \sqrt{I_{c_e}^2(Y) + I_{s_e}^2(Y)}\right) = C_e I_0\left(\frac{\alpha}{N_0} E_e(Y)\right) \quad (3-60)$$

$$= \exp\left\{ \ln \left[I_0 \left(\frac{\alpha}{N_0} E_e(Y) \right) \right] - \frac{\alpha^2 q_1(\theta)}{4N_0} \right\} \quad (3-61)$$

where

$$E_e(Y) \triangleq \sqrt{I_c^2(Y) + I_s^2(Y)} \quad (3-62)$$

and I_0 is the modified Bessel function of the first kind, zeroth order. The above relates to other results, which are well known [5],[6].

Substituting the above results in (3-20) we obtain, after some manipulation, the following:

$$\Lambda_0(Y) = \left(\begin{array}{l} -\frac{\alpha^2 \hat{q}_1(\hat{\theta})}{4N_0} - \frac{\hat{\alpha}}{N_0} \left(\frac{I_{10}(Y)}{I_{00}(Y)} \cdot \frac{I_c(Y)}{E_0(Y)} \int_0^{\hat{T}} \hat{p} \cos \hat{\omega}_0 t dY \right. \\ \quad \left. + \frac{I_{10}(Y)}{I_{00}(Y)} \cdot \frac{I_s(Y)}{E_0(Y)} \int_0^{\hat{T}} \hat{p} \sin \hat{\omega}_0 t dY \right) \\ -\frac{\hat{\alpha} \hat{q}_1(\hat{\theta})}{2N_0} + \frac{1}{N_0} \left(\frac{I_{10}(Y)}{I_{00}(Y)} \cdot \frac{I_c(Y)}{E_0(Y)} \int_0^{\hat{T}} \hat{p} \cos \hat{\omega}_0 t dY \right. \\ \quad \left. + \frac{I_{10}(Y)}{I_{00}(Y)} \cdot \frac{I_s(Y)}{E_0(Y)} \int_0^{\hat{T}} \hat{p} \sin \hat{\omega}_0 t dY \right) \\ -\frac{\hat{\alpha}}{N_0} \left(\frac{I_{10}(Y)}{I_{00}(Y)} \cdot \frac{I_c(Y)}{E_0(Y)} \int_0^{\hat{T}} \hat{p} t \sin \hat{\omega}_0 t dY \right. \\ \quad \left. - \frac{I_{10}(Y)}{I_{00}(Y)} \cdot \frac{I_s(Y)}{E_0(Y)} \int_0^{\hat{T}} \hat{p} t \cos \hat{\omega}_0 t dY \right) \end{array} \right) \quad (3-63)$$

In which new notation appearing is defined as follows:

$$\hat{p} \triangleq p[\theta_A(t) - \hat{\theta}] \quad (3-64)$$

$$\hat{p} \triangleq p[\theta_A(t) - \hat{\theta}] \quad (3-65)$$

$$I_{00}(Y) \triangleq I_0 \left(\frac{\hat{\alpha}}{N_0} E_0(Y) \right) \quad (3-66)$$

$$E_0(Y) \triangleq \sqrt{I_c^2(Y) + I_s^2(Y)} \quad \text{per (3-62)} \quad (3-67)$$

$$I_{c0}(Y) \triangleq \int_0^{\hat{T}} \hat{p} [\theta_A(t) - \hat{\theta}] \cos \hat{\omega}_0 t dY(t) \quad \text{per (3-57)} \quad (3-68)$$

$$I_{s_0}(Y) \triangleq \int_0^T p[\theta_A(t) - \hat{\theta}] \sin \hat{\omega}_0 t dY(t) \quad \text{per (3-58)} \quad (3-69)$$

$$I_{l_0}(Y) \triangleq I_1\left(\frac{\hat{\alpha}}{N_0} E_0(Y)\right) \quad (3-70)$$

where I_1 is the modified Bessel function of the first kind, first order. A simplification of (3-63) is possible with the definition of four more quantities similar to (3-68) and (3-69) above:

$$J_{c_0}(Y) \triangleq \int_0^T p[\theta_A(t) - \hat{\theta}] \cos \hat{\omega}_0 t dY(t) \quad (3-71)$$

$$J_{s_0}(Y) \triangleq \int_0^T p(\theta_A(t) - \hat{\theta}) \sin \hat{\omega}_0 t dY(t) \quad (3-72)$$

$$K_{c_0}(Y) \triangleq \int_0^T p[\theta_A(t) - \hat{\theta}] t \cos \hat{\omega}_0 t dY(t) \quad (3-73)$$

$$K_{s_0}(Y) \triangleq \int_0^T p[\theta_A(t) - \hat{\theta}] t \sin \hat{\omega}_0 t dY(t) \quad (3-74)$$

Further, the quantity $I_{l_1}(Y)/I_{l_0}(Y)$, essentially a soft-limiter function with initial slope = 1/2 and maximum values of ± 1 , will be denoted by $L_0(Y)$; it is closely approximated by an arc tangent expression, i.e.,

$$L_0(Y) \triangleq \frac{I_1\left(\frac{\hat{\alpha}}{N_0} E_0(Y)\right)}{I_0\left(\frac{\hat{\alpha}}{N_0} E_0(Y)\right)} \approx \frac{2}{\pi} \arctan \left[\frac{\pi}{4} \cdot \frac{\hat{\alpha}}{N_0} E_0(Y) \right] \quad (3-75)$$

With these definitions $\Lambda_0(Y)$ can be written

$$\Lambda_0(Y) = \begin{pmatrix} -\frac{\hat{\alpha}^2 q_1(\hat{\theta})}{4N_0} - \frac{\hat{\alpha} L_0(Y)}{N_0 E_0(Y)} [I_{c_0}(Y) J_{c_0}(Y) + I_{s_0}(Y) J_{s_0}(Y)] \\ -\frac{\hat{\alpha} q_1(\hat{\theta})}{2N_0} + \frac{L_0(Y)}{N_0 E_0(Y)} [I_{c_0}^2(Y) + I_{s_0}^2(Y)] \\ -\frac{\hat{\alpha} L_0(Y)}{N_0 E_0(Y)} [I_{c_0}(Y) K_{s_0}(Y) - I_{s_0}(Y) K_{c_0}(Y)] \end{pmatrix} \quad (3-76)$$

which together with (3-67) through (3-69) and (3-71) through (3-74) indicates the amount of processing of the observation $y(t)$ (or $Y(t)$) that is required by the optimal processor which is denied the value of the carrier phase parameter, β . Further, a comparison of (3-33), the known β case, with (3-63) above shows the two expressions for Λ are analogous if the following interpretations are made:

$$\widehat{\cos \beta} = \frac{I_{10}(Y)}{I_{00}(Y)} \cdot \frac{I_{c0}(Y)}{E_0(Y)} = L_0(Y) \left(\frac{I_{c0}(Y)}{E_0(Y)} \right) \quad (3-77)$$

$$\widehat{\sin \beta} = \frac{I_{10}(Y)}{I_{00}(Y)} \cdot \frac{I_{s0}(Y)}{E_0(Y)} = L_0(Y) \left(\frac{I_{s0}(Y)}{E_0(Y)} \right) \quad (3-78)$$

These may not be optimum or even good estimates of $\cos \beta$ and $\sin \beta$ in the usual sense, but locally optimum estimates of θ , α , ω_0 result from their use. Certainly it can be shown that for very large signal-to-noise ratios

$$\widehat{\cos \beta} \rightarrow \cos \beta \quad (3-79)$$

$$\widehat{\sin \beta} \rightarrow \sin \beta . \quad (3-80)$$

In general we settle for less, however, noting, for example

$$(\widehat{\cos \beta})^2 + (\widehat{\sin \beta})^2 = L_0^2(Y) \quad (3-81)$$

which is less than unity for finite signal-to-noise ratios.

This is as far as the study of the locally optimum estimation technique has progressed. The computation of the error covariance matrix Φ_0^{-1} for the random β case has yet to be done (if further effort on this direct-path-signal-plus-noise case is warranted). This matrix is not a function of the observation $Y(t)$; it is needed to complete the solution for the error estimate \hat{e} via (3-19) as well as providing

the desired reference performance measure. The structure of a representative implementation of this receiver algorithm is shown in Figure III-1. The quadrature detection represented by the calculations of I_{c_0} , I_{s_0} , J_{c_0} , J_{s_0} , K_{c_0} , K_{s_0} , (3-68), (3-69) and (3-71) through (3-74) respectively, would be done with analog circuitry, and the remaining calculations associated with the error estimation, (3-19), (3-76), (3-67), (3-75), etc., as well as the A/C angle estimate update, would be done in a digital microprocessor. This algorithm requires a knowledge of the noise power density N_0 . In a baseband simulation of this algorithm the quadrature detection integrations, (3-68), (3-69) and (3-71) through (3-74), would be represented by integrations of the low-frequency (i.e. difference frequency) components of the integrands shown in the equations.

The extension of the locally optimum estimation algorithm to multipath-corrupted signals will be an early objective in the continuation of the project. The problem will center on modeling as a process the reflection component $y_R(t)$ of the received signal $y(t) = y_D(t) + y_R(t) + n(t)$ described in Chapter II, and then calculating the required likelihood ratio (Radon-Nikodym derivative). Kailath's work [6], [7], [8] will help in this second aspect. The successful extension to the multipath-corrupted signal is expected to result in an adaptive algorithm, which approach is discussed further in the conclusion to this chapter.

The complexity of the optimal quadrature detector processors that have resulted motivates a serious consideration of the rectifier-type of envelope detector and the processing optimality of its output to produce the estimate of the A/C angular coordinate. The difficulty in considering this option from the locally optimum estimation viewpoint stems from the possible inapplicability of the latter model (as formulated by Murphy) to the rectified-envelope process and the possibility that a suitable likelihood ratio expression cannot be found in the literature and will have to be derived. These problems are related to the fact that, even in the multipath-free case, the corruption of the envelope process (induced by receiver noise) has the following properties:

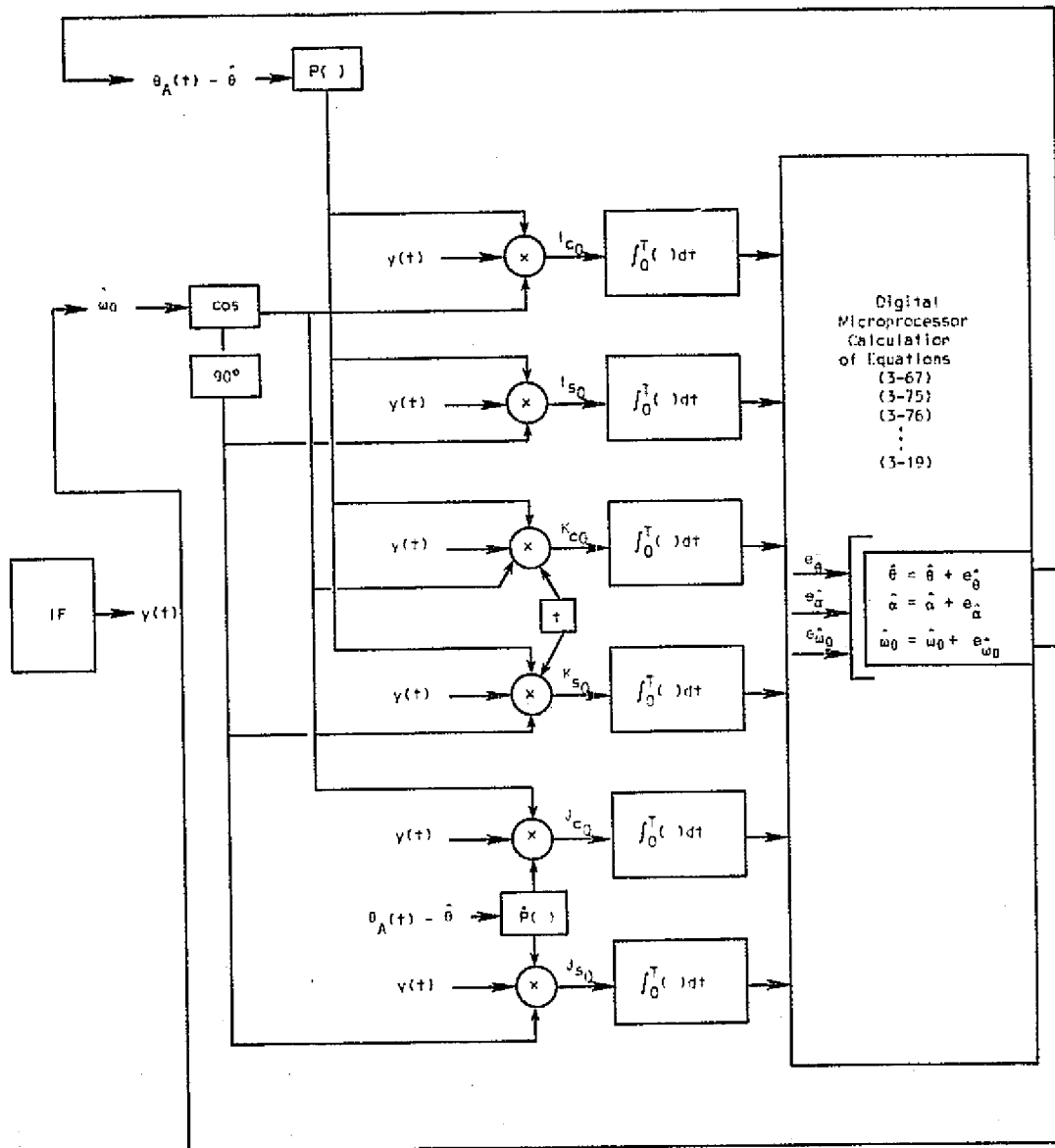


Figure III-1 Structure of a Locally Optimum Estimator Receiver for the Direct-Path Signal + Noise Case

- 1) The corruption is not additive.
- 2) The corruption is not Gaussian.
- 3) The corruption does not have mean value zero.

The rectifier-envelope-detector does seem to offer some economic advantages in implementation, however, and the associated analysis and design problems will be studied. Concern to date for these types of envelope detectors has been somewhat informal and is discussed in Chapter IV on suboptimal design.

Recursive State Estimation

Recursive state estimation (RSE) has some appeal for the MLS application, but algorithms of this class in general have some undesirable characteristics which must be understood and whose effects minimized. In addition, general RSE algorithms are based upon system models in standard state variable forms, and algorithms considered for the MLS application must accommodate the special form and uncertainties in the MLS signal model. The adaptation and evaluation of recursive state estimation techniques for the MLS application is presently at an early stage. This is only a brief description of some relevant properties of recursive state estimators and a discussion of our initial concerns in the direction of inquiry.

Underlying the RSE approach generally are the following:

1. A valid state-variable model
2. A choice of some specific criterion of optimality of estimation
3. An objective of optimal estimation based on all observations from some initial time through the present.

The algorithms that result are characterized generally by both an evolving state estimate and an evolving covariance-of-estimation error matrix (assuming model validity). The importance of the latter is underscored by the presence of the error covariance as a (matrix-) factor in the processing (Kalman) gain for new observations--as was the case in the locally-optimum estimation algorithm (though the error covariance used there for gain calculations was a static quantity).

The updating of the error covariance in RSE, usually in a "downward" direction as the data base grows, is a distinguishing feature of RSE and one that makes model validity so important. For linear systems with a valid model, for example, the algorithm developed under the least mean squared error criterion produces the exact estimate value (without approximation), and the estimator is finite dimensional and globally asymptotically convergent. If the model used is not sufficiently accurate, the expected and characteristic downward drift may be

present in the computed error covariance, but the latter may bear little relation to the covariance of the true error; a form of filter divergence results.

When the system is nonlinear, the exact estimate in general is infinite-dimensional, necessitating for purposes of implementation some form of approximation, which, in turn may affect the modeling validity. Successful extensions of RSE to nonlinear systems in general are finite-dimensional algorithmic approximations which are convergent in the locale of the true state value; from this standpoint RSE appears as a promising approach to tracking algorithm development for optimal MLS receivers.

A valid model is clearly a crucial factor in applications of RSE, and requires careful selection of many parameter values. To ease this task somewhat by reducing the number of parameters, one might be tempted in some cases to remove the stochastic forcing function from his model, i.e., to model his system as either unforced or forced by a known deterministic function. The first implication of this is that the conditional expectation of the state at one point in time, given the state value at some other point in time, is not a random variable; the final consequences may be disastrous. With only observation noise in the model the calculated error covariance matrix tends toward singularity (actually may approach the zero matrix) as time and the (implicit) data base grow arbitrarily large. The Kalman gain then becomes very small, limiting severely the influence of later observation. In this situation the estimator is said to be in "data saturation" and is especially prone to the filter divergence syndrome, caused now, in part, by computational errors, such as round-off, etc.

Two ways to avoid data saturation are as follows:

- 1) Use static noise of sufficient intensity in the model
- 2) Use a limited memory approach to restrict the effective data base to the most recent observations.

The first approach is the usual one taken in RSE applications; the

application of locally optimum estimation to the MLS problem, as described previously, is an example of the second approach. Both approaches effectively place a lower bound on the Kalman gain used in processing new observations.

The digital computation of an evolving error covariance matrix presents certain problems also, arising from the finite-wordlength structure of digital machines. Covariance matrices in general are characterized by the symmetric and non-negative definite properties of matrices. Digital computational errors arising in a RSE algorithm can be categorized into two groups in relation to their effects on filter performance:

1. Those that degrade the performance only slightly in terms of convergence and tracking properties.
2. Those that induce filter divergence.

Computational errors made in the estimate extrapolation and update probably are of the first type and are remedied in subsequent updates. Computational errors made in the covariance matrix extrapolation and update tend to be of the second type; particularly those associated with the loss of the symmetric and non-negative definite properties. Two ways to circumvent this problem are as follows:

1. Integrate the covariance matrix equation off-line, if possible, on a high-precision machine and use the resulting steady-state solution as a matrix constant in the estimator.
2. Reformulate the error covariance propagation problem in terms of propagation of a triangular matrix square root of the error covariance.

The first approach may result in substantially suboptimal performance during certain periods of time, but provides additional benefits of computational simplicity (on-line) and no possibility of data saturation. The second approach insures the (now implicit) covariance matrix will have the requisite matrix properties, but at a moderate increase in computational complexity. Optimality of the estimate is maintained throughout all phases of its evolution, however, a benefit that must be weighed

carefully considering the relative transience of multipath interference in the composite received signal.

Finally, it is noted that straight-forward application of RSE theory to the MLS receiver problem gives algorithms which assume the carrier phase is known, as with the first application of the locally optimum estimation theory. Extension of the RSE theory is needed to treat the case of interest where the carrier phase is a parameter of no intrinsic interest, modeled as a uniformly distributed random variable on $[-\pi, \pi]$. Extensions would be desirable also to the cases where the signal had been preprocessed with linear or quadratic detectors (rectifier-types), and consequently baseband observations were available but which were corrupted effectively by signal dependent noise that was neither Gaussian, additive nor zero mean, as discussed under locally optimum estimation.

Conclusions

Both the locally optimum estimation and recursive state estimation approaches possess both good and bad features in relation to the MLS receiver design problem. It is expected that both algorithms should be considered for application in the final design. RSE could provide the desired extrapolation between scan periods and into fades, as required, given a valid state model. Locally optimum estimation might then be used to provide needed estimates of the state model parameters, which may themselves vary with time but knowledge is lacking of the associated laws of evolution and statistics. Much additional work is needed, of course, to obtain quantitative design and performance data on such a scheme and to describe the effects of such partitioning of the joint problem of identification-state estimation.

Finally, the multipath propagation disturbance should be put back into the model and its effect on the estimation algorithm determined. The preferable type of algorithm would be an adaptive one. A non-adaptive approach would appear possible also in which the averaged performance of a class of multipath environments is optimized, but its performance in any one environment could be poor. The adaptive approach

is expected to be one in which the "gates" of the tracking receiver are modulated in some way by estimates of parameters associated with the multipath interference model.

CHAPTER IV

SUBOPTIMAL DESIGN AND SIMULATION EVALUATION

A suboptimal receiver study was undertaken in order to consider some classical receiver designs involving envelope detection and subsequent processing by a form of early-late gating. This provided an opportunity to improve the computer simulation as well as to produce a candidate receiver design which could be used as a performance standard in evaluating future receivers. No attempt was made to optimally process the envelope-detected signal. Simulation results, however, indicate that such a course may well be worthwhile.

Receiver Algorithm Design

Early design involved the development of a centroid receiver which utilized the relation between envelope pulse centroids and the A/C angular coordinate θ . This receiver recomputed centroid positions (and thus θ) for each TO-FRO scan, rather than computing error in the estimate of θ from the previous scan; i.e., it was not a tracking receiver, and since it processed the signal envelope received over the entire scan interval, it had no multipath suppression ability. Several forms of early-late gate tracking algorithms were then considered, with a square-gate version selected as the new receiver design. A development of the square-gate tracking receiver will now be presented.

The square-gate receiver algorithm produces an estimate of the A/C coordinate by computing the error in the estimate from the previous scan. Let $\theta(t) = \theta(t_k)$ on the k th scan interval (from 2-16), and let $\hat{\theta}(k)$ represent the receiver estimate of $\theta(t_k)$. $\hat{\theta}$ is formed as follows:

$$\hat{\theta}(k+1) \triangleq \hat{\theta}(k) + \Delta\hat{\theta}(k) \quad (4-1)$$

$$\Delta\hat{\theta}(k) \triangleq \int_0^T p_D(\tau) g[\tau, \hat{\theta}(k)] d\tau \quad (4-2)$$

where τ is the local scan time at the A/C (from 2-23), $p_D(\tau)$ is the direct-path signal envelope, on the $(k+1)$ st scan, and $g[\tau, \hat{\theta}(k)]$ is the gating function (see Figure IV-1). The envelope function is given by:

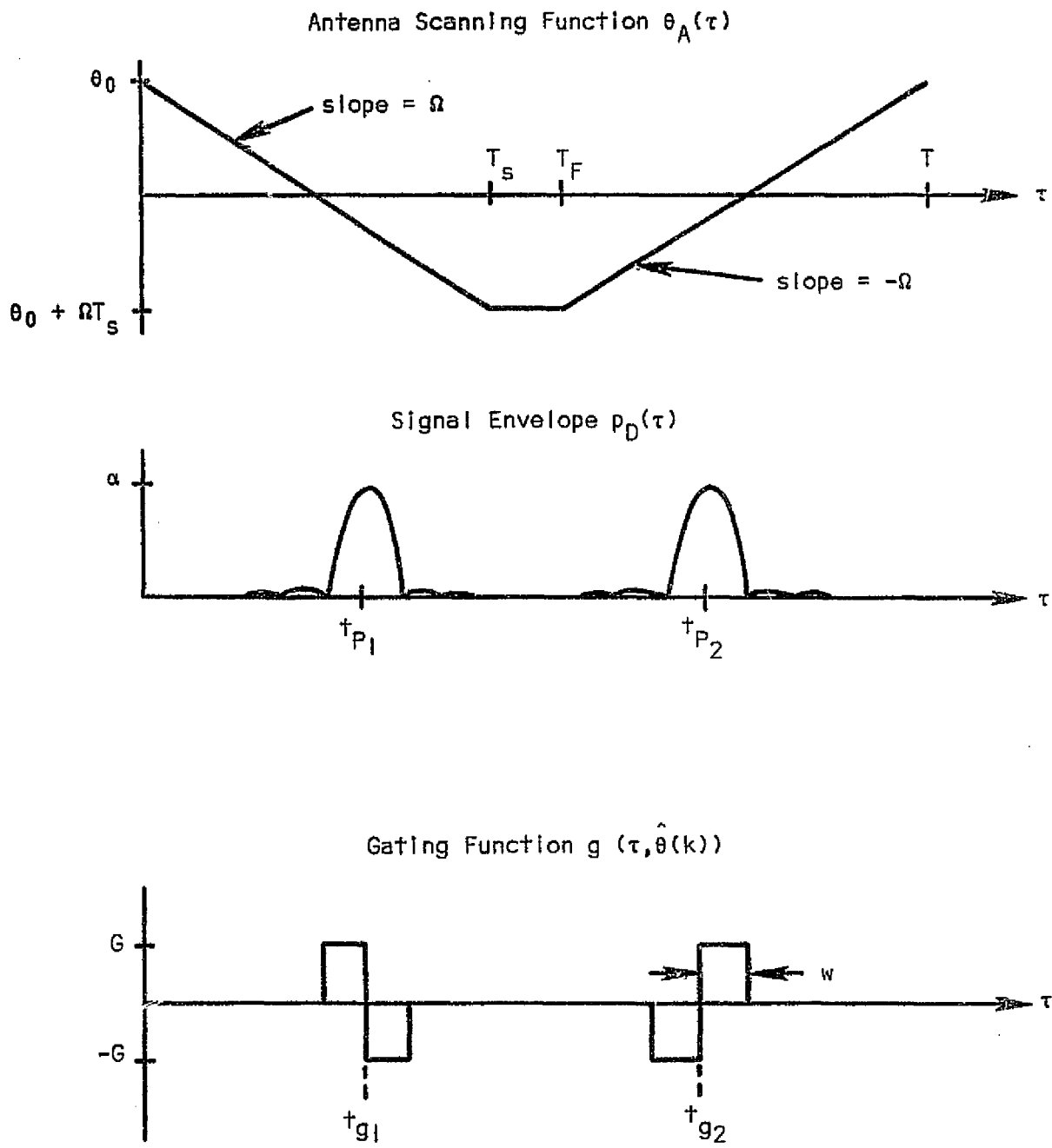


Figure IV-1 Envelope and Gating Functions

$$p_D(\tau) \triangleq \alpha p[\theta_A(\tau) - \theta(t_k)] \quad (4-3)$$

$$\theta_A(\tau) = \begin{cases} \theta_0 + \Omega\tau & : 0 \leq \tau \leq T_s \\ \theta_0 + \Omega T_s & : T_s < \tau < T_F \\ \theta_0 + \Omega T_s - \Omega(\tau - T_F) & : T_F \leq \tau \leq T \end{cases} \quad (4-4)$$

where $p(\cdot)$ is the envelope selectivity function defined by (2-1). In Figure IV-1, t_{p_1} and t_{p_2} are the envelope centroids. The receiver gates are centered at t_{g_1} and t_{g_2} which are estimates of t_{p_1} and t_{p_2} based on $\hat{\theta}(k)$. Each gate has height G and half-width w so that the gating function becomes:

$$g[\tau, \hat{\theta}(k)] = \begin{cases} G: t_{g_1} - w \leq \tau \leq t_{g_1} \text{ or } t_{g_2} \leq \tau \leq t_{g_2} + w \\ -G: t_{g_1} \leq \tau \leq t_{g_1} + w, \text{ or } t_{g_2} - w \leq \tau \leq t_{g_2} \\ 0 \text{ otherwise} \end{cases} \quad (4-5)$$

t_{g_1} and t_{g_2} are the values of τ when $\theta_A(\tau) = \hat{\theta}(k)$ and are given by:

$$t_{g_1} = \frac{\hat{\theta}(k) - \theta_0}{\Omega} \quad (4-6)$$

$$t_{g_2} = T_s + T_F + \frac{\theta_0 - \hat{\theta}(k)}{\Omega} \quad (4-7)$$

Define the error term $\theta_e(k)$ as follows:

$$\theta_e(k) \triangleq \theta(t_{k+1}) - \hat{\theta}(k) \quad (4-8)$$

It follows from (4-1) that $\hat{\theta}(k)$ is an estimate of $\theta_e(k)$. A relation between the gate height and width is desired which will drive $[\theta(t_{k+1}) - \hat{\theta}(k+1)]$ to zero by equating $\Delta\hat{\theta}(k)$ and $\theta_e(k)$. From (4-2) we have:

$$\Delta\hat{\theta}(k) = \int_{t_{g_1}-w}^{t_{g_1}+w} g[\tau, \hat{\theta}(k)] p_D(\tau) d\tau + \int_{t_{g_2}-w}^{t_{g_2}+w} g[\tau, \hat{\theta}(k)] p_D(\tau) d\tau \quad (4-9)$$

$$\begin{aligned}
&= G \int_{-w}^0 p_D(\tau + t_{g_1}) d\tau - G \int_0^w p_D(\tau + t_{g_1}) d\tau - G \int_{-w}^0 p_D(\tau + t_{g_2}) d\tau \\
&\quad + G \int_0^w p_D(\tau + t_{g_2}) d\tau \tag{4-10}
\end{aligned}$$

$p_D(\tau + t_{g_i})$ is found by combining (4-6), (4-7), (4-4), and (4-3). Coupling this result with (4-8), we can rewrite (4-10) as:

$$\hat{\Delta\theta}(k) = \alpha G \left[\int_{-w}^0 p(\Omega\tau - \theta_e) d\tau - \int_0^w p(\Omega\tau - \theta_e) d\tau - \int_{-w}^0 p(-\Omega\tau - \theta_e) d\tau + \int_0^w p(-\Omega\tau - \theta_e) d\tau \right] \tag{4-11}$$

Note that if $\theta_e(k) = 0$, $\hat{\Delta\theta}(k) = 0$, as expected. Assume $\theta_e(k)$ is small.

Then:

$$p(\Omega\tau - \theta_e) \approx p(\Omega\tau) - \theta_e \frac{dp(\Omega\tau)}{d(\Omega\tau)} \tag{4-12}$$

$$\int_{-w}^0 p(\pm\Omega\tau - \theta_e) d\tau \approx \int_{-w}^0 p(\pm\Omega\tau) d\tau \mp \frac{\theta_e}{\Omega} \int_{-\Omega w}^0 dp(\Omega\tau) = P(w) \mp \frac{\theta_e}{\Omega} [p(0) - p(\Omega w)] \tag{4-13}$$

Substituting this result into (4-11) yields:

$$\hat{\Delta\theta}(k) = \alpha G \left[\frac{\theta_e(k)}{\Omega} (4p(\Omega w) - 4p(0)) \right] \tag{4-14}$$

$$= \frac{-4\alpha G \theta_e(k) [1 - p(\Omega w)]}{\Omega} \tag{4-15}$$

Equating $\hat{\theta}(k)$ and $\theta_e(k)$, we have:

$$G = \frac{-\Omega}{4\alpha [1 - p(\Omega w)]} \tag{4-16}$$

It is assumed that the envelope selectivity function $p(\cdot)$ will be known. Thus, given a knowledge of the signal amplitude α , the gate height G can be computed for any desired width w such that $\hat{\theta}(k) = \theta_e(k)$ (assuming that θ_e is sufficiently small). Although α is not known by the A/C, it can be estimated by noting in Figure IV-1 that

$$\alpha = p_D(t_{p_i}), \quad i = 1, 2 \tag{4-17}$$

An estimate of α can be obtained by averaging signal envelope samples taken at t_{g1} and t_{g2} , which are estimates of t_{p1} and t_{p2} . This estimate can then be substituted for α in (4-16) to compute G .

The square gate receiver was developed without considering the effects of additive noise or multipath upon the received signal envelope. This approach can be defended in light of the following:

1. The positive and negative areas of the gating function are equal. It is therefore expected that the effect upon the estimate of noise occurring in a positive gate will be roughly cancelled by that of noise occurring in a negative gate.

2. Any multipath distortions in the envelope occurring outside the gates will be ignored.

The receiver tested in the simulation can be described from (4-1) and (4-2) as:

$$\hat{\theta}(k+1) = \hat{\theta}(k) + \int_0^T M(t_{k+1}, \tau) g[\tau, \hat{\theta}(k)] d\tau \quad (4-18)$$

where $g(\cdot)$ is defined by (4-5) and $p_D(\tau)$ has been replaced with the complete signal envelope $M(t_{k+1}, \tau)$, as presented in (2-53). On the k th scan α is estimated by averaging $M(t_k, t_{g1})$ and $M(t_k, t_{g2})$ (see 4-17), and G is then updated:

$$G = \frac{-\Omega}{2[M(t_k, t_{g1}) + M(t_k, t_{g2})] \times [1 - p(\Omega w)]} \quad (4-19)$$

It was decided to set w equal to the time between centroid and first zero of an envelope pulse of $p_D(\tau)$. This selection of gate width seemed intuitively good in that the gate would include most of the direct signal envelope and yet be narrow enough to exclude most multipath.

The computer simulation involved a discrete-time version of the local scan time τ , so that the square-gate receiver operated on samples of the envelope $M(t_k, \tau)$. This operation will be described in the next section of this chapter.

Simulation Modeling

The simulation objective was to evaluate envelope-detector receivers, making it necessary to model the I.F. signal envelope $M(t_k, \tau)$ in (2-53). The signal modeling was basically that of Chapter II, with the following changes:

1. The "received scan interval" of (2-22) became

$$t_k + \frac{r(t_k)}{c} \leq t \leq t_k + \frac{r(t_k)}{c} + T \quad (4-20)$$

in which fairly insignificant $\frac{\dot{r}(t)}{c}$ terms were dropped. In terms of local scan time τ this interval became (from 2-24)

$$0 \leq \tau \leq T \quad (4-20A)$$

t_{Rk} , defined in (2-25), likewise became

$$t_{Rk} \approx t_k + \frac{r(t_k)}{c} \quad (4-21)$$

2. The signal amplitudes α and α_i in (2-42) and (2-44) were assumed constant. This is valid if the A/C and reflector ranges do not vary appreciably.
3. t_k was dropped from the argument of $\theta_A(\cdot)$ in (2-42) and (2-44), as θ_A is a periodic function which reinitiates at $t = t_k$.
4. The range and angle coordinates of the A/C and reflection points were assumed to be linear functions of time; i.e., \dot{r} , $\dot{\theta}$, $\dot{\phi}$, \dot{r}_{Ri} , $\dot{\theta}_{Ri}$, and $\dot{\phi}_{Ri}$ were made constants. (4-22)

The local scan time τ was discretized to simulate sampling of the received signal envelope $M(t_k, \tau)$. Starting at $\tau = 0$, the envelope was sampled across the entire scan interval at a rate equal to the IF bandwidth B_{IF} (160KHZ). From (4-20A) the number of samples taken in one scan interval would be

$$J_T = T \times B_{IF} + 1 \quad (4-23)$$

The local scan time at the j th sample would thus be:

$$\tau(j) = (j - 1)\delta \quad 1 \leq j \leq J_T \quad (4-24)$$

where $\delta = 1/B_{IF}$. The envelope function $M(t_k, \tau)$ can now be expressed in terms of the discrete local scan time by substituting (4-23) into equations (2-47) through (2-50) and incorporating the new changes in modeling enumerated above:

$$Y_{D_C}(t_k, j) = \alpha p [\theta_A((j - 1)\delta) - \theta(t_k)] \cos[\beta(t_k) - \frac{\omega_c \dot{r}}{c} (j - 1)\delta] \quad (4-25)$$

$$\triangleq P_D(t_k, j) \cos \Psi_D(t_k, j) \quad (4-26)$$

$$Y_{D_S}(t_k, j) = \alpha p [\theta_A((j - 1)\delta) - \theta(t_k)] \sin[\beta(t_k) - \frac{\omega_c \dot{r}}{c} (j - 1)\delta] \quad (4-27)$$

$$\triangleq P_D(t_k, j) \sin \Psi_D(t_k, j) \quad (4-28)$$

$$Y_{R_C}(t_k, j) = \sum_i \alpha_i p [\theta_A((j - 1)\delta - \frac{\Delta r_i(t_k)}{c}) - \theta_{R_i}(t_k)] \cos[\beta_i(t_k) - \frac{\omega_c \dot{r}_i(t_k)}{c} (j - 1)\delta] \quad (4-29)$$

$$\triangleq \sum_i P_{R_i}(t_k, j) \cos \Psi_{R_i}(t_k, j) \quad (4-30)$$

$$Y_{R_S}(t_k, j) = \sum_i \alpha_i p [\theta_A((j - 1)\delta - \frac{\Delta r_i(t_k)}{c}) - \theta_{R_i}(t_k)] \sin[\beta_i(t_k) - \frac{\omega_c \dot{r}_i(t_k)}{c} (j - 1)\delta] \quad (4-31)$$

$$\triangleq \sum_i P_{R_i}(t_k, j) \sin \Psi_{R_i}(t_k, j) \quad (4-32)$$

Note that the RF phase terms $\Psi_D(t_k, j)$ and $\Psi_{R_i}(t_k, j)$ are linear functions of time and can be expressed:

$$\Psi_D(t_k, j) = \begin{cases} \beta(t_k): & j = 1 \\ \Psi_D(t_k, j-1) + \Delta \Psi_D: & 2 \leq j \leq J_T \end{cases} \quad (4-33)$$

$$\text{where } \Delta \Psi_D = -\frac{\omega_c \dot{r}}{c} \delta \quad (4-34)$$

$$\Psi_{R_i}(t_k, j) = \begin{cases} \beta_i(t_k): & j = 1 \\ \Psi_{R_i}(t_k, j-1) + \Delta\Psi_{R_i}(t_k): & 2 \leq j \leq J_T \end{cases} \quad (4-35)$$

$$\text{where } \Delta\Psi_{R_i}(t_k) = \frac{-\omega_c \dot{r}_{T_i}(t_k)}{c} \delta \quad (4-36)$$

The envelope $M(t_k, j)$ now follows directly from (2-54) through (2-56):

$$M(t_k, j) = [(y_{D_c}(t_k, j) + y_{R_c}(t_k, j) + n_c(j))^2 + (y_{D_s}(t_k, j) + y_{R_s}(t_k, j) + n_s(j))^2]^{1/2} \quad (4-37)$$

where $n_c(j)$ and $n_s(j)$ are the quadrature noise components of (2-51).

The simulation must compute $M(t_k, j)$, $j = 1$ to J_T , for every TO-FRO scan of interest. This also involves computing A/C and reflector coordinates and velocities at t_k (and in some cases t_{RK}), as these appear as parameters in the equations just developed. A description of the simulation for the k th scan will now be presented.

Let t_k ($k = 1, 2, \dots, k_{\max}$) be evenly spaced, and define:

$$T_{UD} \triangleq t_k - t_{k-1} \quad (= 75 \text{ milliseconds})$$

From (4-22) we can update the A/C and reflector coordinates:

$$r(t_k) = r(t_{k-1}) + \dot{r} \cdot T_{UD}$$

$$\theta(t_k) = \theta(t_{k-1}) + \dot{\theta} \cdot T_{UD}$$

$$\phi(t_k) = \phi(t_{k-1}) + \dot{\phi} \cdot T_{UD}$$

$$r_{R_i}(t_k) = r_{R_i}(t_{k-1}) + \dot{r}_{R_i} \cdot T_{UD}$$

$$\theta_{R_i}(t_k) = \theta_{R_i}(t_{k-1}) + \dot{\theta}_{R_i} \cdot T_{UD}$$

$$\phi_{R_i}(t_k) = \phi_{R_i}(t_{k-1}) + \dot{\phi}_{R_i} \cdot T_{UD} \quad (4-39)$$

For each reflector we compute $r_{T_i}(t_k)$ from (2-12) through (2-14):

$$\zeta_i(t_k) = \cos\phi(t_k)\cos\phi_{R_i}(t_k)\cos[\theta(t_k) - \theta_{R_i}(t_k)] + \sin\phi(t_k)\sin\phi_{R_i}(t_k) \quad (4-40)$$

$$r_{AR_i}(t_k) = [r^2(t_k) - \zeta_i(t_k)r(t_k)r_{R_i}(t_k) + r_{R_i}^2(t_k)]^{1/2} \quad (4-41)$$

$$r_{T_i}(t_k) = r_{R_i}(t_k) + r_{AR_i}(t_k) \quad (4-42)$$

$$\Delta r_i(t_k) = r_{T_i}(t_k) - r(t_k) \quad (4-43)$$

The time derivative of (4-41) can be shown to be:

$$\dot{r}_{AR_i}(t_k) = \frac{r(t_k)}{r_{AR_i}(t_k)} [\dot{r} - \zeta_i(t_k)\dot{r}_{R_i}] + \frac{r_{R_i}(t_k)}{r_{AR_i}(t_k)} [\dot{r}_{R_i} - \zeta_i(t_k)\dot{r}] \quad (4-44)$$

$$\dot{r}_{T_i}(t_k) = \dot{r}_{R_i} + \dot{r}_{AR_i}(t_k) \quad (4-45)$$

From assumptions (2-20) and (4-21) we obtain:

$$r(t_{RK}) \approx r(t_k) + \dot{r} \frac{r(t_k)}{c} \quad (4-46)$$

$$r_{T_i}(t_{RK}) \approx r_{T_i}(t_k) + \dot{r}_{T_i}(t_k) \frac{r(t_k)}{c} \quad (4-47)$$

$$\Delta r_i(t_{RK}) = r_{T_i}(t_{RK}) - r(t_{RK}) \quad (4-48)$$

$\Delta \psi_{R_i}(t_k)$ is computed from (4-36). Set $\psi_D(t_k, l)$ to $\beta(t_k)$, a uniform random variable on $[-\pi, \pi]$ supplied by a random number generator. From (2-40) and (4-35) compute:

$$\psi_{R_i}(t_k, l) = \beta_i(t_k) = \beta(t_k) + [\beta_i(t_{k-1}) - \beta(t_{k-1})] - \frac{\omega c}{c} [\Delta r_i(t_{RK}) - \Delta r_i(t_{RK-1})] \quad (4-49)$$

Now $M(t_k, j)$ can be computed for each sample on scan K .

For $j = 1$ to J_T :

$$p_D(t_k, j) = \alpha p[\theta_A((j-1)\delta) - \theta(t_k)] \quad (4-50)$$

$$y_{DC}(t_k, j) = p_D(t_k, j) \cos \psi_D(t_k, j) \quad (4-51)$$

$$y_{DS}(t_k, j) = p_D(t_k, j) \sin \psi_D(t_k, j) \quad (4-52)$$

$$\psi_D(t_k, j+1) = \psi_D(t_k, j) + \Delta \psi_D \quad (4-53)$$

$$p_{R_i}(t_k, j) = \alpha_i p[\theta_A((j-1)\delta - \frac{\Delta r_i(t_k)}{c}) - \theta_{R_i}(t_k)] \quad (4-54)$$

$$y_{R_c} = \sum_i p_{R_i}(t_k, j) \cos \psi_{R_i}(t_k, j) \quad (4-55)$$

$$y_{R_s} = \sum_i p_{R_i}(t_k, j) \sin \psi_{R_i}(t_k, j) \quad (4-56)$$

$$\psi_{R_i}(t_k, j+1) = \psi_{R_i}(t_k, j) + \Delta \psi_{R_i}(t_k) \quad (4-57)$$

Obtain quadrature noise samples $n_c(j)$ and $n_s(j)$ from Gaussian random number generator. Compute $M(t_k, j)$ using (4-37).

In the FORTRAN computer simulation, the antenna scanning function $\theta_A(\cdot)$ is computed by the function subprogram THA(T), where the argument T is computed in the main program. $\theta_A(\cdot)$ is defined by (4-4) and illustrated in Figure IV-1. The angular selectivity function $p(\theta)$ is computed by the function subprogram P(THETA), where THETA is computed in the main program. $p(\theta)$ is defined as follows, from reference [1, pp. 2-213, 2-214]:

$$p(\theta) = \begin{cases} \frac{\cos(\frac{\pi}{2} a)}{1 - a^2} & a \neq 1 \\ \frac{\pi}{4} & a = 1 \end{cases} \quad \text{where } a = 2.4\theta \quad (4-58)$$

The simulation program computes $M(t_k, j)$ for $j=1$ to J_T and stores these samples in array M . M is then passed to subroutine RCVR, which contains the square gate tracking receiver algorithm. The algorithm updates the estimate by computing the error in the estimate of the previous scan. It differs from the receiver developed earlier in this chapter as follows:

1. The signal envelope now exists in discrete form so that the integration of (4-18) is performed using a trapezoidal approximation rule.
2. Discontinuities in the gating function (see Figure IV-1) have been forced to occur at the sample times, so that the gates are well defined. Otherwise, the receiver would produce the same value of $\hat{\theta}(k)$ in (4-18) regardless of where between two samples the gate center occurred.

RCVR operates on the samples of array M one by one, with the result stored in array EST. EST thus contains an evolving estimate, where $EST(J_T)$ represents the final estimate $\hat{\theta}(k)$ for the k th scan.

After computing $\hat{\theta}(k)$, the simulation program advances to the next scan and recomputes the envelope and estimate. This is continued for as many scans as desired. For efficiency in computing the simulation has been carried out in two FORTRAN programs. The first, MLSRCVR, performs all simulation calculations and stores results on file. The second program, MLSPLOT, plots these results using a CDC COMPLIT DP-7 digital plotter. Emphasis is placed here on MLSRCVR. The following plots are made:

1. A long-term plot, which plots for every scan K in the simulation:
 - A. the composite signal envelope at the time of direct-signal centroids
 - B. the error in estimate $\hat{\theta}(k)$
2. A plot of signal envelope $M(t_k, j)$ as a function of local scan time for six selected scans.

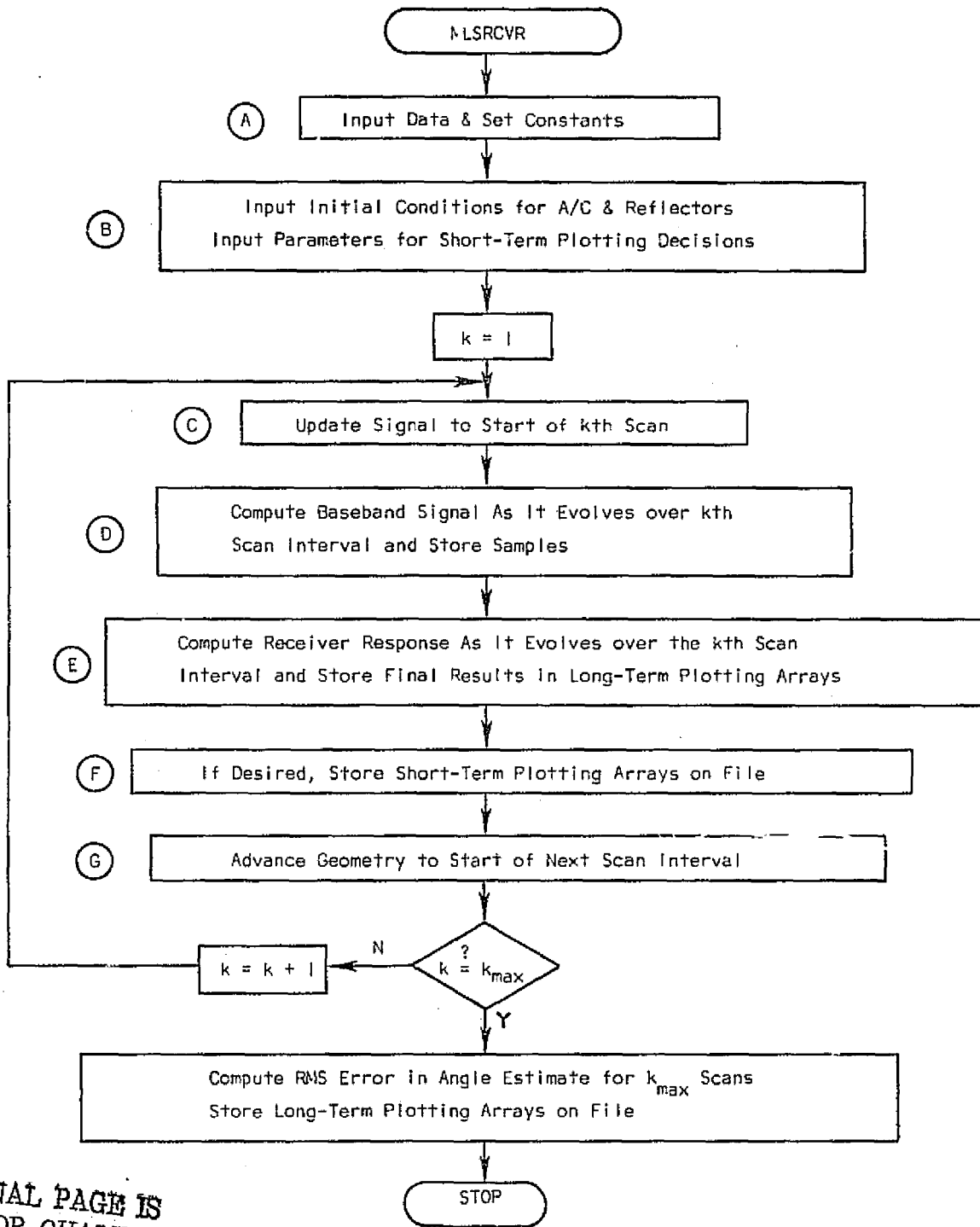
3. A short-term plot, which for one selected scan plots the received envelope $M(t_k, j)$ as well as the evolving estimate as functions of local scan time. Also plotted is the evolving estimate which would result from a received signal containing no noise or multipath.

A flow chart for program MLSRCVR is presented in Figures IV-2 through IV-3, while a basic flowchart for MLSPLOT appears in Figure IV-4. Program listings are contained in Appendix A. It should be noted that variable names used in the flowcharts and programs often differ from those used here.

Performance Evaluation

The square-gate tracking receiver was tested under the following conditions: The A/C with coordinates $r = 10$ N.mi., $\theta = 30^\circ$, $\phi = 3^\circ$ was approaching the runway with airspeed 300 knots ($\dot{\theta} = \dot{\phi} = 0$). A single specular reflector with coordinates $r_{R1} = 1.0$ N.mi., $\theta_{R1} = 33^\circ$, $\phi_{R1} = 1.85^\circ$, was following the circular path $\dot{r}_{R1} = 0$, $\dot{\theta}_{R1} = -3^\circ/\text{second}$, $\dot{\phi}_{R1} = 0$. One second later (scan 14), the reflector was at $\theta_{R1} = 30^\circ$, so that the signal envelope at the A/C due to the reflector was inside the receiver gates and coincident with the envelope due to the direct signal. After another second ($k=27$), the reflector was at $\theta_{R1} = 27^\circ$ and the signal envelope due to reflector was outside the receiver gate again. This was considered to be a realistic test for the square-gate receiver in that in-gate multipath interference intuitively represented a worse case. The simulation was run for 27 scans with the above initial conditions, with signal amplitude $\alpha = 1.0$, and multipath amplitude $\alpha_1 = 0.8$ and for several values of initial RF phase difference $[\beta_1(1) - \beta(1)]$. Also made were two trials with no reflectors and differing signal-to-noise ratios.

All simulation trials were made on the CDC 6400 computer. Plots of receiver performance may be found in Appendix B. Results are tabulated in Figure IV-5. Note that with a 20 db signal-to-noise ratio and no multipath the receiver was able to estimate θ with an R.M.S. error of 0.015° . R.M.S. errors are shown for the trials with multipath, yet



ORIGINAL PAGE IS
OF POOR QUALITY

Figure IV-2 Flowchart for Simulation Program MLSRCVR

(Note: Details of blocks identified with encircled letters are given on subsequent pages.)

BLOCK A

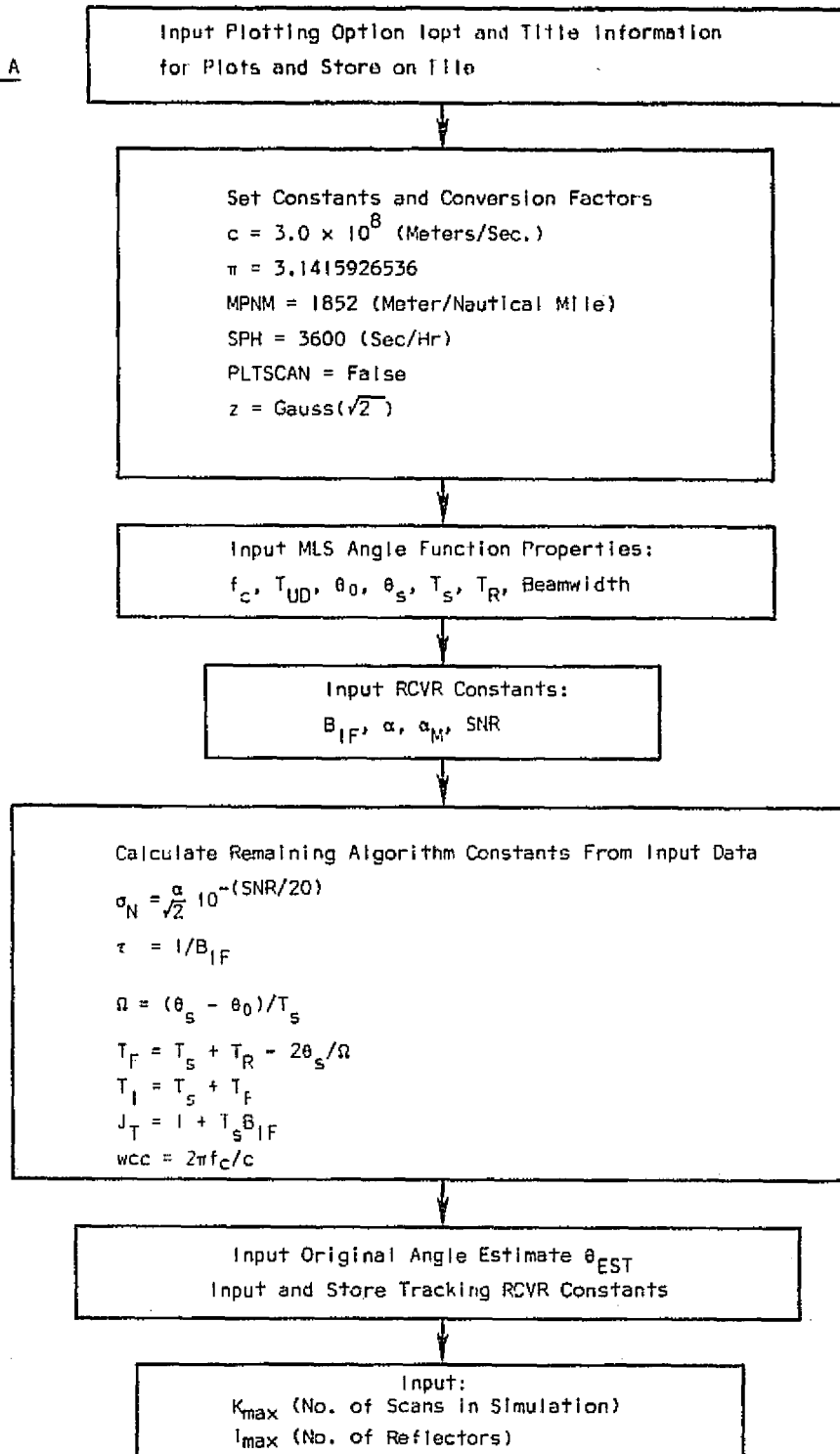


Figure IV-2a Initialization

ORIGINAL PAGE IS
OF POOR QUALITY

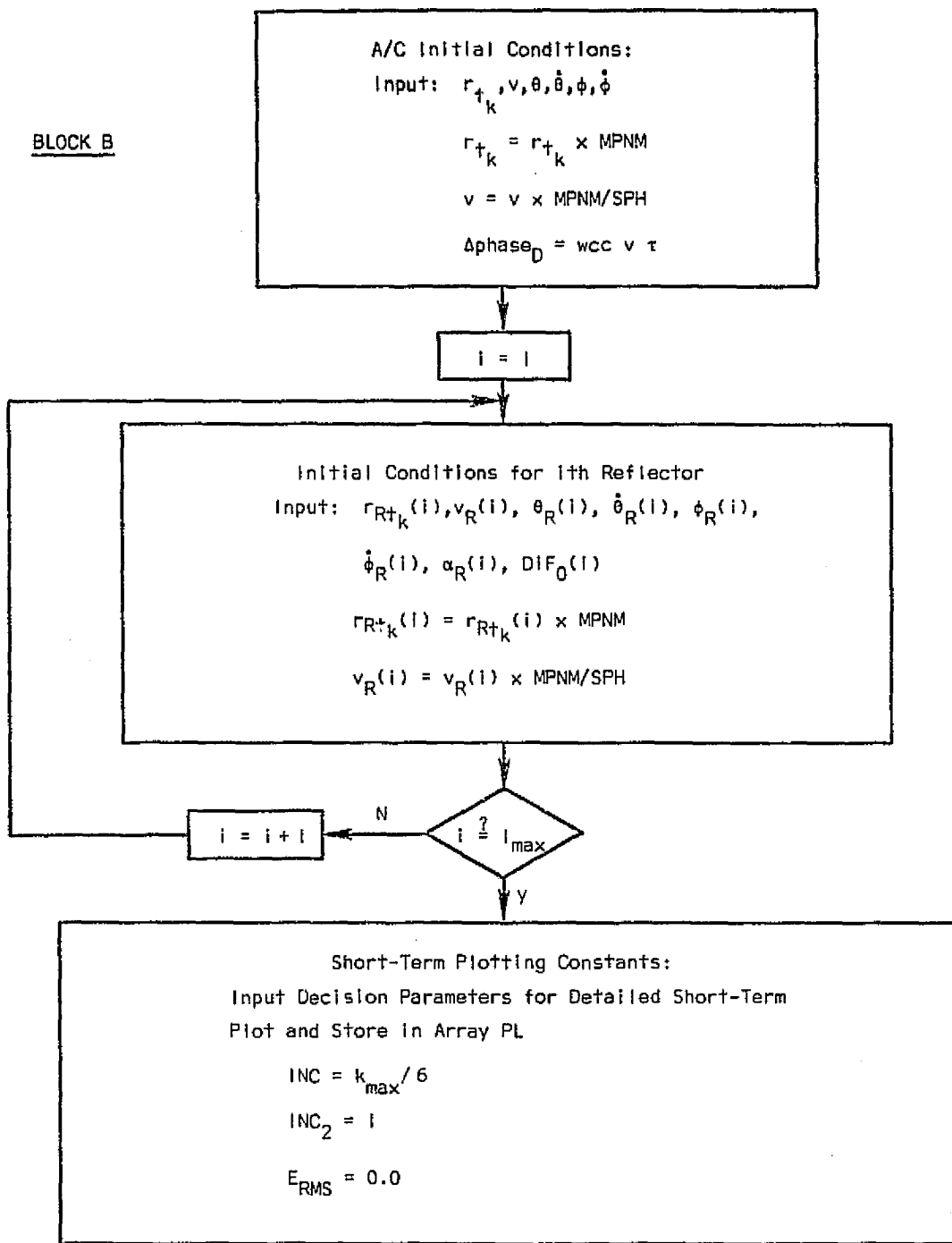


Figure IV-2b A/C and Reflector Initial Conditions

ORIGINAL PAGE IS
OF POOR QUALITY

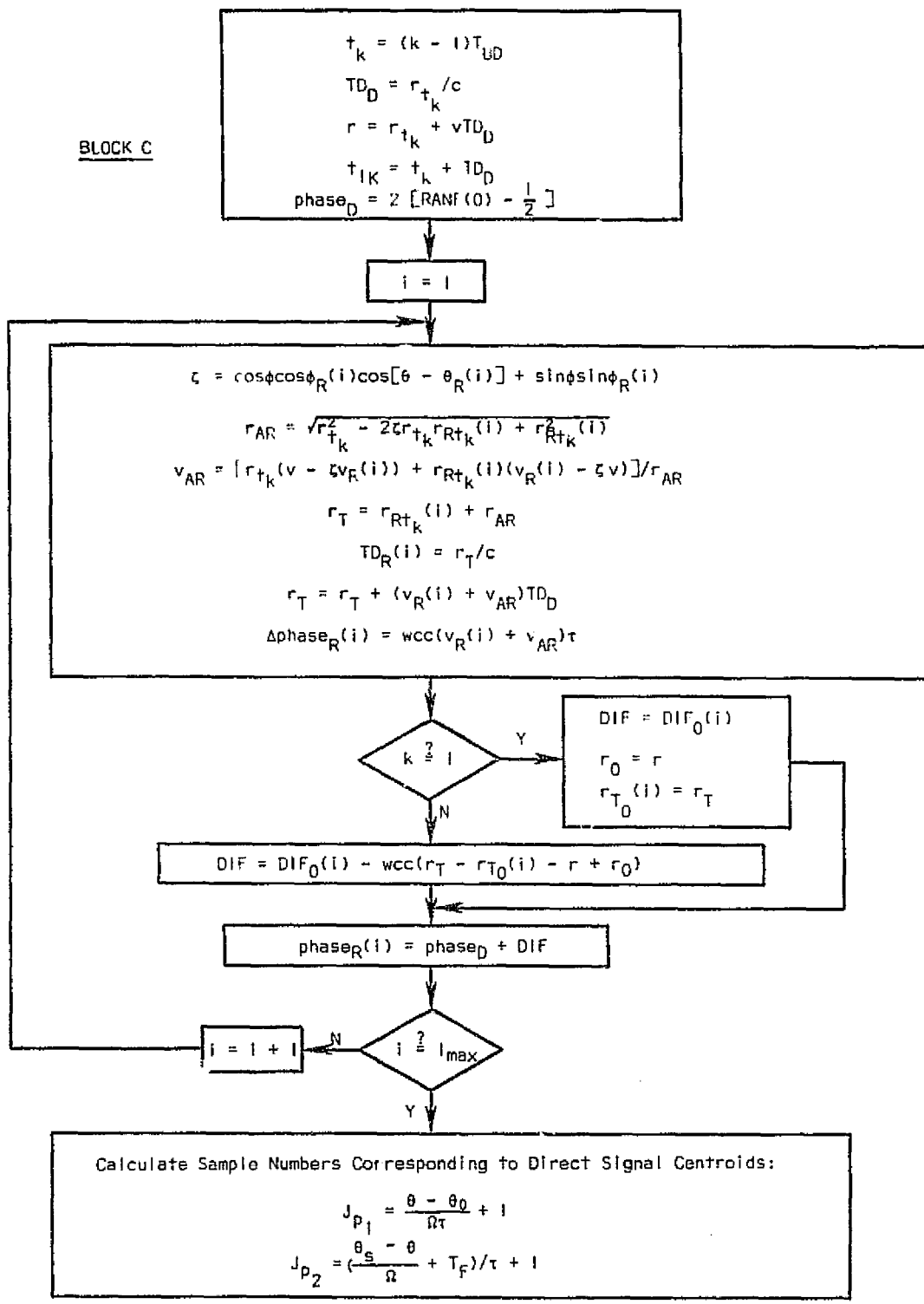
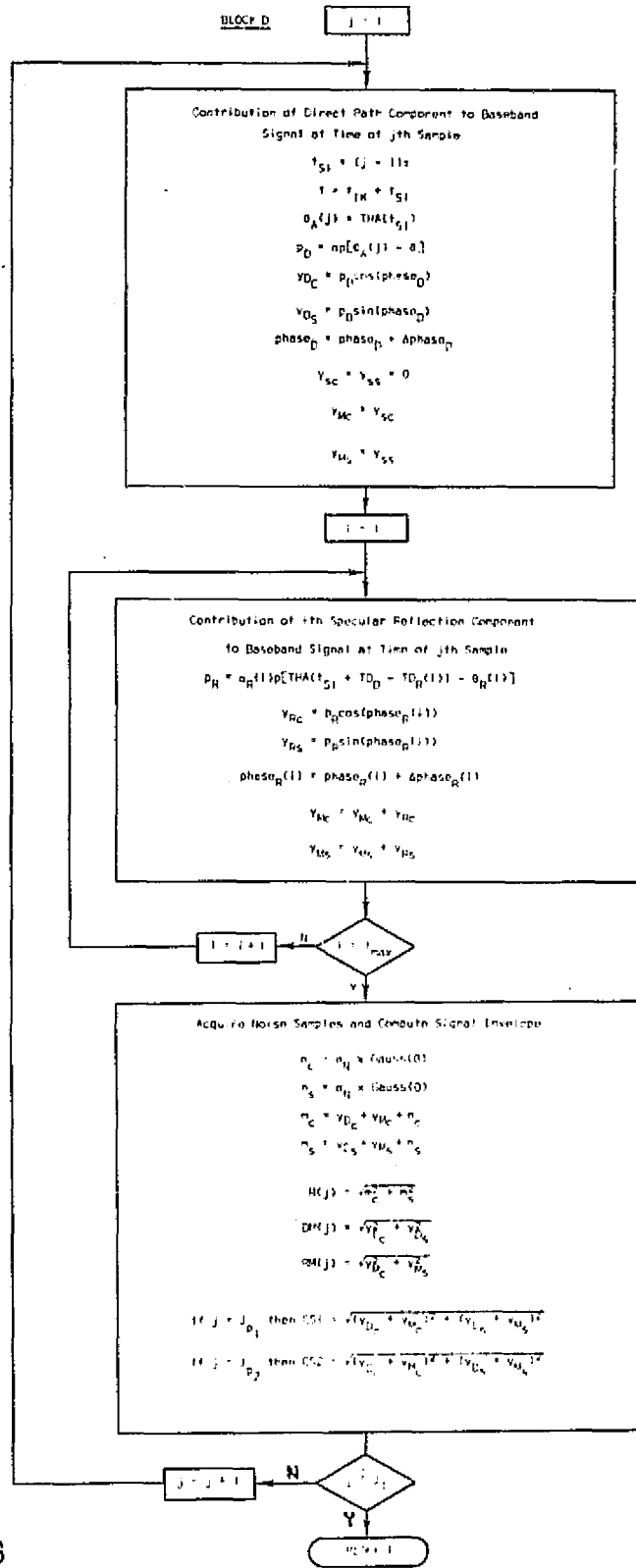


Figure IV-2c Updating Signal to kth Scan



ORIGINAL PAGE IS
OF POOR QUALITY

Figure IV-2d Computing Envelope Samples

BLOCK E

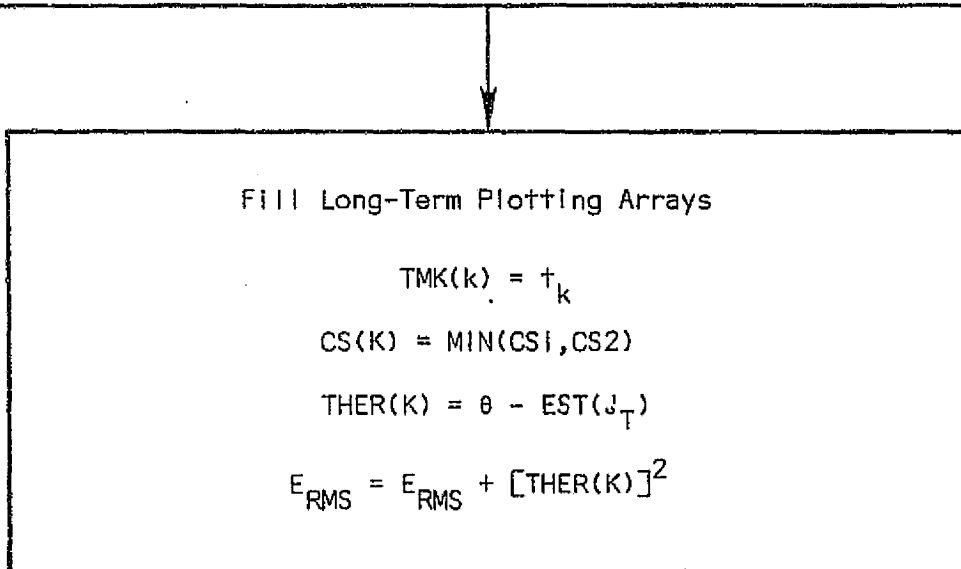
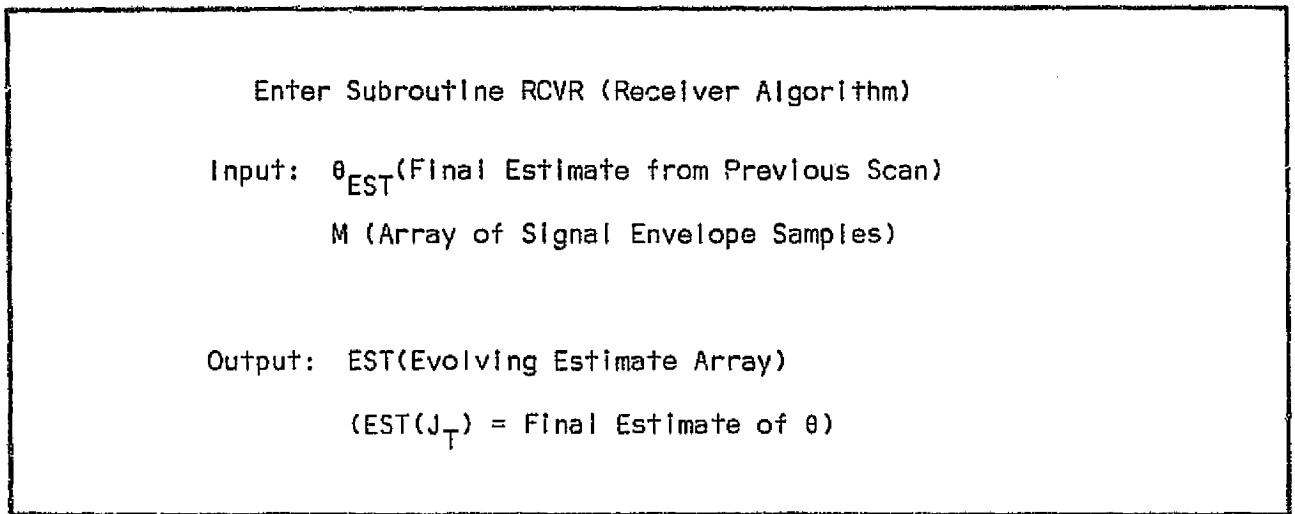


Figure IV-2e Estimate Calculation

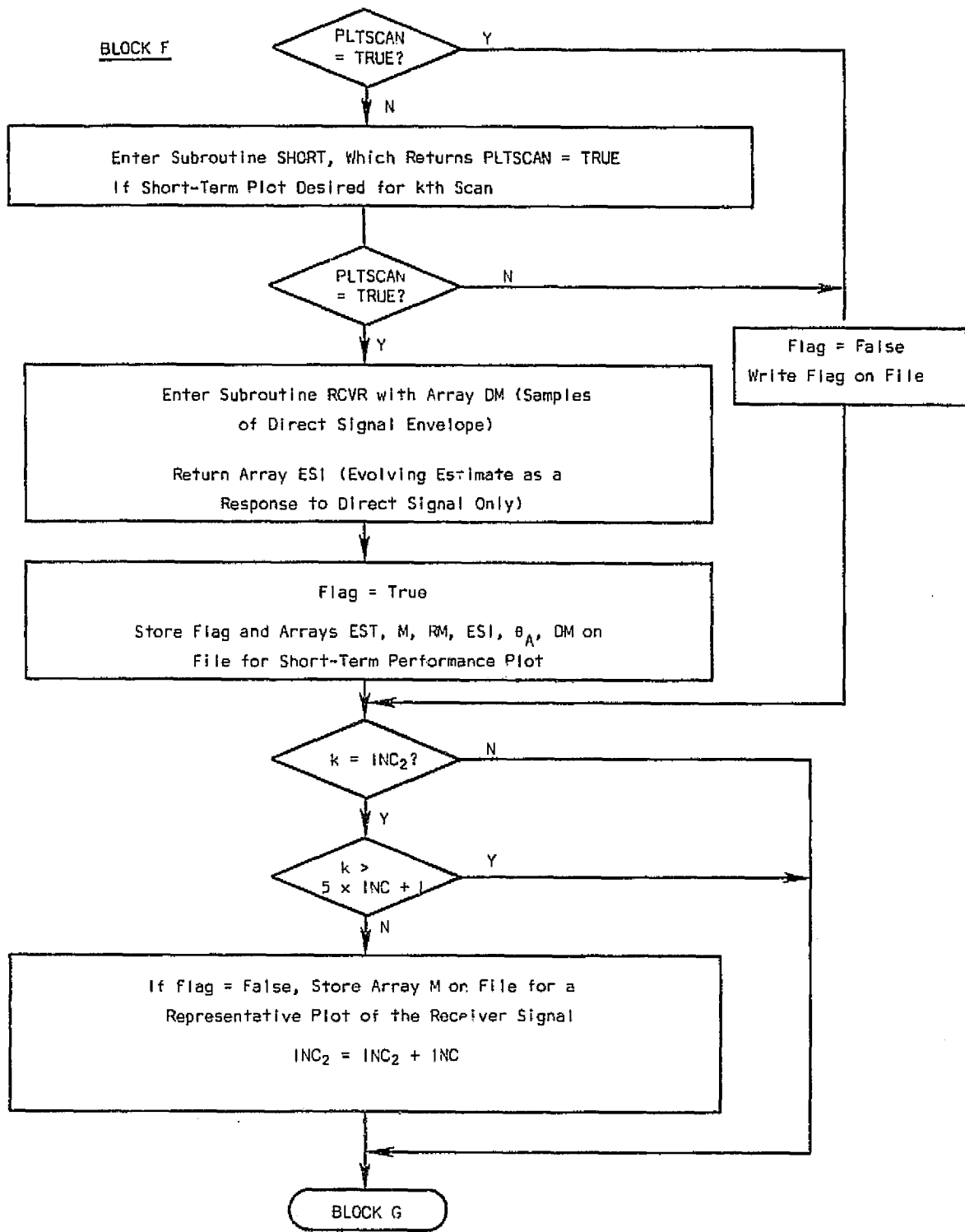


Figure IV-2f Short-Term Plotting Decisions

BLOCK G

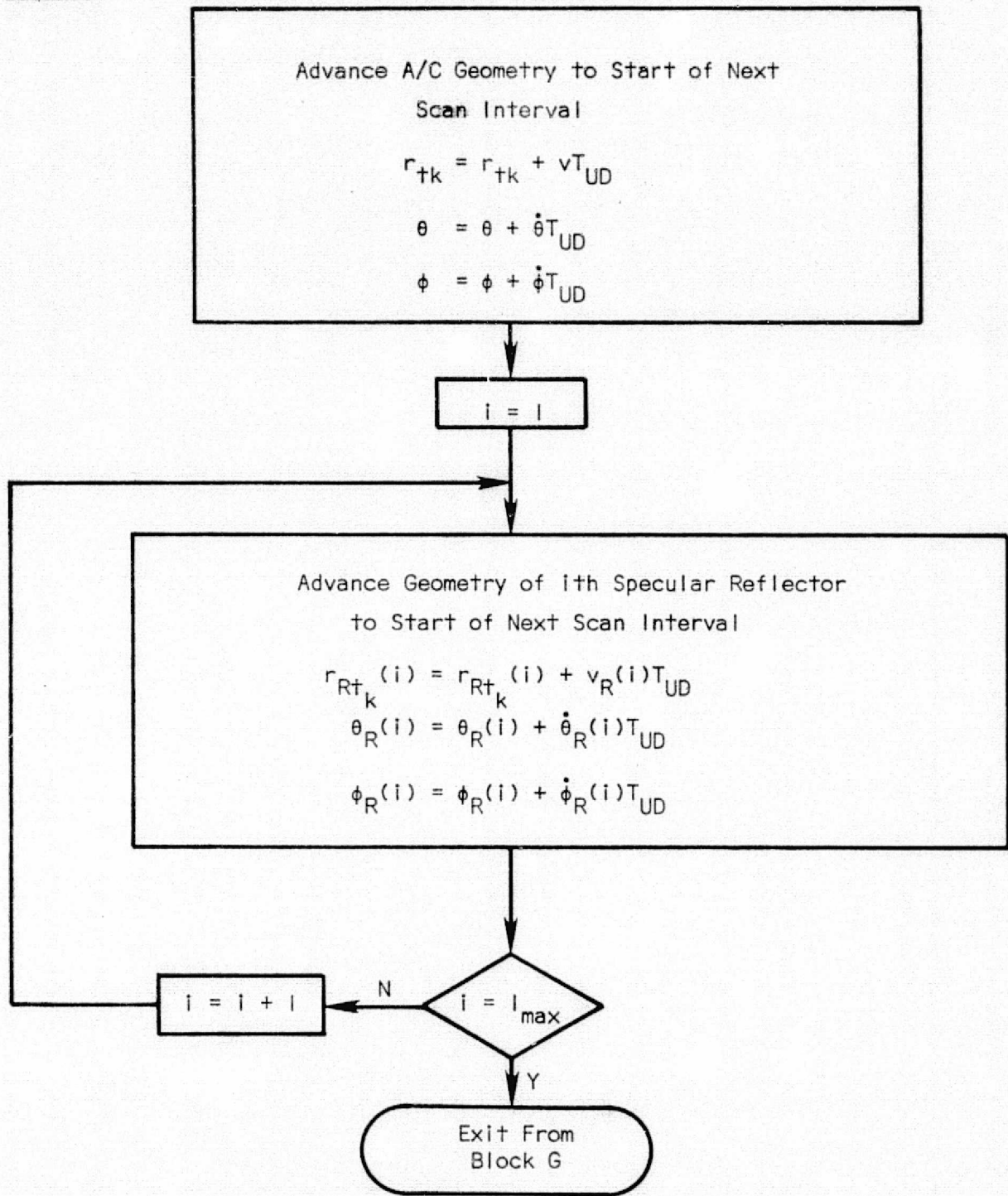


Figure IV-2g Advancing Geometry to Next Scan

BLOCK G

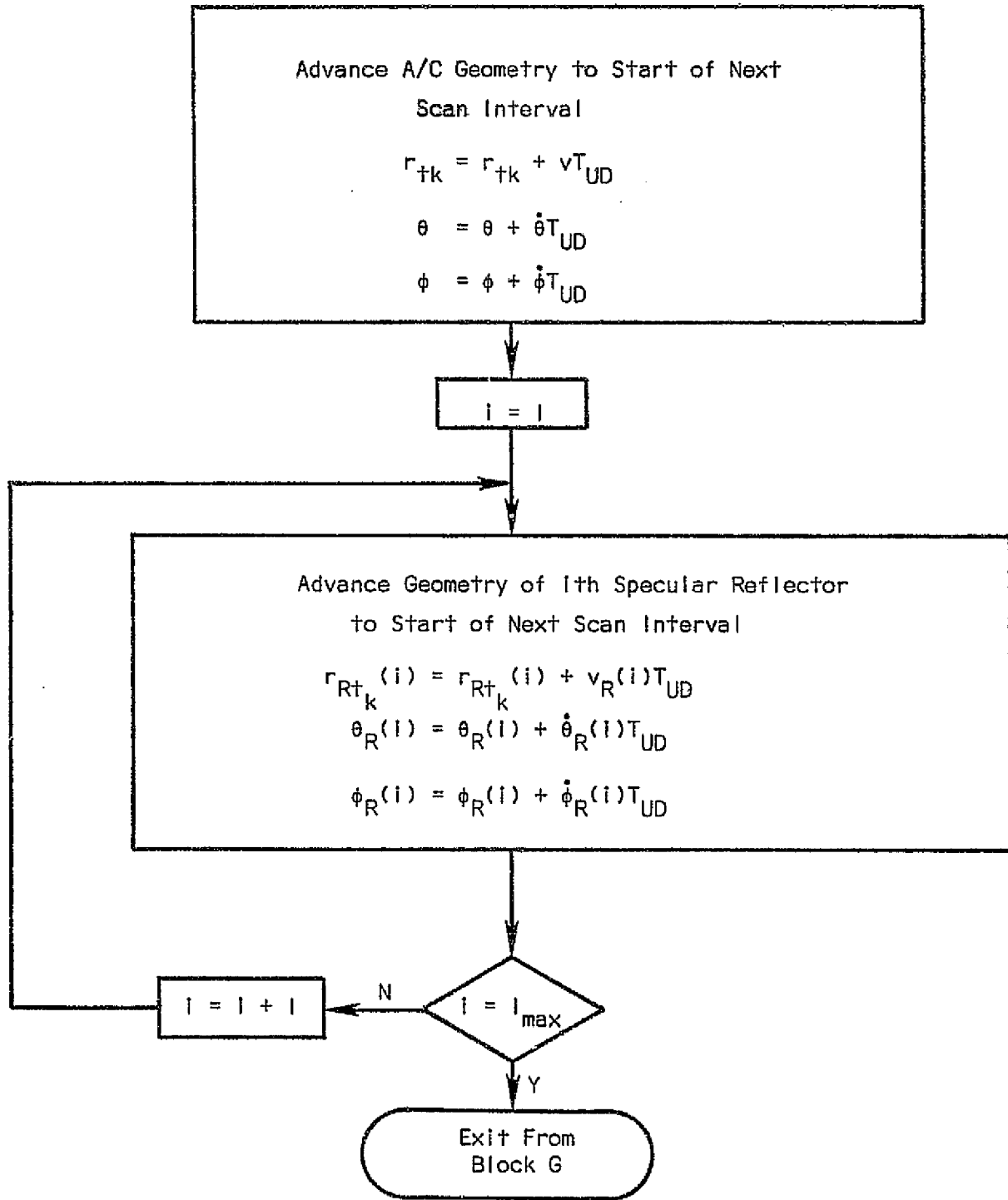
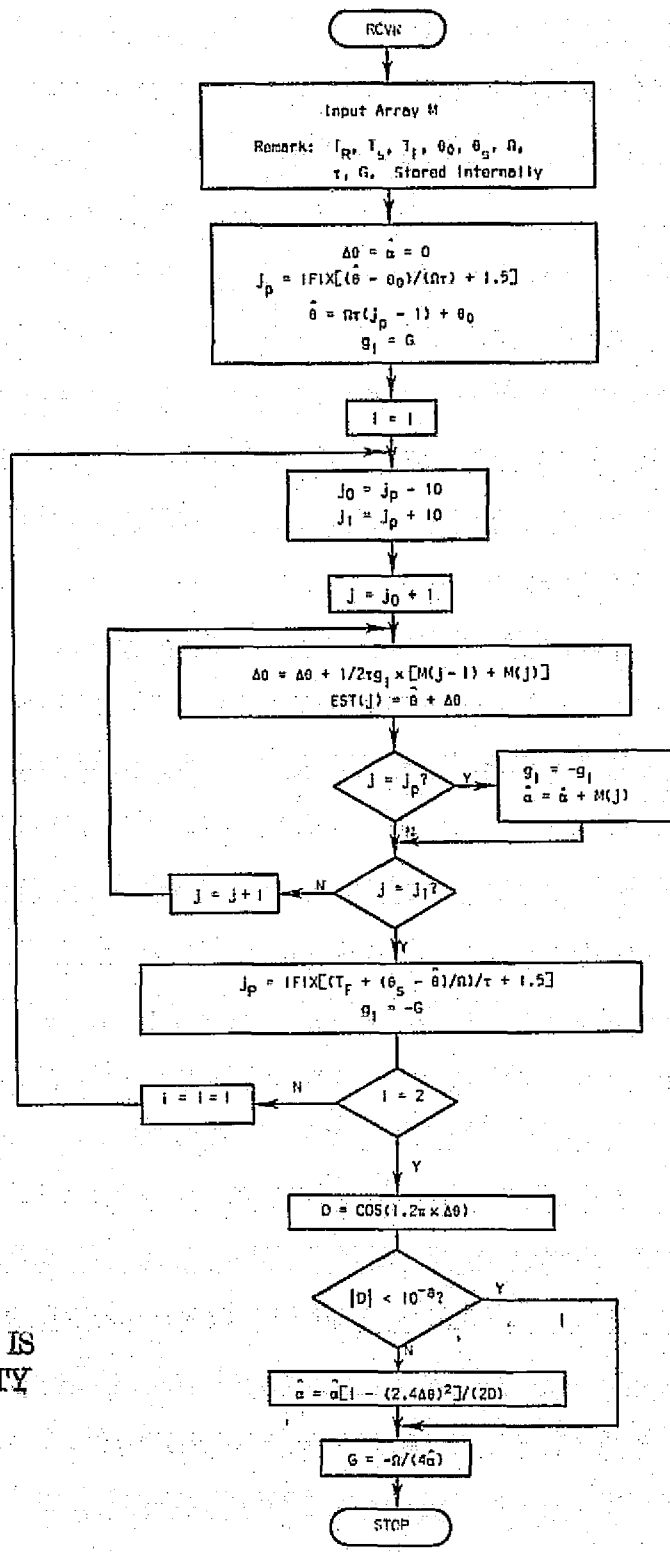
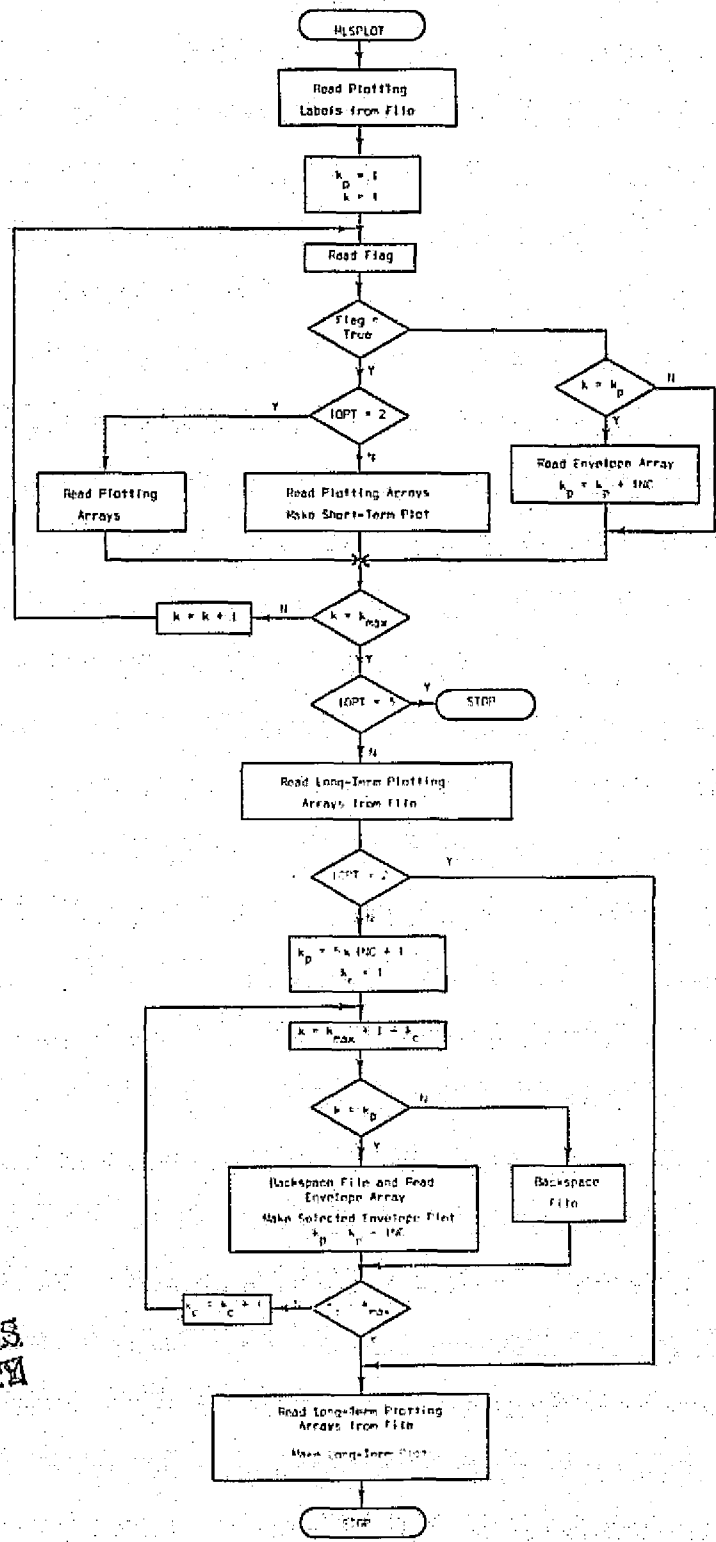


Figure IV-2g Advancing Geometry to Next Scan



ORIGINAL PAGE IS
OF POOR QUALITY

Figure IV-3 Square-Gate Receiver Flowchart



ORIGINAL PAGE IS
OF POOR QUALITY

Figure IV-4 Flowchart for Plotting Program MLSPLOT

Figure	Jobname	SNR(db.)	No. Reflectors	RF Phase Difference at Coincidence	R.M.S. Error	Comments
B-1	MLSRCMP	20	0	-	0.015°	
B-2	MLSRCAZ	8	0	-	0.059°	
B-3	MLSRCJO	8	1	180°	0.247°	
B-4	MLSRCFG	20	1	180°	0.203°	Fade; Greatest Error Coming out of Fade
B-5	MLSRC5C	20	1	0°	0.162°	Phase Enhancement
B-6	MLSRC8E	20	1	90°	0.173°	
B-7	MLSRC7Q	20	1	270°	0.201°	

Figure IV-5 Simulation Results

these quantities may not be very useful comparison measures in general. This is especially true for differing multipath environments, since R.M.S. is a time-averaging process and the multipath interference may be non-stationary. A more useful measure may be peak error, which is available on the plots.

Note in Figure B-4.a how the signal fades when the direct and reflected signals are beam coincident but 180° out of phase (scan 14). Also note that the greatest error in the estimate $\hat{\theta}(k)$ occurs not at the fade, but as the signal comes out of the fade. In Figure B-4.b one can see how the reflected signal envelope moves across the direct signal envelope as the simulation progresses, and how at scan 13 (1 scan before coincidence) the two signals have nearly cancelled each other. This is contrasted with Figure B-5.b, where phase enhancement causes the signal envelope to increase in amplitude on scan 13. Also note that in general the simulation trials with multipath have very low error near the beginning and end of the trials. This is expected, since a reflector removed 3° in azimuth from the A/C would produce an out-of-gate signal envelope pulse.

Conclusion

This study has produced and demonstrated a receiver algorithm of basically intuitive design which has some commendable performance features. The value of the simulation developed for evaluation of candidate algorithms was also demonstrated.

The study of this algorithm suggested two options for further consideration:

1. An algorithm which optimally uses the detected envelope to estimate the A/C angular coordinate.
2. An algorithm not closely coupled to the exact form of the selectivity function $p(\cdot)$, and hence, inherently suboptimal, but perhaps less sensitive to variations in the shape of $p(\cdot)$ arising from cross-coupling of the angle channels and site-to-site design and installation variations, etc.

The simulation appears to be validated in the results presented. The principal use in the near future of this tool will be in the study of optimal tracking algorithms. Some refinements will have to be made as we consider both quadrature detection and envelope detection estimation algorithms. Also, a linear evolution of A/C and/or reflector coordinates seems more plausible in a Cartesian frame than in a spherical system. This modification will be made to test the validity of assumption, equations (2-15) through (2-20), made in signal modeling.

CHAPTER V

CONCLUSIONS AND RECOMMENDATIONS

A summary has been presented of both theoretical and simulation study results, including

1. The development of detailed signal models cast in the time frame of the A/C receiver;
2. Preliminary optimal estimation studies, involving first an application of the locally optimum estimating algorithm to the direct-signal and noise specialization, then a critical overview of some relevant characteristics of recursive state estimation approaches;
3. Design of a suboptimal square-gate tracking algorithm which accepts the baseband output signal of a standard linear AM demodulator, and then evaluation of this algorithm in simulation.

The greater significance of the work done to date is in identifying and bringing into focus concrete problems and problem areas that should be considered, and in suggesting methods of attack.

First among these is the modeling of the total reflection component of the signal; the modeling results described gives support to the belief a random field defined with respect to a low-dimension parameter space may be a suitable model. This would motivate a multipath-adaptive approach.

Another problem stems from our ignorance of the law of evolution of the A/C angular coordinate and the general and unknown variability with time of the law. One approach which should be considered involves simultaneous model identification and state estimation, possibly in a "layered" algorithm with different criteria of estimation optimality for parameters on different levels.

The study of processors using the output of AM detection should be broadened to include both linear and quadratic AM detection, and also an objective to process optimally the detector outputs in calculating

an estimate of the A/C angular coordinate. The most attractive estimation algorithm for the MLS receiver may well come from such an approach.

Finally, in support of the prototype construction effort to be done in the project continuation a number of decisions must be considered and made, dealing with the choice of algorithm, choice of microprocessor and choice of interface equipment. Synchronization and acquisition details must be clarified and a system plan worked out which will allow the microprocessor to perform all its jobs in the requisite real time frame. These tasks are under consideration presently.

REFERENCES

1. "Microwave Landing System," Final Report of the MLS Scanning Beam Working Group, December, 1974.
2. G. A. McAlpine, J. H. Highfill, III, S. H. Irwin, Jr., "Microwave Landing System Airborne Receiver Analysis," Report No. EE-4029-102-75, Research Laboratories for the Engineering Sciences, School of Engineering and Applied Science, University of Virginia, Charlottesville, Virginia, May 1975.
3. James T. Murphy, Jr., "Locally Optimum Estimation with Applications to Communication Theory," Ph.D. Dissertation, University of Florida, 1968.
4. A. P. Sage, J. L. Melsa, Estimation Theory with Applications to Communications and Control, New York: McGraw-Hill, 1971.
5. C. W. Helstrom, Statistical Theory of Signal Detection, London: Pergamon Press, 1960.
6. T. Kailath, "A General Likelihood-Ratio Formula for Random Signals in Gaussian Noise," IEEE Transactions on Information Theory, IT-15:3, May 1969, pp. 350-361.
7. ———, "Likelihood Ratios for Gaussian Processes," IEEE Transactions on Information Theory, IT-16, May 1970, pp. 276-288.
8. ———, "A Further Note on a General Likelihood Formula for Random Signals in Gaussian Noise," IEEE Transactions on Information Theory, IT-16, July 1970, pp. 393-396.

APPENDIX A
COMPUTER PROGRAMS

PROGRAM MLSRCVR(INPUT,OUTPUT,TAPE20)

C
CC MICROWAVE LANDING SYSTEM RECEIVER S.H. IRWIN, JR. 9/1/75
C REVISED 10/3/75C
CC MLS RECEIVER SIMULATION PROGRAM. IN THIS PROGRAM THE RECEIVED SIGNAL IS
C GENERATED AND RECEIVER PERFORMANCE EVALUATED. OUTPUT DATA IS STORED ON A
C PERMANENT FILE, WHICH IS THEN ACCESSED BY A PLOTTING PROGRAM.C
C

C THE FOLLOWING MUST BE ON DATA CARDS AT THE END OF THE PROGRAM:

C
CC IOPT I1
C NAME(I), I=1,3 3A10
C (NRCVR(I), I=1,3), (NRCVR2(I), I=1,3) 6A10
C CHAN 3A10C ERSPEC E20,1
C FC, TUD, THO, THS, TS, TR, BEAMWTH 7E10,2C BIF, ALPHA 2F10,3
C ALPHAM F10,3C SNR F10,3
C THES E20,1C (RA(I), I=1,5) 5E15,1
C IMAX, KMAX 2I10C RTK, V, THETA, DTH, PHI, DPH 6(E10,1)
C RRTK(I), VR(I), THETAR(I), DTHR(I), PHIR(I), DPHR(I), ALPHAR(I), DIFO(I) 8E10,1C (FOR I=1 TO IMAX)
C (PL(I), I=1,5) 5E15,1C
C

C

LOGICAL PLTSCAN, FLAG

REAL M, MPNM, MC, MS, NC, NS

DIMENSION M(2000), DM(2000), RM(2000), TM(2000), EST(2000), ESI(2000)

DIMENSION RRTK(10), THETAR(10), DTHR(10), PHIR(10), DPHR(10)

DIMENSION ALPHAR(10), DIFO(10), TDR(10), PHASER(10), DPHASER(10)

DIMENSION VR(10), NRCVR(3), NAME(3), RT0(10)

DIMENSION CS(30), TMK(30), THER(30), TA(2000)

DIMENSION RA(5), RA1(5), RA2(5), NRCVR2(3), PL(5)

COMMON TR, TS, TF, THO, THS, OMG, TAU

COMMON/PLT/KMAX, ERR, PL

COMMON/SEL/BEAMWTH

COMMON/TRACK/THES, RA

C
C

C INPUT PLOTTING OPTION IOPT, WHERE:

C IOPT=1: GENERATE ALL PLOTS

C IOPT=2: GENERATE LONG-TERM PLOT ONLY

C IOPT=3: GENERATE SHORT-TERM PLOT ONLY

C

READ 11, IOPT

11 FORMAT(I1)

C
C

C INPUT TITLE INFORMATION FOR PLOTTING PROGRAM

C

```

C
C NAME=USERS NAME
C NRCVR=NAME OF RECEIVER ALGORITHM
C NRCVR2=ADDITIONAL RCVR INFORMATION (IF NEEDED)
C CHAN=MLS CHANNEL OF INTEREST
C ERSPEC=ERROR SPEC
C
C READ 10,(NAME(J),J=1,3)
10 FORMAT(6A10)
C READ 10,(NRCVR(J),J=1,3),(NRCVR2(I),I=1,3)
C READ 10,CHAN
C READ 20,ERSPEC
20 FORMAT(E20.1)
C JB=JOBNAME(X)
C DAY=DATE(X)
C WRITE(20) *OPT,NAME,NRCVR,NRCVR2,CHAN,ERSPEC,JB,DAY
C
C
C *****
C * *
C * *
C * INITIALIZATION- INPUT DATA, SET CONSTANTS *
C * *
C * *
C *****
C
C
C SET CONSTANTS AND CONVERSION FACTORS
C
C C=SPEED OF LIGHT IN METERS PER SECOND
C MPNM=METERS PER NAUTICAL MILE
C SPH=SECONDS PER HOUR
C
C C=3.0E8
C PI=3.1415926536
C MPNM=1852.
C SPH=3600.
C
C
C
C INPUT PROPERTIES OF MLS ANGLE FUNCTION
C
C FC=CARRIER FREQUENCY (HZ)
C TUD(UPDATE TIME)-TIME BETWEEN THE START OF A SCAN AND THE START OF
C THE NEXT SCAN OF THE SAME ANGLE FUNCTION.
C TH0(THETA-0)-SCAN ANGLE AT THE BEGINNING OF THE TO SCAN
C THS(THETA-S)-SCAN ANGLE AT THE END OF THE TO SCAN
C TS(SCAN TIME)-LENGTH IN SECONDS OF THE TO SCAN
C TR(REFERENCE TIME)-TIME IN SECONDS BETWEEN ZERO-DEGREE CROSSINGS
C OF THE SCAN ANGLE
C BEAMWTH=BEAMWIDTH OF THE SCANNING ANTENNA PATTERN
C
C READ 100,FC,TUD,TH0,THS,TS,TR,BEAMWTH
100 FORMAT(7E10.2)
C

```



```

C
C INITIALIZE PLTSCAN AND GAUSS
C
C   PLTSCAN=.F.
C   ZZ=GAUSS(SQRT(2.))
C
C
C
C INPUT RECEIVER CONSTANTS
C
C BIF=IF BANDWIDTH
C ALPHA=PEAK DIRECT SIGNAL STRENGTH
C ALPHAM=AMPLITUDE OF SCATTERED MULTIPATH
C SNR=SIGNAL TO NOISE RATIO IN DB
C
C   READ 200,BIF,ALPHA
C   200 FORMAT(2F10.3)
C   READ 300,ALPHAM
C   READ 300,SNR
C   300 FORMAT(F10.3)
C   SIGMA=ALPHA/SQRT(2.0)*10.0**(-SNR/20.0)
C
C
C CALCULATE ALGORITHM CONSTANTS FROM INPUT DATA
C
C
C TAU=TIME IN SECONDS BETWEEN SAMPLES
C OME(OMEGA)=SCAN RATE(DEGREES/SEC)
C TF=TIME IN SECONDS FROM START OF TO SCAN TO START OF FRO SCAN
C JT=TOTAL NUMBER OF SAMPLES
C
C   TAU=1./BIF
C   OME=(IHS-TH0)/TS
C   TF=TS+TR-2.*THS/OMG
C T1=SCAN INTERVAL FROM START OF TO SCAN TO END OF FRO SCAN
C
C   T1=TS+TF
C   JT=1+IFIX(T1*BIF+0.5)
C   WCC=2.*PI*FC/C
C
C
C
C INPUT TRACKING RCVR CONSTANTS:
C
C
C THES=ESTIMATE OF THE A/C ANGULAR POSITION CALCULATED ON THE PREVIOUS SCAN
C RA= ARRAY OF CONSTANTS PECULIAR TO A SPECIFIC TRACKING ALGORITHM (COMPUTED
C EXTERNALLY). RA MUST BE COMPLETELY FILLED. IF 5 PARAMETERS ARE NOT
C REQUIRED, LEFT-OVER POSITIONS ARE SET TO ZERO.
C
C
C   READ 330,THES
C   330 FORMAT(2E20.1)
C   READ 340,(RA(I),I=1,5)
C   340 FORMAT(5E15.1)
C   DO 350 I=1,5
C   RA1(I)=RA(I)

```



```

DPHASED=WCC*V*TAU
C
C
C
C INPUT INITIAL CONDITIONS OF THE ITH REFLECTOR
C
C
IF(IMAX.EQ.0) GO TO 1030
DO 1000 I=1,IMAX
READ 800,RRTK(I),VR(I),THETAR(I),DTHR(I),PHIR(I),DPHR(I),ALPHAR(I)
1,DIF0(I)
800 FORMAT(8E10,1)
PRINT 1513,I
1513 FORMAT(1H0,/,20X,*INITIAL CONDITIONS FOR REFLECTOR*,I2)
PRINT 1512,RRTK(I),VR(I),THETAR(I),DTHR(I),PHIR(I),DPHR(I)
PRINT 1514,ALPHAR(I),DIF0(I)
1514 FORMAT(1H0,10X,*ALPHA=*,F7.2,10X,*PHASE DIF. FROM DIRECT SIGNAL(RA
1D.) =*,E16,8)
IF(I.LE.3) WRITE(20) RRTK(I),VR(I),THETAR(I),DTHR(I),PHIR(I),DPHR(
1I),ALPHAR(I)
RRTK(I)=RRTK(I)*MPNM
VR(I)=VR(I)*MPNM/SPH
1000 CONTINUE
IF(IMAX.GE.3) GO TO 1050
1030 IJ=3-IMAX
DO 1040 I=1,IJ
WRITE(20) C,C,C,C,C,C,C
1040 CONTINUE
C
C
C INPUT SHORT-TERM PLOTTING CONSTANTS:
C
C
C ARRAY PL CONTAINS CONSTANTS FOR ACCESS BY SUBROUTINE SHORT, WHICH DETERMINES
C WHAT SCAN WILL HAVE A DETAILED SHORT-TERM PLOT OF RECEIVER PERFORMANCE.
C IF ARRAY PL IS NOT NEEDED, IT MUST BE FILLED WITH ZEROS.
C
C
1050 READ 340,(PL(I),I=1,5)
PRINT 1515,(PL(I),I=1,5)
1515 FORMAT(1H0,10X,*PL= (*,5(2X,E16,8),*)*)
INC=KMAX/6
INC2=1
ERMS=0,0
C
C
C
C *****
C * *
C * UPDATE GEOMETRY TO KTH SCAN *
C * *
C * *
C *****
C
C
DO 1525 J=1,JT

```

```

      TM(J)=(J-1)*TAU
1525 CONTINUE
      WRITE(20) TM
      DO 50000 K=1,KMAX
      TK=(K-1)*TUD
      IDD=RTK/C
      I1K=TK+IDD
      R=RTK+V*TOD
      PHASED=2.0*PI*(RANF(0.0)-.5)
      PRINT 1517,K,R,THETA,PHI
1517 FORMAT(1H0,///,5X,*SCAN*,I3,10X,*R(METERS)=*,E16.8,5X,*THETA(DEG)
1=*,E16.8,5X,*PHI(DEG) =*,E16.8)
      IF(IMAX.EQ.0) GO TO 2050
      DO 2000 I=1,IMAX
      ZETA=CGS(PHI)*COS(PHIR(I))*COS(THETA-THETA(I))+SIN(PHI)*SIN(PHIR(
1I))
      RAR=SQRT(RTK**2-2.*ZETA*RTK*RRTK(I)+(RRTK(I))**2)
      VAR=(RTK*(V-ZETA*VR(I))+RRTK(I)*(VR(I)-ZETA*V))/RAR
      TDR(I)=(RRTK(I)+RAR)/C
      RR=RRTK(I)+VR(I)*TDR(I)
      RAR=RAR+VAR*TDR(I)
      RT=RR+RAR
      DPHASER(I)=WCC*(VR(I)+VAR)*TAU
      IF(K.NE.1) GO TO 1900
      DIF=DIF0(I)
      R0=R
      RT0(I)=RT
      GO TO 1950
1900 DIF=DIF0(I)-WCC*(RT-RT0(I)-R+R0)
      DO 1800 JK=1,10
      IF(ABS(DIF).LT.2.0*PI) GO TO 1950
      IF(DIF.GT.0.0) DIF=DIF-2.0*PI
      IF(DIF.LT.0.0) DIF=DIF+2.0*PI
1800 CONTINUE
1950 PHASER(I)=PHASED+DIF
      DIFD=DIF*180.0/PI
      PRINT 1518,I,RR,THETA(I),PHIR(I)
1518 FORMAT(1H0,10X,*REFLECTOR*,I3,5X,*R=*,E16.8,5X,*THETA=*,E16.8,5X,*
1PHI=*,E16.8)
      PRINT 1519,DIFD
1519 FORMAT(1H0,10X,*RF PHASE DIFFERENCE FROM DIRECT SIGNAL=*,E16.8,*DE
1GREES*)
2000 CONTINUE
C
C
C GET SAMPLE NUMBERS CORRESPONDING TO DIRECT PATH CENTROIDS
C
2050 JP1=1+IFIX((THETA-TH0)/(TAU*OMG) +0.5)
      JP2=1+IFIX(((THS-THETA)/OMG+TF)/TAU+0.5)
C
C
C
C *****
C *
C * COMPUTE BASEBAND SIGNAL FOR THE KTH SCAN AND STORE SAMPLES
C *
C *

```

```

C *****
C
C
DO 10000 J=1, JT
TSI=(J-1)*TAU
T=T1K+TSI
TA(J)=THA(TSI)
PD=P(TA(J)-THETA)
YDC=PD*COS(PHASED)
YDS=PU*SIN(PHASED)
PHASED=PHASED+DPHASED
YSC=0.
YSS=0.
YMC=YSC
YMS=YSS
IF(IMAX.EQ.0) GO TO 3100
DO 3000 I=1, IMAX
PR=ALPHAR(I)*P(THA(TSI+TDD-TDR(I))-THETA(I))
YRC=PR*COS(PHASER(I))
YRS=PR*SIN(PHASER(I))
YMC=YMC+YRC
YMS=YMS+YRS
PHASER(I)=PHASER(I)+DPHASER(I)
3000 CONTINUE
3100 NC=SIGMA*GAUSS(0.0)
NS=SIGMA*GAUSS(0.0)
MC=YDC+YMC+NC
MS=YDS+YMS+NS
M(J)=SQRT(MC**2+MS**2)
DM(J)=SQRT(YDC**2+YDS**2)
RM(J)=SQRT(YMC**2+YMS**2)
CSG=SQRT((YDC+YMC)**2+(YDS+YMS)**2)
IF(J.EQ.JP1) CS1=CSG
IF(J.EQ.JP2) CS2=CSG
10000 CONTINUE
C
C
C
C *****
C *
C * CALCULATE THE RESPONSE ON THE SCAN INTERVAL OF THE *
C * CANDIDATE RECEIVER ALGORITHM *
C *
C *
C *****
C
C
C
15000 THES1=THES
CALL RCVR(M, JT, EST)
C
C
C STORE VALUES FOR LONG-TERM PLOT
C
C
TMK(K)=TK

```

ORIGINAL PAGE IS
OF POOR QUALITY

```

CS(K)=AMIN1(CS1,CS2)
ERR=THETA-EST(JT)
THER(K)=ERR
ERMS=ERMS+(THER(K))**2
PRINT 1526,EST(JT),THETA,THER(K)
1526 FORMAT(1H0,/,11X,*FINAL ESTIMATE=*,E16.8,5X,*THETA=*,E16.8,5X,*ERR
10R=*,E16.8)
C
C
C
C DECIDE IF SHORT-TERM PLOT IS DESIRED
C IF PLTSCAN IF TRUE,S.T. PLOT HAS ALREADY BEEN MADE
C
C
IF(PLTSCAN)40000,25000
25000 CSK=CS(K)
CALL SHORT(CSK,K,PLTSCAN)
C
C
C IF SHORT RETURNS PLTSCAN=TRUE, A SHORT-TERM PLOT IS TO BE MADE FOR THIS SCAN
IF(PLTSCAN) 26000,40000
C
C
C STORE ON FILE THE ARRAYS NEEDED FOR THE SHORT-TERM PLOT
C
26000 FLAG=.T.
PRINT 26050
26050 FORMAT(1H0,/,*A SHORT-TERM PERFORMANCE PLOT WILL BE MADE FOR THIS
1SCAN*)
EST(JT+1)=THETA
DO 27000 I=1,5
RA2(I)=RA(I)
RA(I)=RA1(I)
27000 CONTINUE
THES2=THES
THES=THES1
CALL RCVR(DM,JT,ESI)
DO 28000 I=1,5
RA(I)=RA2(I)
28000 CONTINUE
THES=THES2
PRINT 28100,ESI(JT)
28100 FORMAT(1H0,10X,*ESTIMATE FOR DIRECT SIGNAL= *,E16.8)
WRITE(20) FLAG
WRITE(20) EST
WRITE(20) M
WRITE(20) RM
WRITE(20) ESI
WRITE(20) TA
WRITE(20) DM
GO TO 43000
40000 FLAG=.F.
WRITE(20) FLAG
C
C
C
C CHECK TO SEE IF THIS IS ONE OF THE 6 SCANS FOR WHICH A SHORT-TERM PLOT OF THE
C RECEIVED SIGNAL IS DESIRED

```

```

C
C
43000 IF(K.NE.INC2) GO TO 45000
      IF(K.GT.1+5*INC) GO TO 45000
C STORE ON FILE THE SAMPLES OF THE RECEIVED SIGNAL (UNLESS THIS IS THE SAME
C SCAN FOR WHICH THE DETAILED SHORT-TERM PLOT IS TO BE MADE).
      IF(.NOT.FLAG) WRITE(20) M
      INC2=INC2+INC
C
C
C UPDATE A/C AND REFLECTOR COORDINATES FOR THE NEXT SCAN
C
C
45000 RTK=RTK+V*TUD
      PRINT 1521,FLAG
      1521 FORMAT(1H0,10X,*FLAG=*,L2)
      THETA=THETA+DTH*TUD
      PHI=PHI+DPH*TUD
      IF(IMAX.EQ.0) GO TO 50000
      DO 41000 I=1,IMAX
        RRTK(I)=RRTK(I)+VR(I)*TUD
        THETAR(I)=THETAR(I)+DTHR(I)*TUD
        PHIR(I)=PHIR(I)+DPHR(I)*TUD
      41000 CONTINUE
      50000 CONTINUE
      ERMS=SQRT(ERMS/KMAX)
C
C
C STORE ON FILE THE ARRAYS NEEDED FOR THE LONG-TERM PLOT
C
C
      WRITE(20)ERMS, TMK, CS, THER
      PRINT 1527
      1527 FORMAT(1H1,9X,*SCAN K*,12X,*TMK(K) (MILLSEC)*,13X,*CS(K)*,17X,*THE
        1R(K) (DEG)*,/)
      DO 60000 K=1,KMAX
        PRINT 1528,K, TMK(K), CS(K), THER(K)
      1528 FORMAT(11X,I3,3(10X,E16.8))
      60000 CONTINUE
      PRINT 1529,ERMS
      1529 FORMAT(1H0,/,11X,*RMS ERROR= *,E16.8)
      STOP
      END

```

FUNCTION GAUSS(X)

```
C
C GAUSSIAN RANDOM NO. GENERATOR S.H. IRWIN, JR. 2/25/75
C
C GAUSS UTILIZES THE FORTRAN RANDOM NO. FUNCTION RANF( ) TO GENERATE RANDOM
C NUMBERS WITH STANDARD GAUSSIAN DISTRIBUTION(ZERO MEAN, UNITY VARIANCE).
C
C THE 1ST CALL TO GAUSS IN THE MAIN PROGRAM SHOULD BE WITH X AS AN IRRATIONAL
C NUMBER(EG.,X=SQRT(2.)) TO INITIALIZE RANF. ALL OTHER CALLS TO GAUSS ARE MADE
C WITH X=0.
C
LOGICAL HAS
IF(X.EQ.0.) GO TO 1000
A=RANF(X)
HAS=.FALSE.
1000 IF(HAS) 2000,3000
2000 GAUSS=SAVED
HAS=.FALSE.
RETURN
3000 A=SQRT(-2.0*ALOG(RANF(0.)))
P=3.141592705
T=2*P*RANF(0.)
SAVED=A*SIN(T)
GAUSS=A*COS(T)
HAS=.TRUE.
RETURN
END
```

ORIGINAL PAGE IS
OF POOR QUALITY

FUNCTION THA(T)

```

C
C THETA-A          S.H. IRWIN, JR.      7/25/75
C
C THA IS THE MLS SCAN ANGLE (XMITTER ANTENNA BORESIGHT ORIENTATION) IN
C DEGREES, WHERE:
C
C TS (SCAN TIME) = TIME IN SECONDS FROM BEGINNING OF TO SCAN UNTIL END OF
C TO SCAN
C TR (REFERENCE TIME) = TIME IN SECONDS FROM WHEN THA=0 IN TO SCAN UNTIL WHEN
C THA=0 DURING FRO SCAN.
C TF = TIME IN SECONDS FROM BEGINNING OF TO SCAN UNTIL BEGINNING OF FRO SCAN
C TH0 (THETA-0) = VALUE OF THA AT BEGINNING OF TO SCAN
C THS (THETA-S) = VALUE OF THA AT BEGINNING OF FRO SCAN
C OMG = OMEGA, THE SCAN RATE IN DEGREES/SECOND.
C
C
C COMMON TR,TS,TF,TH0,THS,OMG,TAU
C T1=TS+TF
C IF(T.GE.0.0) GO TO 50
C THA=TH0
C RETURN
C 50 IF(T.GT.TS) GO TO 100
C THA=TH0+OMG*T
C RETURN
C 100 IF(T.GE.TF) GO TO 200
C THA=THS
C RETURN
C 200 IF(T.GT.T1) GO TO 250
C THA=THS-OMG*(T-TF)
C RETURN
C 250 THA=TH0
C RETURN
C END

```

FUNCTION P(THETA)

```
C
C ANTENNA SELECTIVITY FUNCTION      7/25/75      S.H. IRWIN, JR.
C
C P(THETA) IS THE ANTENNA SELECTIVITY AS A FUNCTION OF THETA, THE DIFFERENCE
C BETWEEN SCAN ANGLE AND AIRCRAFT ANGULAR POSITION (A/C DEVIATION IN DEGREES
C FROM SCANNING ANTENNA BORESIGHT).
C
C IF THE ABSOLUTE VALUE OF (1-A**2) IS LESS THAN MIN, P(A) IS SET TO P(1.0)=PI/4
C (BY L. HOSPITALS RULE).
C
COMMON/SEL/BEAMWTH
MIN=1.0E-10
PI=3.1415926536
A=2.4*THETA/BEAMWTH
B=1.0-A**2
B1=ABS(B)
IF(B1.GT.MIN) GO TO 1000
P=PI/4.0
RETURN
1000 P=ABS(COS(PI*A/2.0))/B
RETURN
END
```

```
SUBROUTINE SHORT(S,K,PS)
LOGICAL PS
DIMENSION PL(5)
COMMON/PLT/KMAX,ERR,PL
PS=.F.
IF(K,EQ,17) PS=.T.
RETURN
END
```

ORIGINAL PAGE IS
OF POOR QUALITY

SUBROUTINE RCVR(M, JT, EST)

```

C
C SQUARE-GATE TRACKING RECEIVER ALGORITHM          S.H. IRWIN, JR.      9/10/75
C
C
REAL M
DIMENSION M(JT), EST(JT), RA(5)
COMMON TR, TS, TF, TH0, THS, OMG, TAU
COMMON/TRACK/THES, RA
PI=3.1415926536
G=RA(1)
DEL=0.0
ALEST=0.0
THES1=THES
JP=IFIX((THES-TH0)/(OMG*TAU)+1.5)
THES=OMG*TAU*FLOAT(JP-1)+TH0
G1=G
PRINT 101
101 FORMAT(1H0,/,11X,*RECEIVER CALCULATIONS:*)
102 FORMAT(1H0,13X,*STARTING ESTIMATE=*,E16.8)
PRINT 102,THES
PRINT 103,G
103 FORMAT(1H,13X,*GATE HEIGHT=*,E16.8)
PRINT 104
104 FORMAT(1H0,13X,*FOR TO AND FRO SCANS, RESPECTIVELY:*,/)
DO 5000 I=1,2
  J0=JP-10
  J1=JP+10
  MN=J0+1
  DO 2000 J=MN,J1
    DEL=DEL+0.5*TAU*G1*(M(J-1)+M(J))
    EST(J)=THES+DEL
    IF(J.NE.JP) GO TO 2000
    G1=-G1
    ALEST=ALEST+M(JP)
  2000 CONTINUE
  PRINT 105,J0,JP,J1,DEL
  105 FORMAT(15X,*J0=*,I5.5X,*JP=*,I5.5X,*J1=*,I5.5X,*DEL=*,E16.8)
  IF(I.EQ.2) GO TO 3000
  DO 2100 J=1,J0
    EST(J)=THES1
  2100 CONTINUE
  MIN=J1+1
  JK=J1
  3000 JP=IFIX((TF+(THS-THES)/OMG)/TAU+1.5)
  G1=-G
  5000 CONTINUE
  THES=EST(J1)
  DEN=COS(1.2*PI*DEL)
  IF(ABS(DEN).LT.1.0E-8) GO TO 5100
  ALEST=ALEST*(1.0-(2.4*DEL)**2)/(2.0*DEN)
  RA(1)=-OMG/(4.0*ALEST)
  5100 DO 5500 J=MIN,J0
    EST(J)=EST(JK)
  5500 CONTINUE
  MN=J1+1
  DO 6000 J=MN,JT

```

EST(J)=EST(J1)
6000 CONTINUE
RETURN
END

ORIGINAL PAGE IS
OF POOR QUALITY

PROGRAM MLSPLOT(INPUT,OUTPUT,TAPE12,TAPE13,TAPE15)

C
C
C TAPE12=PLOT FILE TAPE13=PERMANENT FILE
C THIS PROGRAM PLOTS THE RESULTS OF THE PROGRAM MLSRCVR, WHICH ARE
C STORED FOR A SHORT TIME ON PERMANENT FILE. ALL INFORMATION NEEDED BY
C THIS PROGRAM IS TO BE READ FROM THE FILE IN UNFORMATTED FORM. THE
C ORDER IS AS FOLLOWS, A SLASH DENOTING END-OF-RECORD:
C IOPT,NAME,NRCVR,CHAN,ERSPEC,JB,DAY/
C KMAX,IMAX,ALPHA,ALPHAM,SNR,SIGMA,T1,JT/
C RTK,V,THETA,DTH,PHI,DPH/
C RRTK(1),VR(1),THETAR(1),DTHR(1),PHIR(1),DPHR(1),ALPHAR(1)/
C RRTK(2),VR(2),THETAR(2),DTHR(2),PHIR(2),DPHR(2),ALPHAR(2)/
C RRTK(3),VR(3),THETAR(3),DTHR(3),PHIR(3),DPHR(3),ALPHAR(3)/
C TM/ (SCAN TIME ARRAY)
C DATA FOR DETAILED AND SPECTED SHORT-TERM PLOTS/ (EACH SCAN IS
C REPRESENTED BY A FLAG. IF FLAG= .TRUE., A DETAILED SHORT TERM PLOT
C IS TO BE MADE. PLOTS OF THE COMPOSITE SIGNAL WILL BE MADE FOR SIX
C UNIFORMLY SPACED SCANS, BEGINNING WITH THE FIRST.)
C ESTERR,TK,CS,THEP/
C
C

LOGICAL FLAG

REAL NOISE ,M1,M2

DIMENSION CS(30),THEP(30),TK(30),NOISE(30),TM(2000),Y(2000)

DIMENSION ERSPCA(4),ACPOS(5),SR1POS(5),SR2POS(5),SR3POS(5)

DIMENSION ACRATE(5),SR1RAT(4),SR2RAT(4),SR3RAT(4),DPAMPA(2)

DIMENSION RIAMPA(2),R2AMPA(2),R3AMPA(2),SMA(2),SNRDBA(2),KTKA(2)

DIMENSION ESTCRA(4),NRCVR(3),KMAXA(3),STLBL(3),TRANGL(3),NAME(3)

DIMENSION RRTK(3),VR(3),THETAR(3),DTHR(3),PHIR(3),DPHR(3),ALPHAR(3)
1),NRCVR2(3)

CALL CALCOMP(12)

C
C
C READ INITIALIZATION DATA FROM FILE

READ(13) IOPT,NAME,NRCVR,NRCVR2,CHAN,ERSPEC,JB,DAY

READ(13) KMAX,IMAX,ALPHA,ALPHAM,SNR,SIGMA,T1,JT

READ(13) RTK,V,THETA,DTH,PHI,DPH

DO 10 I=1,3

READ(13) RRTK(I),VR(I),THETAR(I),DTHR(I),PHIR(I),DPHR(I),ALPHAR(I)

10 CONTINUE

C
C
C ENCODE PLOT LABELS

ENCODE(27,5,KMAXA)KMAX

ENCODE(10,10,DPAMPA)ALPHA

ENCODE(10,10,RIAMPA)ALPHAR(1)

ENCODE(10,10,R2AMPA)ALPHAR(2)

ENCODE(10,10,R3AMPA)ALPHAR(3)

ENCODE(10,10,SMA)ALPHAM

ENCODE(45,15,ACPOS)RTK,THETA,PHI

ENCODE(42,20,ACRATE)V,DTH,DPH

ENCODE(41,25,SR1POS)RRTK(1),THETAR(1),PHIR(1)

ENCODE(37,30,SR1RAT)VR(1),DTHR(1),DPHR(1)

ENCODE(41,25,SR2POS)RRTK(2),THETAR(2),PHIR(2)

ORIGINAL PAGE IS
OF POOR QUALITY

```

ENCODE(37,30,SR2RAT)VR(2),DTHR(2),DPHR(2)
FNCODE(41,25,SR3POS)RRTK(3),THETAR(3),PHIR(3)
ENCODE(37,30,SR3RAT)VR(3),DTHR(3),DPHR(3)
SN2=SIGMA*SQRT(2.0)
ENCODE(6,35,SNA)SN2
ENCODE(16,40,SNRDBA)SNR
ENCODE(40,50,ERSPCA)ERSPEC
5 FORMAT(*LONG-TERM PLOT FOR *,I2,* SCANS*)
10 FORMAT(*AMPLITUDE = *,F6.2)
15 FORMAT(*INITIAL A/C POSITION = *,F6.2,*, *,F6.2,*, *,F6.2)
20 FORMAT(*INITIAL A/C RATE = *,F7.2,*, *,F6.2,*, *,F6.2)
25 FORMAT(*INITIAL POSITION = *,F6.2,*, *,F6.2,*, *,F6.2)
30 FORMAT(*INITIAL RATE = *,F6.2,*, *,F6.2,*, *,F6.2)
35 FORMAT(F6.2)
40 FORMAT(*(SNR = *,F5.2,* DB)*)
50 FORMAT(*RMS ERROR SPECIFICATION = *,F6.3,* DEGREES*)
C
C
C READ SCAN TIME AXIS AND SCALE FOR PLOTTING
C
READ(13) TM
CALL SCALE(TM,25.0,JT,1)
VMIN=TM(JT+1)*1000
DELTA=TM(JT+2)*1000
C
C
C INITIALIZE FOR SELECTED SHORT-TERM PLOTS
C
INC=KMAX/6
KPLT=1
DO 6000 K=1,KMAX
READ(13) FLAG
IF(.NOT.FLAG) GO TO 2000
KTRUE=K
IF(K.NE.KPLT) GO TO 4050
KPLT=KPLT+INC
4050 IF(IOPT.NE.2) GO TO 5000
DO 4500 KS=1,6
READ(13) Y
4500 CONTINUE
GO TO 6000
2000 IF(K.EQ.KPLT) GO TO 3000
GO TO 6000
3000 IF(K.GT.5*INC+1) GO TO 6000
KPLT=KPLT+INC
READ(13) Y
GO TO 6000
C
C
C
C *****
C * *
C * *
C * GENERATE DETAILED SHORT-TERM PLOT *
C * *
C * *
C *****
C

```

C
C DRAW EDGES AND FOLDING MARKS

C
5000 LBL=1
GO TO 62000
62100 CONTINUE
READ(13) Y
THETA1=Y(JT+1)
CALL SCALE(Y,2.0,JT,1)
ESI1=Y(JT+1)
EST2=Y(JT+2)
READ(13) Y
CALL SCALE(Y,2.0,JT,1)
S21=Y(JT-2)
READ(13) Y
CALL SCALE(Y,2.0,JT,1)
S22=Y(JT+2)
READ(13) Y
CALL SCALE(Y,2.0,JT,1)
ESI1=Y(JT+1)
ESI2=Y(JT+2)
READ(13) Y
READ(13) Y
CALL SCALE(Y,2.0,JT,1)
S23=Y(JT+2)
M1=0.0
M2=AMAX1(S21,S22,S23)*2.0
BACKSPACE 13
BACKSPACE 13
BACKSPACE 13
BACKSPACE 13
BACKSPACE 13
BACKSPACE 13
READ(13) Y
IF(ESI2.GT.EST2) GO TO 5110
ESI1=EST1
ESI2=EST2
GO TO 5130
5110 EST1=ESI1
EST2=ESI2
EST2=ESI2
5130 Y(JT+1)=EST1
Y(JT+2)=EST2

C
C
C DRAW THE RECEIVER OUTPUT FROM THE COMPOSITE SIGNAL

C
CALL PLOT(0.0,0.2,-3)
S=-EST1/EST2
IF(EST1.GT.0.0) S=0.0
XMAX=T1/TM(JT+2)
XM1=XMAX+0.1
XM2=XMAX+0.2
CALL PLOT(0.0,S,3)
CALL PLOT(XMAX,S,2)
CALL AXIS(0.0,0.0,1H,1,2.0,90.0,EST1,EST2)
S1=(Y(1)-EST1)/EST2+0.1
CALL SYMBOL(0.1,S1,0.14,14H(DEG.),0.0+14)


```

IF(Y(1).GE.1.0) GO TO 5134
CALL SYMBOL(0.5,S1,0.14,1H0,0.0,1)
5134 CALL NUMBER(0.2,S1,0.14,Y(1),0.0,4HF7.2)
C EST
CALL LINE(TM,Y,JT,1,0,0)
S1=(Y(JT)-EST1)/EST2
CALL SYMBOL(XM1,S1,0.14,14H(      DEG.),0.0,14)
IF(Y(JT).GE.1.0) GO TO 5135
XM3=XM2+0.3
CALL SYMBOL(XM3,S1,0.14,1H0,0.0,1)
5135 CALL NUMBER(XM2,S1,0.14,Y(JT),0.0,4HF7.2)
CALL SYMBOL(-2.5,1.56,0.14,9HCANDIDATE,0.0,9)
CALL SYMBOL(-2.5,1.28,0.14,11HRCVR OUTPUT,0.0,11)
CALL SYMBOL(-2.5,1.00,0.14,9H(DEGREES),0.0,9)
CALL SYMBOL(-2.5,0.58,0.14,16HCOMPOSITE SIGNAL,0.0,16)
CALL SYMBOL(-2.5,0.30,0.14,10HPLUS NOISE,0.0,10)
C
C
C DRAW THE COMPOSITE SIGNAL AMPLITUDE VS TIME PLOT
C
READ(13) Y
Y(JT+1)=M1
Y(JT+2)=M2
CALL PLOT(0.0,2.5,-3)
CALL PLOT(XMAX,0.0,2)
CALL AXIS(0.0,0.0,1H ,1,1.0,90.0,Y(JT+1),Y(JT+2))
C M
CALL LINE(TM,Y,JT,1,0,0)
CALL SYMBOL(-2.5,0.7,0.14,12HAMPLITUDE OF,0.0,12)
CALL SYMBOL(-2.5,0.42,0.14,16HCOMPOSITE SIGNAL,0.0,16)
CALL SYMBOL(-2.5,0.14,0.14,10HPLUS NOISE,0.0,10)
C
C
C DRAW THE MULTIPATH AMPLITUDE VS TIME PLOT
C
READ(13) Y
Y(JT+1)=M1
Y(JT+2)=M2
CALL PLOT(0.0,1.5,-3)
CALL PLOT(XMAX,0.0,2)
CALL AXIS(0.0,0.0,1H ,1,1.0,90.0,Y(JT+1),Y(JT+2))
C RM
CALL LINE(TM,Y,JT,1,0,0)
CALL SYMBOL(-2.5,0.7,0.14,12HAMPLITUDE OF,0.0,12)
CALL SYMBOL(-2.5,0.42,0.14,9HMULTIPATH,0.0,9)
CALL SYMBOL(-2.5,0.14,0.14,12HINTERFERENCE,0.0,12)
C
C
C DRAW THE RECEIVER OUTPUT VS TIME PLOT (ONLY DIRECT SIGNAL PRESENT)
C
CALL PLOT(0.0,1.5,-3)
READ(13) Y
Y(JT+1)=ESI1
Y(JT+2)=ESI2
S=-ESI1/ESI2
IF(ESI1.GT.0.0) S=0.0
CALL PLOT(0.0,S,3)
CALL PLOT(XMAX,S,2)

```

```

CALL AXIS(0.0,0.0,0.1H ,1,2.0,90.0,ESI1,ESI2)
S1=(Y(1)-ESI1)/ESI2+0.1
CALL SYMBOL(0.1,S1,0.14,14H(      DEG.),0.0,14)
IF(Y(1).GE.1.0) GO TO 5138
CALL SYMBOL(0.5,S1,0.14,1H0,0.0,1)
5138 CALL NUMBER(0.2,S1,0.14,Y(1),0.0,4HF7,2)
C ESI
CALL LINE(TM,Y,JT,1,0,0)
S1=(Y(JT)-ESI1)/ESI2
CALL SYMBOL(XM1,S1,0.14,14H(      DEG.),0.0,14)
IF(Y(JT).GE.1.0)GO TO 5136
XM3=XM2+0.3
CALL SYMBOL(XM3,S1,0.14,1H0,0.0,1)
5136 CALL NUMBER(XM2,S1,0.14,Y(JT),0.0,4HF7,2)
CALL SYMBOL(-2.5,1.56,0.14,9HCANDIDATE,0.0,9)
CALL SYMBOL(-2.5,1.28,0.14,11HRCVR OUTPUT,0.0,11)
CALL SYMBOL(-2.5,1.00,0.14,9H(DEGREES),0.0,9)
CALL SYMBOL(-2.5,0.58,0.14,11HDIRECT PATH,0.0,11)
CALL SYMBOL(-2.5,0.30,0.14,14HCOMPONENT ONLY,0.0,14)
C
C
C DRAW THE SCAN ANGLE AND DIRECT SIGNAL AMPLITUDE VS TIME PLOTS
C
CALL PLOT(0.0,2.5,-3)
READ(13) Y
CALL SCALE(Y,2.0,JT,1)
S=-Y(JT+1)/Y(JT+2)
CALL PLOT(0.0,S,3)
CALL PLOT(XMAX,S,2)
CALL AXIS(0.0,0.0,0.1H ,1,2.0,90.0,Y(JT+1),Y(JT+2))
C TA
CALL DASHLN(TM,Y,JT,1,0,0)
CALL SYMBOL(-2.5,1.3,0.14,10HSCAN ANGLE,0.0,10)
CALL SYMBOL(-2.5,1.02,0.14,9H(DEGREES),0.0,9)
CALL SYMBOL(-2.5,0.6,0.14,8H(DASHED),0.0,8)
CALL PLOT(0.0,S,-3)
READ(13) Y
Y(JT+1)=M1
Y(JT+2)=M2
C DM
CALL LINE(TM,Y,JT,1,0,0)
CALL AXIS(XMAX,0.0,0.1H ,-1,1.0,90.0,Y(JT+1),Y(JT+2))
CALL SYMBOL(25.25,0.65,0.14,12HAMPLITUDE OF,0.0,12)
CALL SYMBOL(25.25,0.37,0.14,11HDIRECT PATH,0.0,11)
CALL SYMBOL(25.25,0.06,0.14,9HCOMPONENT,0.0,9)
CALL SYMBOL(25.25,-.25,0.14,12H(SOLID LINE),0.0,12)
C
C
C SET ORIGIN AN INCH PAST LAST FOLD AND AT BOTTOM OF PAGE
C
ADJUST=8.9+S
CALL PLOT(26.5,-ADJUST,-3)
C
C
C LABEL TITLE BLOCK
C
ENCODE(27,5100,STLBL)K
5100 FORMAT(*SHORT-TERM PLOT FOR SCAN *,I2)

```

ORIGINAL PAGE IS
OF POOR QUALITY

```

      KTK=(K-1)*75
      ENCODE(15,5150,STLBL2)KTK
5150  FORMAT(*TK = *,I4,*MSEC.*)
      ENCODE(29,5200,TRANGL)THETA1
5200  FORMAT(*A/C AT *,F6.2,* DLGREES AZIMUTH*)
      CALL SYMBOL(1,0,10,22,0,14,STLBL,0,0,27)
      GO TO 64000
64100 CONTINUE
      CALL SYMBOL(.75,.865,0.14,TRANGL,0,0,29)
      CALL SYMBOL(0.75,0.586,0.14,STLBL2,0,0,15)
6000  CONTINUE
      IF(IOPT,EQ,3) GO TO 17000
      READ(13) ESTERR,TKM,CS,THERR
      IF(IOPT,EQ,2) GO TO 16000
      CALL NEWBLOK
      BACKSPACE 13
      KPLT=5*INC+1

```

C
C
C
C
C
C
C
C
C
C
C
C
C
C

```

*****
*
*
*   GENERATE SELECTED SHORT-TERM PLOTS OF THE RECEIVED SIGNAL
*
*
*
*****

```

```

      LBL=2
      N1=1
      GO TO 62000
62200 CONTINUE
      CALL PLOT(0,0,0.2,-3)
      DO 15000 KCOM=1,KMAX
      K=KMAX+1-KCOM
      FLAG=.FALSE.
      IF(K,EQ,KTRUE) GO TO 8000
      IF(K,NE,KPLT) GO TO 14000
      KPLT=KPLT-INC
      BACKSPACE 13
12000 READ(13) Y
      IF(K,EQ,5*INC+1) GO TO 12500
      CALL PLOT(0,0,1.75,-3)
12500 CALL PLOT(25,0,0,0,2)
      IF(N1,NE,1) GO TO 12510
      CALL SCALE(Y,1.0,JT,1)
      AM1=0.0
      AM2=Y(JT+2)
      N1=2
12510 Y(JT+1)=AM1
      Y(JT+2)=AM2
      CALL AXIS(0,0,0,0,1H ,1,1,0,90,0,Y(JT+1),Y(JT+2))
      CALL LINE(TM,Y,JT,1,0,1)
      BACKSPACE 13
      IF(.NOT,FLAG) GO TO 14000
      BACKSPACE 13
14000 BACKSPACE 13

```

15000 CONTINUE

C

C

C LABEL AXES

C

DO 65050 NK=1,6
NSCAN=1+(NK-1)*INC
ENCODE(7,65010,NSCANA)NSCAN

65010 FORMAT(*SCAN *,I2)

KTK=75*(NSCAN-1)

ENCODE(12,65020,KTK)KTK

65020 FORMAT(*TK = *,I4,* MS*)

CALL SYMBOL(-2.5,0.57,0.14,NSCANA,0,0,7)

CALL SYMBOL(-2.5,0.29,0.14,KTK,0,0,12)

IF(NK.EQ.6) GO TO 65050

CALL PLOT(0.0,-1.75,-3)

65050 CONTINUE

CALL PLOT(26.5,-0.9,-3)

CALL SYMBOL(0,0,10.22,0.14,40AMPLITUDE OF COMPOSITE SIGNAL PLUS N
NOISE,0,0,40)

GO TO 64000

64200 CONTINUE

CALL NEWBLOK

GO TO 16000

8000 IF(K.NE.KPLT) GO TO 9000

FLAG=.TRUE.

KPLT=KPLT-INC

DO 11000 KB=1,5

BACKSPACE 13

11000 CONTINUE

GO TO 12000

9000 DO 10000 KB=1,6

BACKSPACE 13

10000 CONTINUE

GO TO 14000

C

C

C

C *****

C *

*

C *

*

C * GENERATE LONG-TERM PLOT *

C *

*

C *

*

C *****

C

C

16000 LBL=3

C

C FILL NOISE ARRAY FOR PLOT

C

DO 68000 KL=1,KMAX

NOISE(KL)=SIGMA*SQRT(2.0)

68000 CONTINUE

C

C

C DRAW THE EDGES AND FOLDING MARKS

C

```

CALL PLOT(0.0,-0.5,3)
CALL PLOT(0.0,10.5,2)
CALL SYMBOL(8.5,-.4,0.21,13,0.0,-1)
CALL SYMBOL(8.5,10.4,0.21,13,0.0,-1)
CALL SYMBOL(14.5,-.4,0.21,13,0.0,-1)
CALL SYMBOL(14.5,10.4,0.21,13,0.0,-1)
CALL PLOT(20.5,-0.5,3)
CALL PLOT(20.5,10.5,2)

C
C
C MOVE ORIGIN TO 3/4 INCH FROM BOTTOM OF PAPER
C
C
C CALL PLOT(0,0.25,-3)
C
C LABEL TOP AXIS
C
CALL SYMBOL(1.5,8.35,0.14,16HAV. AMPLITUDE OF,0.0,16)
CALL SYMBOL(1.5,8.07,0.14,16HCOMPOSITE SIGNAL,0.0,16)
CALL SYMBOL(1.5,7.79,0.14,17HAT TIME OF DIRECT,0.0,17)
CALL SYMBOL(1.5,7.51,0.14,15HSIGNAL CENTROID,0.0,15)
CALL SYMBOL(1.5,7.23,0.14,12H(SOLID LINE),0.0,12)
CALL SYMBOL(1.5,6.67,0.14,15HRMS NOISE LEVEL,0.0,15)
CALL SYMBOL(1.5,6.39,0.14,13H(DASHED LINE),0.0,13)

C
C LABEL BOTTOM AXIS
C
CALL SYMBOL(1.5,2.1,0.14,16HESTIMATION ERROR,0.0,16)
CALL SYMBOL(1.5,1.82,0.14,16H(A/C ANGLE-EST.),0.0,16)
CALL SYMBOL(1.8,1.54,0.14,9H(DEGREES),0.0,9)

C
C MOVE ORIGIN AN INCH TO RIGHT OF LETTERING AND UP
C
C CALL PLOT(4,5,5.5,-3)
C
C SCALE THE DATA FOR THE ERROR PLOT
C
CALL SCALE(TMK,7.0,KMAX,1)
CS(KMAX+1)=0.0
CALL SCALE(CS,4.0,KMAX+1,1)
CS(KMAX+1)=CS(KMAX+2)
CS(KMAX+2)=CS(KMAX+3)
NOISE(KMAX+1)=CS(KMAX+1)
NOISE(KMAX+2)=CS(KMAX+2)

C
C DRAW AXES
C
CALL AXIS(0.0,0.0,0.35HTIME(SEC) SINCE START OF FIRST SCAN,-35,7.0,
10.0,TMK(KMAX+1),TMK(KMAX+2))
CALL AXIS(0.0,0.0,0.1H .1,4.0,90.0,CS(KMAX+1),CS(KMAX+2))

C
C DRAW PLOT WITH AN ASTERISK AT SELECTED POINTS
C
CALL LINE(TMK,CS,KMAX,1,0,0)
IF(IOPT,EQ,2) GO TO 3005
IMX=5*INC+1
DO 3001 I=1,IMX,INC
SX=(TMK(I)-TMK(KMAX+1))/TMK(KMAX+2)

```

ORIGINAL PAGE IS
OF POOR QUALITY

```

S1=(CS(I)-CS(KMAX+1))/CS(KMAX+2)
CALL SYMBOL(SX,S1,0.14,11,0.0,-1)
3001 CONTINUE
SX=(TMK(KTRUE)-TMK(KMAX+1))/TMK(KMAX+2)
S1=(CS(KTRUE)-CS(KMAX+1))/CS(KMAX+2)
CALL SYMBOL(SX,S1,0.14,11,0.0,-1)
3005 CALL DASHLN(TMK,NOISE,KMAX,1,0,0)
C
C MOVE ORIGIN BACK DOWN
C
CALL PLOT(0,0,-5.5,-3)
C
C SCALE ERROR DATA
C
CALL SCALE(THER,4.0,KMAX,1)
C
C COMPUTE TRUE ORIGIN
C
TOR=0.0
IF(THER(KMAX+1).GE.0) GO TO 3111
TOR=-THER(KMAX+1)/THER(KMAX+2)
3111 CONTINUE
C
C DRAW AXES
C
CALL AXIS(0,0,TOR,35HTIME(SEC) SINCE START OF FIRST SCAN,-35,
17,0,0,0,TMK(KMAX+1),TMK(KMAX+2))
CALL AXIS(0,0,0,0,1H,1,4,0,90,0,THER(KMAX+1),THER(KMAX+2))
C
C DRAW PLOT WITH AN ASTERISK AT SELECTED POINTS
C
CALL LINE(TMK,THER,KMAX,1,0,0)
IF(IOPT.EQ.2) GO TO 3006
DO 3009 I=1,IMX,INC
SX=(TMK(I)-TMK(KMAX+1))/TMK(KMAX+2)
S1=(THER(I)-THER(KMAX+1))/THER(KMAX+2)
CALL SYMBOL(SX,S1,0.14,11,0.0,-1)
3009 CONTINUE
SX=(TMK(KTRUE)-TMK(KMAX+1))/TMK(KMAX+2)
S1=(THER(KTRUE)-THER(KMAX+1))/THER(KMAX+2)
CALL SYMBOL(SX,S1,0.14,11,0.0,-1)
C
C MOVE ORIGIN AND CREATE TITLE BLOCK
C
3006 CALL PLOT(9.75,-0.75,-3)
CALL SYMBOL(1,0,10,22,0.14,KMAX,0,0,27)
GO TO 64000
64300 CONTINUE
ENCODE(36,45,ESTERA)ESTERR
45 FORMAT(*RMS ESTIMATION ERROR = *,F5.3,* DEGREES*)
CALL SYMBOL(.75,.865,0.14,16HESTIMATION ERROR,0,0,16)
CALL SYMBOL(.95,.655,0.105,ESTERA,0,0,36)
CALL SYMBOL(.95,.445,0.105,ERSPCA,0,0,40)
IF(IOPT.EQ.2) GO TO 17000
CALL SYMBOL(.75,.165,0.07,11,0,-1)
CALL SYMBOL(.85,.165,0.07,45HSHORT-TERM PLOT OF COMPOSITE SIGNAL A
1AVAILABLE,0,0,45)
CALL SYMBOL(0.75,0.025,0.07,11,0,0,-1)

```



```
1AL MILES, (0.0,47)
CALL SYMBOL(.75,7.84,0.07,41HDEGREES OF AZIMUTH, DEGREES OF ELEVAT
1ION, (0.0,41)
CALL SYMBOL(.75,7.7,0.07,46HRATES SPECIFIED BY VELOCITY IN KNOTS,
1 DEGREES (0.0,46)
CALL SYMBOL(.75,7.56,0.07,35HAZIMUTH/SEC, DEGREES ELEVATION/SEC,
10.0,35)
```

C ADJUST ORIGIN

```
CALL PLOT(0.0,0.5,-3)
CALL SYMBOL(.95,6.78,0.14,11HDIRECT PATH,0.0,11)
CALL SYMBOL(1.05,6.57,0.105,DPAMPA,0.0,18)
CALL SYMBOL(1.05,6.36,0.105,ACPOS,0.0,45)
CALL SYMBOL(1.05,6.15,0.105,ACRATE,0.0,41)
CALL SYMBOL(.95,5.765,0.14,18HSPECULAR MULTIPATH,0.0,18)
IF(IMAX,GE,1)GO TO 64010
CALL SYMBOL(3.2,5.765,0.14,5H-NONE,0.0,5)
GO TO 64020
64010 CALL SYMBOL(.95,5.485,0.1225,11HREFLECTOR 1,0.0,11)
CALL SYMBOL(1.05,5.275,0.105,R1AMPA,0.0,18)
CALL SYMBOL(1.05,5.065,0.105,SR1POS,0.0,41)
CALL SYMBOL(1.05,4.855,0.105,SR1RAT,0.0,37)
IF(IMAX,EQ,1) GO TO 64020
CALL SYMBOL(.95,4.61,0.1225,11HREFLECTOR 2,0.0,11)
CALL SYMBOL(1.05,4.40,0.105,R2AMPA,0.0,18)
CALL SYMBOL(1.05,4.19,0.105,SR2POS,0.0,41)
CALL SYMBOL(1.05,3.98,0.105,SR2RAT,0.0,37)
IF(IMAX,EQ,2) GO TO 64020
CALL SYMBOL(.95,3.735,0.1225,11HREFLECTOR 3,0.0,11)
CALL SYMBOL(1.05,3.525,0.105,R3AMPA,0.0,18)
CALL SYMBOL(1.05,3.315,0.105,SR3POS,0.0,41)
CALL SYMBOL(1.05,3.105,0.105,SR3RAT,0.0,37)
64020 CALL SYMBOL(.95,2.72,0.14,19HSCATTERED MULTIPATH,0.0,19)
CALL SYMBOL(1.05,2.51,0.105,SMA,0.0,18)
CALL SYMBOL(.95,2.125,0.14,24HFRONT-END RECEIVER NOISE,0.0,24)
CALL SYMBOL(1.05,1.915,0.105,3HO =,0.0,3)
CALL PLOT(1.1,2.02,3)
CALL PLOT(1.15,2.02,2)
CALL SYMBOL(1.14,1.915,0.07,1HN,0.0,1)
CALL SYMBOL(1.4,1.915,0.105,SNA,0.0,6)
CALL SYMBOL(1.05,1.705,0.105,SNRDBA,0.0,16)
CALL SYMBOL(.75,1.285,0.14,20HCANDIDATE RECEIVER:,0.0,20)
CALL SYMBOL(1.05,1.075,0.105,NRCVR,0.0,30)
CALL SYMBOL(1.05,0.87,0.105,NRCVR2,0.0,30)
CALL PLOT(0.0,-0.41,-3)
GO TO(64100,64200,64300)LBL
```

C

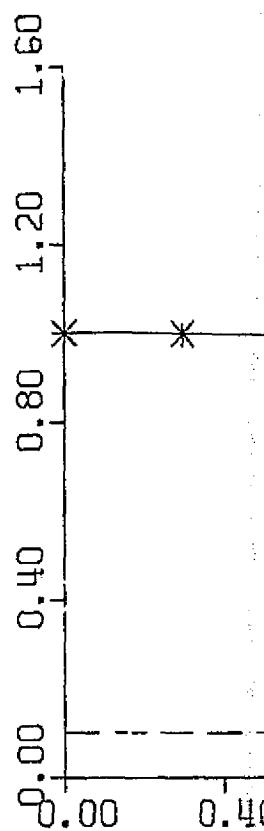
C

```
17000 CALL ENDPLT
STOP
END
```

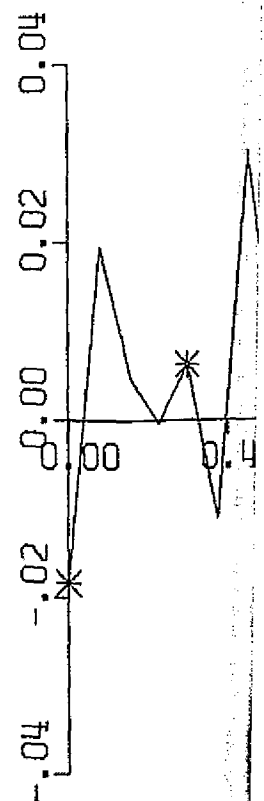

APPENDIX B
COMPUTER PLOTS

AV. AMPLITUDE OF
COMPOSITE SIGNAL
AT TIME OF DIRECT
SIGNAL CENTROID
(SOLID LINE)

RMS NOISE LEVEL
(DASHED LINE)

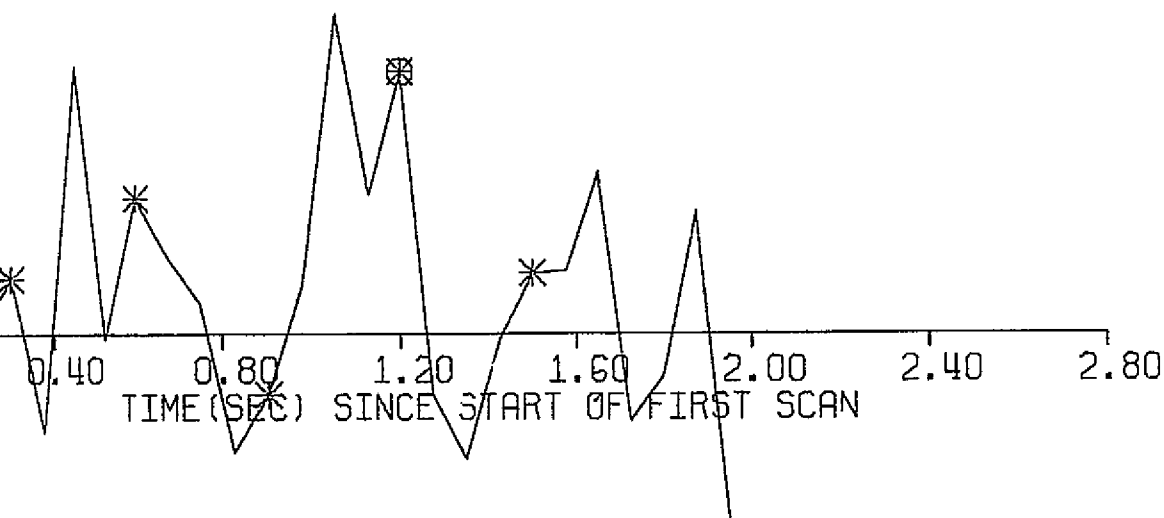
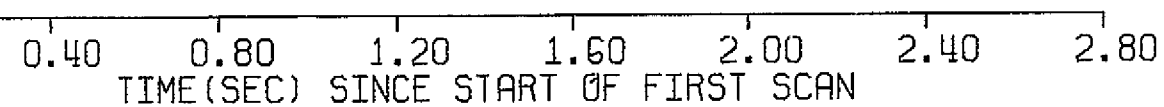
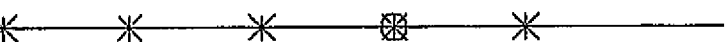


ESTIMATION ERROR
(A/C ANGLE-EST.)
(DEGREES)



PRECEDING PAGE BLANK NOT FILMED

FOLDOUT FRAME |



FOLDOUT FRAME 1

FIGURE B-1.a

LONG-TERM PLOT FOR 27 SCANS

DATE: 10/07/75

PROGRAM: MLSRCVR

JOBNAME: MLSRCMP

S. H. IRWIN, JR.

CHANNEL: AZIMUTH

SIGNAL MAKEUP

POSITION SPECIFIED BY RANGE IN NAUTICAL MILES,
DEGREES OF AZIMUTH, DEGREES OF ELEVATION,
RATES SPECIFIED BY VELOCITY IN KNOTS, DEGREES
AZIMUTH/SEC, DEGREES ELEVATION/SEC.

DIRECT PATH

AMPLITUDE = 1.00

INITIAL A/C POSITION = 10.00, 30.00, 3.00

INITIAL A/C RATE = -300.00, .00, .0

SPECULAR MULTIPATH -NONE

SCATTERED MULTIPATH

AMPLITUDE = .00

FRONT-END RECEIVER NOISE

$\sigma_n = .10$

(SNR = 20.00 DB)

CANDIDATE RECEIVER:

SQUARE GATE TRACKING RECEIVER

(60-BIT WORD LENGTH)

ESTIMATION ERROR

RMS ESTIMATION ERROR = .015 DEGREES

RMS ERROR SPECIFICATION = .010 DEGREES

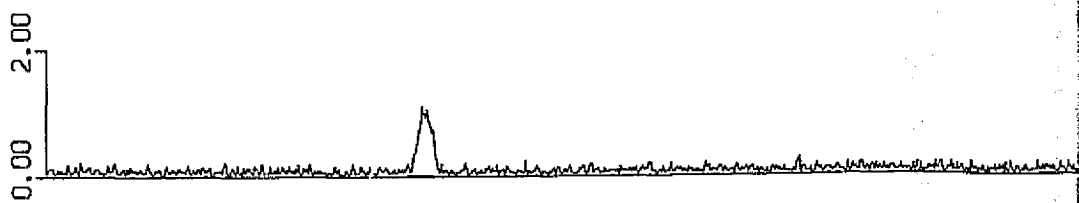
* SHORT-TERM PLOT OF COMPOSITE SIGNAL AVAILABLE
O DETAILED SHORT-TERM PERFORMANCE PLOT AVAILABLE

FOLDOUT FRAME

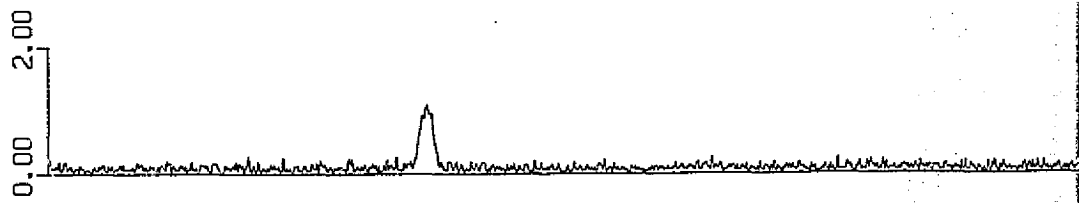
3

C.M.

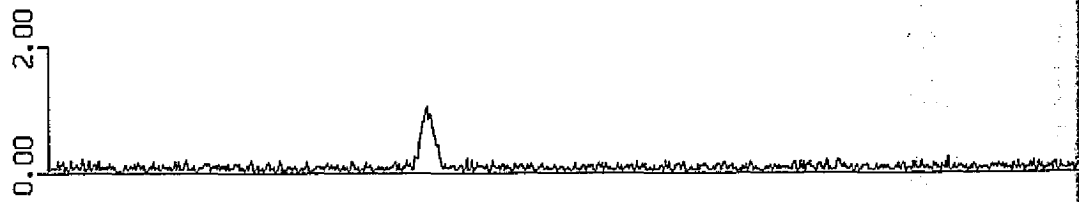
SCAN 1
TK = 0 MS



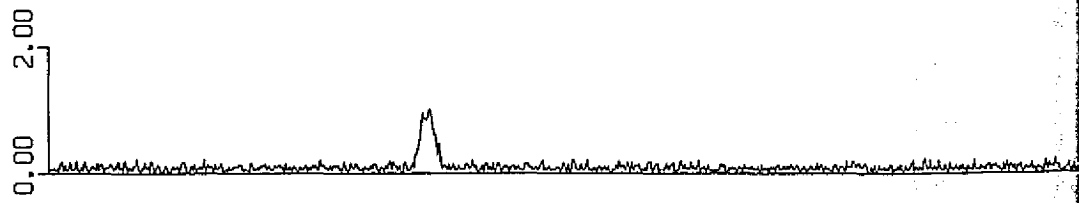
SCAN 5
TK = 300 MS



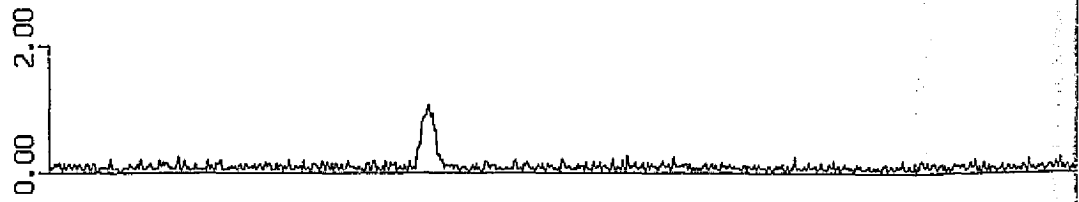
SCAN 9
TK = 600 MS



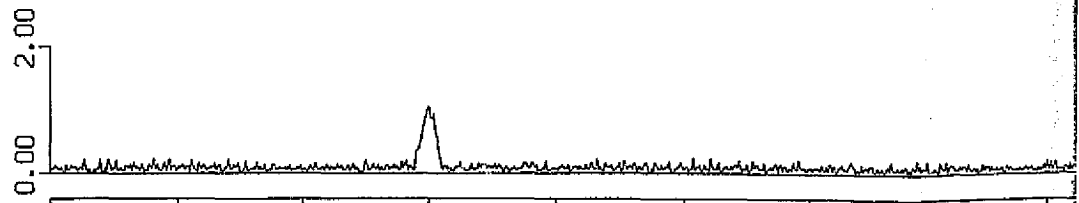
SCAN 13
TK = 900 MS



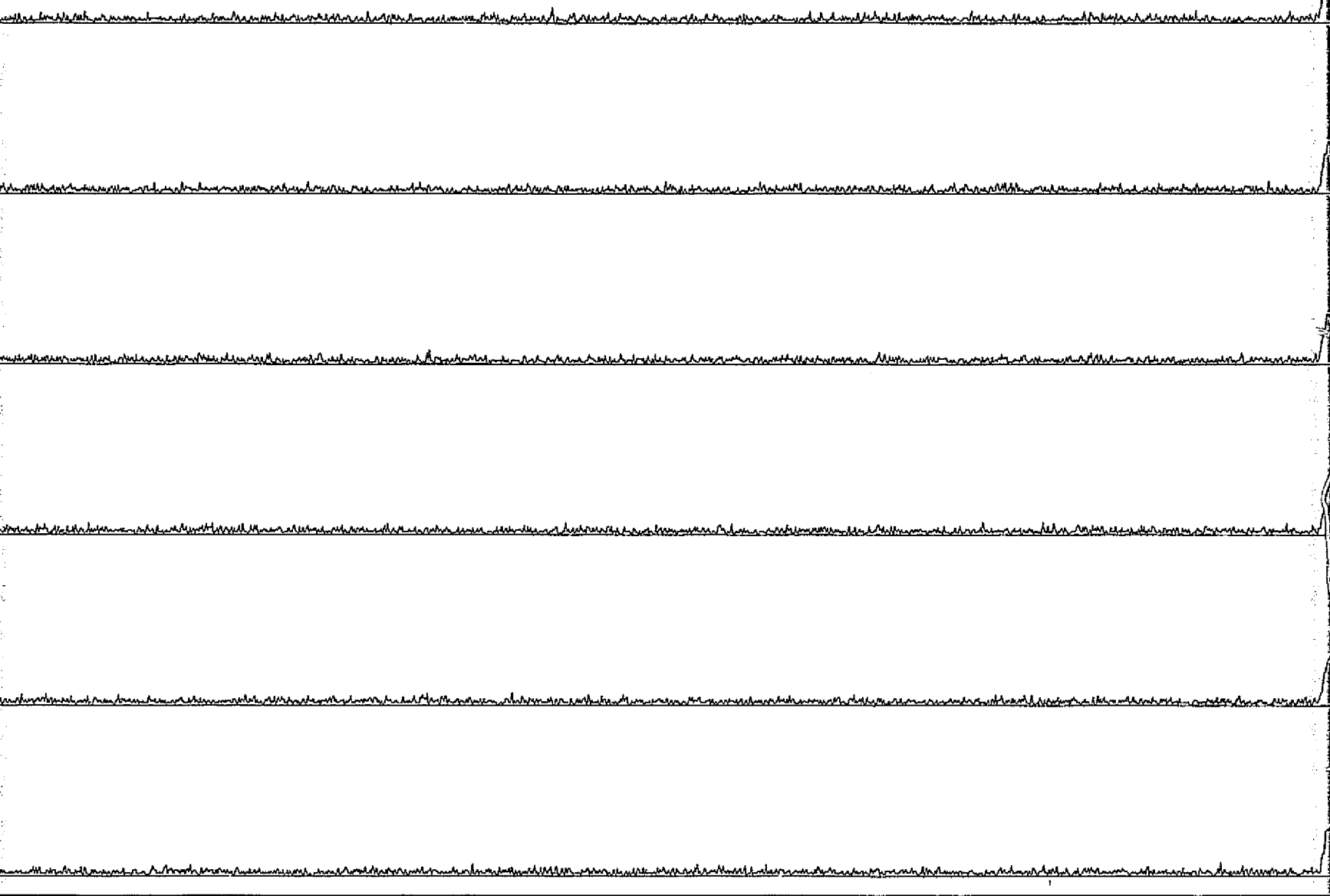
SCAN 17
TK = 1200 MS



SCAN 21
TK = 1500 MS



FOLDBOUT FRAME |



4.00 4.50 5.00 5.50 6.00 6.50 7.00 7.50 8.00 8.50 9.00 9.50 10.00 10.50
RECEIVER SCAN TIME (MILLISECONDS)

FOLDBOUT FRAME 2

FIGURE B-1b

AMPLITUDE OF COMPOSITE SIGNAL, PLUS NOISE

DATE: 10/07/75

PROGRAM: MLSRCVR

JOBNAME: MLSRCMP

S. H. IRWIN, JR.

CHANNEL: AZIMUTH

SIGNAL MAKEUP

POSITION SPECIFIED @ RANGE IN NAUTICAL MILES,
DEGREES OF AZIMUTH, DEGREES OF ELEVATION,
RATES SPECIFIED @ VELOCITY IN KNOTS, DEGREES
AZIMUTH/SEC, DEGREES ELEVATION/SEC.

DIRECT PATH

AMPLITUDE = 1.00

INITIAL A/C POSITION = 10.00, 30.00, 3.00

INITIAL A/C RATE = -300.00, .00, .0

SPECULAR MULTIPATH -NONE

SCATTERED MULTIPATH

AMPLITUDE = .00

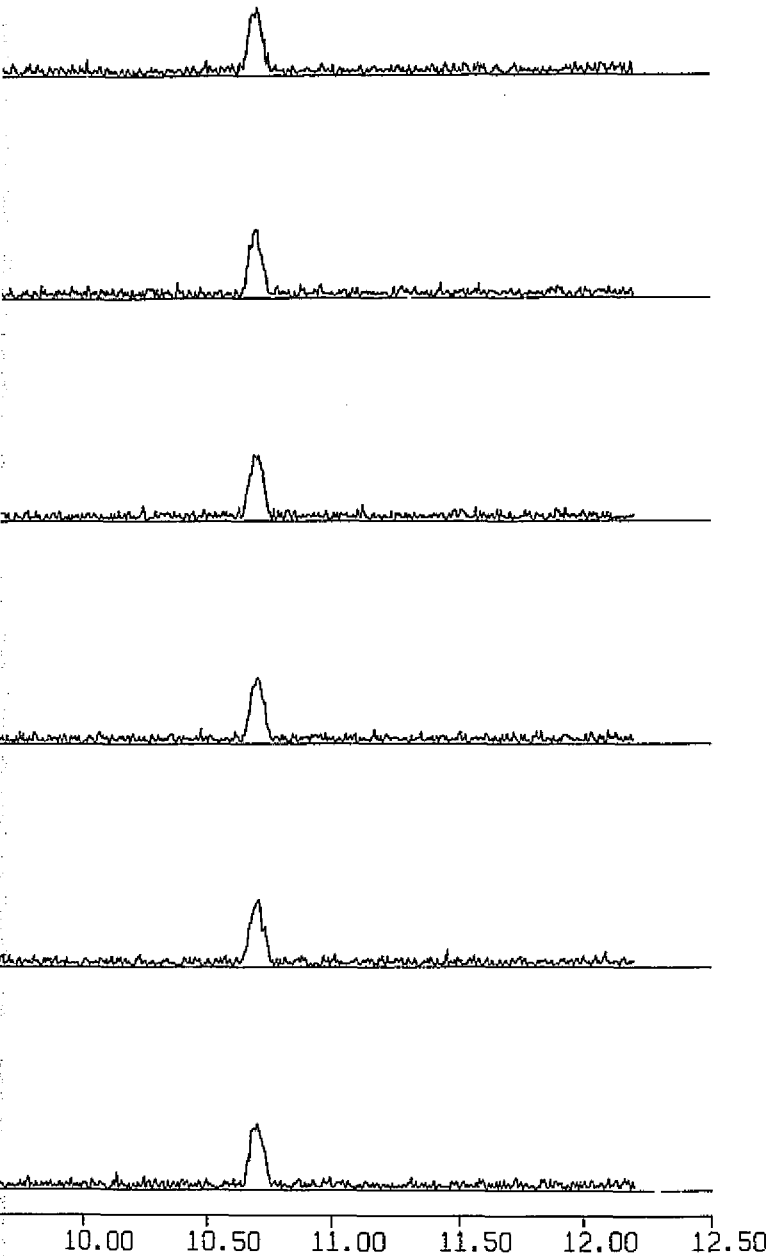
FRONT-END RECEIVER NOISE

$\sigma_n = .10$

(SNR = 20.00 DB)

CANDIDATE RECEIVER:

SQUARE GATE TRACKING RECEIVER
(60-BIT WORD LENGTH)



FOLBOUT FRAME 5

SCAN ANGLE
(DEGREES)
(DASHED)

CANDIDATE
RCVR OUTPUT
(DEGREES)

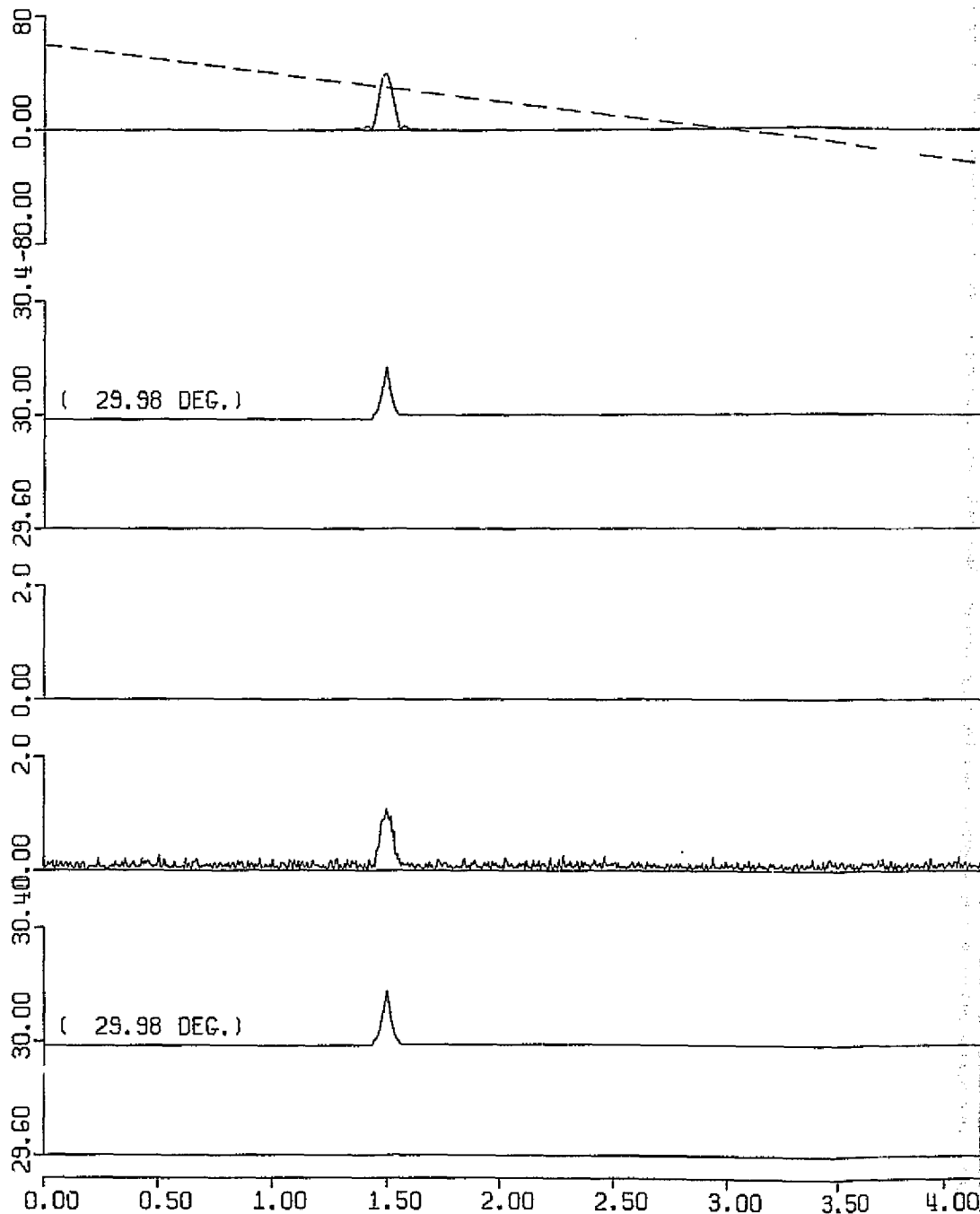
DIRECT PATH
COMPONENT ONLY

AMPLITUDE OF
MULTIPATH
INTERFERENCE

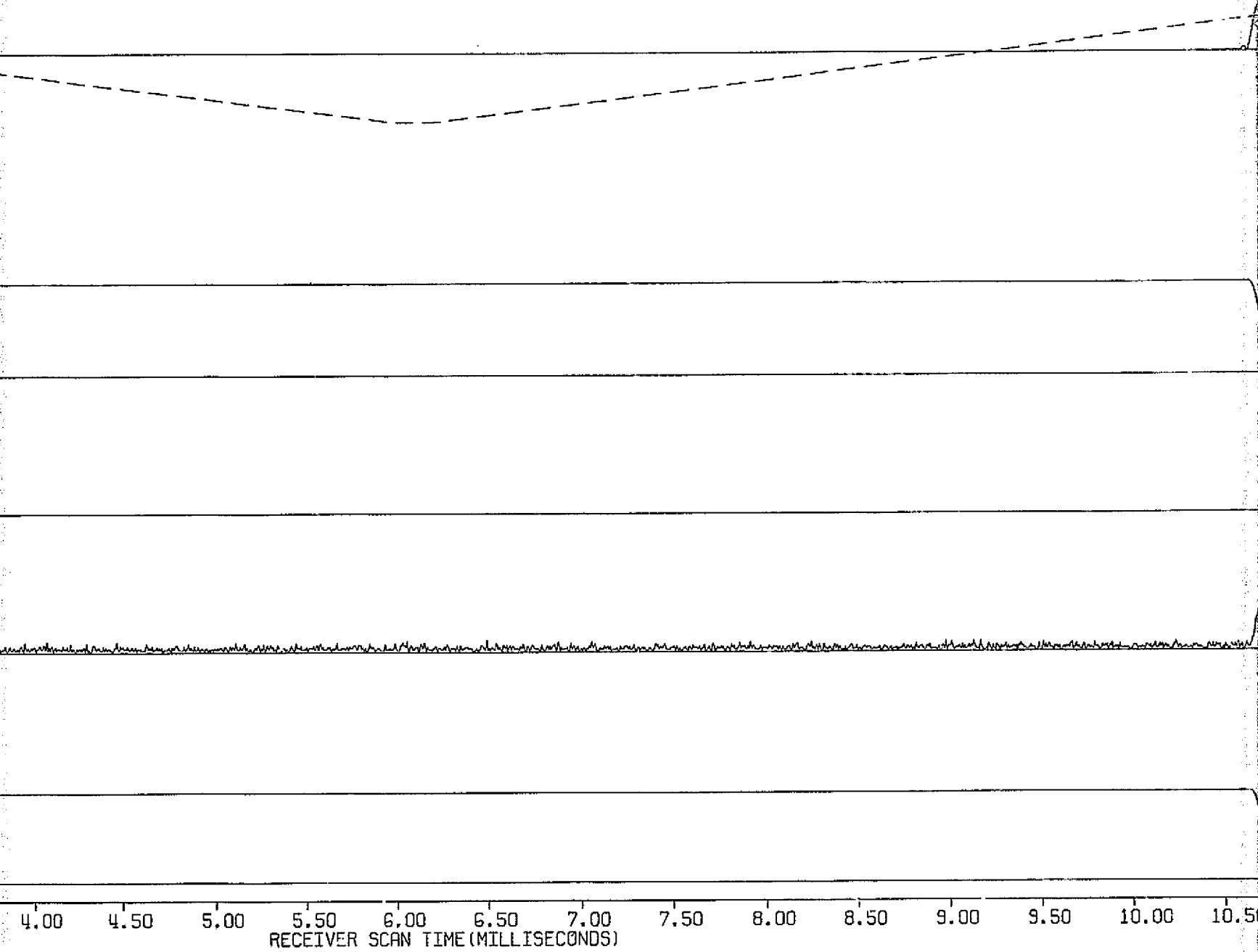
AMPLITUDE OF
COMPOSITE SIGNAL
PLUS NOISE

CANDIDATE
RCVR OUTPUT
(DEGREES)

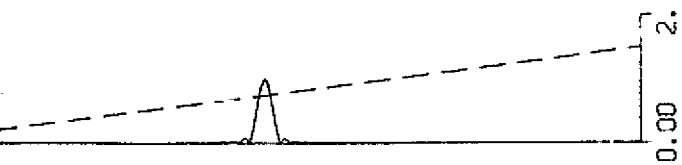
COMPOSITE SIGNAL
PLUS NOISE



FOLDOUT FRAME



FOLDOUT FRAME 2



AMPLITUDE OF
DIRECT PATH
COMPONENT
(SOLID LINE)

FIGURE B-1.c

SHORT-TERM PLOT FOR SCAN 17

DATE: 10/07/75

PROGRAM: MLSRCVR

JOBNAME: MLSRCMP

S. H. IRWIN, JR.

CHANNEL: AZIMUTH

SIGNAL MAKEUP

POSITION SPECIFIED BY RANGE IN NAUTICAL MILES,
DEGREES OF AZIMUTH, DEGREES OF ELEVATION,
RATES SPECIFIED BY VELOCITY IN KNOTS, DEGREES
AZIMUTH/SEC, DEGREES ELEVATION/SEC

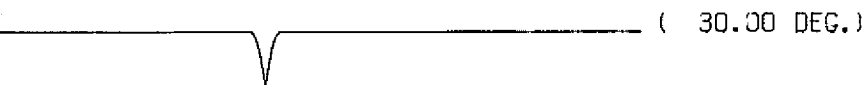
DIRECT PATH

AMPLITUDE = 1.00

INITIAL A/C POSITION = 10.00, 30.00, 3.00

INITIAL A/C RATE = -300.00, .00, .0

SPECULAR MULTIPATH -NONE



SCATTERED MULTIPATH

AMPLITUDE = .00

FRONT-END RECEIVER NOISE

$\sigma_n = .10$

(SNR = 20.00 DB)

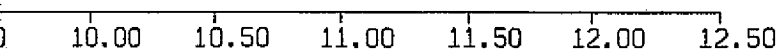
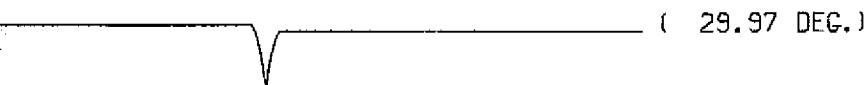
CANDIDATE RECEIVER:

SQUARE GATE TRACKING RECEIVER

(60-BIT WORD LENGTH)

A/C AT 30.00 DEGREES AZIMUTH

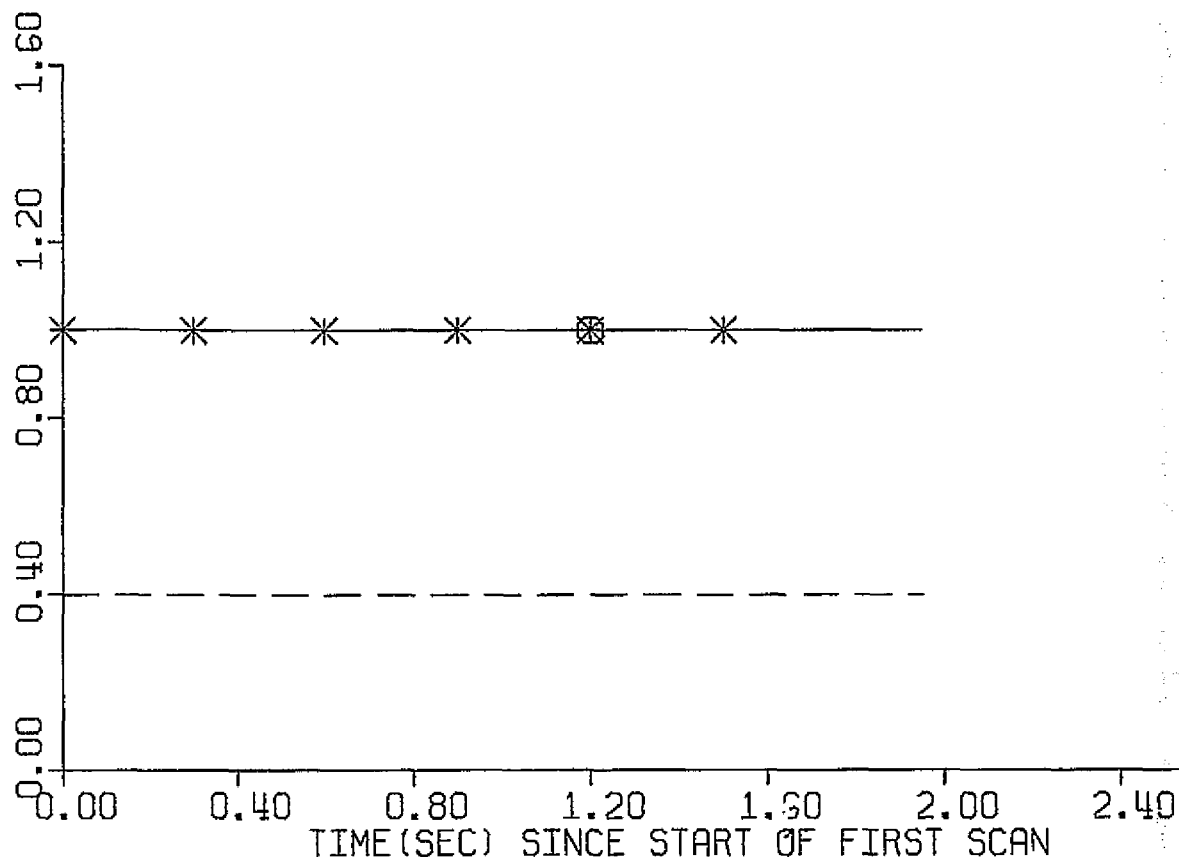
TK = 1200MSEC.



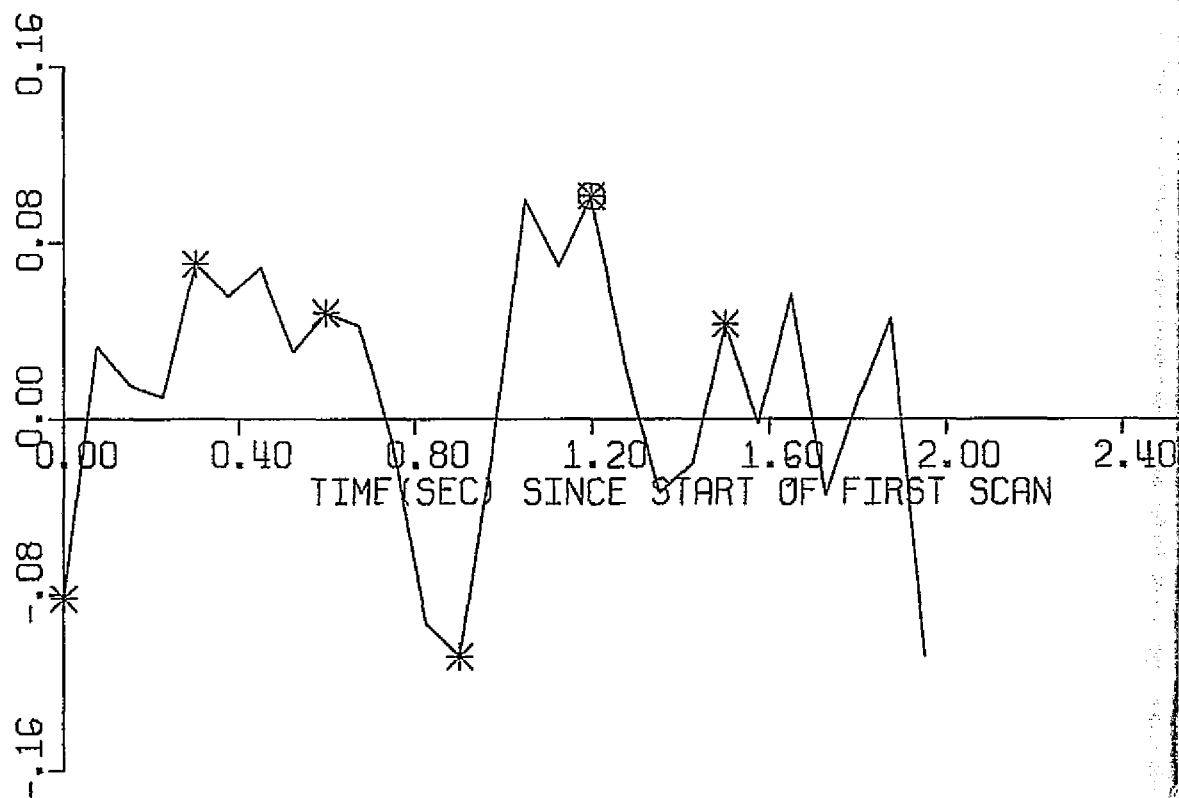
FOLOUT FRAME

AV. AMPLITUDE OF
COMPOSITE SIGNAL
AT TIME OF DIRECT
SIGNAL CENTROID
(SOLID LINE)

RMS NOISE LEVEL
(DASHED LINE)



ESTIMATION ERROR
(A/C ANGLE-EST.)
(DEGREES)



FOLIOUR FRAME (

FIGURE B-2.a

LONG-TERM PLOT FOR 27 SCANS

DATE: 10/08/75

PROGRAM: MLSRCVR

JOBNAME: MLSRCAZ

S. H. IRWIN, JR.

CHANNEL: AZIMUTH

SIGNAL MAKEUP

POSITION SPECIFIED BY RANGE IN NAUTICAL MILES,
DEGREES OF AZIMUTH, DEGREES OF ELEVATION.
RATES SPECIFIED BY VELOCITY IN KNOTS, DEGREES
AZIMUTH/SEC, DEGREES ELEVATION/SEC.

DIRECT PATH

AMPLITUDE = 1.00

INITIAL A/C POSITION = 10.00, 30.00, 3.00

INITIAL A/C RATE = -300.00, .00, .0

SPECULAR MULTIPATH -NONE

2.40 2.80

SCATTERED MULTIPATH

AMPLITUDE = .00

FRONT-END RECEIVER NOISE

$\sigma_n = .40$

(SNR = 8.00 DB)

2.40 2.80

CANDIDATE RECEIVER:

SQUARE GATE TRACKING RECEIVER
(60-BIT WORD LENGTH)

ESTIMATION ERROR

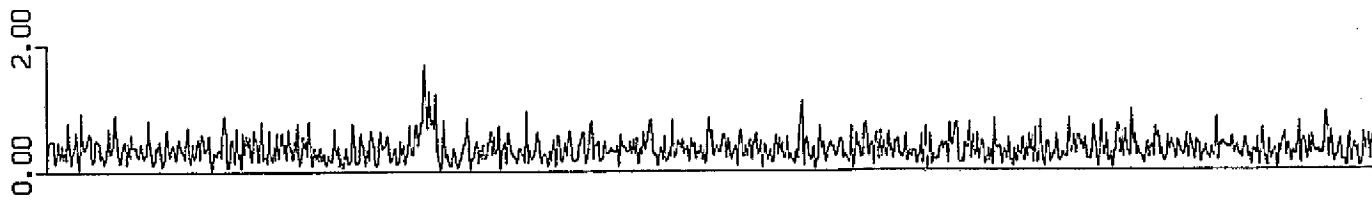
RMS ESTIMATION ERROR = .059 DEGREES

RMS ERROR SPECIFICATION = .010 DEGREES

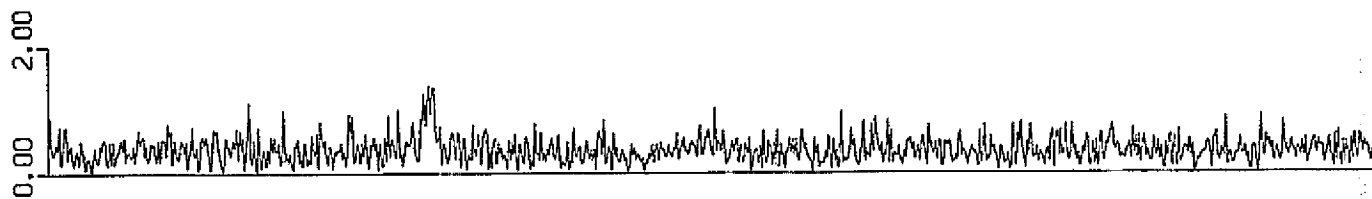
* SHORT-TERM PLOT OF COMPOSITE SIGNAL AVAILABLE
© DETAILED SHORT-TERM PERFORMANCE PLOT AVAILABLE

FOLIOUT FRAME

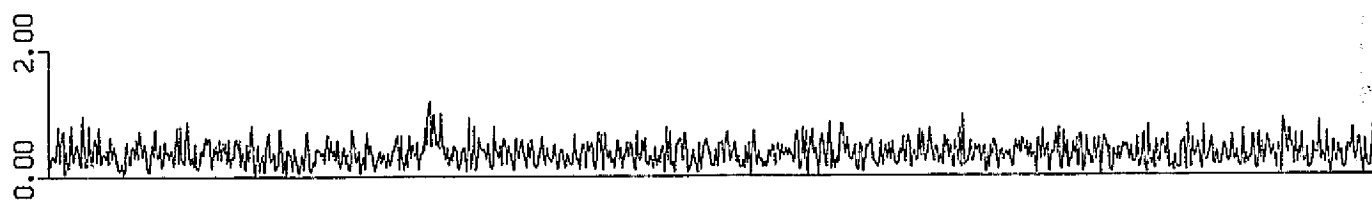
SCAN 1
TK = 0 MS



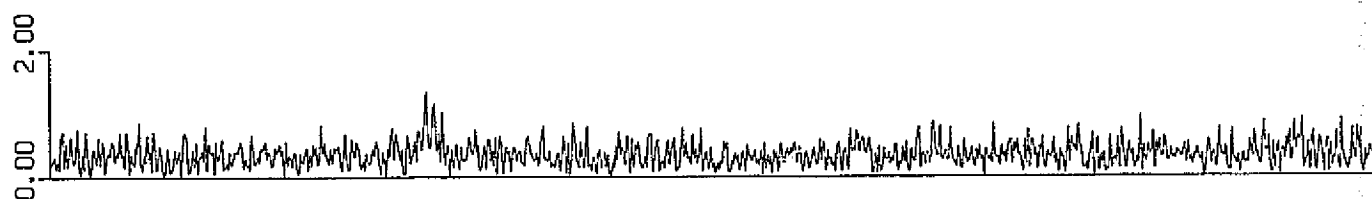
SCAN 5
TK = 300 MS



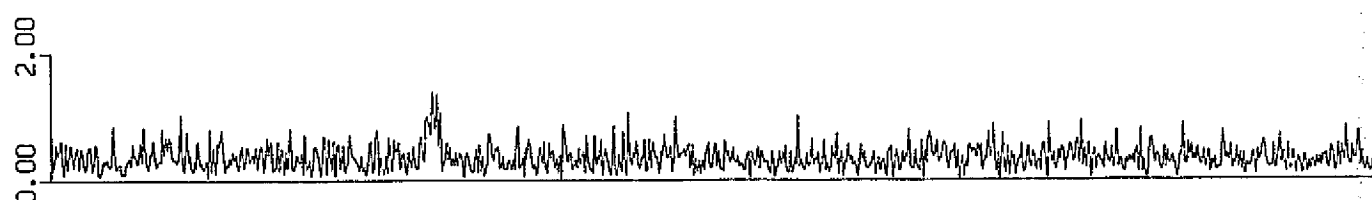
SCAN 9
TK = 600 MS



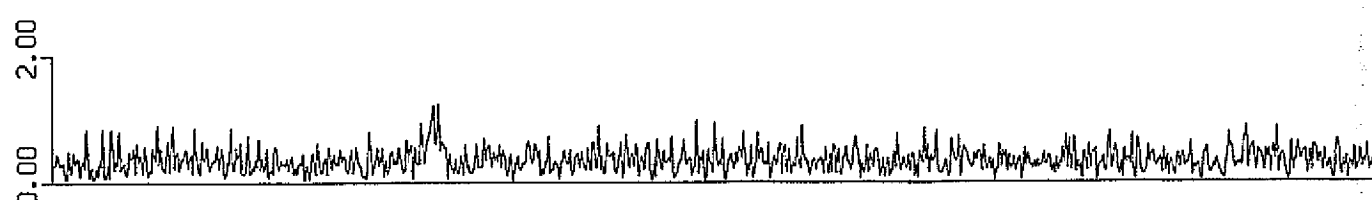
SCAN 13
TK = 900 MS



SCAN 17
TK = 1200 MS

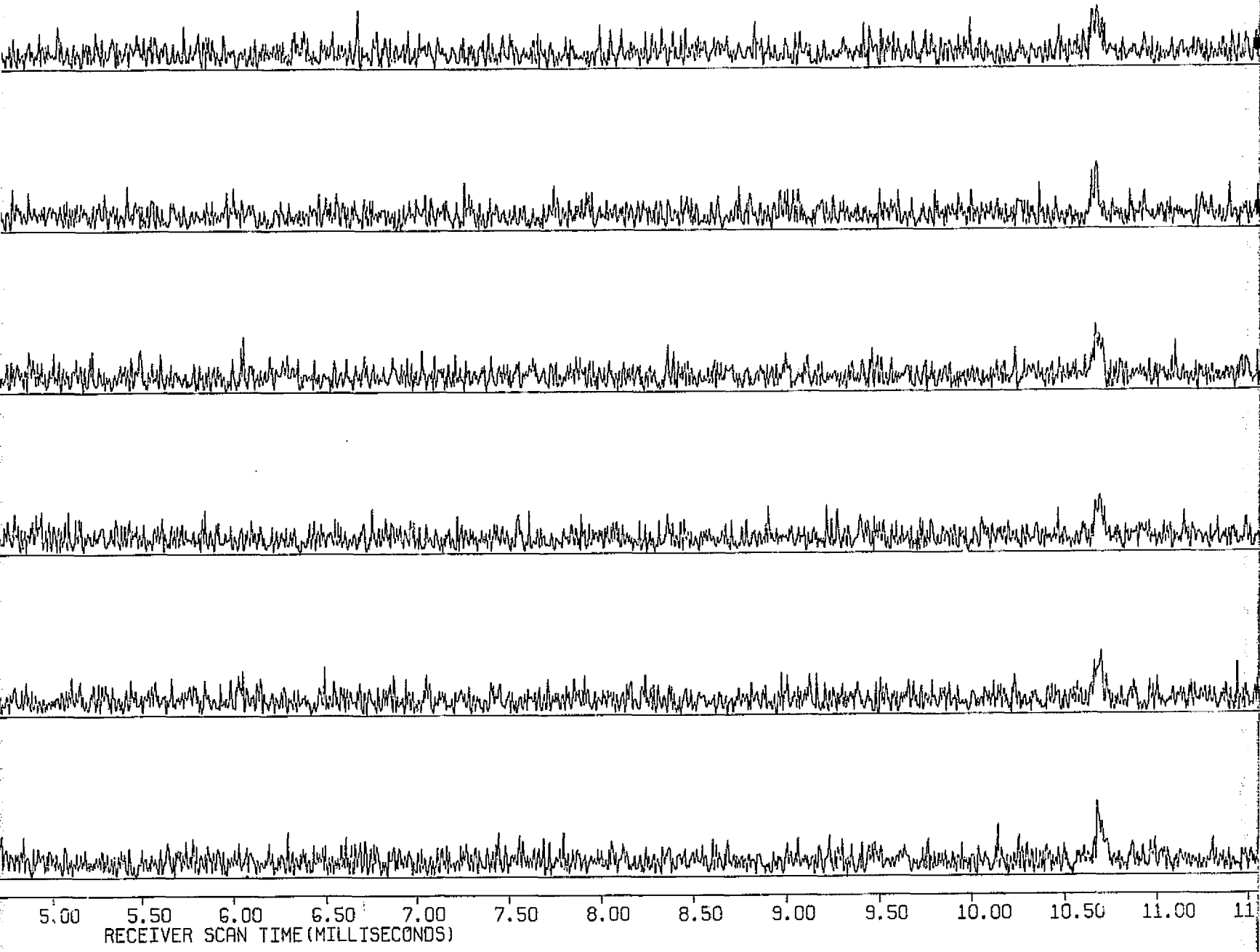


SCAN 21
TK = 1500 MS



.00 0.50 1.00 1.50 2.00 2.50 3.00 3.50 4.00 4.50 5.00

FOLDBOUT FRAME |



FOLDOUT FRAME ²

FIGURE B-2.b

AMPLITUDE OF COMPOSITE SIGNAL PLUS NOISE

DATE: 10/08/75

PROGRAM: MLSRCVR

JOBNAME: MLSRCVZ

S. H. IRWIN, JR.

CHANNEL: AZIMUTH

SIGNAL MAKEUP

POSITION SPECIFIED BY RANGE IN NAUTICAL MILES,
DEGREES OF AZIMUTH, DEGREES OF ELEVATION,
RATES SPECIFIED BY VELOCITY IN KNOTS, DEGREES
AZIMUTH/SEC, DEGREES ELEVATION/SEC.

DIRECT PATH

AMPLITUDE = 1.00

INITIAL A/C POSITION = 10.00, 30.00, 3.00

INITIAL A/C RATE = -300.00, .00, .0

SPECULAR MULTIPATH -NONE

SCATTERED MULTIPATH

AMPLITUDE = .00

FRONT-END RECEIVER NOISE

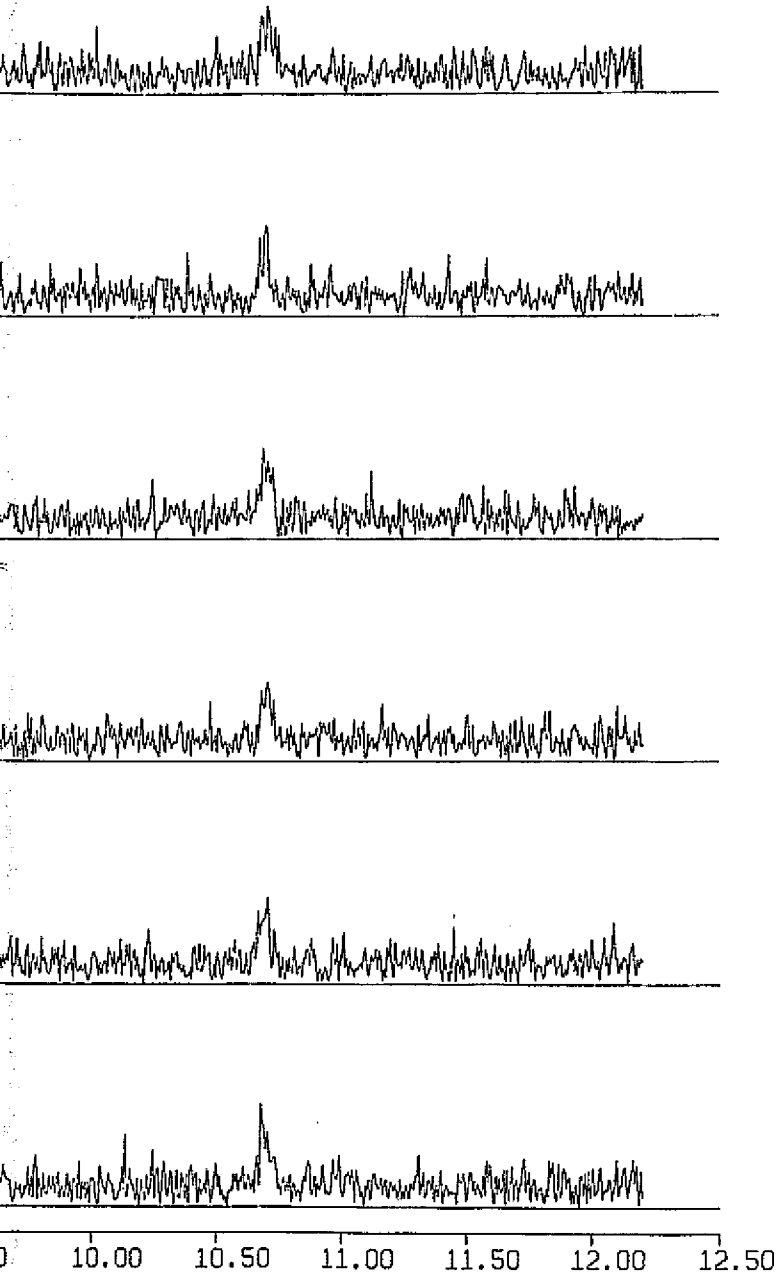
$\sigma_n = .40$

(SNR = 8.00 DB)

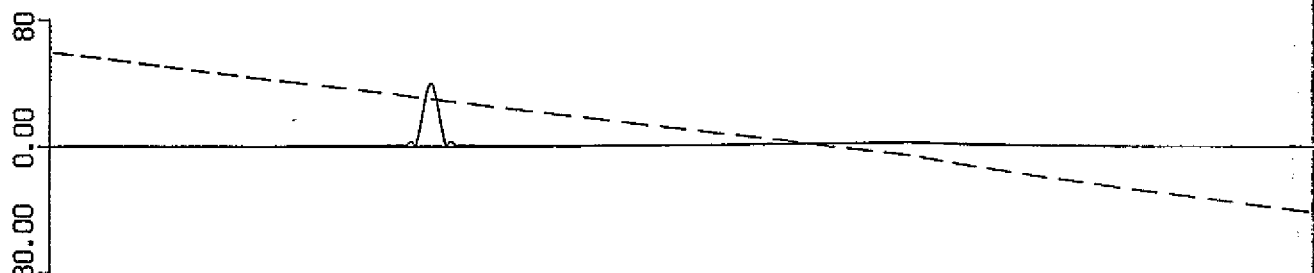
CANDIDATE RECEIVER:

SQUARE GATE TRACKING RECEIVER

(60-BIT WORD LENGTH)



SCAN ANGLE
(DEGREES)
(DASHED)



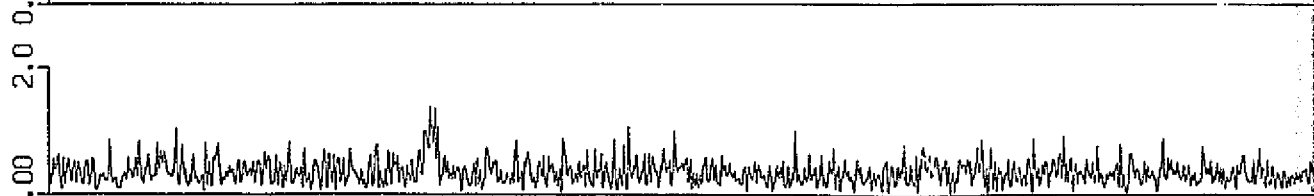
CANDIDATE
RCVR OUTPUT
(DEGREES)
DIRECT PATH
COMPONENT ONLY



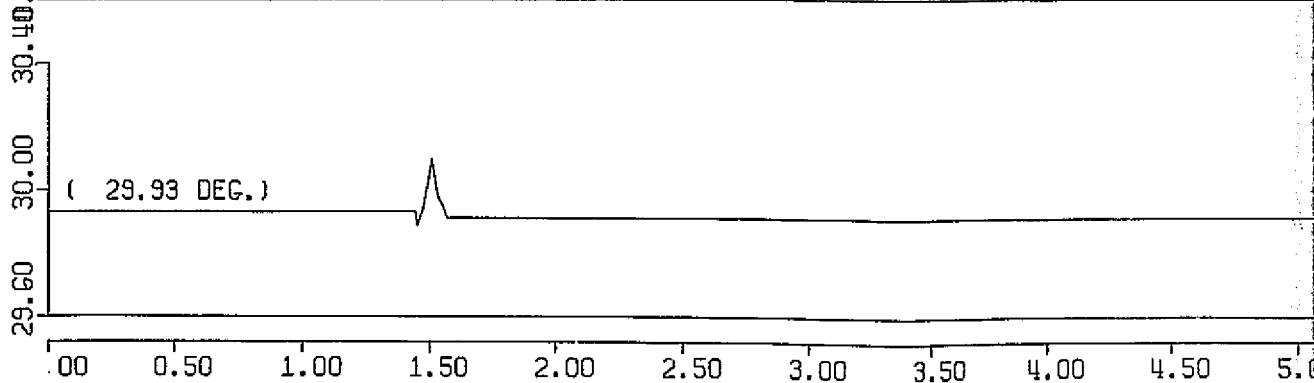
AMPLITUDE OF
MULTIPATH
INTERFERENCE

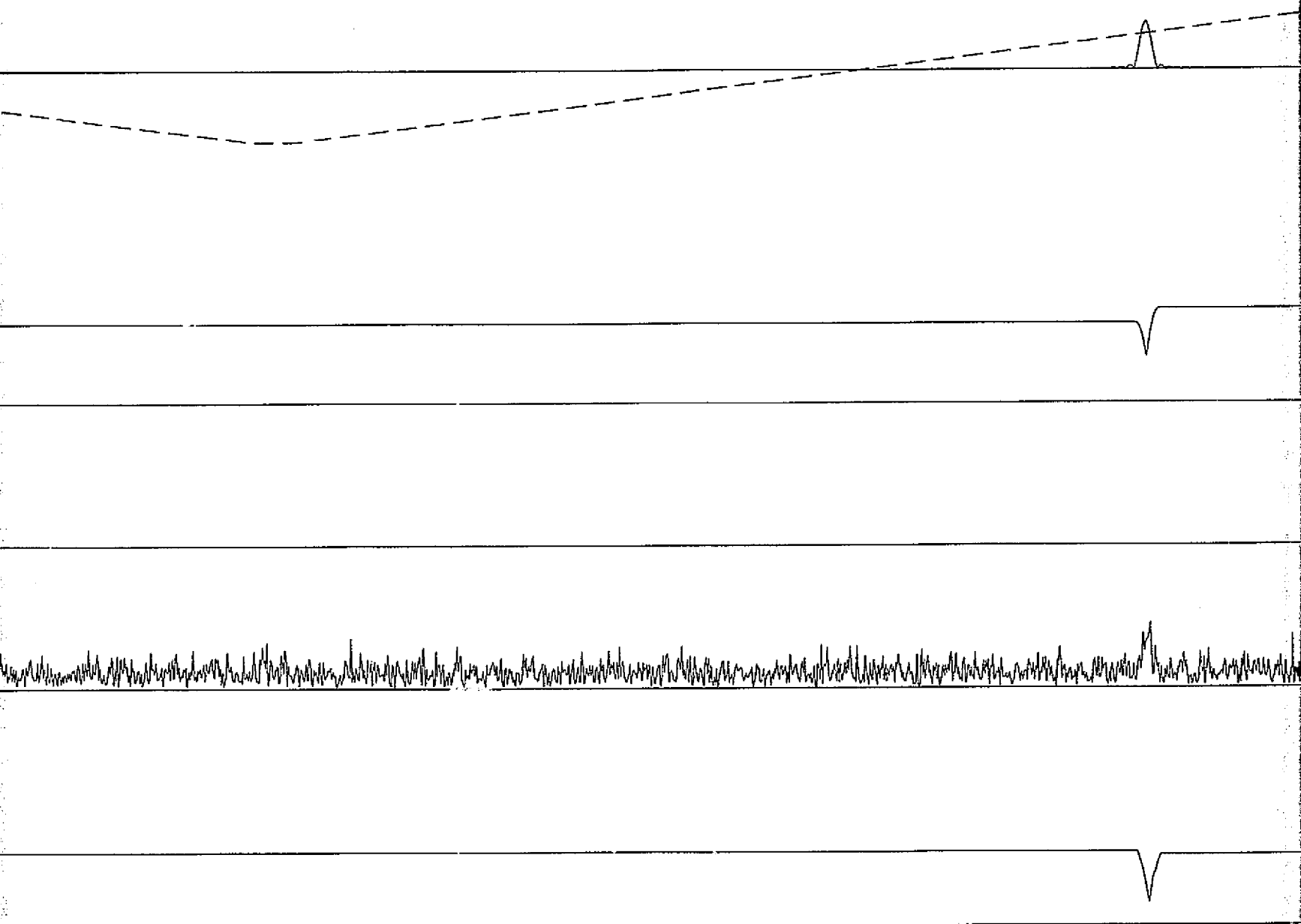


AMPLITUDE OF
COMPOSITE SIGNAL
PLUS NOISE



CANDIDATE
RCVR OUTPUT
(DEGREES)
COMPOSITE SIGNAL
PLUS NOISE





5.00 5.50 6.00 6.50 7.00 7.50 8.00 8.50 9.00 9.50 10.00 10.50 11.00
RECEIVER SCAN TIME (MILLISECONDS)

FOLDOUT FRAME 2



AMPLITUDE OF
DIRECT PATH
COMPONENT
(SOLID LINE)

FIGURE B-2.c

SHORT-TERM PLOT FOR SCAN 17

DATE: 10/08/75

PROGRAM: MLSRCVR

JOBNAME: MLSRCVZ

S. H. IRWIN, JR.

CHANNEL: AZIMUTH

SIGNAL MAKEUP

POSITION SPECIFIED BY RANGE IN NAUTICAL MILES,
DEGREES OF AZIMUTH, DEGREES OF ELEVATION,
RATES SPECIFIED BY VELOCITY IN KNOTS, DEGREES
AZIMUTH/SEC, DEGREES ELEVATION/SEC.

DIRECT PATH

AMPLITUDE = 1.00

INITIAL A/C POSITION = 10.00, 30.00, 3.00

INITIAL A/C RATE = -300.00, .00, .0

SPECULAR MULTIPATH -NONE



0 10.00 10.50 11.00 11.50 12.00 12.50

SCATTERED MULTIPATH

AMPLITUDE = .00

FRONT-END RECEIVER NOISE

ON = .40

(SNR = 8.00 DB)

CANDIDATE RECEIVER:

SQUARE GATE TRACKING RECEIVER

(60-BIT WORD LENGTH)

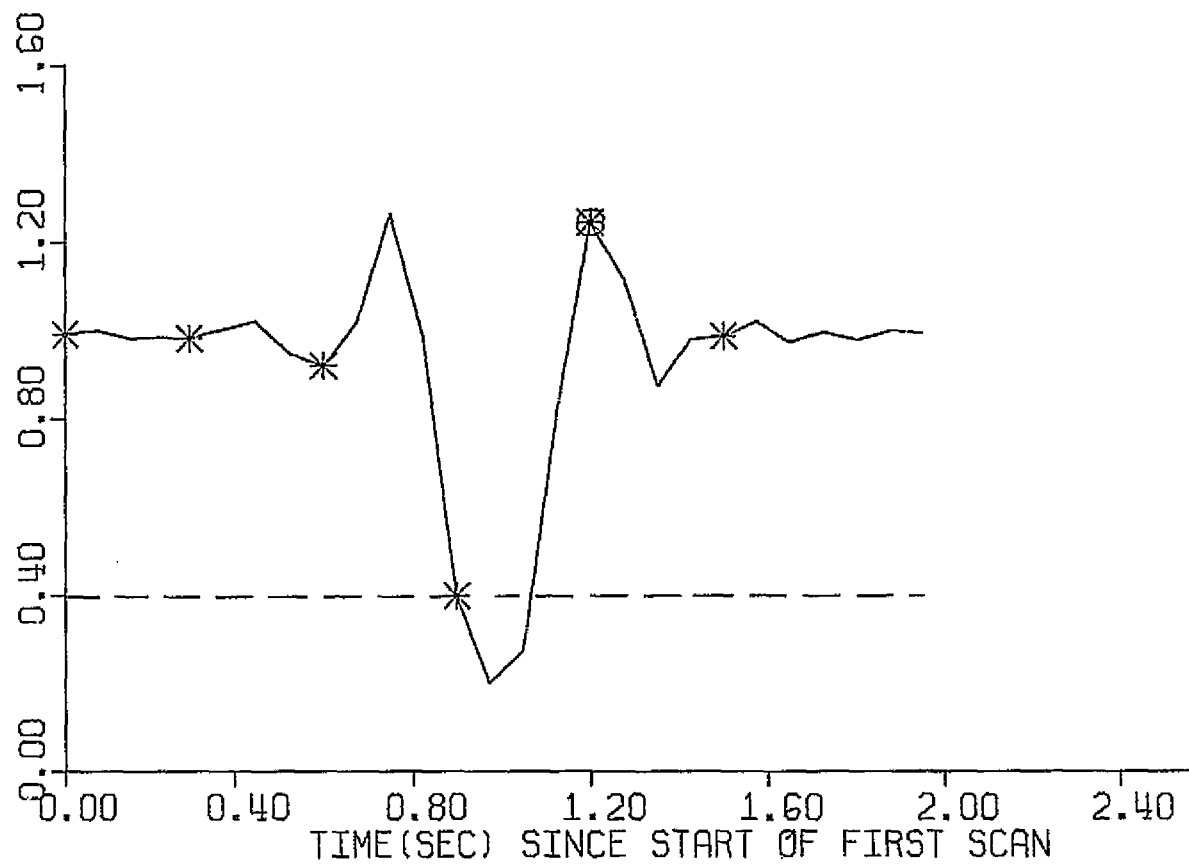
A/C AT 30.00 DEGREES AZIMUTH

TK = 1200MSEC.

FOLDOUT FRAME 3

AV. AMPLITUDE OF
COMPOSITE SIGNAL
AT TIME OF DIRECT
SIGNAL CENTROID
(SOLID LINE)

RMS NOISE LEVEL
(DASHED LINE)



ESTIMATION ERROR
(A/C ANGLE-EST.)
(DEGREES)

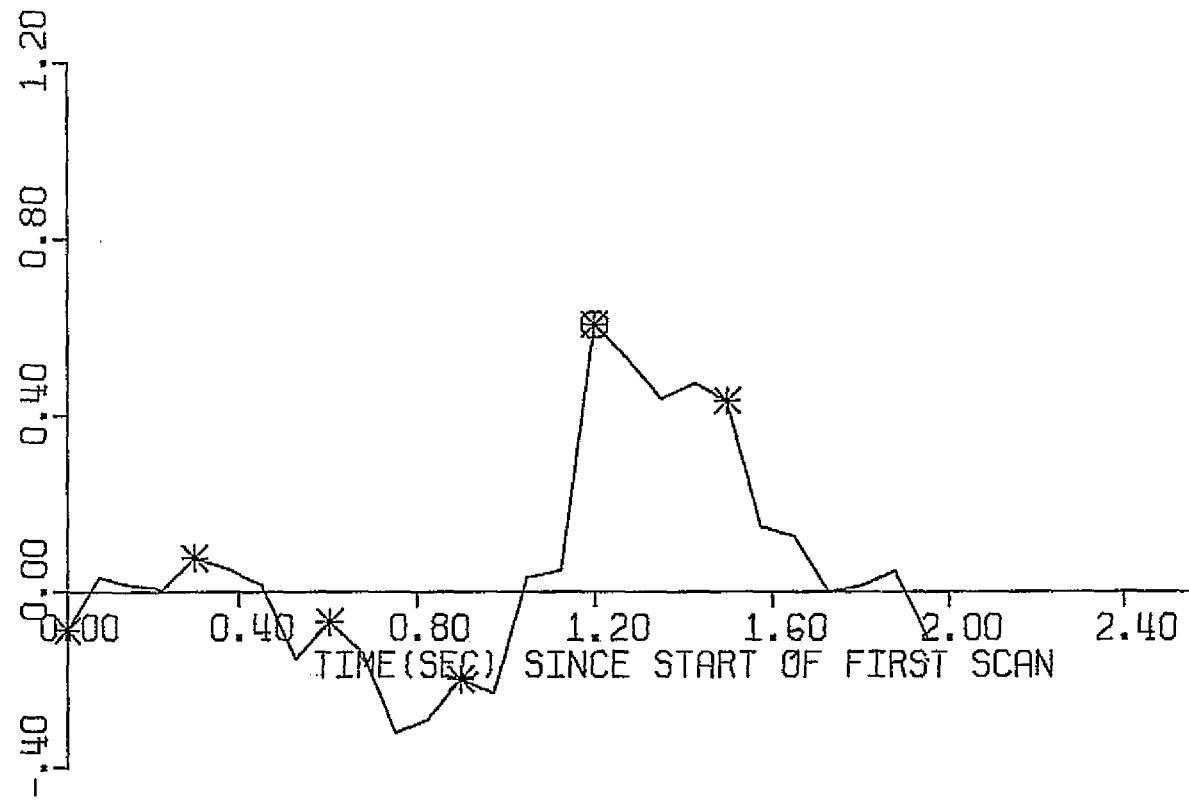


FIGURE B-3.a

LONG-TERM PLOT FOR 27 SCANS

DATE: 10/07/75

PROGRAM: MLSRCVR

JOBNAME: MLSRCJO

S. H. IRWIN, JR.

CHANNEL: AZIMUTH

SIGNAL MAKEUP

POSITION SPECIFIED BY RANGE IN NAUTICAL MILES,
DEGREES OF AZIMUTH, DEGREES OF ELEVATION.
RATES SPECIFIED BY VELOCITY IN KNOTS, DEGREES
AZIMUTH/SEC, DEGREES ELEVATION/SEC.

DIRECT PATH

AMPLITUDE = 1.00

INITIAL A/C POSITION = 10.00, 30.00, 3.00

INITIAL A/C RATE = -300.00, .00, .0

SPECULAR MULTIPATH

REFLECTOR 1

AMPLITUDE = .80

INITIAL POSITION = 1.00, 33.00, 1.85

INITIAL RATE = .00, -3.04, .00

R.F. PHASE DIFFERENCE = 180° AT PULSE

COINCIDENCE

SCATTERED MULTIPATH

AMPLITUDE = .00

FRONT-END RECEIVER NOISE

$\sigma_n = .40$

(SNR = 8.00 DB)

CANDIDATE RECEIVER:

SQUARE GATE TRACKING RECEIVER

(60-BIT WORD LENGTH)

ESTIMATION ERROR

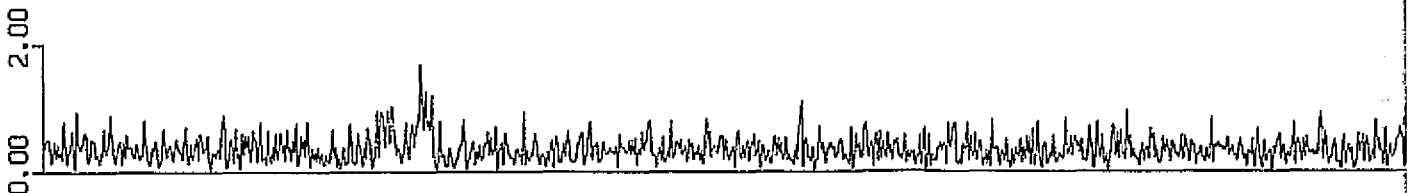
RMS ESTIMATION ERROR = .247 DEGREES

RMS ERROR SPECIFICATION = .010 DEGREES

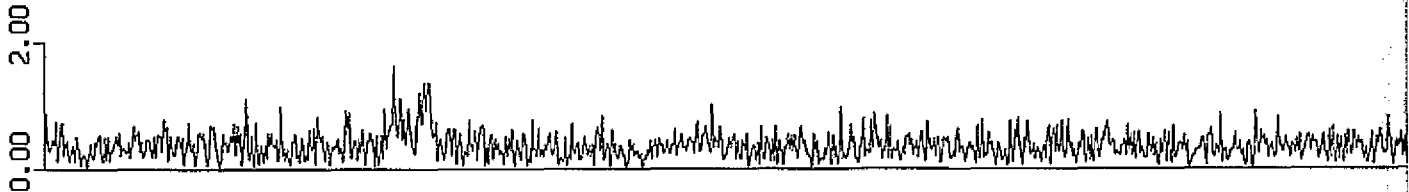
* SHORT-TERM PLOT OF COMPOSITE SIGNAL AVAILABLE
© DETAILED SHORT-TERM PERFORMANCE PLOT AVAILABLE

FOLDOUT FRAME 2

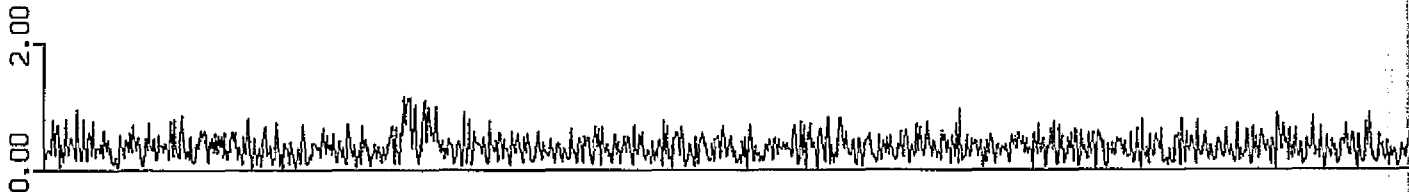
SCAN 1
TK = 0 MS



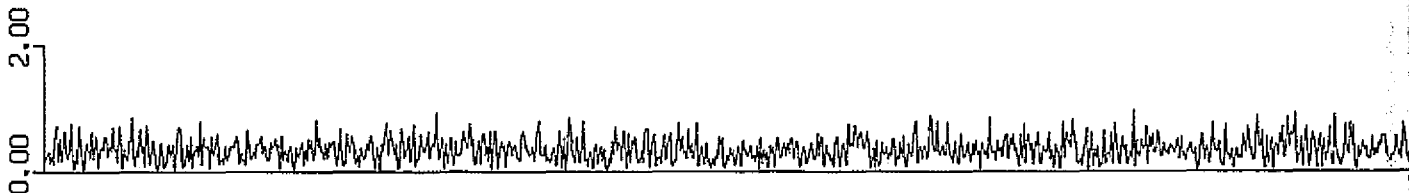
SCAN 5
TK = 300 MS



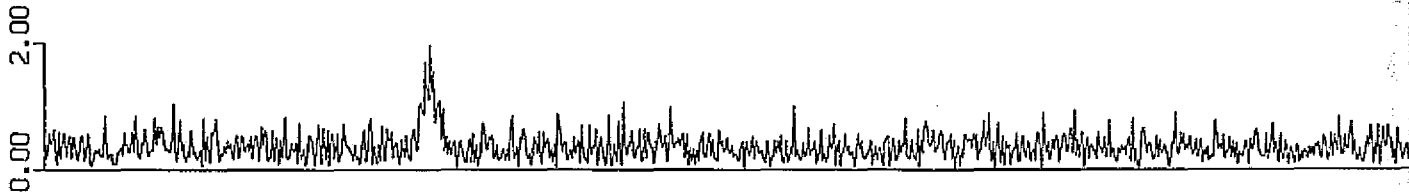
SCAN 9
TK = 600 MS



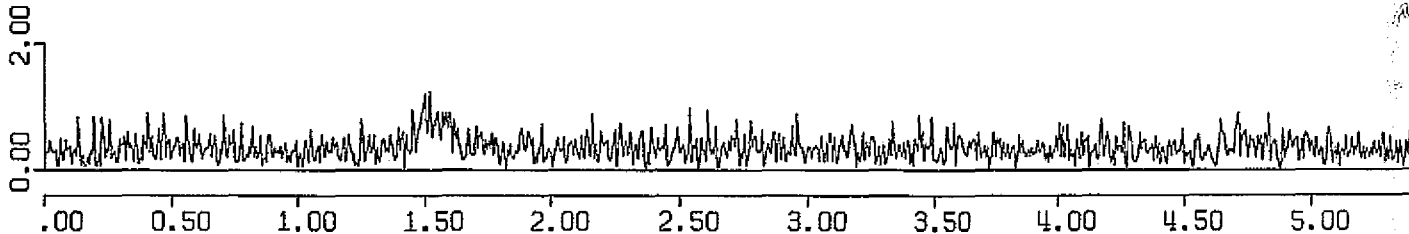
SCAN 13
TK = 900 MS



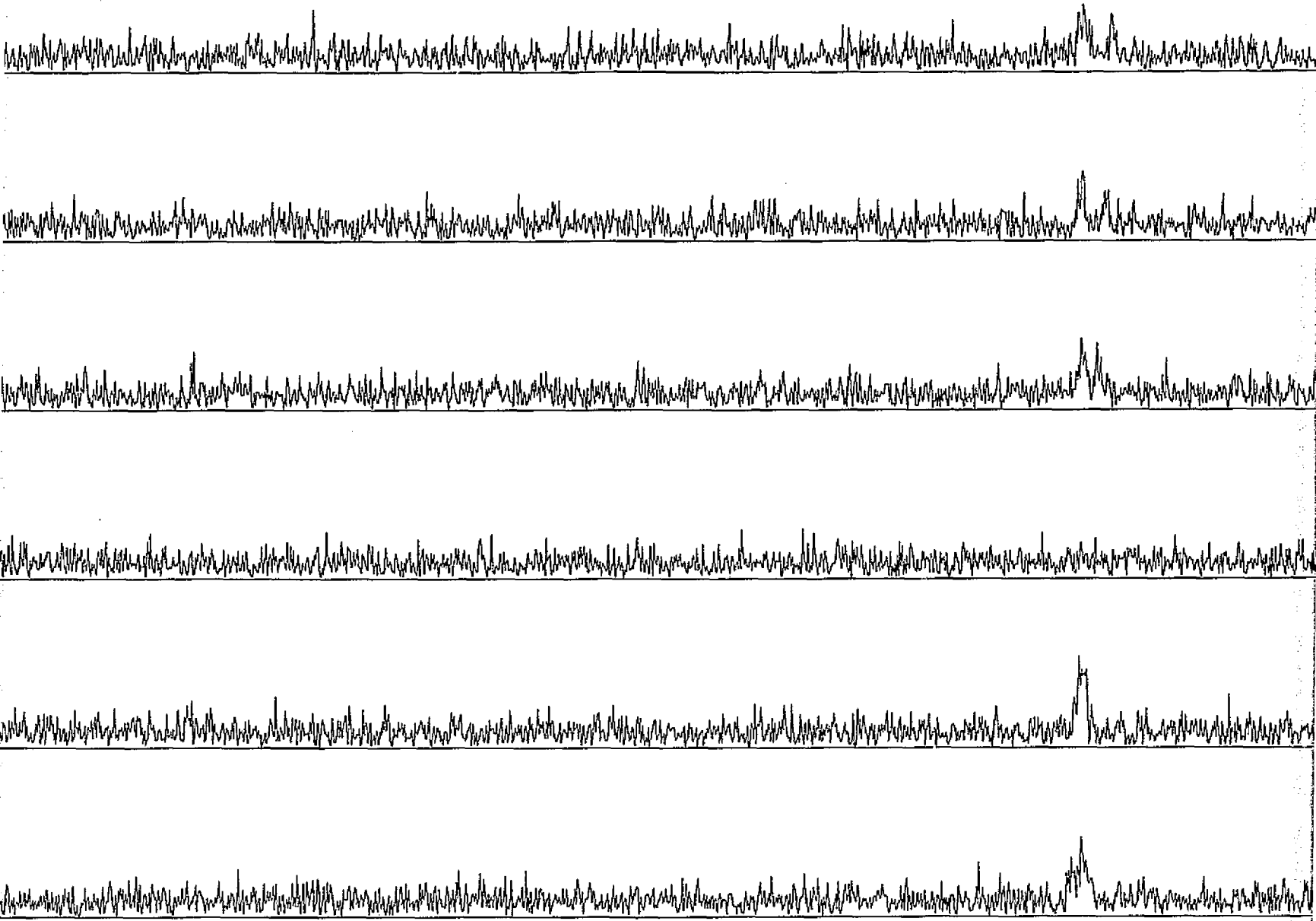
SCAN 17
TK = 1200 MS



SCAN 21
TK = 1500 MS



FOLDOUT FRAME



00 5.50 6.00 6.50 7.00 7.50 8.00 8.50 9.00 9.50 10.00 10.50 11.00 11.50

RECEIVER SCAN TIME (MILLISECONDS)

FOLDOUT FRAME 2

1

FIGURE B-3.b

AMPLITUDE OF COMPOSITE SIGNAL PLUS NOISE

DATE: 10/07/75

PROGRAM: MLSRCVR

JOBNAME: MLSRCJO

S. H. IRWIN, JR.

CHANNEL: AZIMUTH

SIGNAL MAKEUP

POSITION SPECIFIED BY RANGE IN NAUTICAL MILES,
DEGREES OF AZIMUTH, DEGREES OF ELEVATION.
RATES SPECIFIED BY VELOCITY IN KNOTS, DEGREES
AZIMUTH/SEC DEGREES ELEVATION/SEC

DIRECT PATH

AMPLITUDE = 1.00

INITIAL A/C POSITION = 10.00, 30.00, 3.00

INITIAL A/C RATE = -300.00, .00, .0

SPECULAR MULTIPATH

REFLECTOR 1

AMPLITUDE = .80

INITIAL POSITION = 1.00, 33.00, 1.85

INITIAL RATE = .00, -3.04, .00

RF PHASE DIFFERENCE = 180° AT PULSE

COINCIDENCE

SCATTERED MULTIPATH

AMPLITUDE = .00

FRONT-END RECEIVER NOISE

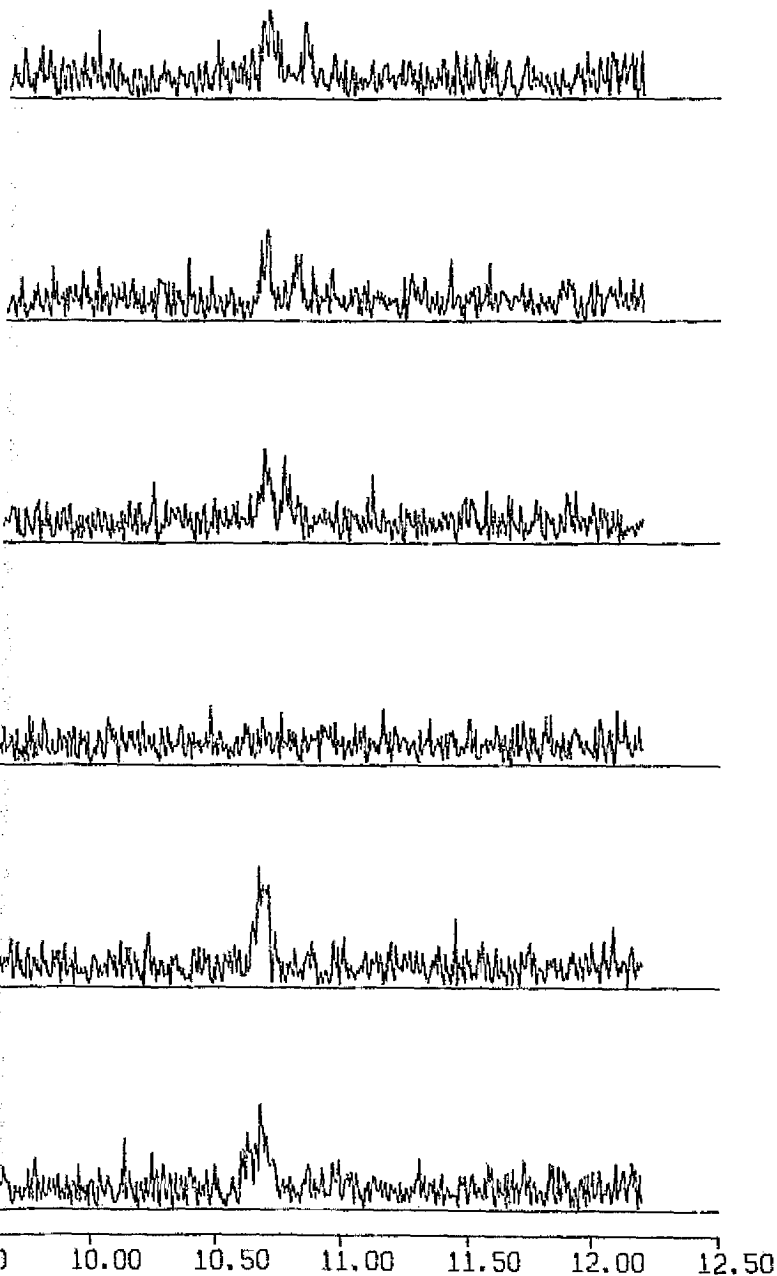
$C/N = .40$

(SNR = 8.00 DB)

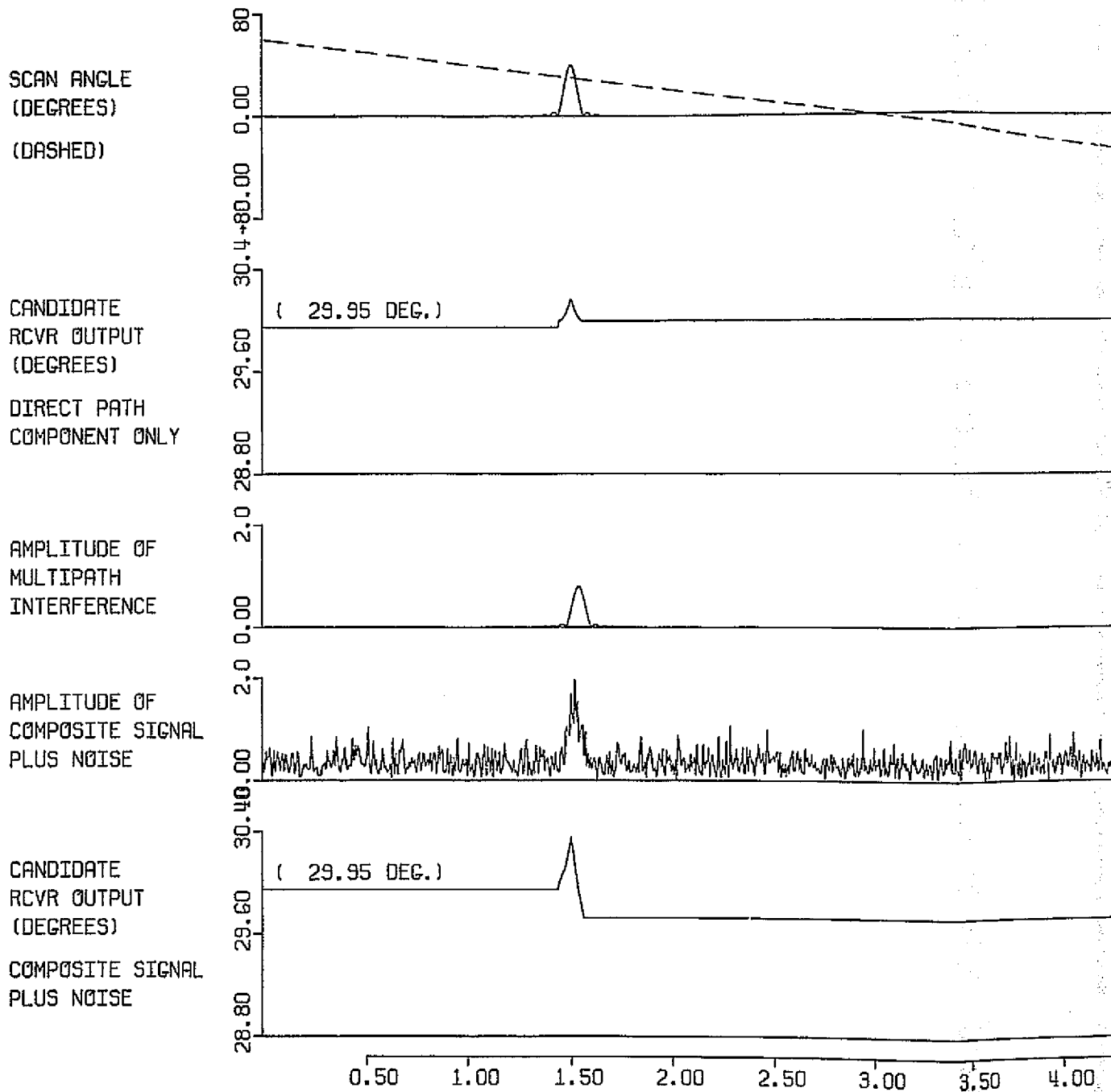
CANDIDATE RECEIVER:

SQUARE GATE TRACKING RECEIVER

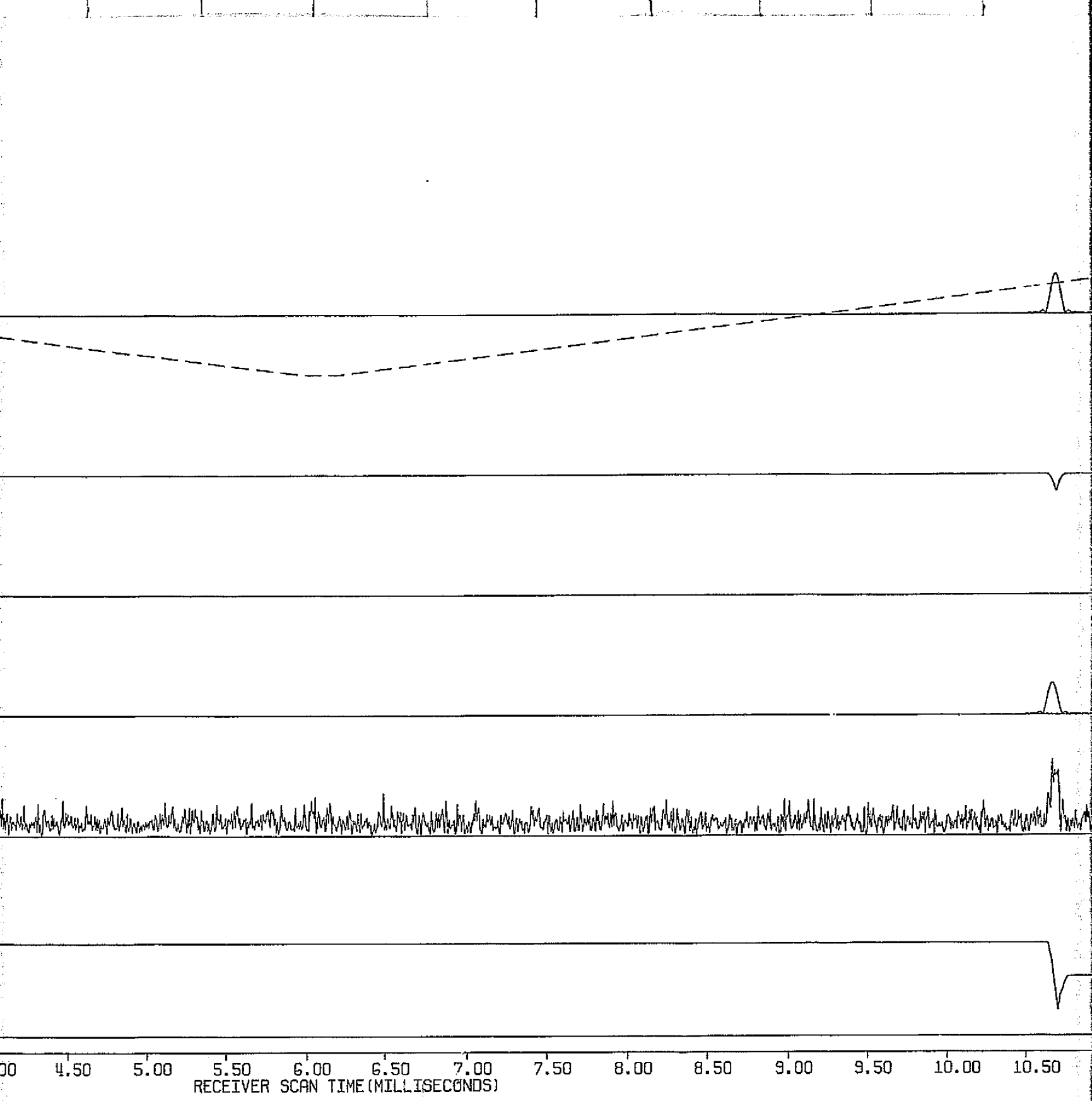
(60-BIT WORD LENGTH)



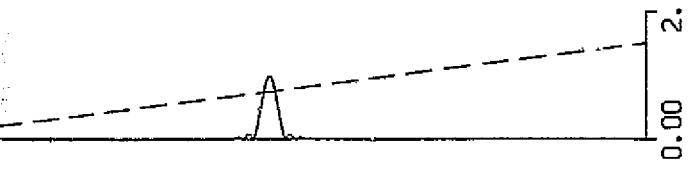
FOLDOUT FRAME 3



FOLDOUT FRAME /

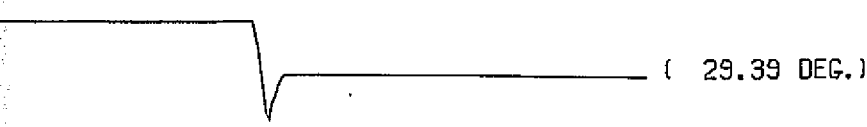
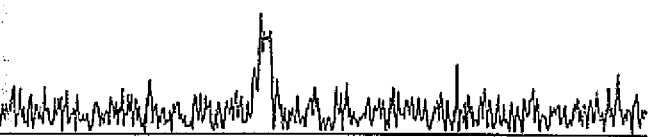
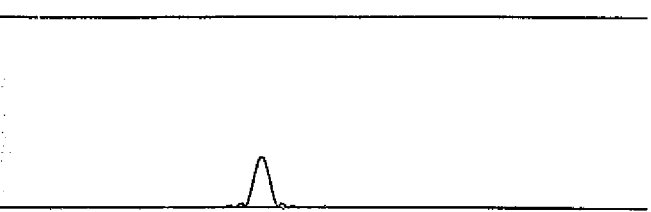
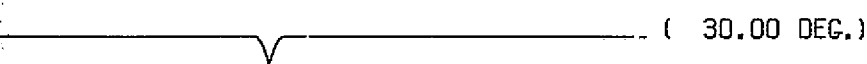


FOLDOUT FRAME 2



AMPLITUDE OF
DIRECT PATH
COMPONENT
(SOLID LINE)

FIGURE B-3.c
SHORT-TERM PLOT FOR SCAN 17
DATE: 10/07/75
PROGRAM: MLSRCVR
JOBNAME: MLSRCJO
S. H. IRWIN, JR.



10.00 10.50 11.00 11.50 12.00 12.50

CHANNEL: AZIMUTH

SIGNAL MAKEUP
POSITION SPECIFIED BY RANGE IN NAUTICAL MILES,
DEGREES OF AZIMUTH, DEGREES OF ELEVATION.
RATES SPECIFIED BY VELOCITY IN KNOTS, DEGREES
AZIMUTH/SEC, DEGREES ELEVATION/SEC.

DIRECT PATH
AMPLITUDE = 1.00
INITIAL A/C POSITION = 10.00, 30.00, 3.00
INITIAL A/C RATE = -300.00, .00, .0

SPECULAR MULTIPATH
REFLECTOR 1
AMPLITUDE = .80
INITIAL POSITION = 1.00, 33.00, 1.85
INITIAL RATE = .00, -3.04, .00
RF PHASE DIFFERENCE = 180° AT PULSE
COINCIDENCE

SCATTERED MULTIPATH
AMPLITUDE = .00
FRONT-END RECEIVER NOISE
 $\sigma_n = .40$
(SNR = 8.00 DB)

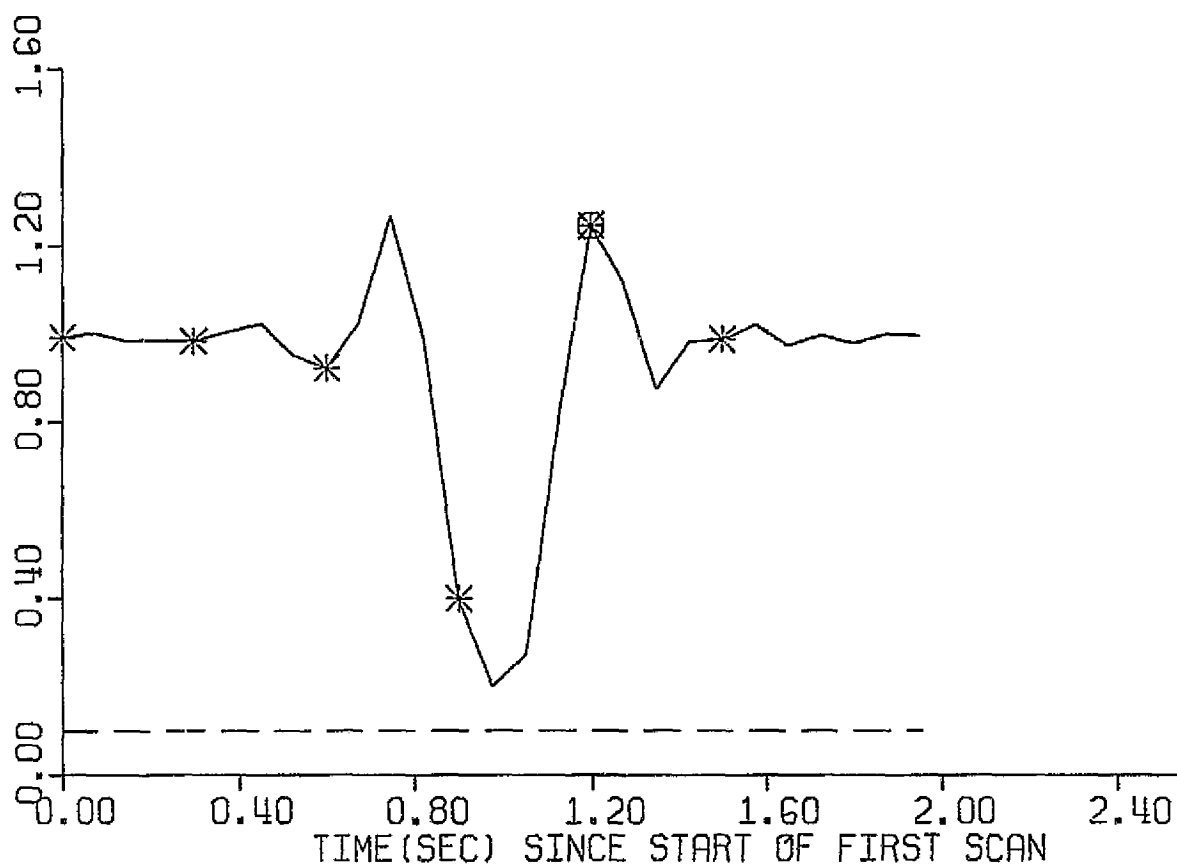
CANDIDATE RECEIVER:
SQUARE GATE TRACKING RECEIVER
(60-BIT WORD LENGTH)

A/C AT 30.00 DEGREES AZIMUTH
TK = 1200MSEC.

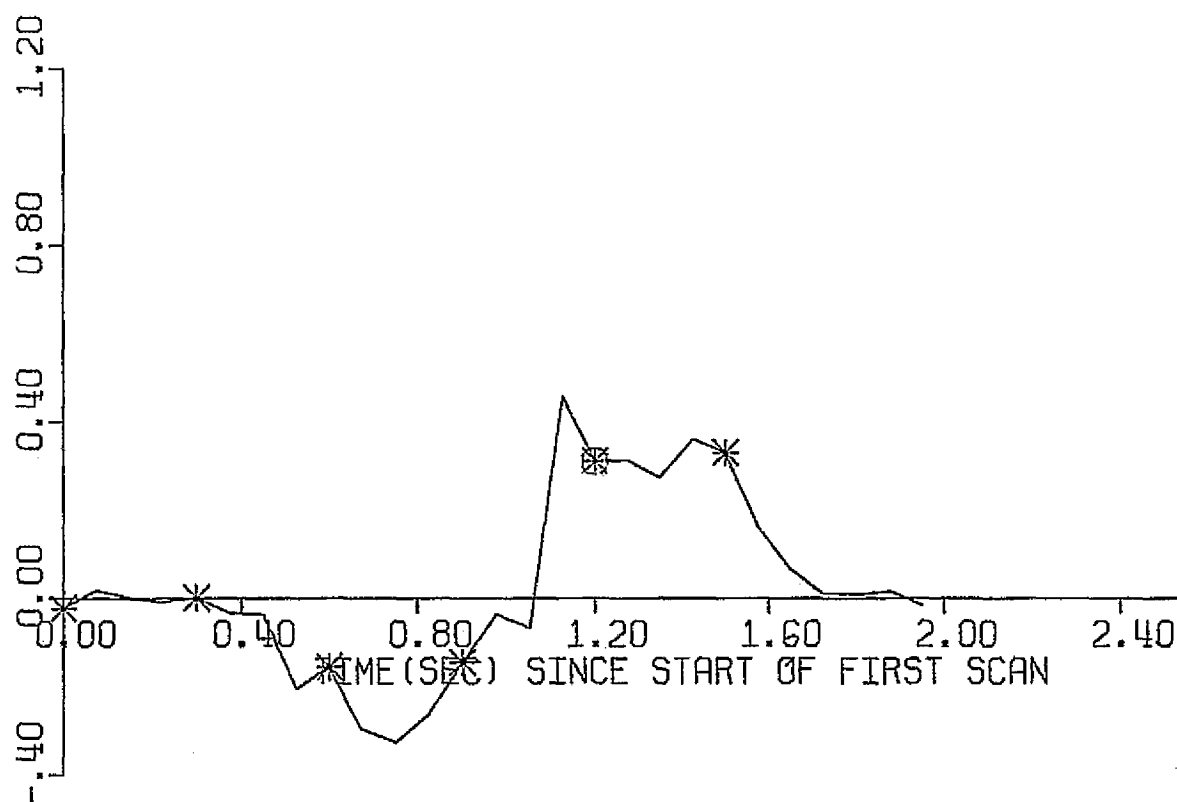
FOLDOUT FRAME 3

AV. AMPLITUDE OF
COMPOSITE SIGNAL
AT TIME OF DIRECT
SIGNAL CENTROID
(SOLID LINE)

RMS NOISE LEVEL
(DASHED LINE)



ESTIMATION ERROR
(A/C ANGLE-EST.)
(DEGREES)



FOLDOUT FRAME

FIGURE B-4.a

LONG-TERM PLOT FOR 27 SCANS

DATE: 10/06/75

PROGRAM: MLSRCVR

JOBNAME: MLSRCFG

S. H. IRWIN, JR.

CHANNEL: AZIMUTH

SIGNAL MAKEUP

POSITION SPECIFIED BY RANGE IN NAUTICAL MILES,
DEGREES OF AZIMUTH, DEGREES OF ELEVATION.
RATES SPECIFIED BY VELOCITY IN KNOTS, DEGREES
AZIMUTH/SEC, DEGREES ELEVATION/SEC.

DIRECT PATH

AMPLITUDE = 1.00

INITIAL A/C POSITION = 10.00, 30.00, 3.00

INITIAL A/C RATE = -300.00, .00, .0

SPECULAR MULTIPATH

REFLECTOR 1

AMPLITUDE = .80

INITIAL POSITION = 1.00, 33.00, 1.85

INITIAL RATE = .00, -3.04, .00

RF PHASE DIFFERENCE = 180° AT PULSE
COINCIDENCE

SCATTERED MULTIPATH

AMPLITUDE = .00

FRONT-END RECEIVER NOISE

$\sigma_n = .10$

(SNR = 20.00 DB)

CANDIDATE RECEIVER:

SQUARE GATE TRACKING RECEIVER

(60-BIT WORD LENGTH)

ESTIMATION ERROR

RMS ESTIMATION ERROR = .203 DEGREES

RMS ERROR SPECIFICATION = .010 DEGREES

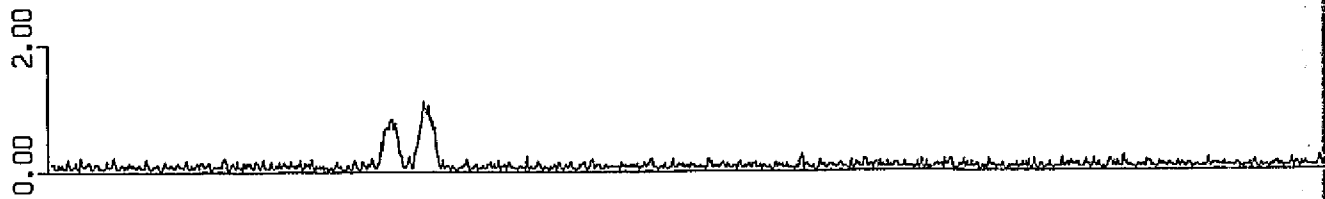
* SHORT-TERM PLOT OF COMPOSITE SIGNAL AVAILABLE
O DETAILED SHORT-TERM PERFORMANCE PLOT AVAILABLE

WOLDOUT FRAME 2

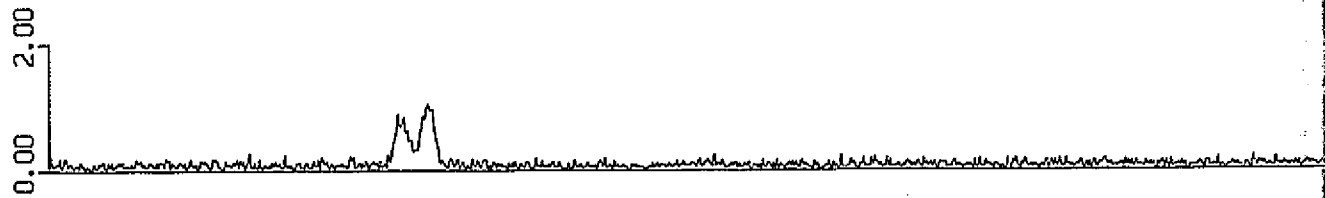
2.80

2.80

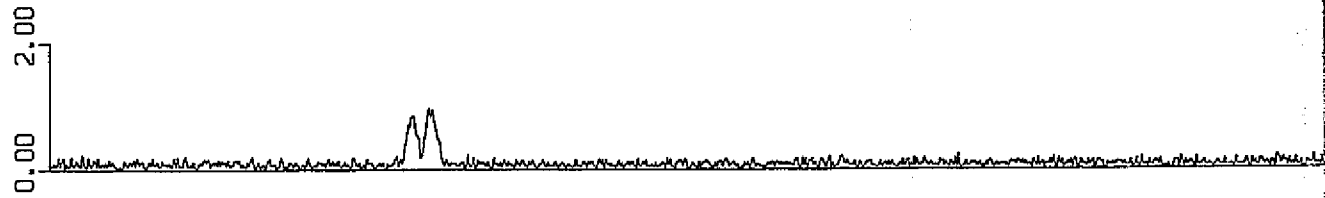
SCAN 1
TK = 0 MS



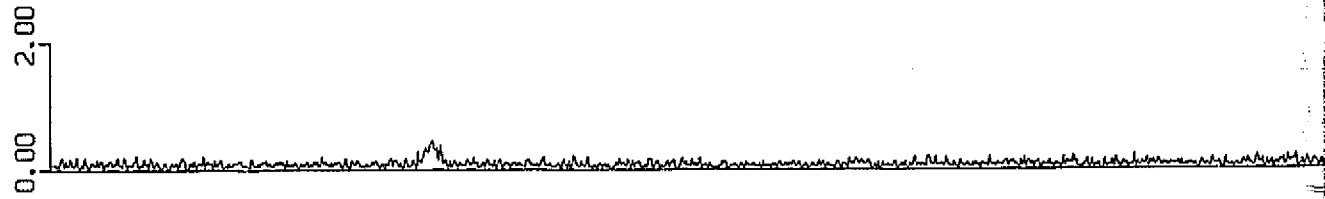
SCAN 5
TK = 300 MS



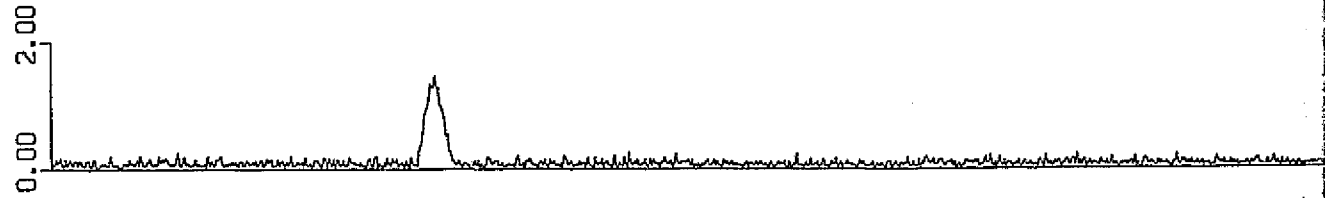
SCAN 9
TK = 600 MS



SCAN 13
TK = 900 MS



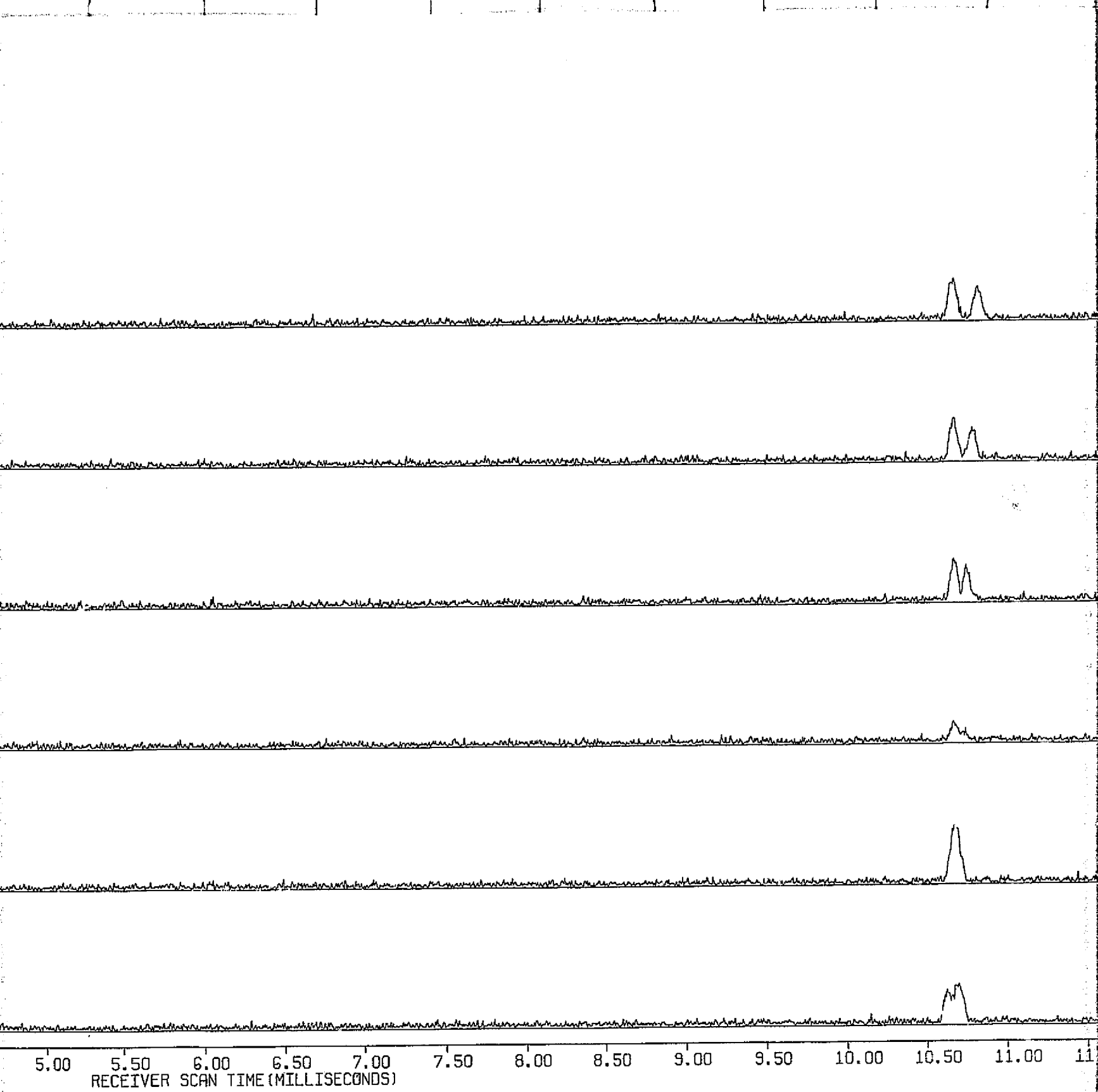
SCAN 17
TK = 1200 MS



SCAN 21
TK = 1500 MS



FOLDOUT FRAME (



FOLDOUT FRAME 2

FIGURE B-4.b

AMPLITUDE OF COMPOSITE SIGNAL PLUS NOISE

DATE: 10/06/75

PROGRAM: MLSRCVR

JOBNAME: MLSRCFG

S. H. IRWIN, JR.

CHANNEL: AZIMUTH

SIGNAL MAKEUP

POSITION SPECIFIED BY RANGE IN NAUTICAL MILES,
DEGREES OF AZIMUTH, DEGREES OF ELEVATION.
RATES SPECIFIED BY VELOCITY IN KNOTS, DEGREES
AZIMUTH/SEC, DEGREES ELEVATION/SEC.

DIRECT PATH

AMPLITUDE = 1.00

INITIAL A/C POSITION = 10.00, 30.00, 3.00

INITIAL A/C RATE = -300.00, .00, .0

SPECULAR MULTIPATH

REFLECTOR 1

AMPLITUDE = .80

INITIAL POSITION = 1.00, 33.00, 1.85

INITIAL RATE = .00, -3.04, .00

RF PHASE DIFFERENCE = 180° AT PULSE
COINCIDENCE

SCATTERED MULTIPATH

AMPLITUDE = .00

FRONT-END RECEIVER NOISE

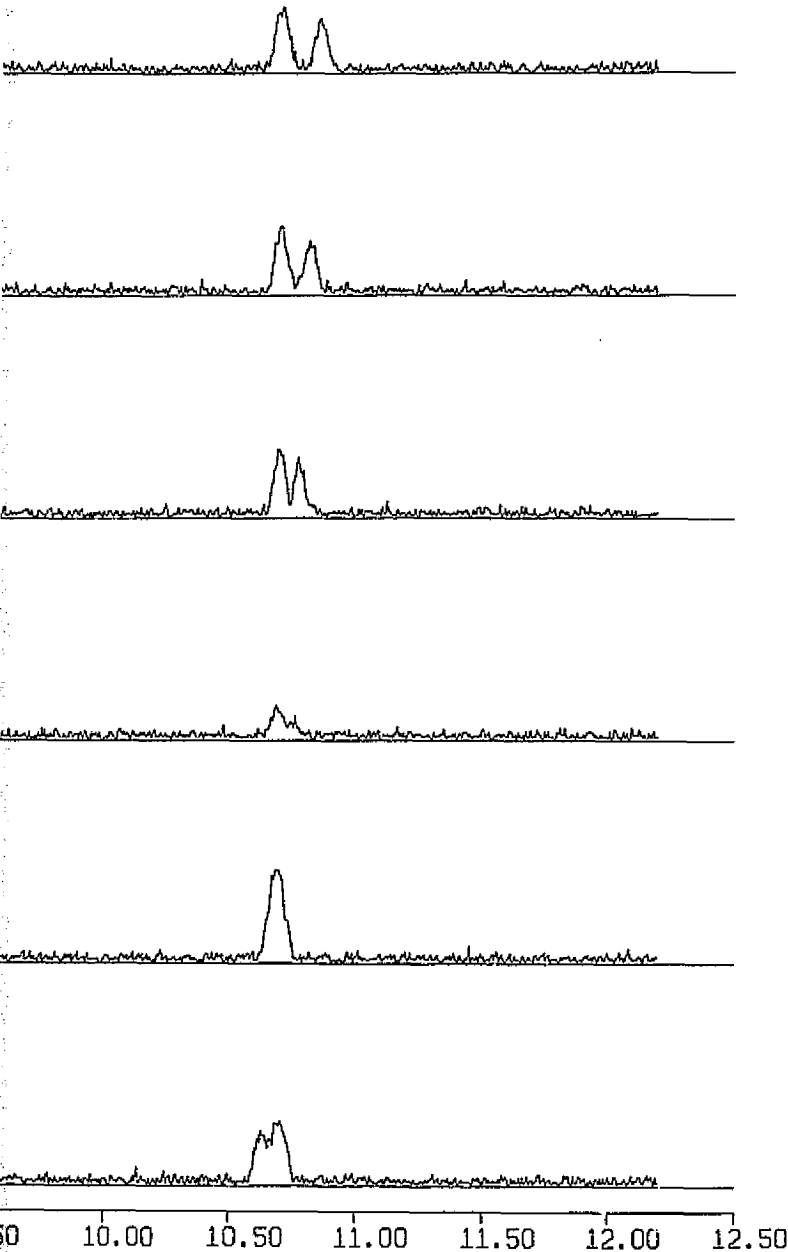
$\sigma_n = .10$

(SNR = 20.00 DB)

CANDIDATE RECEIVER:

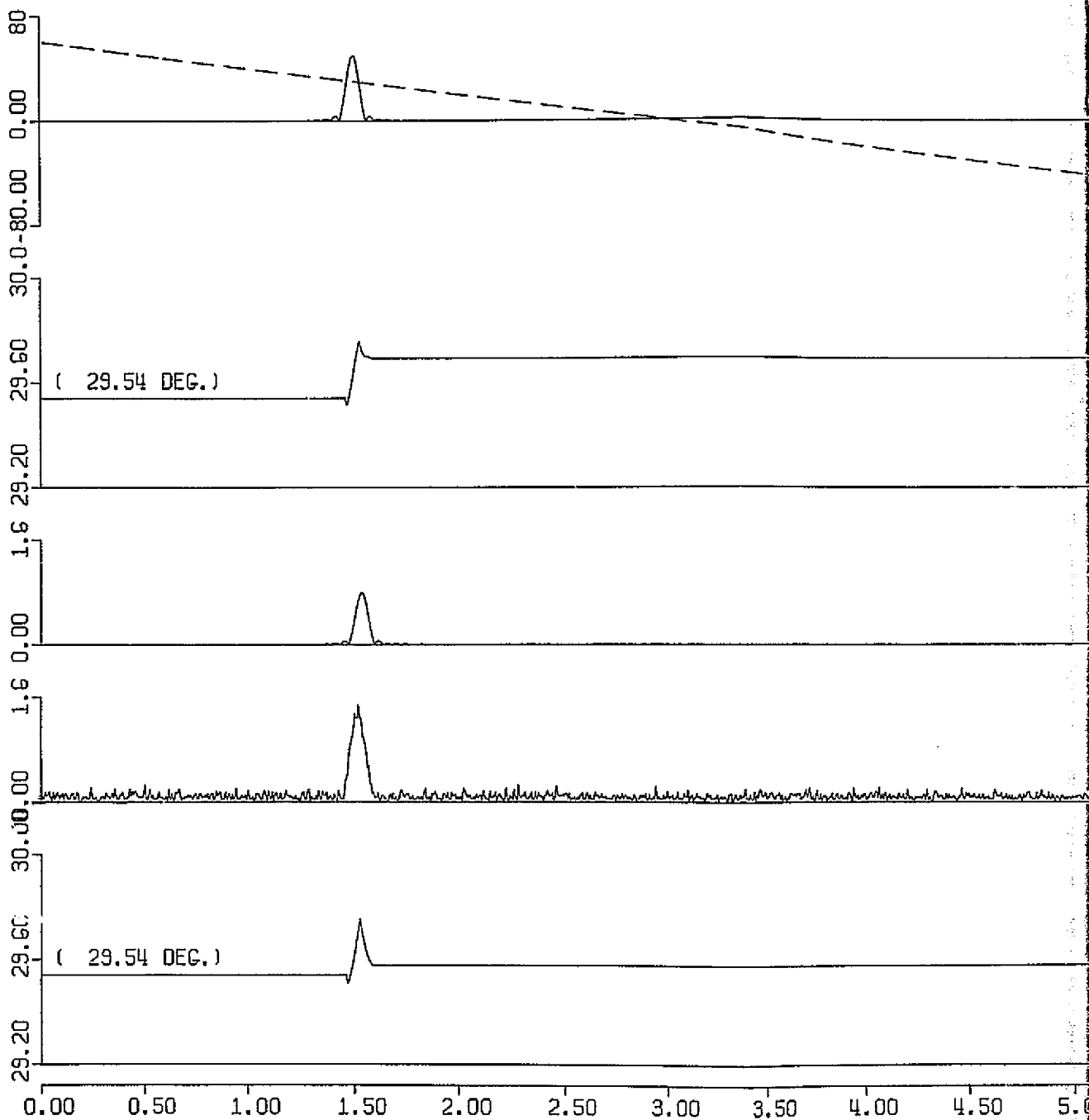
SQUARE GATE TRACKING RECEIVER

(60-BIT WORD LENGTH)



FOLDOUT FRAME 2

SCAN ANGLE
(DEGREES)
(DASHED)



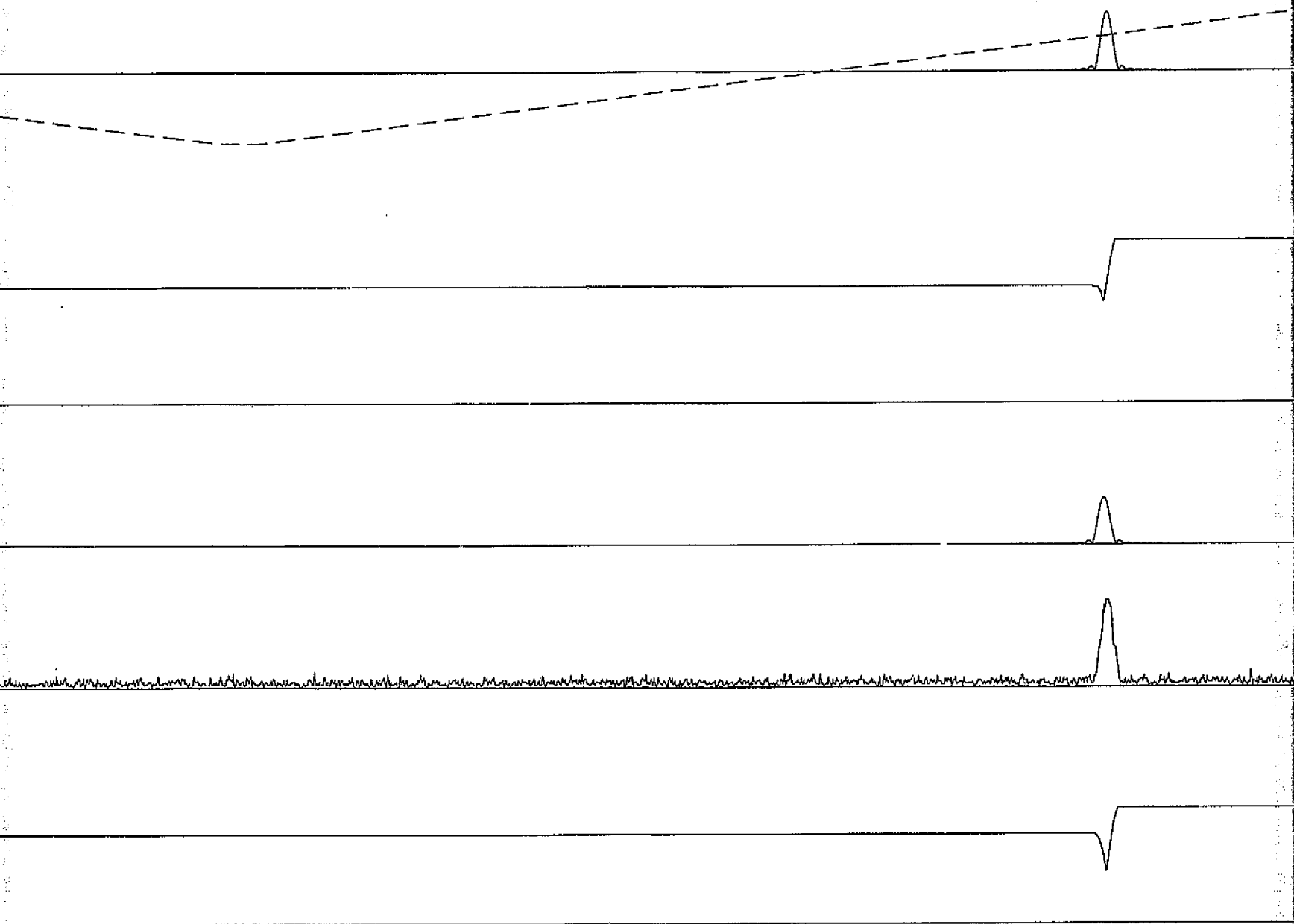
CANDIDATE
RCVR OUTPUT
(DEGREES)
DIRECT PATH
COMPONENT ONLY

AMPLITUDE OF
MULTIPATH
INTERFERENCE

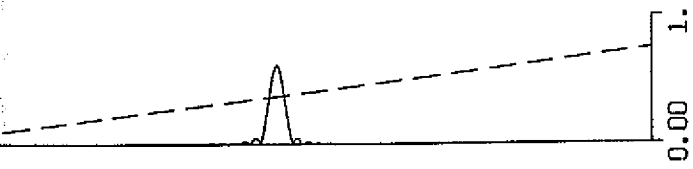
AMPLITUDE OF
COMPOSITE SIGNAL
PLUS NOISE

CANDIDATE
RCVR OUTPUT
(DEGREES)
COMPOSITE SIGNAL
PLUS NOISE

FOLDOUT FRAME



5.00 5.50 6.00 6.50 7.00 7.50 8.00 8.50 9.00 9.50 10.00 10.50 11.00 11.50
RECEIVER SCAN TIME (MILLISECONDS)



AMPLITUDE OF
DIRECT PATH
COMPONENT
(SOLID LINE)

FIGURE B-4.c

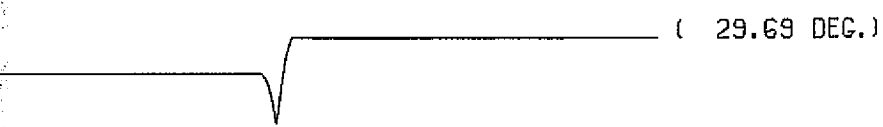
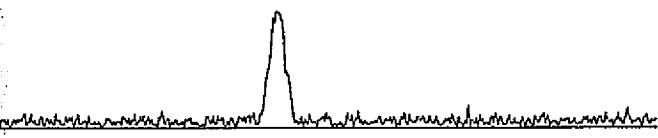
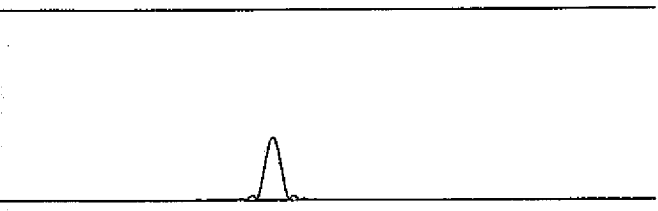
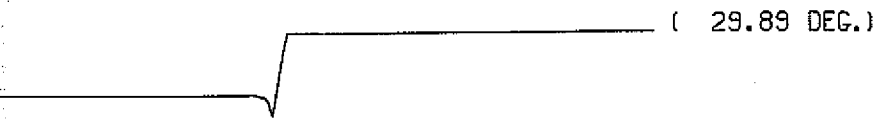
SHORT-TERM PLOT FOR SCAN 17

DATE: 10/06/75

PROGRAM: MLSRCVR

JOBNAME: MLSRCFC

S. H. IRWIN, JR.



10.00 10.50 11.00 11.50 12.00 12.50

CHANNEL: AZIMUTH

SIGNAL MAKEUP

POSITION SPECIFIED BY RANGE IN NAUTICAL MILES,
DEGREES OF AZIMUTH, DEGREES OF ELEVATION.
RATES SPECIFIED BY VELOCITY IN KNOTS, DEGREES
AZIMUTH/SEC, DEGREES ELEVATION/SEC.

DIRECT PATH

AMPLITUDE = 1.00
INITIAL A/C POSITION = 10.00, 30.00, 3.00
INITIAL A/C RATE = -300.00, .00, .0

SPECULAR MULTIPATH

REFLECTOR 1

AMPLITUDE = .80
INITIAL POSITION = 1.00, 33.00, 1.85
INITIAL RATE = .00, -3.04, .00
RF PHASE DIFFERENCE = 180° AT PULSE
COINCIDENCE

SCATTERED MULTIPATH

AMPLITUDE = .00

FRONT-END RECEIVER NOISE

DN = .10
(SNR = 20.00 DB)

CANDIDATE RECEIVER:

SQUARE GATE TRACKING RECEIVER
(60-BIT WORD LENGTH)

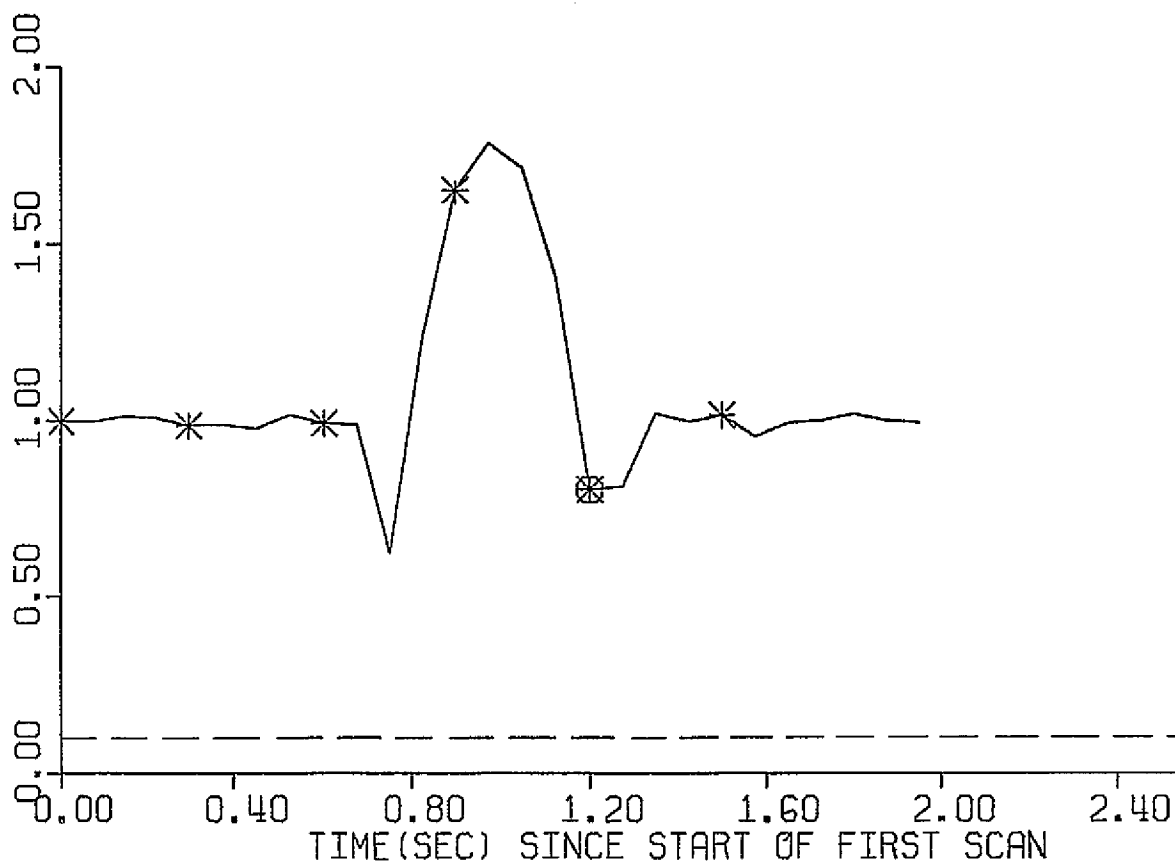
A/C AT 30.00 DEGREES AZIMUTH

TK = 1200MSEC.

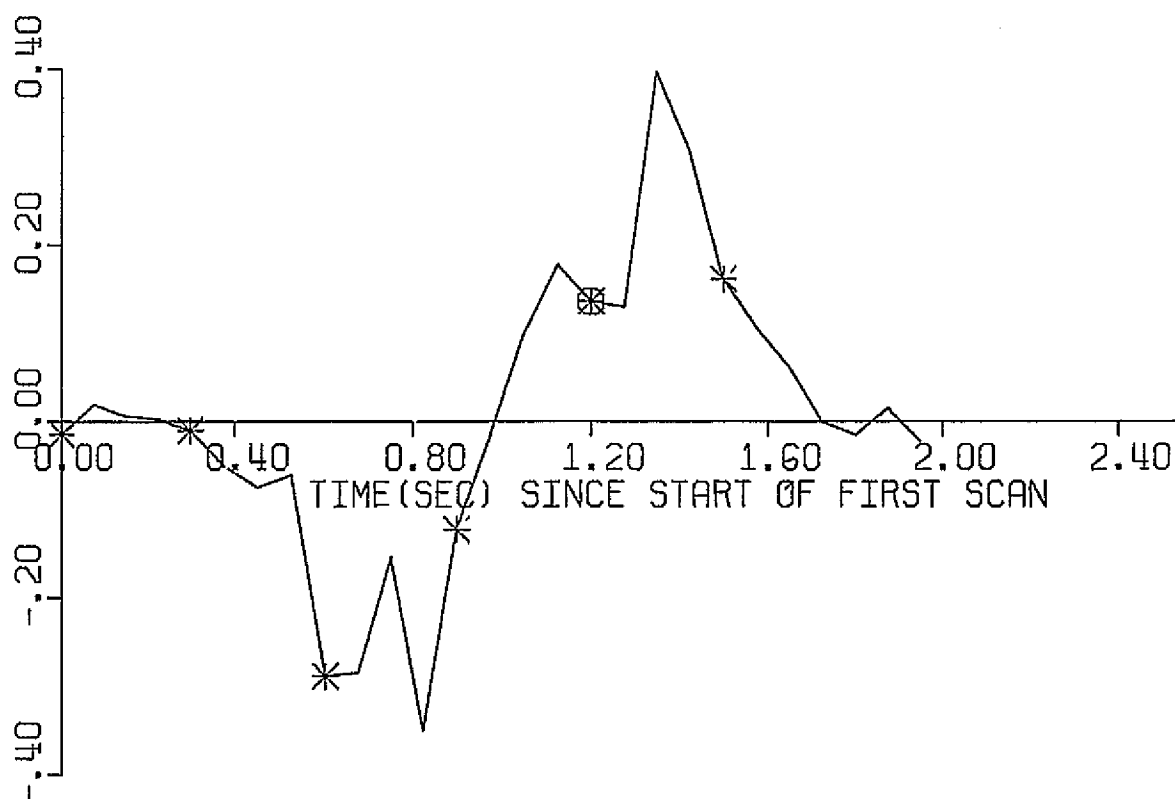
FOLDOUT FRAME 3

AV. AMPLITUDE OF
COMPOSITE SIGNAL
AT TIME OF DIRECT
SIGNAL CENTROID
(SOLID LINE)

RMS NOISE LEVEL
(DASHED LINE)



ESTIMATION ERROR
(A/C ANGLE-EST.)
(DEGREES)



FOLDOUT FRAME

FIGURE B - 5.a

LONG-TERM PLOT FOR 27 SCANS

DATE: 10/10/75

PROGRAM: MLSRCVR

JOBNAME: MLSRC5C

S. H. IRWIN, JR.

CHANNEL: AZIMUTH

SIGNAL MAKEUP

POSITION SPECIFIED BY RANGE IN NAUTICAL MILES
DEGREES OF AZIMUTH, DEGREES OF ELEVATION.
RATES SPECIFIED BY VELOCITY IN KNOTS, DEGREES
AZIMUTH/SEC, DEGREES ELEVATION/SEC.

DIRECT PATH

AMPLITUDE = 1.00

INITIAL A/C POSITION = 10.00, 30.00, 3.00

INITIAL A/C RATE = -300.00, .00, .0

SPECULAR MULTIPATH

REFLECTOR 1

AMPLITUDE = .80

INITIAL POSITION = 1.00 33.00 1.85

INITIAL RATE = .00 -3.04, .00

RF PHASE DIFFERENCE = 0° AT PULSE
COINCIDENCE

SCATTERED MULTIPATH

AMPLITUDE = .00

FRONT-END RECEIVER NOISE

σ_n = .10

(SNR = 20.00 DB)

CANDIDATE RECEIVER:

SQUARE GATE TRACKING RECEIVER
(60-BIT WORD LENGTH)

ESTIMATION ERROR

RMS ESTIMATION ERROR = .162 DEGREES

RMS ERROR SPECIFICATION = .010 DEGREES

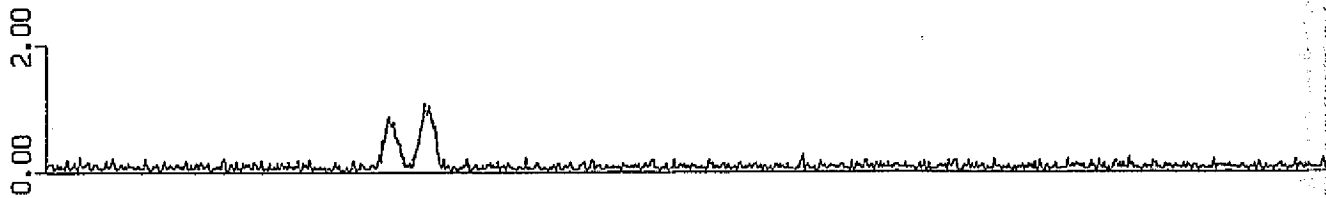
* SHORT-TERM PLOT OF COMPOSITE SIGNAL AVAILABLE
⊙ DETAILED SHORT-TERM PERFORMANCE PLOT AVAILABLE

FOLDOUT FRAME 5

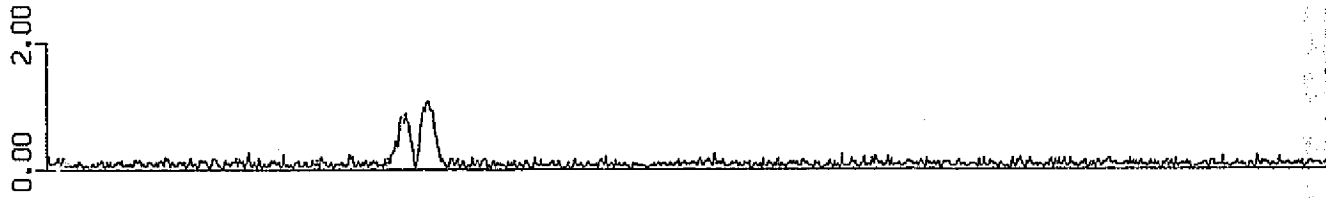
.40 2.80

.40 2.80

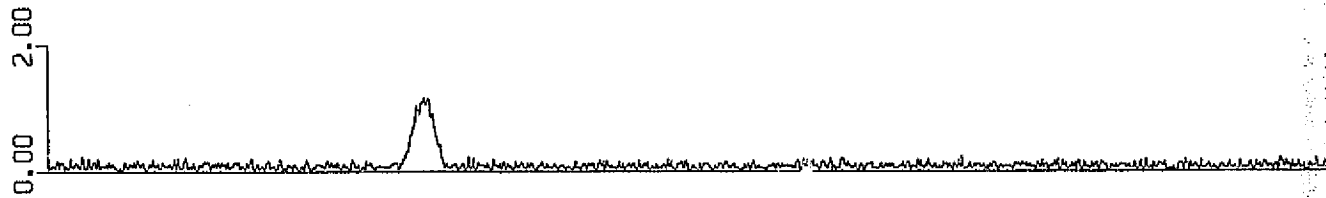
SCAN 1
TK = 0 MS



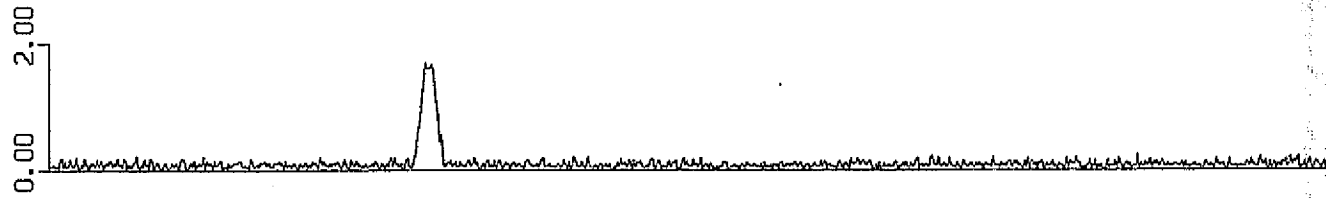
SCAN 5
TK = 300 MS



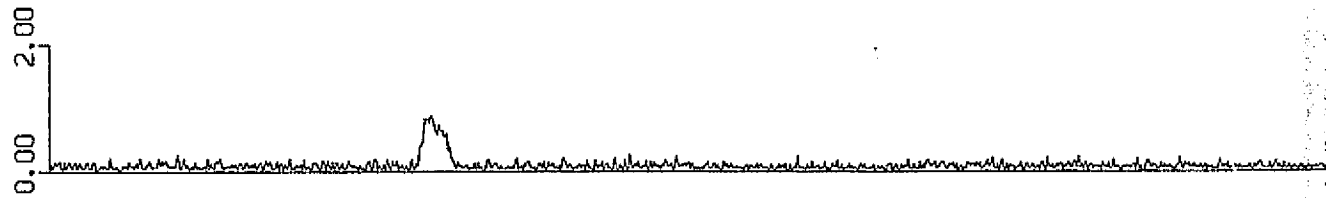
SCAN 9
TK = 600 MS



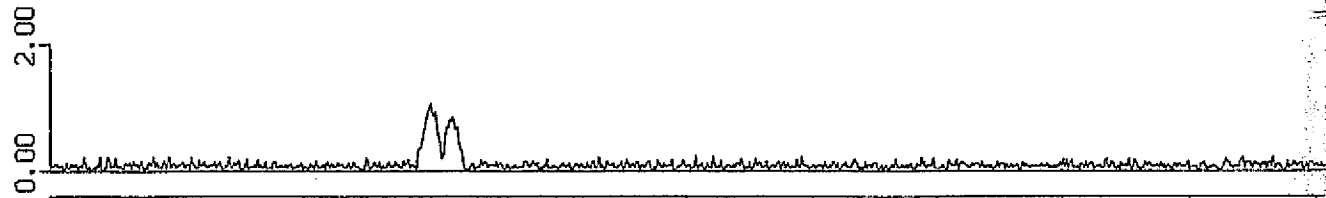
SCAN 13
TK = 900 MS



SCAN 17
TK = 1200 MS

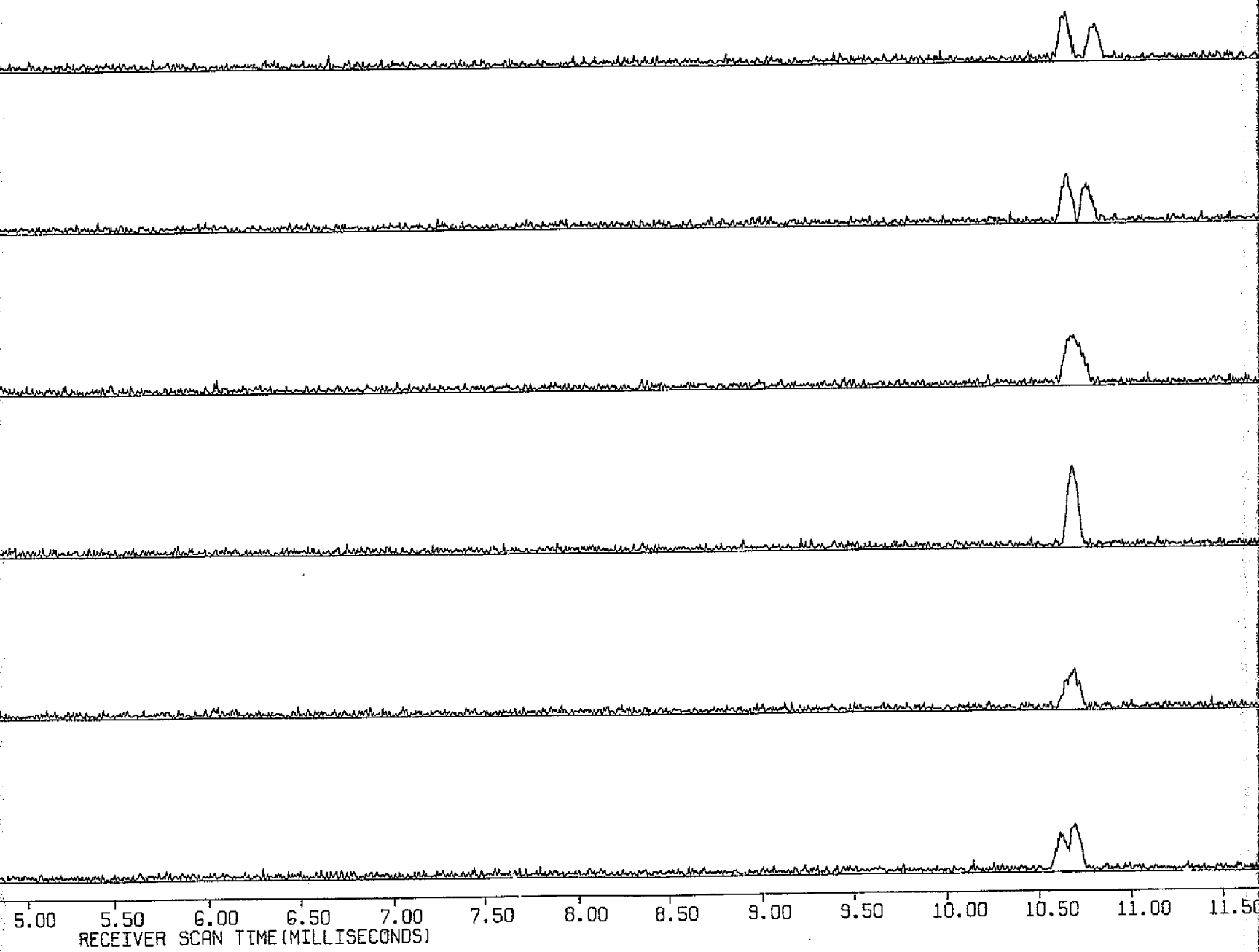


SCAN 21
TK = 1500 MS



00 0.50 1.00 1.50 2.00 2.50 3.00 3.50 4.00 4.50 5.00

HOLDOUT FRAME)



FOLDOUT FRAME 2

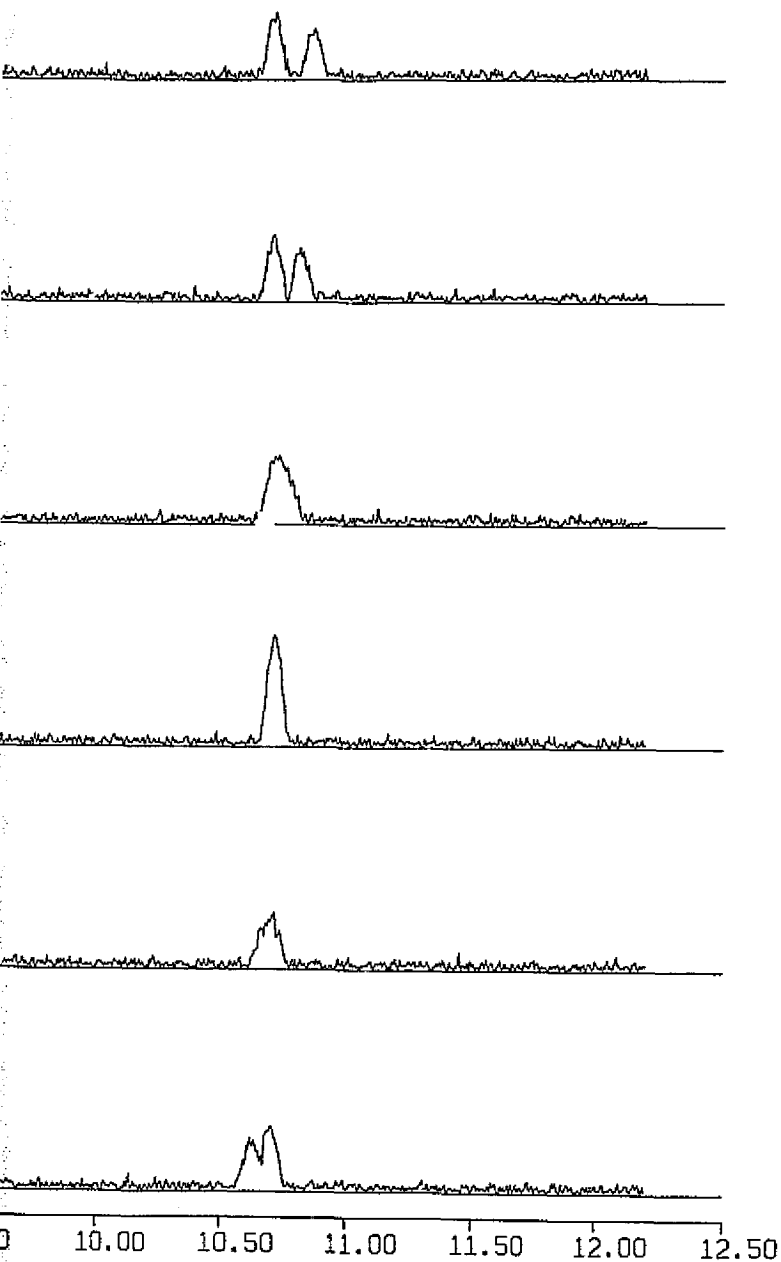


FIGURE B-5.b

AMPLITUDE OF COMPOSITE SIGNAL PLUS NOISE

DATE: 10/10/75

PROGRAM: MLSRCVR

JOBNAME: MLSRC5C

S. H. IRWIN, JR.

CHANNEL: AZIMUTH

SIGNAL MAKEUP

POSITION SPECIFIED BY RANGE IN NAUTICAL MILES,
 DEGREES OF AZIMUTH, DEGREES OF ELEVATION,
 RATES SPECIFIED BY VELOCITY IN KNOTS, DEGREES
 AZIMUTH/SEC, DEGREES ELEVATION/SEC.

DIRECT PATH

AMPLITUDE = 1.00
 INITIAL A/C POSITION = 10.00, 30.00, 3.00
 INITIAL A/C RATE = -300.00, .00, .0

SPECULAR MULTIPATH

REFLECTOR 1

AMPLITUDE = .80
 INITIAL POSITION = 1.00, 33.00, 1.85
 INITIAL RATE = .00 -3.04 .00
 RF PHASE DIFFERENCE = 0° AT PULSE
 COINCIDENCE

SCATTERED MULTIPATH

AMPLITUDE = .00

FRONT-END RECEIVER NOISE

$\sigma_n = .10$
 (SNR = 20.00 DB)

CANDIDATE RECEIVER:

SQUARE GATE TRACKING RECEIVER
 (60-BIT WORD LENGTH)

FOLDOUT FRAME 5

SCAN ANGLE
(DEGREES)
(DASHED)

CANDIDATE
RCVR OUTPUT
(DEGREES)

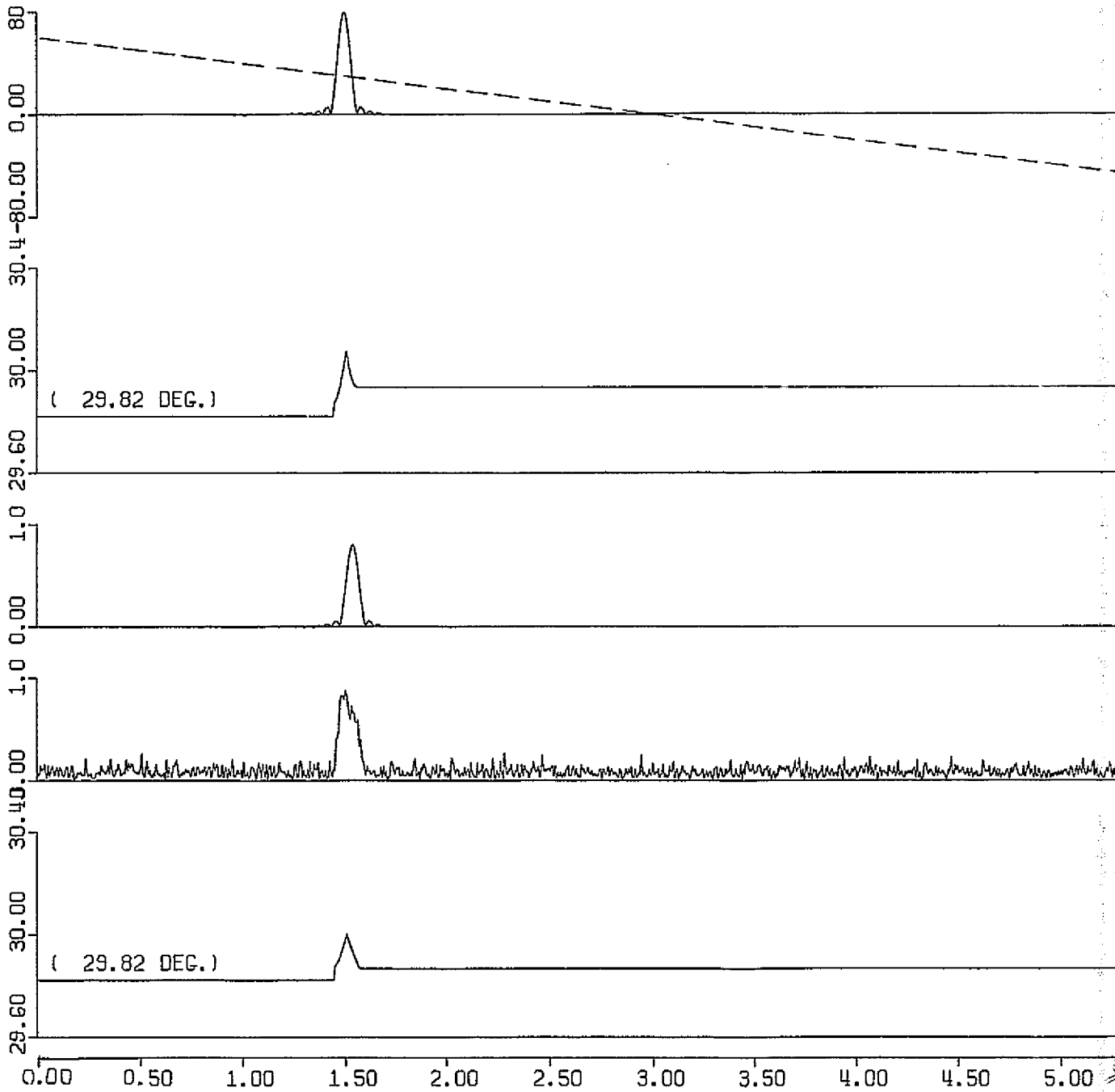
DIRECT PATH
COMPONENT ONLY

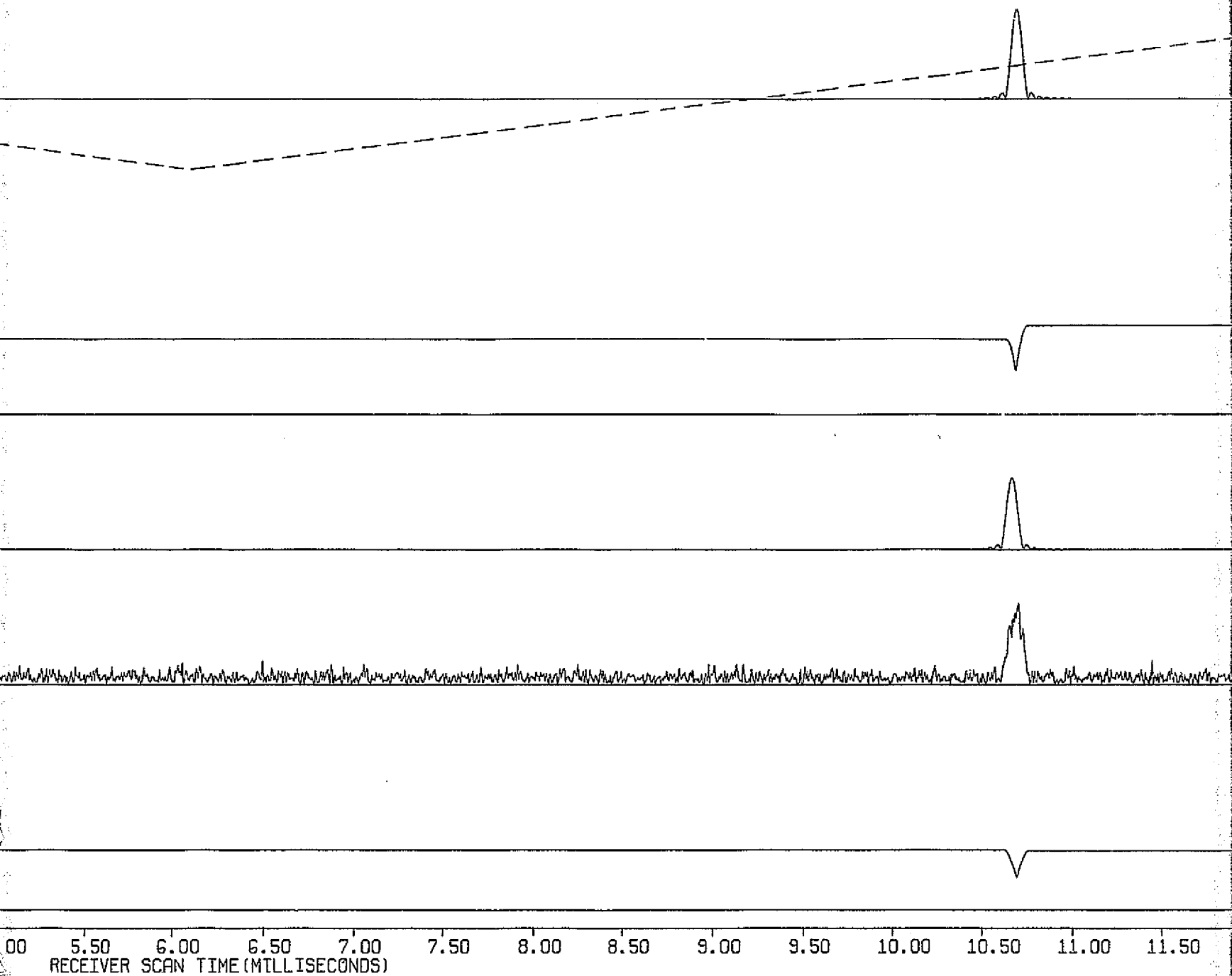
AMPLITUDE OF
MULTIPATH
INTEREERENCE

AMPLITUDE OF
COMPOSITE SIGNAL
PLUS NOISE

CANDIDATE
RCVR OUTPUT
(DEGREES)

COMPOSITE SIGNAL
PLUS NOISE





00 5.50 6.00 6.50 7.00 7.50 8.00 8.50 9.00 9.50 10.00 10.50 11.00 11.50
RECEIVER SCAN TIME (MILLISECONDS)

FOLDOUT FRAME 2

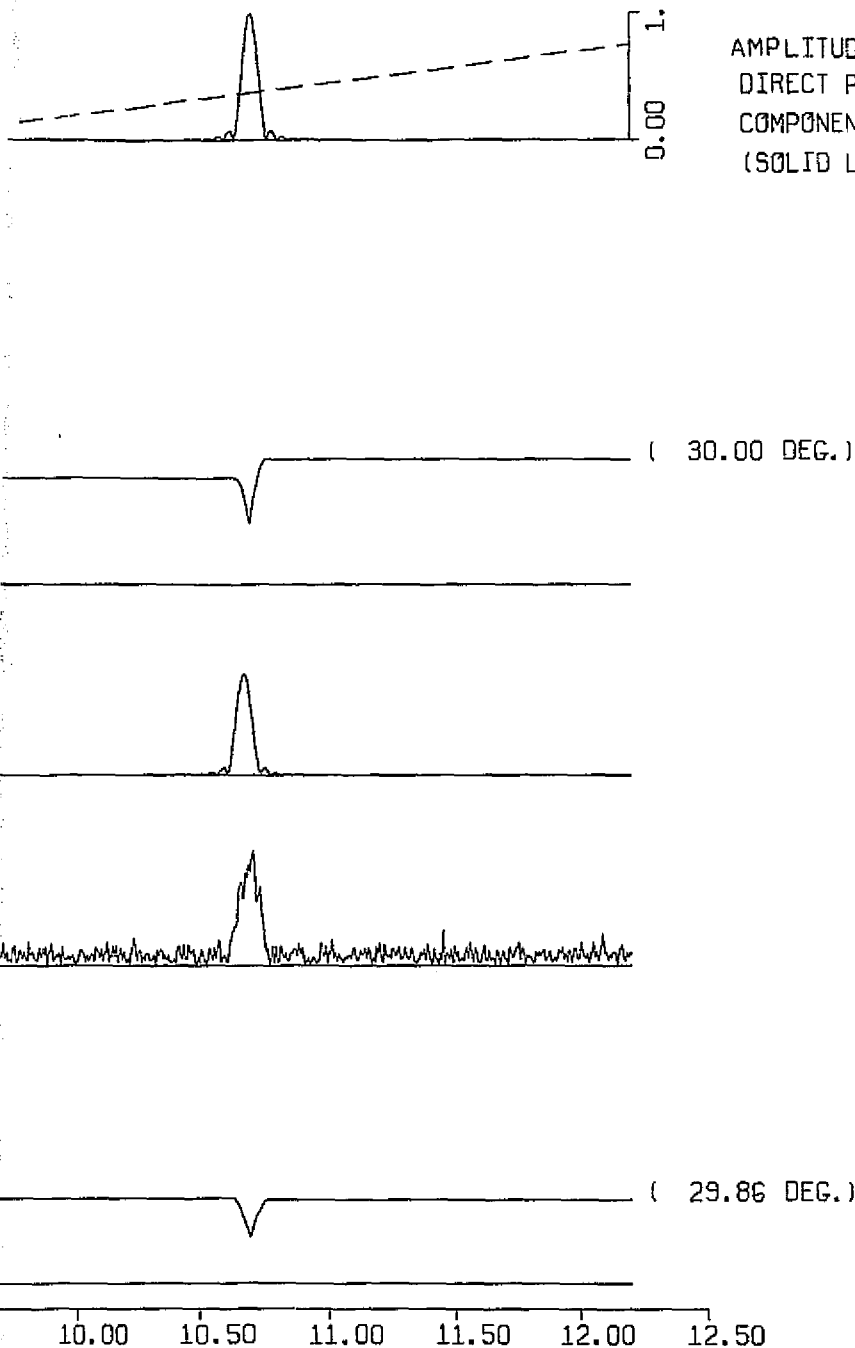


FIGURE B-5.c

SHORT-TERM PLOT FOR SCAN 17

DATE: 10/10/75

PROGRAM: MLSRCVR

JOBNAME: MLSRC5C

S. H. IRWIN, JR.

CHANNEL: AZIMUTH

SIGNAL MAKEUP

POSITION SPECIFIED BY RANGE IN NAUTICAL MILES
DEGREES OF AZIMUTH, DEGREES OF ELEVATION.
RATES SPECIFIED BY VELOCITY IN KNOTS, DEGREES
AZIMUTH/SEC., DEGREES ELEVATION/SEC.

DIRECT PATH

AMPLITUDE = 1.00
INITIAL A/C POSITION = 10.00, 30.00, 3.00
INITIAL A/C RATE = -300.00 .00 .0

SPECULAR MULTIPATH

REFLECTOR 1

AMPLITUDE = .80
INITIAL POSITION = 1.00 33.00 1.85
INITIAL RATE = .00, -3.04, .00
RF PHASE DIFFERENCE = 0° AT PULSE
COINCIDENCE

SCATTERED MULTIPATH

AMPLITUDE = .00

FRONT-END RECEIVER NOISE

σ_n = .10
(SNR = 20.00 DB)

CANDIDATE RECEIVER:

SQUARE GATE TRACKING REC. TVER
(60-BIT WORD LENGTH)

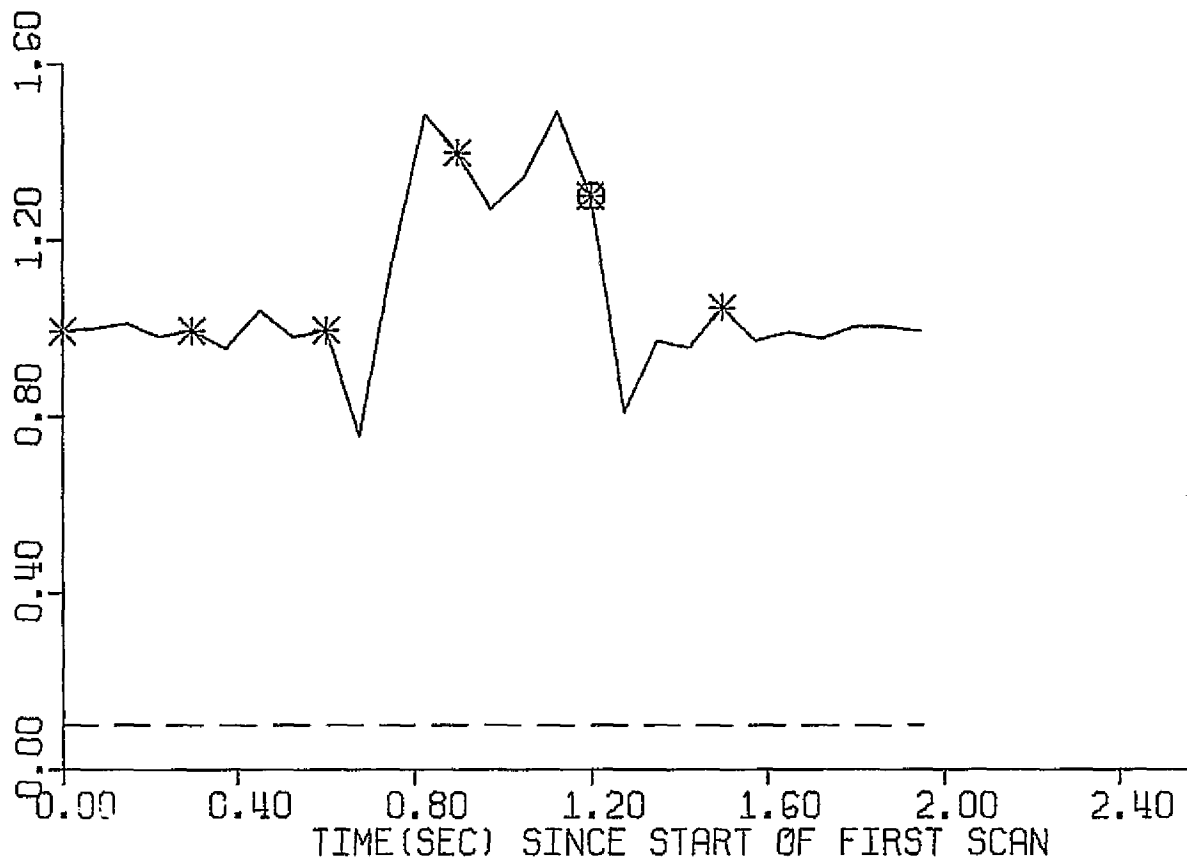
A/C AT 30.00 DEGREES AZIMUTH

TK = 1200MSEC.

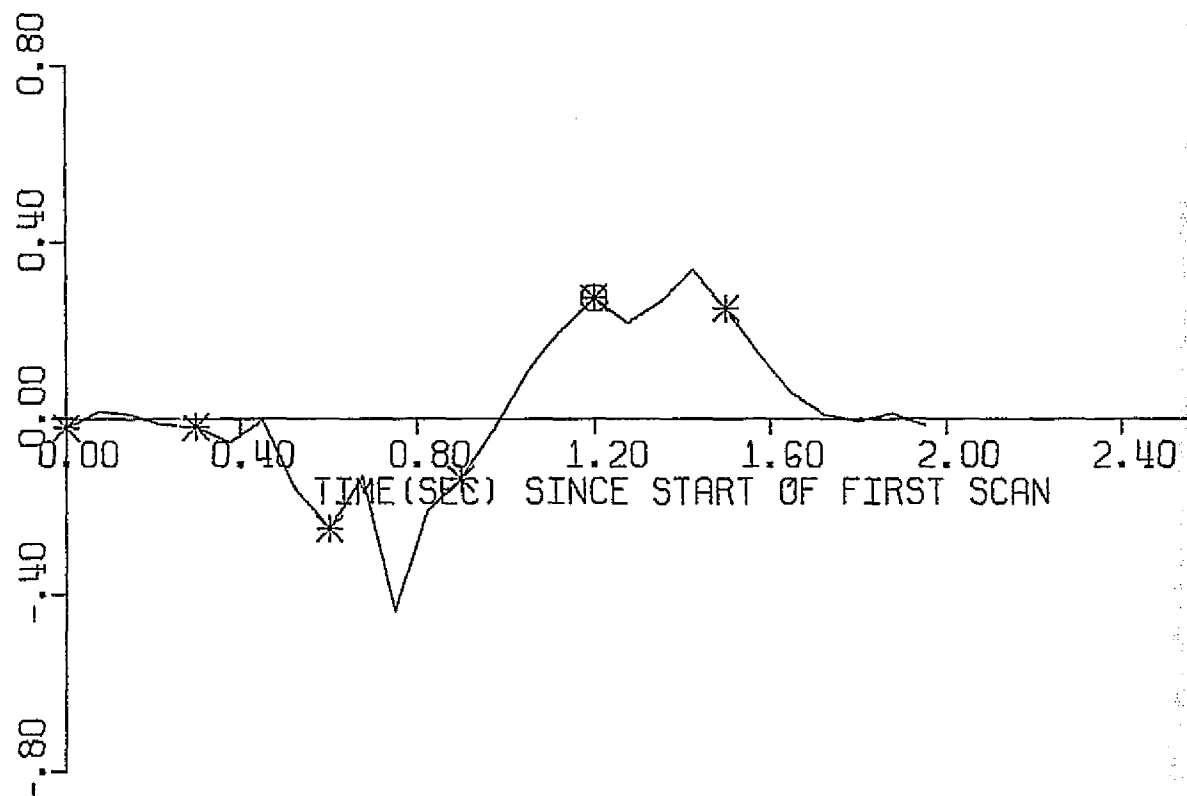
FOLDOUT FRAME 3

AV. AMPLITUDE OF
COMPOSITE SIGNAL
AT TIME OF DIRECT
SIGNAL CENTROID
(SOLID LINE)

RMS NOISE LEVEL
(DASHED LINE)



ESTIMATION ERROR
(A/C ANGLE-EST.)
(DEGREES)



FOLDOUT FRAME)

FIGURE B-6.a

LONG-TERM PLOT FOR 27 SCANS

DATE: 10/10/75

PROGRAM: MLSRCVR

JOBNAME: MLSRC8E

S. H. IRWIN, JR.

CHANNEL: AZIMUTH

SIGNAL MAKEUP

POSITION SPECIFIED BY RANGE IN NAUTICAL MILES,
DEGREES OF AZIMUTH, DEGREES OF ELEVATION.
RATES SPECIFIED BY VELOCITY IN KNOTS, DEGREES
AZIMUTH/SEC, DEGREES ELEVATION/SEC.

DIRECT PATH

AMPLITUDE = 1.00

INITIAL A/C POSITION = 10.00, 30.00, 3.00

INITIAL A/C RATE = -300.00, .00, .0

SPECULAR MULTIPATH

REFLECTOR 1

AMPLITUDE = .80

INITIAL POSITION = 1.00, 33.00, 1.85

INITIAL RATE = .00, -3.04, .00

RF PHASE DIFFERENCE = 90° AT PULSE

COINCIDENCE

SCATTERED MULTIPATH

AMPLITUDE = .00

FRONT-END RECEIVER NOISE

$\sigma_n = .10$

(SNR = 20.00 DB)

CANDIDATE RECEIVER:

SQUARE GATE TRACKING RECEIVER

(60-BIT WORD LENGTH)

ESTIMATION ERROR

RMS ESTIMATION ERROR = .173 DEGREES

RMS ERROR SPECIFICATION = .010 DEGREES

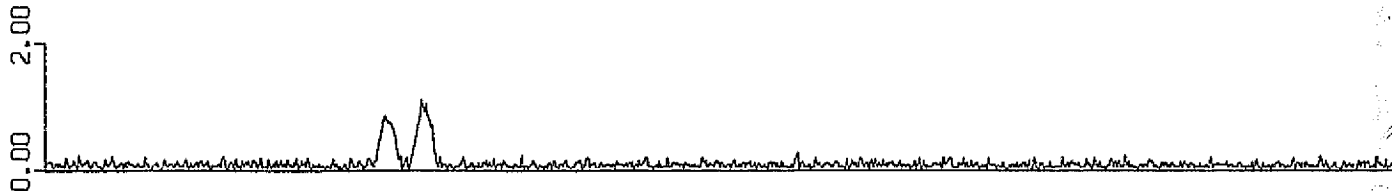
* SHORT-TERM PLOT OF COMPOSITE SIGNAL AVAILABLE
① DETAILED SHORT-TERM PERFORMANCE PLOT AVAILABLE

FOLDOUT FRAME 2

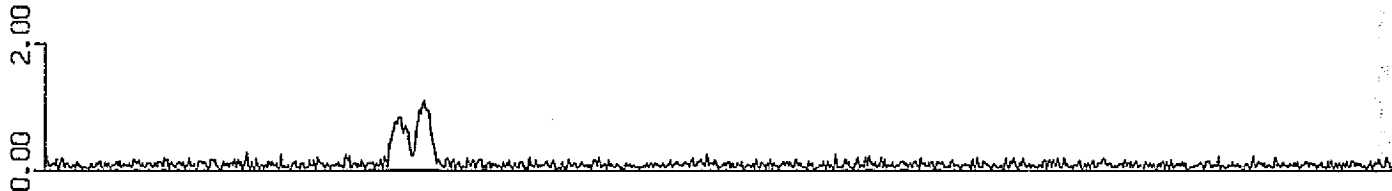
2.80

2.80

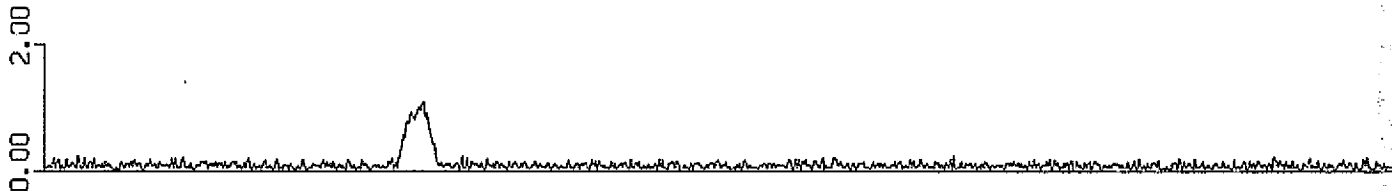
SCAN 1
TK = 0 MS



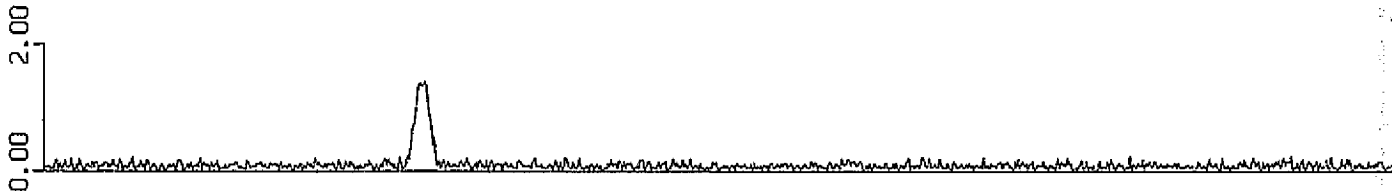
SCAN 5
TK = 300 MS



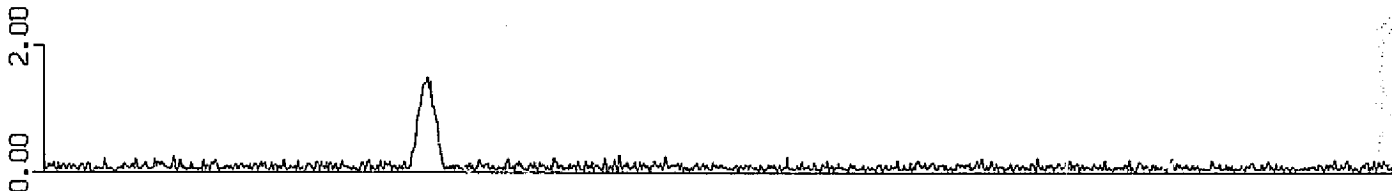
SCAN 9
TK = 600 MS



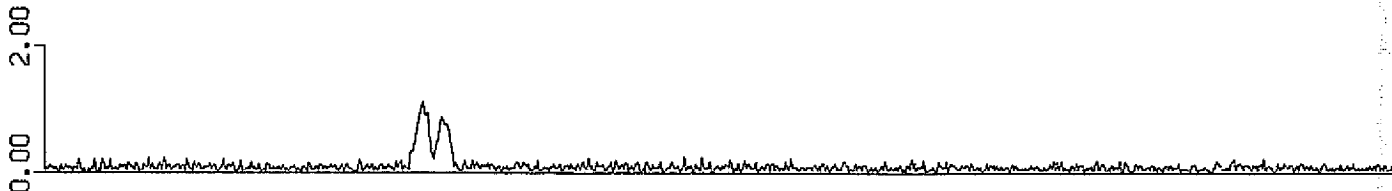
SCAN 13
TK = 900 MS



SCAN 17
TK = 1200 MS

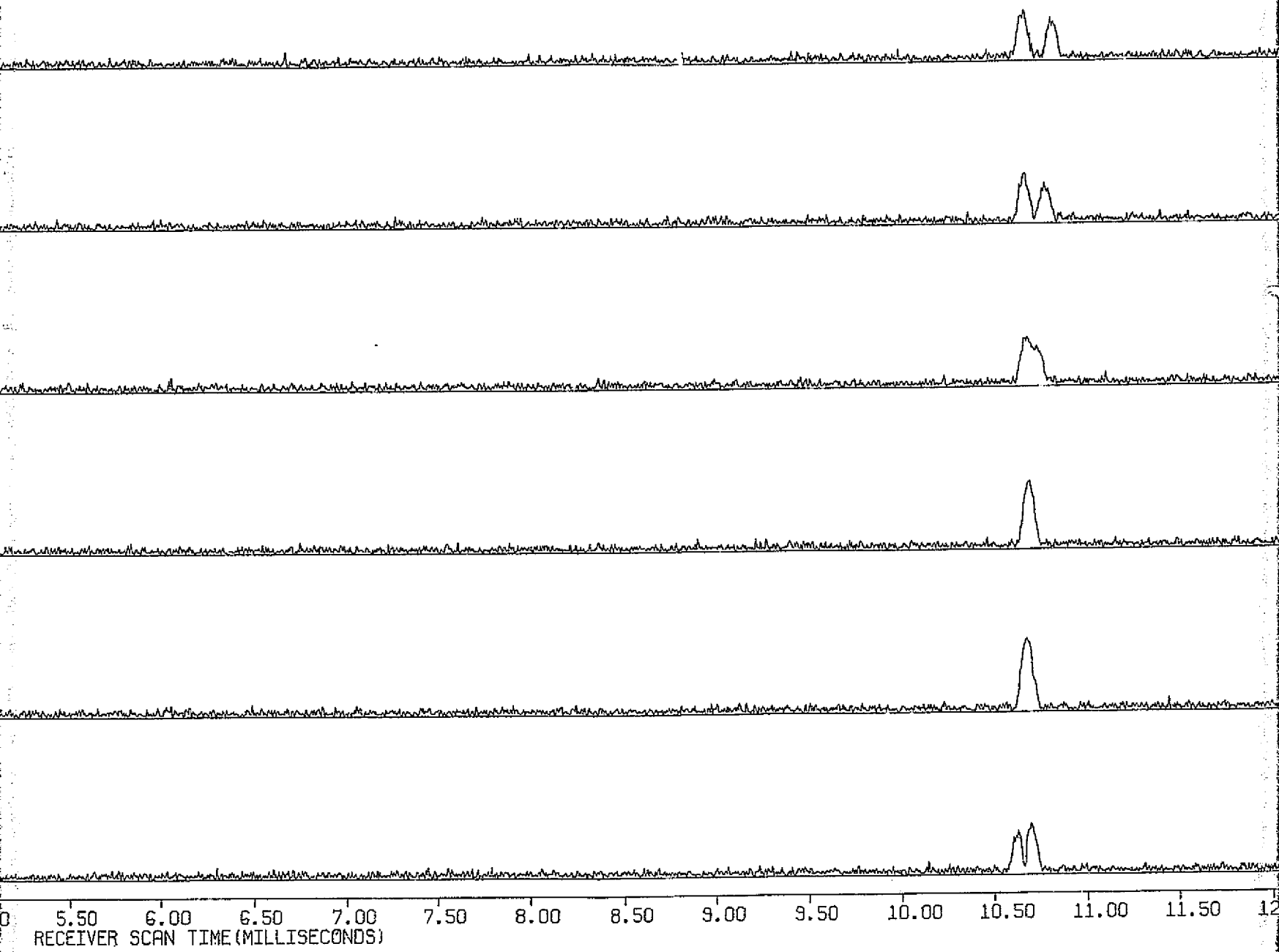


SCAN 21
TK = 1500 MS



0.00 0.50 1.00 1.50 2.00 2.50 3.00 3.50 4.00 4.50 5.00

FOLDOUT FRAME



TOLDOUT FRAME 2

FIGURE B-6.b

AMPLITUDE OF COMPOSITE SIGNAL PLUS NOISE

DATE: 10/10/75

PROGRAM: MLSRCVR

JOBNAME: MLSRCBE

S. H. IRWIN, JR.

CHANNEL: AZIMUTH

SIGNAL MAKEUP

POSITION SPECIFIED BY RANGE IN NAUTICAL MILES,
DEGREES OF AZIMUTH, DEGREES OF ELEVATION.
RATES SPECIFIED BY VELOCITY IN KNOTS, DEGREES
AZIMUTH/SEC, DEGREES ELEVATION/SEC.

DIRECT PATH

AMPLITUDE = 1.00

INITIAL A/C POSITION = 10.00, 30.00, 3.00

INITIAL A/C RATE = -300.00, .00, .0

SPECULAR MULTIPATH

REFLECTOR 1

AMPLITUDE = .80

INITIAL POSITION = 1.00, 33.00, 1.85

INITIAL RATE = .00, -3.04, .00

RF PHASE DIFFERENCE = 90° AT PULSE

COINCIDENCE

SCATTERED MULTIPATH

AMPLITUDE = .00

FRONT-END RECEIVER NOISE

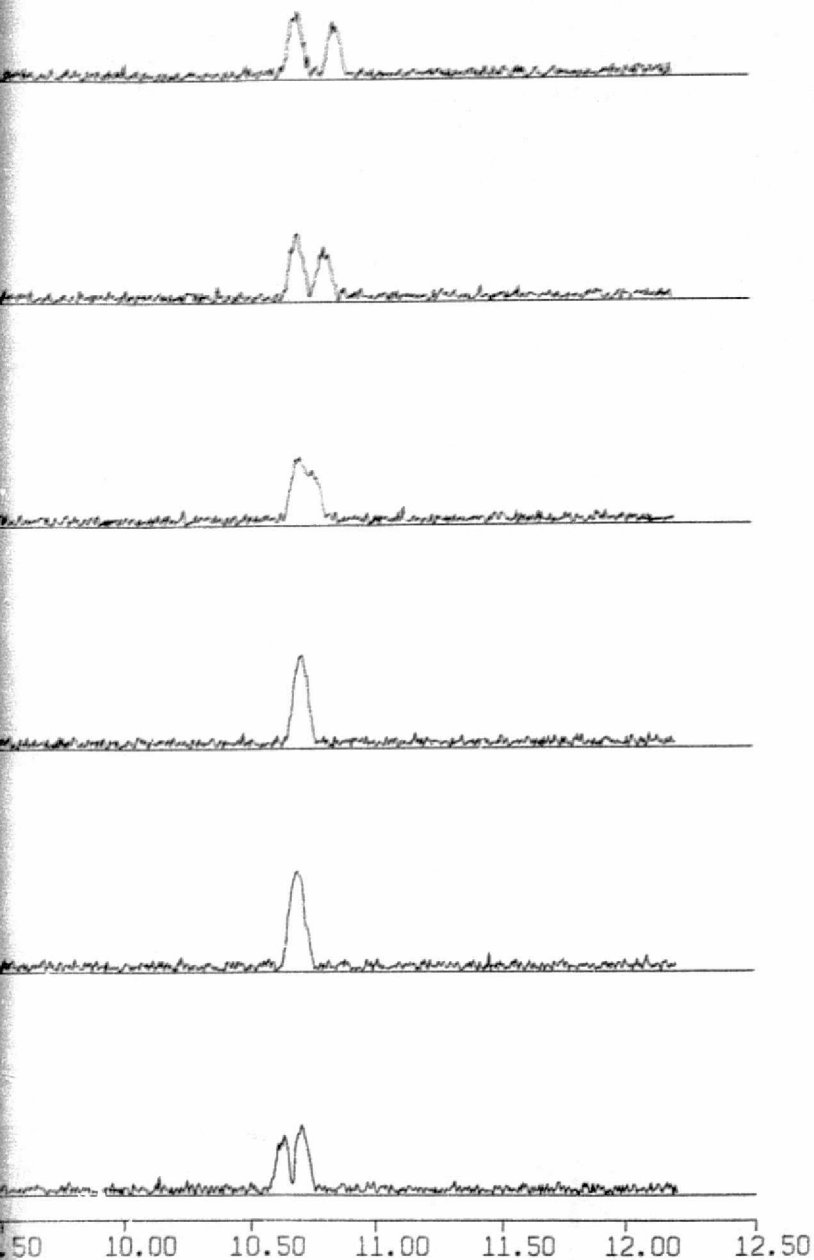
$\sigma_n = .10$

(SNR = 20.00 DB)

CANDIDATE RECEIVER:

SQUARE GATE TRACKING RECEIVER

(60-BIT WORD LENGTH)



FOLDOUT FRAME 3

FIGURE 5-6b

AMPLITUDE OF COMPOSITE SIGNAL PLUS NOISE

DATE: 10/10/75

PROGRAM: MLSACVR

JOBNAME: MLSAC8E

S. H. IRWIN, JR.

CHANNEL: AZIMUTH

SIGNAL MAKEUP

POSITION SPECIFIED BY RANGE IN METERS, KILES,
DEGREES OF AZIMUTH, DEGREES OF ELEVATION.
RATES SPECIFIED BY VELOCITY IN KNOTS, DEGREES
PER SECOND, DEGREES ELEVATION/SEC.

DIRECT PATH

AMPLITUDE = 1.00

INITIAL A/C POSITION = 10.00, 30.00, 3.00

INITIAL A/C RATE = -300.00, .00, .0

SPECULAR MULTIPATH

REFLECTOR 1

AMPLITUDE = .80

INITIAL POSITION = 1.00, 33.00, 1.85

INITIAL RATE = .00, -3.04, .00

RF PHASE DIFFERENCE = 90° AT PULSE

COINCIDENCE

SCATTERED MULTIPATH

AMPLITUDE = .00

FRONT-END RECEIVER NOISE

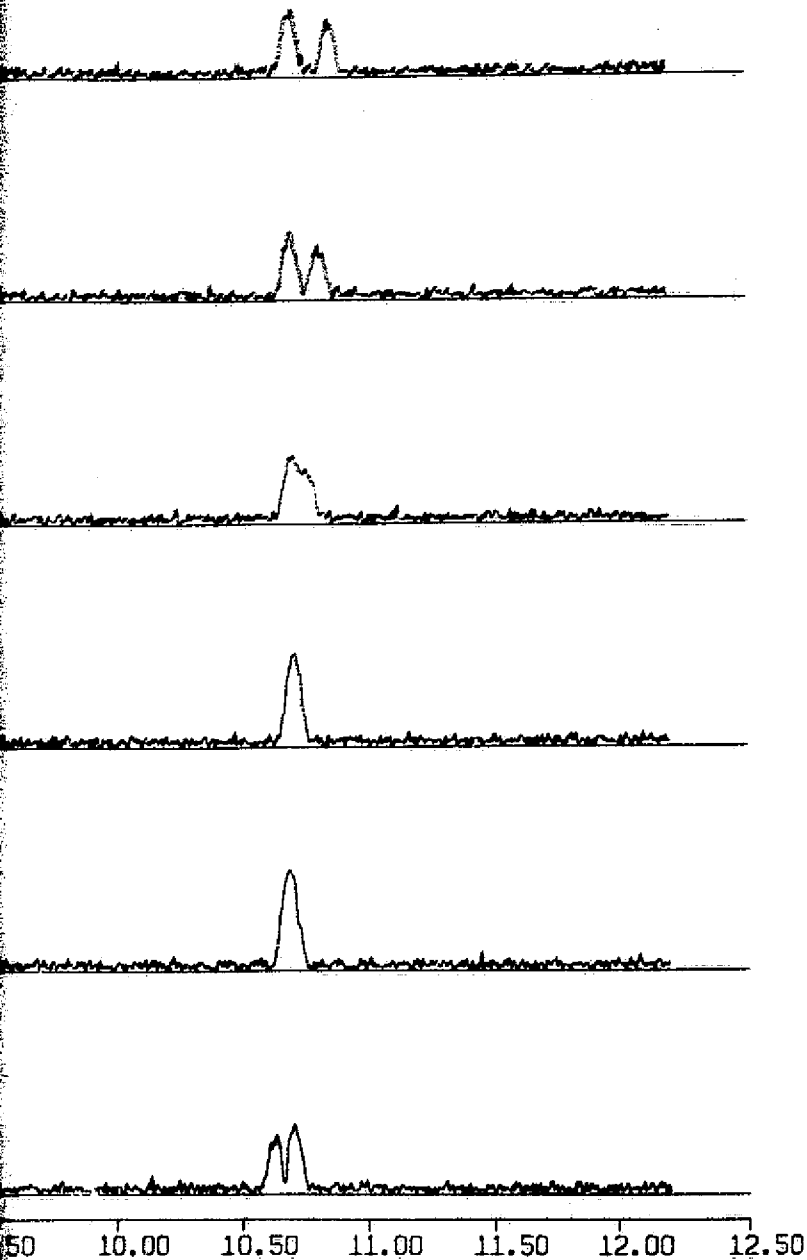
DN = .10

(SNR = 20.00 DB)

CANDIDATE RECEIVER:

SQUARE GATE TRACKING RECEIVER

(60-BIT WORD LENGTH)

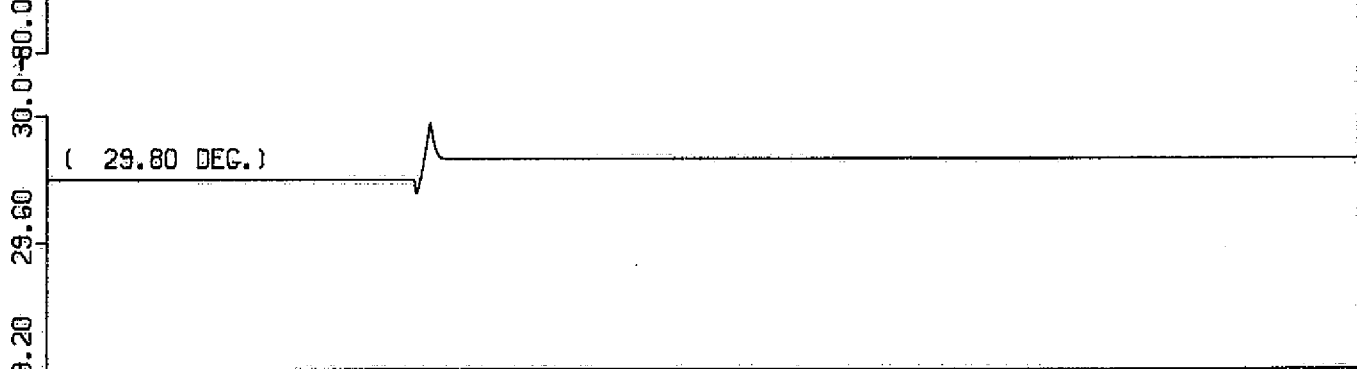


FOLDER TRAIN 5

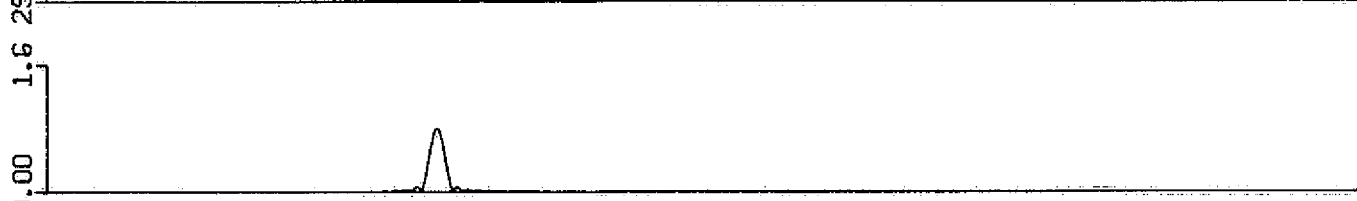
SCAN ANGLE
(DEGREES)
(DASHED)



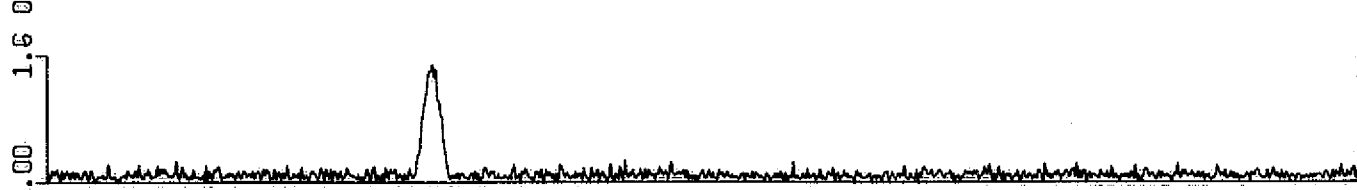
CANDIDATE
RCVR OUTPUT
(DEGREES)
DIRECT PATH
COMPONENT ONLY



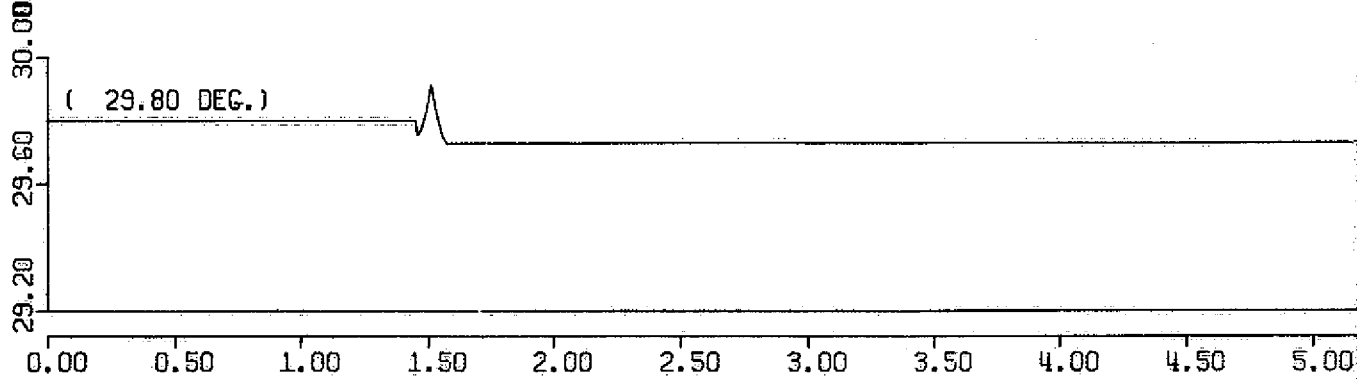
AMPLITUDE OF
MULTIPATH
INTERFERENCE



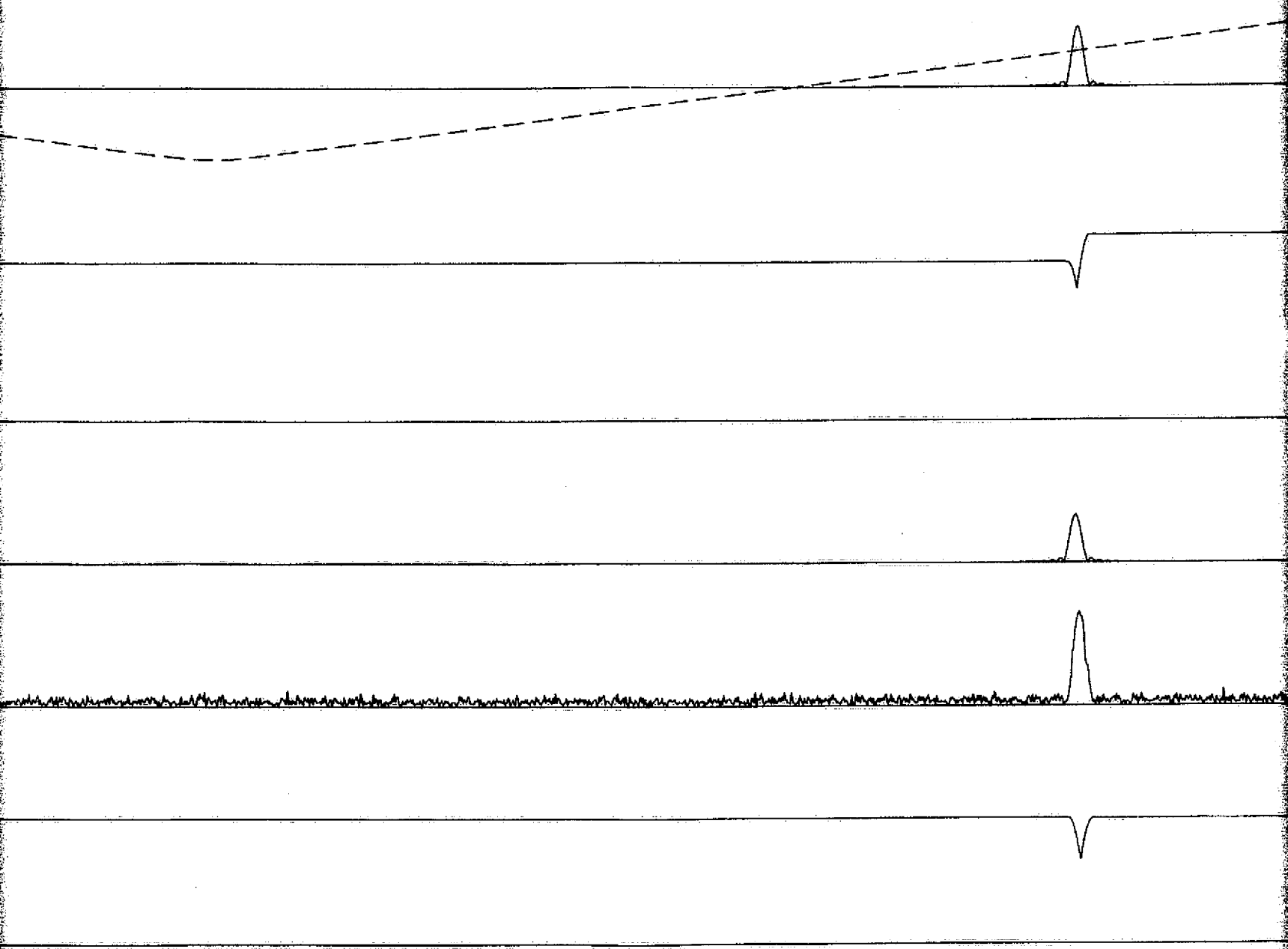
AMPLITUDE OF
COMPOSITE SIGNAL
PLUS NOISE



CANDIDATE
RCVR OUTPUT
(DEGREES)
COMPOSITE SIGNAL
PLUS NOISE

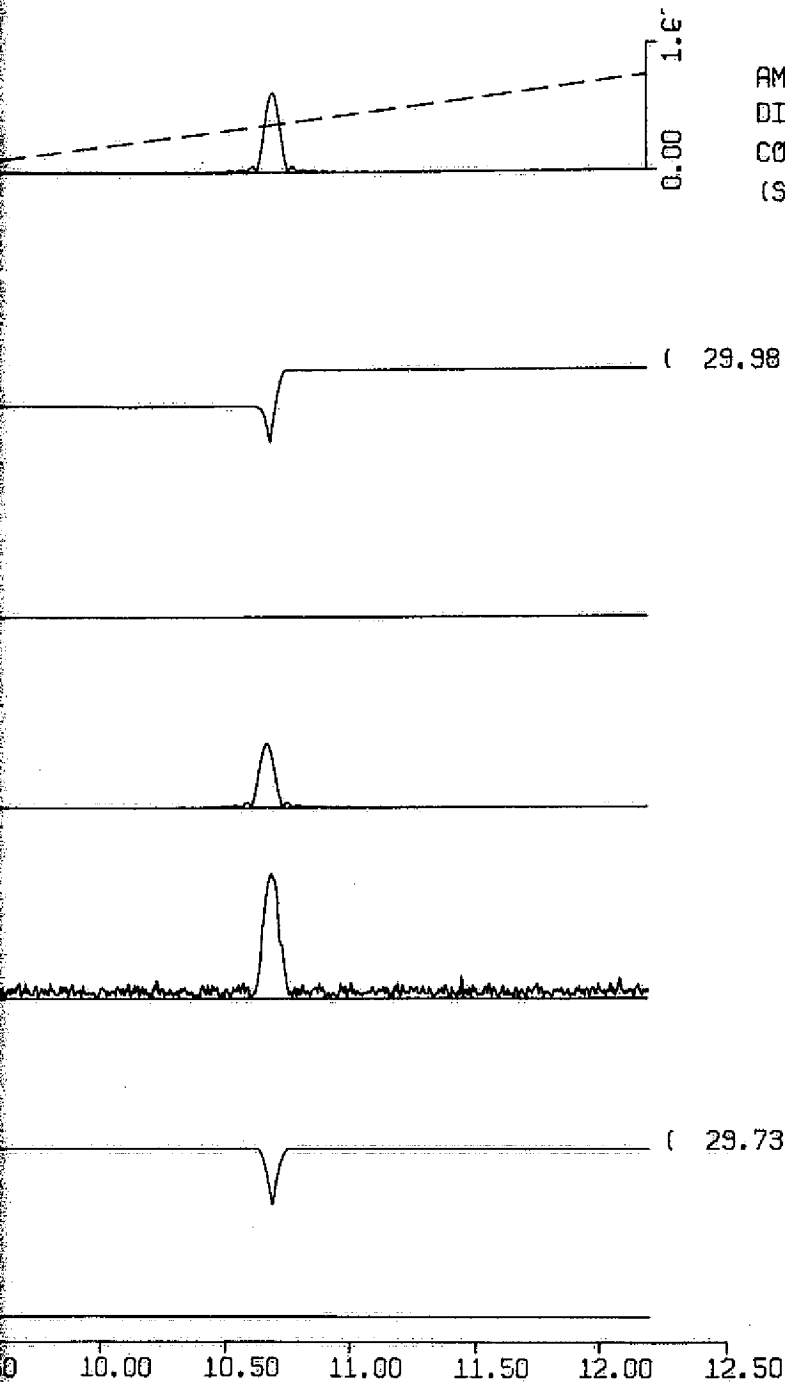


0.00 0.50 1.00 1.50 2.00 2.50 3.00 3.50 4.00 4.50 5.00



5.00 5.50 6.00 6.50 7.00 7.50 8.00 8.50 9.00 9.50 10.00 10.50 11.00 11.50
RECEIVER SCAN TIME (MILLISECONDS)

FOLDOUT FRAME 3



AMPLITUDE OF
DIRECT PATH
COMPONENT
(SOLID LINE)

FIGURE B-6.c

SHORT-TERM PLOT FOR SCAN 17

DATE: 10/10/75

PROGRAM: MLSRCVR

JOBNAME: MLSRC8E

S. H. IRWIN, JR.

CHANNEL: AZIMUTH

SIGNAL MAKEUP

POSITION SPECIFIED BY RANGE IN NAUTICAL MILES,
DEGREES OF AZIMUTH, DEGREES OF ELEVATION.
RATES SPECIFIED BY VELOCITY IN KNOTS, DEGREES
AZIMUTH/SEC, DEGREES ELEVATION/SEC.

DIRECT PATH

AMPLITUDE = 1.00

INITIAL A/C POSITION = 10.00, 30.00, 3.00

INITIAL A/C RATE = -300.00, .00, .0

SPECULAR MULTIPATH

REFLECTOR 1

AMPLITUDE = .80

INITIAL POSITION = 1.00, 33.00, 1.85

INITIAL RATE = .00, -3.04, .00

RF PHASE DIFFERENCE = 90° AT PULSE

COINCIDENCE

SCATTERED MULTIPATH

AMPLITUDE = .00

FRONT-END RECEIVER NOISE

$C_n = .10$

(SNR = 20.00 DB)

CANDIDATE RECEIVER:

SQUARE GATE TRACKING RECEIVER

(60-BIT WORD LENGTH)

A/C AT 30.00 DEGREES AZIMUTH

TK = 1200MSEC.

HOLDON FRANK

FIGURE B-7.a

LONG-TERM PLOT FOR 27 SCANS

DATE: 10/10/75

PROGRAM: MLSRCVR

JOBNAME: MLSRC7Q

S. H. IRWIN, JR.

CHANNEL: AZIMUTH

SIGNAL MAKEUP

POSITION SPECIFIED BY RANGE IN NAUTICAL MILES,
DEGREES OF AZIMUTH, DEGREES OF ELEVATION.
RATES SPECIFIED BY VELOCITY IN KNOTS, DEGREES
AZIMUTH/SEC, DEGREES ELEVATION/SEC.

DIRECT PATH

AMPLITUDE = 1.00

INITIAL A/C POSITION = 10.00, 30.00, 3.00

INITIAL A/C RATE = -300.00, .00, .0

SPECULAR MULTIPATH

REFLECTOR 1

AMPLITUDE = .80

INITIAL POSITION = 1.00, 33.00, 1.85

INITIAL RATE = .00, -3.04, .00

RF PHASE DIFFERENCE = 270° AT PULSE

COINCIDENCE

SCATTERED MULTIPATH

AMPLITUDE = .00

FRONT-END RECEIVER NOISE

$\sigma_n = .10$

(SNR = 20.00 DB)

CANDIDATE RECEIVER:

SQUARE GATE TRACKING RECEIVER

(60-BIT WORD LENGTH)

ESTIMATION ERROR

RMS ESTIMATION ERROR = .201 DEGREES

RMS ERROR SPECIFICATION = .010 DEGREES

* SHORT-TERM PLOT OF COMPOSITE SIGNAL AVAILABLE
□ DETAILED SHORT-TERM PERFORMANCE PLOT AVAILABLE

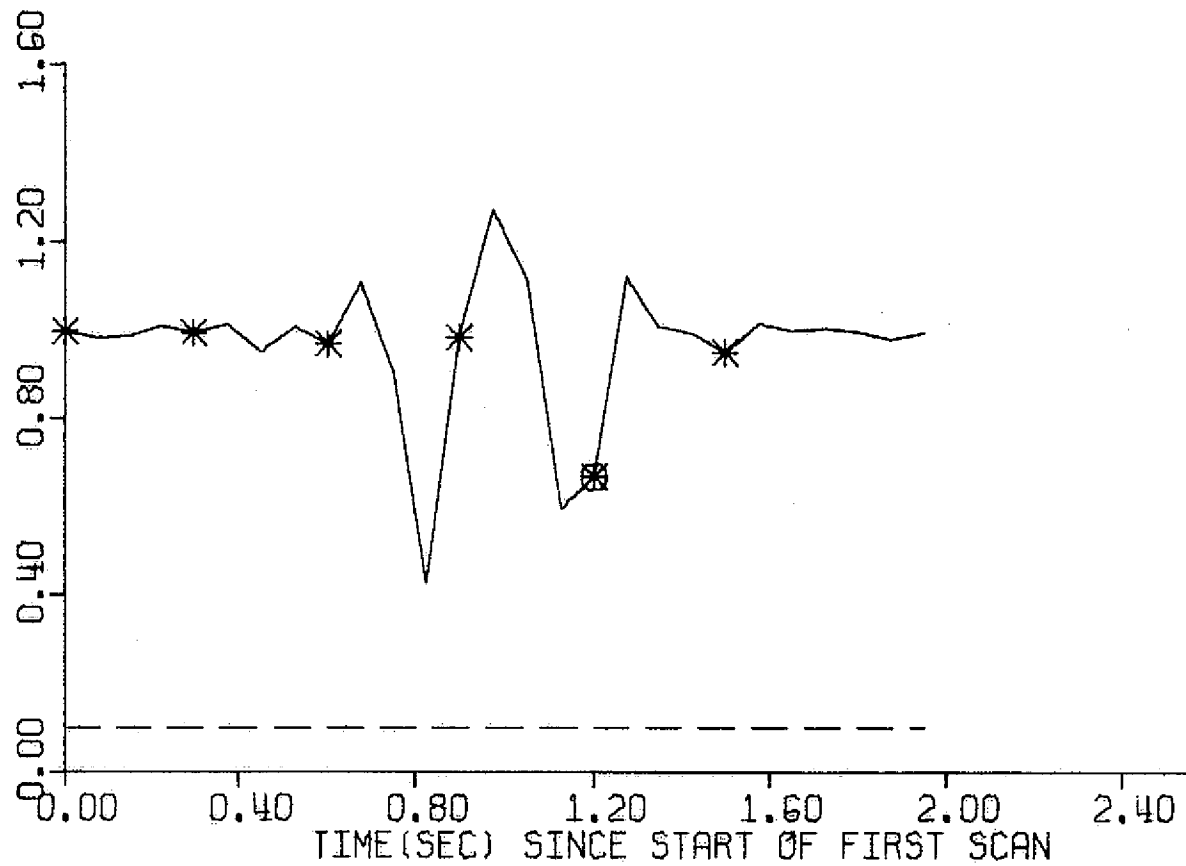
2.80

2.80

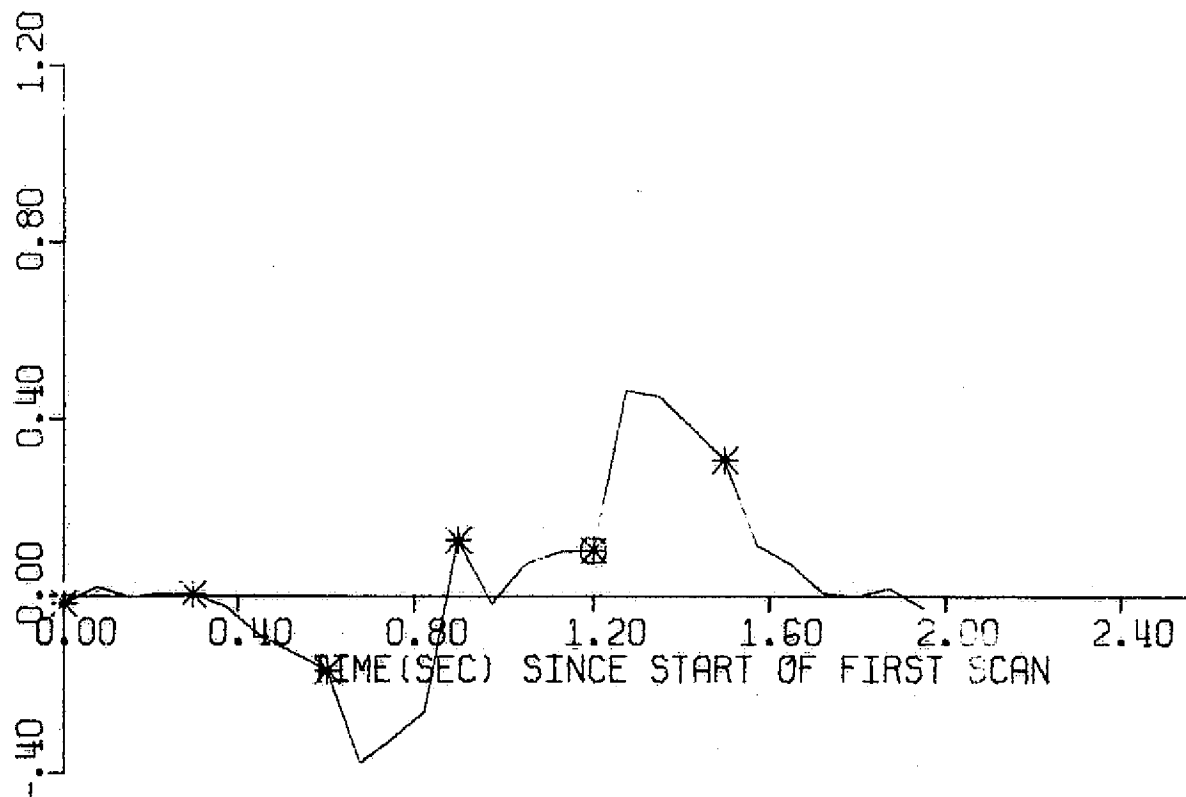
EXPLODED FRAME 2

AV. AMPLITUDE OF
COMPOSITE SIGNAL
AT TIME OF DIRECT
SIGNAL CENTROID
(SOLID LINE)

RMS NOISE LEVEL
(DASHED LINE)



ESTIMATION ERROR
(A/C ANGLE-EST.)
(DEGREES)

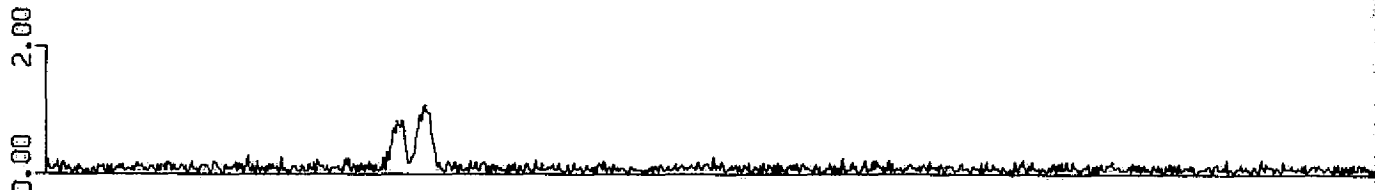


FOLDOUT FRAME

SCAN 1
TK = 0 MS



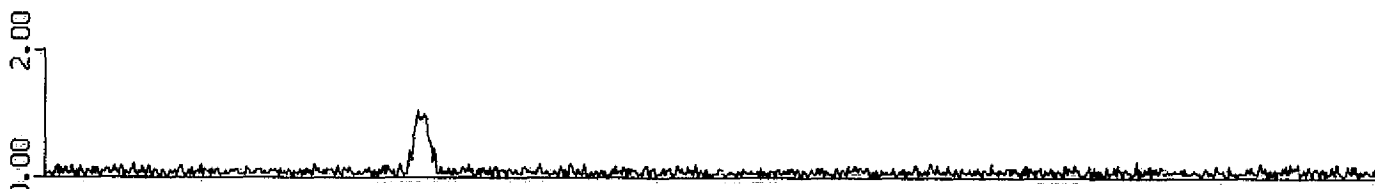
SCAN 5
TK = 300 MS



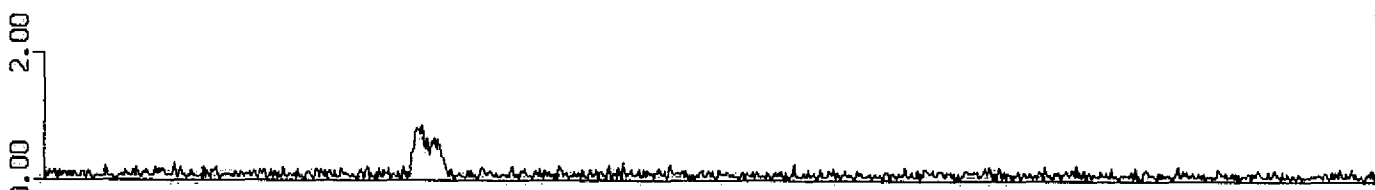
SCAN 9
TK = 600 MS



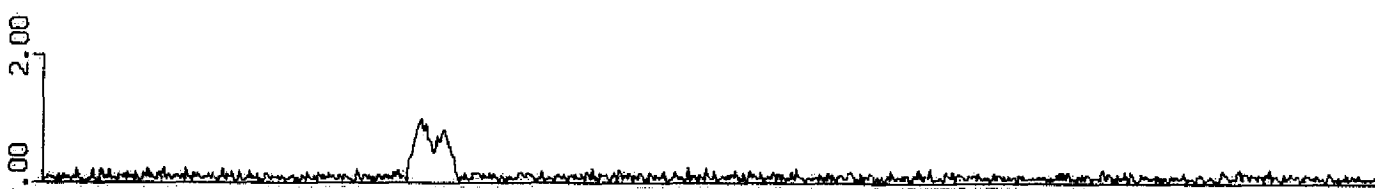
SCAN 13
TK = 900 MS



SCAN 17
TK = 1200 MS

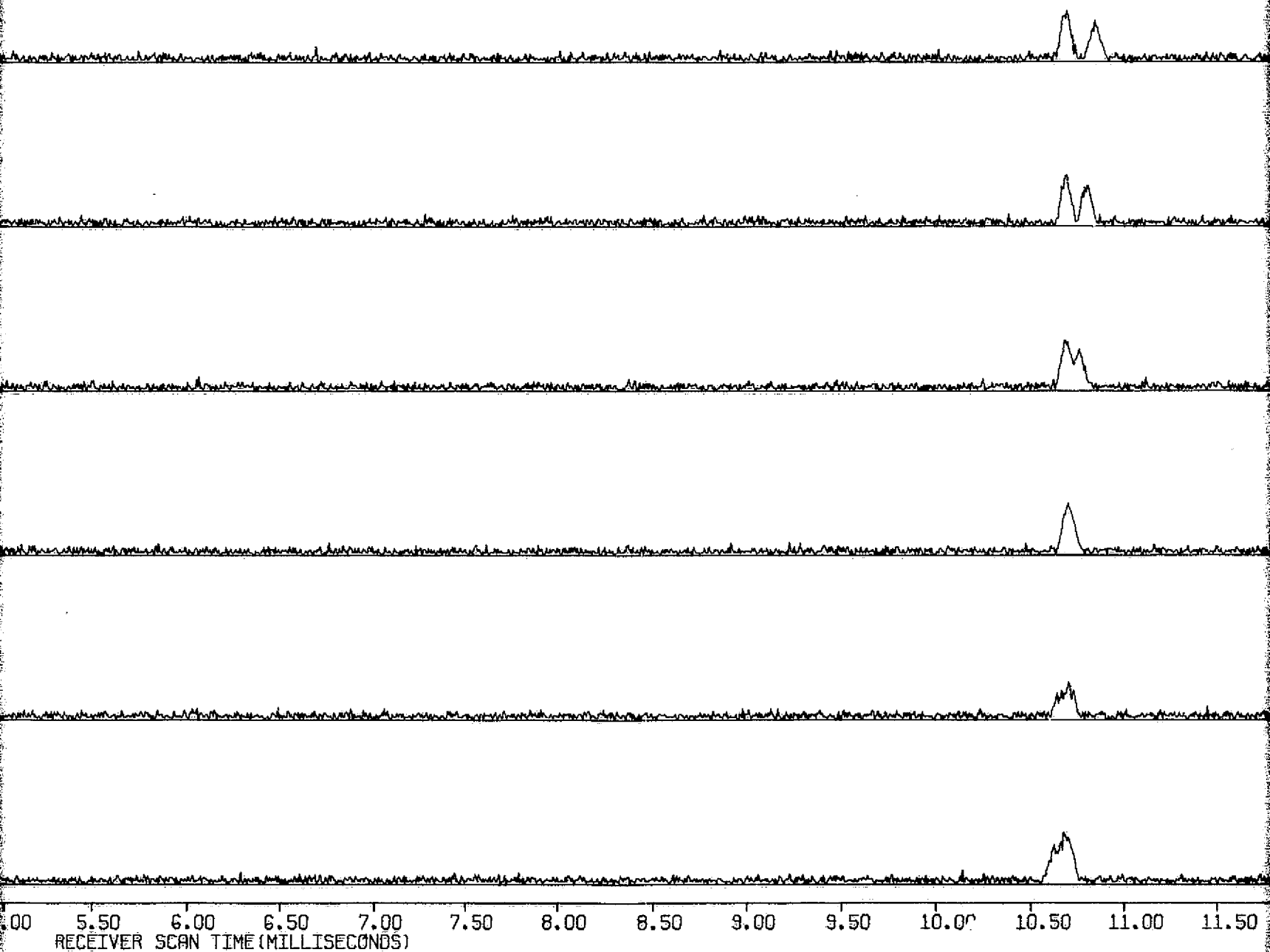


SCAN 21
TK = 1500 MS



0.00 0.50 1.00 1.50 2.00 2.50 3.00 3.50 4.00 4.50 5.00

FOLDOUT FRAME 1



FOLDOUT FRAME 3

FIGURE B-7.b

AMPLITUDE OF COMPOSITE SIGNAL PLUS NOISE

DATE: 10/10/75

PROGRAM: MLSRCVR

JOBNAME: MLSRC7Q

S. H. IRWIN, JR.

CHANNEL: AZIMUTH

SIGNAL MAKEUP

POSITION SPECIFIED BY RANGE IN NAUTICAL MILES,
DEGREES OF AZIMUTH, DEGREES OF ELEVATION.
RAVES SPECIFIED BY VELOCITY IN KNOTS, DEGREES
AZIMUTH/SEC, DEGREES ELEVATION/SEC.

DIRECT PATH

AMPLITUDE = 1.00

INITIAL A/C POSITION = 10.00, 30.00, 3.00

INITIAL A/C RATE = -300.00, .00, .0

SPECULAR MULTIPATH

REFLECTOR 1

AMPLITUDE = .80

INITIAL POSITION = 1.00, 33.00, 1.85

INITIAL RATE = .00, -3.04, .00

RF PHASE DIFFERENCE = 270° AT PULSE
COINCIDENCE

SCATTERED MULTIPATH

AMPLITUDE = .00

FRONT-END RECEIVER NOISE

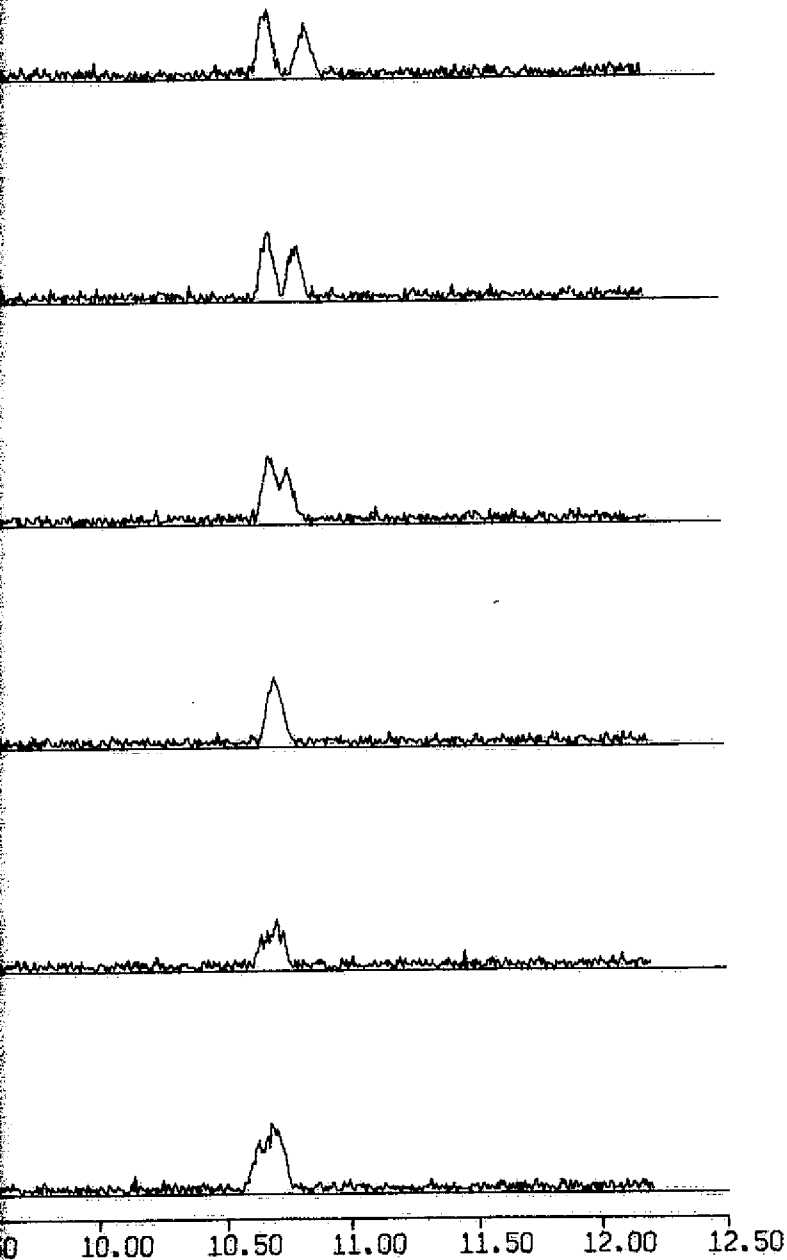
σ_n = .10

(SNR = 20.00 DB)

CANDIDATE RECEIVER:

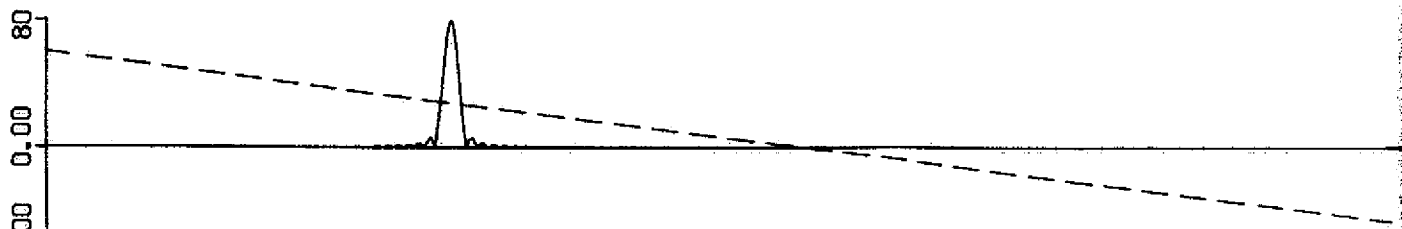
SQUARE GATE TRACKING RECEIVER

(60-BIT WORD LENGTH)

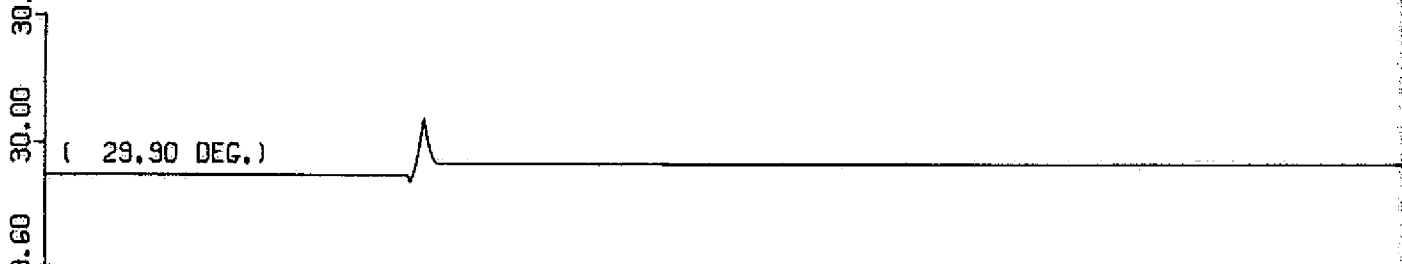


FOLDOUT FRAME 3

SCAN ANGLE
(DEGREES)
(DASHED)



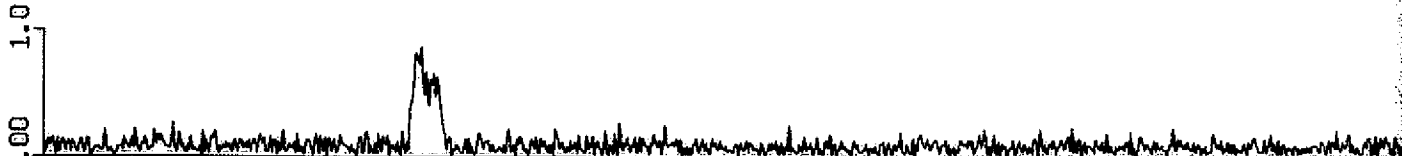
CANDIDATE
RCVR OUTPUT
(DEGREES)
DIRECT PATH
COMPONENT ONLY



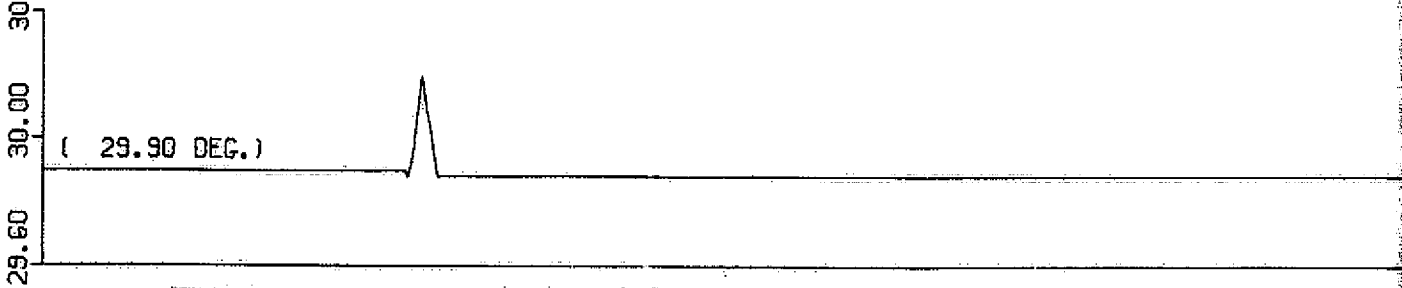
AMPLITUDE OF
MULTIPATH
INTERFERENCE



AMPLITUDE OF
COMPOSITE SIGNAL
PLUS NOISE

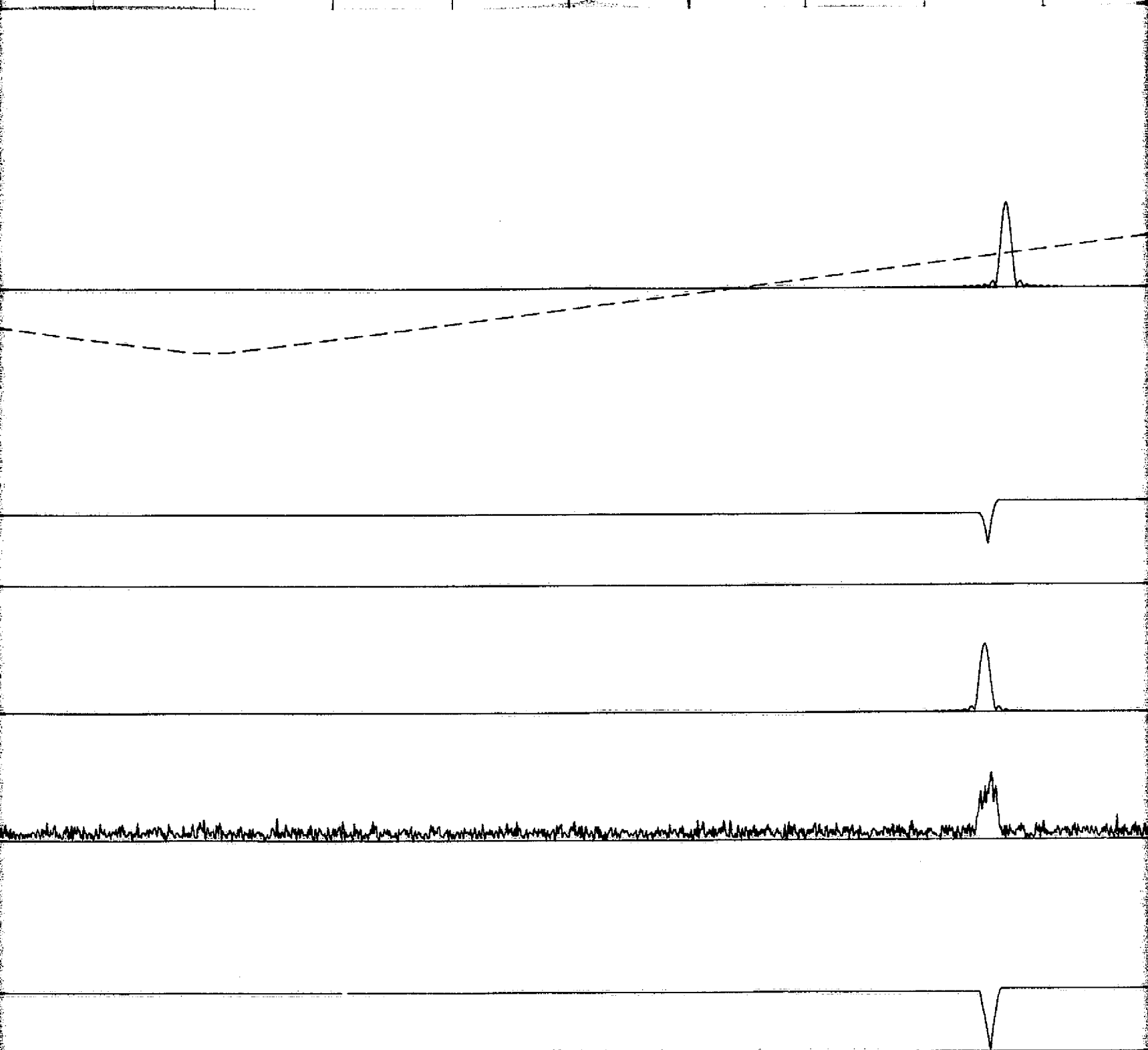


CANDIDATE
RCVR OUTPUT
(DEGREES)
COMPOSITE SIGNAL
PLUS NOISE



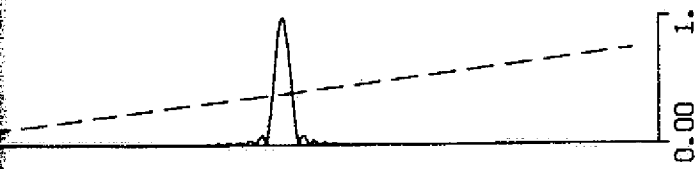
0.50 1.00 1.50 2.00 2.50 3.00 3.50 4.00 4.50 5.00

FOLDOUT FRAME



RECEIVER SCAN TIME (MILLISECONDS)

FOLDOUT FRAME 2



AMPLITUDE OF
DIRECT PATH
COMPONENT
(SOLID LINE)

FIGURE B-7.c

SHORT-TERM PLOT FOR SCAN 17

DATE: 10/10/75

PROGRAM: MLSRCVR

JOBNAME: MLSRC7Q

S. H. IRWIN, JR.

CHANNEL: AZIMUTH

SIGNAL MAKEUP

POSITION SPECIFIED BY RANGE IN NAUTICAL MILES,
DEGREES OF AZIMUTH, DEGREES OF ELEVATION.
RATES SPECIFIED BY VELOCITY IN KNOTS, DEGREES
AZIMUTH/SEC, DEGREES ELEVATION/SEC.

DIRECT PATH

AMPLITUDE = 1.00

INITIAL A/C POSITION = 10.00, 30.00, 3.00

INITIAL A/C RATE = -300.00, .00, .0

SPECULAR MULTIPATH

REFLECTOR

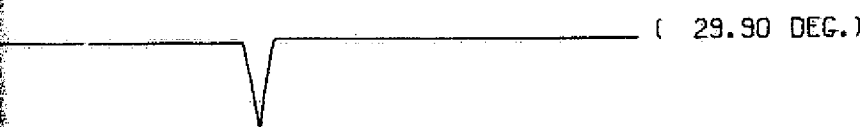
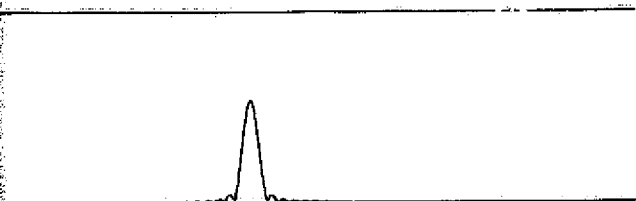
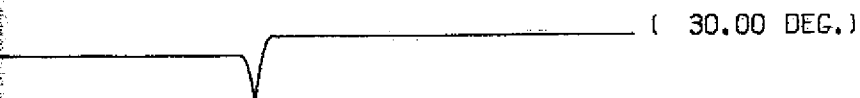
AMPLITUDE = .80

INITIAL POSITION = 1.00, 39.00, 1.85

INITIAL RATE = .00, -3.04, .00

RF PHASE DIFFERENCE = 270° AT PULSE

COINCIDENCE



SCATTERED MULTIPATH

AMPLITUDE = .00

FRONT-END RECEIVER NOISE

DN = .10

(SNR = 20.00 DB)

CANDIDATE RECEIVER:

SQUARE GATE TRACKING RECEIVER

(60-BIT WORD LENGTH)

A/C AT 30.00 DEGREES AZIMUTH

TK = 1200MSEC.

10.00 10.50 11.00 11.50 12.00 12.50

BOLDOUT FRAME 3